INTRINSIC PROPERTIES AND NETWORK CONFIGURATION OF SYMPATHETIC PREMOTOR NEURONS IN THE ROSTRAL VENTROLATERAL MEDULLA

LAMA BOU FARAH

AUSTRALIAN SCHOOL OF ADVANCED MEDICINE

MACQUARIE UNIVERSITY

A thesis submitted in fulfilment of the requirements for the degree of Doctor of Philosophy in Medicine

17/02/2015

SUPERVISOR:	DR SIMON MCMULLAN
ASSOCIATE SUPERVISORS:	ASSOCIATE PROFESSOR ANN K GOODCHILD
	PROFESSOR MARK CONNOR
CO-SUPERVISOR:	DR. ANITA TURNER

TABLE OF CONTENTS

ABSTRACT

Sympathetic premotor neurons within the rostral ventrolateral medulla (RVLM) exhibit tonic activity *in vivo,* which is thought to be critical for generating sympathetic nerve activity (SNA) and maintaining blood pressure. The mechanisms responsible for the generation of spontaneous activity in these neurons are therefore a topic of considerable research interest. In the current thesis we examine intrinsic and extrinsic mechanisms that contribute to the excitability of these neurons *in vitro*.

First we investigated two candidate mechanisms for mediating the hypoxia-sensitivity of these cells. We initially examined the evidence for expression and function of the putative oxygen-sensor heme oxygenase 2 (HO-2) on bulbospinal neurons. We found no HO-2 immunoreactivity on spinally projecting or catecholaminergic RVLM neurons, and found no effect of HO-2 blockade on electrophysiological responses to acute cyanide hypoxia. We then demonstrated that extracellular ATP release is critically important for mediating responses to hypoxia, and that destruction of brainstem glia abolishes cyanide sensitivity, indicating a previous unrecognized role for glia in driving hypoxic responses.

Second, we examined the role played by RVLM sympathetic premotor neurons in driving adrenaline release in response to acute glucoprivation. We found that RVLM bulbospinal neurons are not sensitive to changes in extracellular glucose concentration *in vitro*, but that RVLM neurons are activated by an orexinergic relay originating in the perifornical hypothalamus (PeH) in response to systemic or PeH glucoprivation *in vivo*.

Third, we examined the cellular mechanisms responsible for the dramatic sympathoinhibition evoked by microinjection of somatostatin (Sst) into the RVLM *in vivo*, despite the limited expression of the SST2A receptor on putative sympathetic premotor neurons. Consistent with our previous anatomical data we found that Sst hyperpolarises only 50% of bulbospinal RVLM neurons (via an inwardly rectifying potassium channel). Given the profound effect of Sst receptor agonists in this region and the limited distribution of the SST2A-R and sensitivity of bulbospinal neurons to Sst, these findings support our previous suggestion that Sst-sensitive neurons may play a critical role in generating vasomotor tone.

Finally, we examined the hypothesis that synaptic coupling between spinally projecting RVLM neurons contributes to the burst generation in sympathetic nerves *in vivo*. We did not

find any evidence of monosynaptic connections between simultaneously recorded pairs of RVLM bulbospinal neurons and conclude that synaptic mechanisms does not contribute to the synchronisation of these neurons.

Overall, these data extend our knowledge of the innate properties of bulbospinal RVLM neurons and the neuronal networks in which they reside.

DECLARATION OF ORIGINALITY

I declare that the work in this thesis entitled “Intrinsic properties and network configuration of sympathetic premotor neurons in the rostral ventrolateral medulla” has not been submitted for a degree nor has been submitted as part of the requirements for a degree to any other university or institution other than Macquarie University.

In addition, I certify that the contents of this thesis represent the original experimental and written work of the candidate except where due acknowledgment is made.

All research presented in this thesis was conducted following approval of Macquarie University Ethics Committees (protocol numbers: 2009/045 and 2011/055).

Lama Bou Farah

Student ID: 42193761

DECLARATION OF CONTRIBUTION TO CHAPTERS

Chapter 2

The candidate performed all electrophysiological experiments and data analysis. Drafting of the manuscript was made by the candidate and Dr. Simon McMullan. Dr. Anita Turner taught the candidate how to perform recovery surgeries on pups and spinal cord tracer injections. A/Prof. Ann Goodchild provided essential intellectual contribution.

Chapter 3

The candidate performed all in vitro electrophysiological experiments and data analysis and contributed to writing the corresponding parts of the manuscript. Dr. Willian Korim performed all in vivo experiments and contributed to drafting this part of the manuscript.

Chapter 4

Dr. Simon McMullan and Dr. Anita Turner conducted RVLM tracer injections for adult rats; Dr. Sarah Hassan assessed prefrontal cortex regions for labelling; Dr. Belinda Ramirez performed combined in situ hybridisation and immunohistochemical protocols and conducted all tracer/ double labelling data analysis; the candidate conducted all patch slice experiments and analysis; Phill Bokiniec assisted in immunohistochemical processing of patch slices; the candidate was a major contributor to the manuscript, with a major contribution also from Dr. Belinda Ramirez, and intellectual input from A/Prof. Ann Goodchild and Dr. Simon McMullan.

Chapter 5

The candidate performed all electrophysiological experiments and data analysis and wrote the manuscript with the assistance of Dr. Simon McMullan.

PUBLICATIONS ARISING FROM THIS THESIS

Korim WS, **Bou Farah L**, McMullan S, Verberne AJ (2014) Orexinergic activation of medullary premotor neurons modulates the adrenal sympathoexcitation to hypothalamic glucoprivation. Diabetes 63:1895-1906.

Bou Farah L, Bowman BR, Bokiniec P, Karim S, Le S, Goodchild AK, McMullan S (2015) Somatostatin in the rat rostral ventrolateral medulla: Origins and mechanism of action. J Comp Neurol [In Press, accepted 23 June 2015).

In Preparation

Bou Farah L, Dempsey B, Turner A, Goodchild AK and McMullan S. The hypoxia sensitivity of sympathetic premotor neurons in the rostral ventrolateral medulla is due to glial ATP release, not the activation of heme oxygenase 2.

Bou Farah L and McMullan S. RVLM sympathetic premotor neurons are not synaptically linked to each other.

Publications arising from the period of candidature (not included in this thesis)

Dempsey, B., Turner, A. J., Le, S., Sun, Q. J., **Bou Farah, L.**, Allen, A. M., Goodchild, A. K., McMullan, S. (2015). Recording, labeling, and transfection of single neurons in deep brain structures. Physiol Rep **3**(1), doi:10.14814/phy2.12246.

In preparation from the period of candidature (not included in this thesis)

Phillip Wisinski-Bokiniec, **Lama Bou Farah**, Nicolle H Packer, Simon McMullan, Ann K Goodchild. Cardiovascular responses following enzymatic removal of PSA-NCAM from the nucleus of the solitary tract.

Communications

Bou Farah L, Turner A, Dempsey B, Goodchild AK, McMullan S (2012). The oxygen sensitivity of sympathetic premotor neurons does not involve heme oxygenase-2 (HO-2). Poster presentation at the Macquarie University Biofocus Research Conference, Sydney, Australia.

Bou Farah L, Turner A, Dempsey B, Goodchild AK, McMullan S (2013). The oxygen sensitivity of sympathetic premotor neurons does not involve heme oxygenase-2 (HO-2). Poster presentation at the 33rd Annual meeting of the Australian Neuroscience Society, Melbourne, Australia.

Dempsey B, Turner A, **Bou Farah L** and McMullan S (2013). A novel technique that combines single cell electroporation with extracellular recordings *in vitro* and *in vivo*. Poster presentation at the 33rd Annual meeting of the Australian Neuroscience Society, Melbourne, Australia.

Bou Farah L, Turner A, Dempsey B, Goodchild AK and McMullan S (2013). The oxygen sensitivity of sympathetic premotor neurons is mediated by non-neuronal release of ATP, not heme oxygenase-2 (HO-2). Oral presentation at the 8th Congress of the International Society for Autonomic Neuroscience (ISAN) and the 15th Meeting of the European Federation of Autonomic Societies (EFAS), Giessen, Germany.

Dempsey B, Turner A, **Bou Farah L**, Le S and McMullan S (2013). A novel technique that combines single cell electroporation with extracellular recordings *in vitro* and *in vivo*. Poster presentation at the 8th Congress of the International Society for Autonomic Neuroscience (ISAN) and the 15th Meeting of the European Federation of Autonomic Societies (EFAS), Giessen, Germany.

Bou Farah L, Turner A, Dempsey B, Goodchild AK and McMullan S (2013). The oxygen sensitivity of sympathetic premotor neurons is mediated by non-neuronal release of ATP, not heme oxygenase-2 (HO-2). Poster presentation at the 37th International Congress of Physiological Sciences, Birmingham, United Kingdom.

Dempsey B, Turner A, **Bou Farah L**, Le S and McMullan S (2012). A novel technique that combines single cell electroporation with extracellular recordings *in vitro* and *in vivo*. Poster presentation at the 37th International Congress of Physiological Sciences, Birmingham, United Kingdom.

Bou Farah L, Turner A, Dempsey B, Goodchild AK, McMullan S. (2013). Oxygen sensitivity of brainstem sympathoexcitatory neurons is mediated by glial ATP release, not heme oxygenase-2 (HO-2). Oral presentation at the Central Cardiovascular and Respiratory Control: Future Directions, Sydney, Australia.

Dempsey B, Turner A, **Bou Farah L**, Le S and McMullan S (2013). A novel technique that combines single cell electroporation with extracellular recordings *in vitro* and *in vivo*. Poster presentation at the Central Cardiovascular and Respiratory Control: Future Directions, Sydney, Australia.

Bou Farah L and McMullan S. (2013). RVLM sympathetic premotor neurons are not synaptically linked to each other. Poster presentation at the Macquarie University Biofocus Research Conference, Sydney, Australia. ***Awarded the best poster in the conference.***

Bou Farah L and McMullan S. (2014). RVLM sympathetic premotor neurons are not synaptically linked to each other. Poster presentation at the Experimental Biology Conference, San Diego, United States of America.

Bou Farah L, Turner A, Dempsey B, Goodchild AK, McMullan S. (2014). The hypoxia sensitivity of RVLM sympathetic premotor neurons is mediated by glial ATP release. Poster presentation at the Experimental Biology Conference, San Diego, United States of America.

ACKNOWLEDGMENTS

First and foremost, thanks to my supervisor, Dr. Simon McMullan, for his support, guidance, patience, clever ideas, friendship and mentorship. Simon, you have been a constant source of knowledge, I am very lucky, proud and grateful for being your first PhD student. I learned heaps of skills from you Simon, and most importantly is to be critical in everything I do.

Thanks also to my associate supervisors, A/Prof. Ann Goodchild and Prof. Mark Connor for the constant encouragement and intellectual contribution provided during the whole period of my candidature.

To my Co-supervisor, Dr. Anita Turner, thank you so much, for teaching me important skills in science and most importantly how to stay young at heart and being a close friend. I was not able to finish up this thesis without your constant encouragement.

To my friends: Bowen, Sheng, Erin, Phillip, Belinda, Sarah, Willian, and Rhadika you have been a constant source of inspiration and support. Thank you to everyone else in ASAM for the psychological support and encouragement.

To my husband, Bichara, thanks for your unending love and support, this thesis would not have happened without your strong support. You were always asking me to go forward and to move toward perfection. I love you.

To my daughter, Tia, I really hope that one day you will say it is true that I started day care when I was 4 weeks old but I am very proud of my mum who achieved her goal and at the same time she was always there for me. You are the source of my patience and inspiration. To my Son, Elias, I was expecting you when I was writing my thesis; you did a good job in keeping me awake… your kicks are unforgettable… the last two months of my candidature you were also doing a great job by keeping me awake because you needed to feed every hour… you should be proud because you will be called a thesis boy.

To my family, especially dad and mum, I wish you are proud of me… your famous sentence “never give up” helped me heaps especially at the end of my candidature. You were always driving me toward more knowledge… thanks for the no ending encouragement. Dad, I know that this thesis means a lot for you, I am sorry for not being strong enough at some stages and I mistrusted my ability to finish this work.

I dedicate this thesis to my husband (Bichara), daughter (Tia), son (Elias) and especially to my parents (Nabih and Marie). I could not have chosen better partners…

To dad, I will never forget how many times in the last four years you told me this:

"A little knowledge that acts is worth infinitely more than
much knowledge that is idle…"

Gebran Khalil Gebran

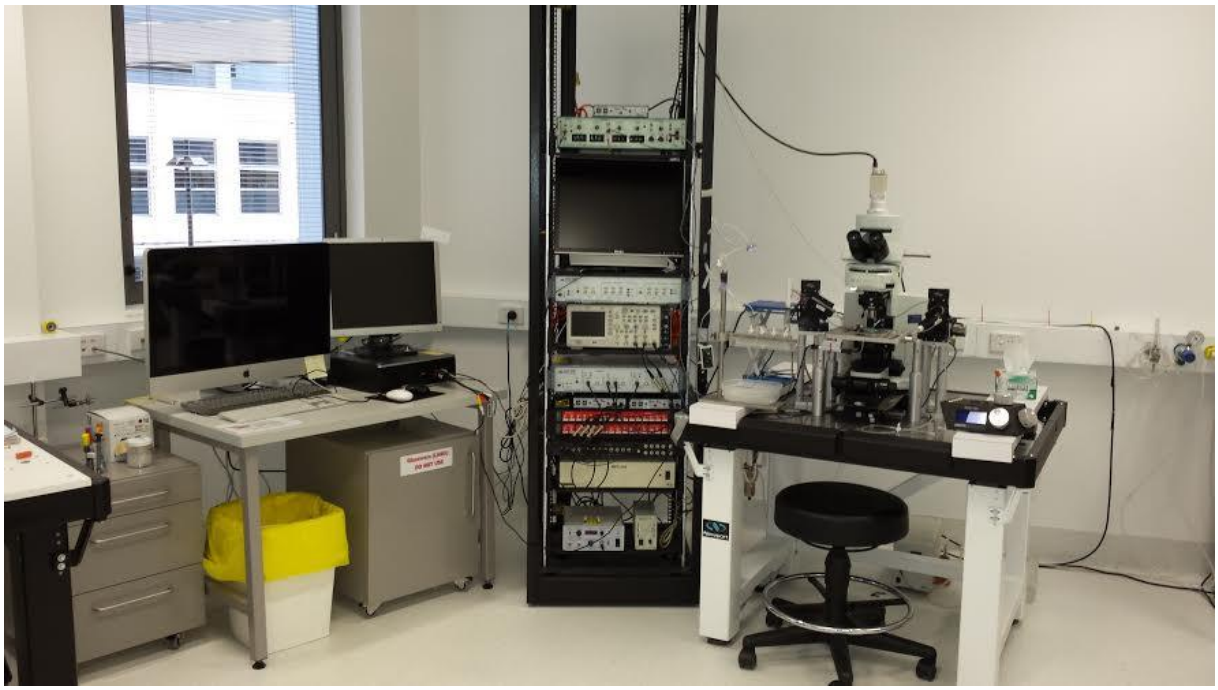

My thesis building block toy

ABBREVIATIONS

aCSF	Artificial cerebrospinal fluid
ANOVA	analysis of variance
ASNA	Adrenal sympathetic nerve activity
BNST	Bed nucleus of the stria terminalis
BSA	Bovine serum albumin
C1	first adrenergic cell group
CeA	central nucleus of the amygdala
CNS	central nervous system
CTB	cholera toxin B
CVLM	caudal ventrolateral medulla
DβH	dopamine beta hydroxylase
DIG	Digoxigenin
DMSO	Dimethyl sulfoxide
DMV	dorsal motor nucleus of the vagus
EDTA	ethylenediamine tetraacetic acid
EPSP	excitatory post synaptic potential
EGFP	Enhanced green fluorescent protein
GABA	γ-Aminobutyric acid
GIRK	Inwardly rectifying potassium channel
HO-1	Heme oxygenase-1
HO-2	Heme oxygenase-2
HO-3	Heme oxygenase-3
IML	intermediolateral cell column
IPAC	interstitial nucleus of the posterior limb of the anterior commissure
Iv	Intravenous
KF	kölliker fuse
LPAG	lateral periaqueductal gray area
LPB	lateral parabrachial nucleus
LSNA	Lumbar sympathetic nerve activity
mRNA	messenger ribonucleic acid

NaCN	Sodium cyanide
NK-1	neurokinin-1
NMDA	N-methyl-D-aspartate
NTS	nucleus of the solitary tract
OxA	Orexin A
Pa5	paratrigeminal nucleus
PACAP	pituitary adenylyl cyclase-activating polypeptide
$PaCO_2$	Partial pressure of carbon dioxide
PAG	periaqueductal grey
PBS	Phosphate buffered solution
PeH	Perifornical hypothalamus
PNMT	phenylethanolamine N-methyltransferase
PPADS	Pyridoxalphosphate-6-azophenyl-2',4' disulfonic acid
PPS	Preprosomatostatin
PVN	paraventricular nucleus of the hypothalamus
RTN	Retrotrapezoid nucleus
RVLM	rostral ventrolateral medulla
RVMM	rostral ventromedial medulla
SLEA	sublenticular extended amygdala
SNA	Sympathetic nerve activity
SPN	sympathetic preganglionic neurons
SST	Somatostatin
TH	tyrosine hydroxylase
TTX	Tetrodotoxin
VGLUT	vesicular glutamate transporter
VLM	ventrolateral medulla
VLPAG	ventrolateral periaqueductal grey area
VRC	Ventral respiratory column
5HT1A	5-hyroxytryptamine
2-DG	2-deoxy-D-glucose
5-TG	5-thio-D-glucose

CHAPTER 1: LITERATURE REVIEW

Cardiovascular disease is the major determinant of life expectancy worldwide; an Australian dies from cardiovascular disease every ten minutes. One of the major risk factors for all cardiovascular diseases is high blood pressure, but the reasons why blood pressure becomes high are unclear. In many cases, it seems that the part of the brain that normally maintains blood pressure within the healthy range ceases to function normally.

Blood pressure is controlled by networks of cardiovascular control neurons in the brainstem and spinal cord (the sympathetic nervous system). Although we understand how the individual neurons that compose these networks work, we don't really understand how the behaviour of an individual neuron is influenced by the rest of the neuronal network, or how a single neuron can modify the overall behaviour of this network. This is important because it is the dysfunction of the whole network, rather than of individual neurons that can lead to serious cardiovascular diseases like hypertension.

In this thesis I attempt to solve some of the mysteries that surround our understanding of the functional properties and organisation of the neurons that compose the sympathetic nervous system.

ARTERIAL BLOOD PRESSURE CONTROL

The autonomic nervous system controls diverse functions and has specific targets such as the kidneys, blood vessels, heart, lungs, liver, sweat glands and gut. It is composed of the parasympathetic nervous system responsible for the 'rest and digest' responses which stimulate digestion for example; and the sympathetic nervous system responsible for the 'fight or flight' responses such as increasing the blood pressure and heart rate following stressful conditions. Both systems regulate pathways of preganglionic and cholinergic neurons residing in the central nervous system (CNS), peripheral ganglionic networks, glands and organs.

The activity of sympathetic nerves determines the flow of blood between different parts of the body and is responsible for maintaining blood pressure. It is responsible for regulating the total peripheral resistance and the increases in cardiac output which have direct effect on the elevation of blood pressure (Cornish et al., 1990, Guyenet, 2006). The end-diastolic volume, heart rate and myocardial contractility determine the cardiac output (Guyenet, 2006). Total peripheral resistance is controlled by the constriction of arterial resistance

vessels which is maintained by ongoing sympathetic nerve activity and adjusted according to continuous physiological demand (Share and Crofton, 1984, Mancia et al., 1997, Esler, 2000, Grisk, 2005).

Sympathetic activity regulating vasomotor targets is tonically active and varies greatly with internal and external stressors (such as fear, heat/cold exposure, exercise etc.) reflecting adaptive responses. Sympathetic nerve activity is controlled by sympathetic premotor neurons residing in the brainstem and midbrain (for review, see Dampney, 1994). These neurons receive inputs that are directly related to the psychological and physiological state of an animal, which are then integrated in the brain to provide the appropriate sympathetic output.

Elevated sympathetic nerve activity has been detected in different disease states such as obesity, sleep apnoea and heart failure which are known to be causative of hypertension (Malpas, 2010). There is strong evidence that increases in sympathetic nerve activity are causative or contributory to hypertension aetiology (Rahn, 1999, Smith et al., 2004); sympathetic hyperactivity is seen in humans and animals that go on to develop hypertension prior to any measurable increase in blood pressure.

Spinally projecting neurons within the rostral ventrolateral medulla (RVLM) in the brainstem appears to play a key role in the generation of sympathetic tone, these neurons are a major driver of sympathetic nerve activity (Guyenet, 2006). The spontaneous activity of these neurons corresponds with the sympathetic nerve activity and blood pressure, all three are sensitive to the same type of stimuli and afferent inputs such as hypoxia and baroreceptor activation (Brown and Guyenet, 1985). The neural mechanisms responsible for the generation of sympathetic nerve activity have emerged as a major research goal (Coote, 2007). In this chapter I will review the main populations of neurons that are involved in cardiovascular regulation, with a particular focus on sympathetic premotor neurons in the RVLM.

SYMPATHETIC PREGANGLIONIC NEURONS (SPN)

The sympathetic control of the heart and blood vessels comes from noradrenergic sympathetic excitatory neurons located in the pre- and para-vertebral ganglia (Janig and Habler, 2003). These neurons receive excitatory cholinergic input from sympathetic

preganglionic neurons (SPN) (Strack et al., 1988). SPN cell bodies with vasomotor targets tend to be distributed in longitudinal cell clusters in the thoracic and lumbar interomediolateral cell column (IML) within the spinal cord (Figure 1.1. adapted from Strack et al. (1988)), topographically distributed in accordance with the ganglia or peripheral target organs they innervate (Strack et al., 1988).

Maintained by excitatory input from neurons in multiple supraspinal premotor nuclei, the ongoing activity of SPNs plays a key role in maintaining sympathetic vasomotor tone and arterial pressure. The main source of this excitatory drive to SPN originates from the release of excitatory transmitters, mainly glutamate, from the terminals of presympathetic neurons (Morrison et al., 1991, Deuchars et al., 1995, Deuchars et al., 1997, Lewis and Coote, 2008). SPN activity and excitability is also influenced by other transmitters such as: GABA, serotonin, catecholamines, substance P and opioids originating from presympathetic neurons and spinal interneurons (Guyenet and Cabot, 1981, Yoshimura et al., 1986, Inokuchi et al., 1993, Matsumoto et al., 1994, Deuchars et al., 1997, Stornetta et al., 2001, Minson et al., 2002). Spinal interneurons known to mainly inhibit SPN do not play a key role in maintaining sympathetic tone. The functional role of inhibition of SPN activity, and the architecture of spinal sympathetic circuitry, is yet to be determined.

SYMPATHETIC PREMOTOR NEURONS

In the rat brain, supraspinal inputs arise from five different regions of the brainstem and hypothalamus (for review, see Dampney, 1994): the RVLM, the rostral ventromedial medulla (RVMM), the caudal medullary raphe nuclei, the A5 noradrenergic cell group in the pons, and the paraventricular nucleus (PVN) in the hypothalamus (Figure 1.2. adapted from Strack et al. (1989a)). These presympathetic groups are considered to be the main source of innervation of the SPN (Meckler and Weaver, 1985). Although physiological evidence indicates that activation of each of these groups increases sympathetic outflow (Morrison, 2001, Guyenet, 2006, Coote, 2007), one cell group in particular, the RVLM has emerged as the major focus for the maintenance of vasomotor sympathetic tone and the elaboration of homeostatic sympathetic reflexes (Brown and Guyenet, 1985, Pilowsky and Goodchild, 2002). The mechanisms that regulate the activity of these neurons is the major topic of the current thesis.

Chemical and electrical activation of the RVLM produces a large increase in the activity of vasomotor sympathetic nerves (Morrison, 1999, Rathner and McAllen, 1999, Cao and Morrison, 2003). Critically, inhibition of neurons within the RVLM, but not nuclei containing other putative sympathetic premotor neurons, is sufficient to produce a pronounced fall in blood pressure and sympathetic nerve activity to spinal levels (50 mmHg), similar to C1 spinal cord transection or ganglionic blockade (Guertzenstein and Silver, 1974) and to disrupt cardiovascular reflex pathways that converge in the RVLM (Dampney and Moon, 1980, Stornetta et al., 1989, Zanzinger et al., 1994, Nagata et al., 1995). These observations have led many investigators to conclude that the RVLM plays a key role in generating sympathetic nerve activity and in integrating homeostatic reflex pathways that control blood pressure. As a result, the RVLM has emerged as the major focus of research into the mechanisms that control blood pressure in normal and pathophysiological conditions.

In the following sections, the location, neurochemistry, connections and functional role of RVLM presympathetic neurons are reviewed.

THE ROSTRAL VENTROLATERAL MEDULLA (RVLM)

The activity of RVLM neurons located immediately caudal to the facial motor nucleus determines ongoing vasomotor and reflex activity in sympathetic efferent pathways (Reis et al., 1984, Dampney, 1994, Pilowsky and Goodchild, 2002, Guyenet, 2006). In cats, bilateral inhibition of neurons near the ventral medullary surface using pentobarbital, glycine or γ-Aminobutyric acid (GABA), caused a large reduction in arterial pressure (Feldberg and Guertzenstein, 1972, 1976). Many other studies in a variety of species (rabbits, rats and cats), have provided evidence that the RVLM plays a crucial role in the maintenance of arterial pressure and sympathetic nerve discharge following stimulation, inhibition or destruction of the RVLM using either electrical, chemical, optogenetic or pharmacogenetic techniques (Dampney and Moon, 1980, Willette et al., 1983b, Ross et al., 1984, McAllen, 1985, Pilowsky et al., 1985, Abbott et al., 2009c, Marina et al., 2011).

Following excitation of the RVLM, large increases in arterial pressure and activity in sympathetic nerves innervating the heart, blood vessels and adrenal medulla have been recorded (Goodchild et al., 1982, Willette et al., 1983a, Ross et al., 1984, McAllen, 1986). This increased activity was not recorded in sympathetic nerves that stimulate non-

vasomotor organs such as smooth muscle of the gut and sweat glands (McAllen, 1986). Anatomical (Amendt et al., 1979, Ross et al., 1981, Dampney et al., 1982, Caverson et al., 1983) and electrophysiological (Deuchars et al., 1995, Oshima et al., 2006, Oshima et al., 2008) evidence suggest that the sympathoexcitation evoked by RVLM stimulation is due to monosynaptic activation of thoracic SPN. Following inhibition of the RVLM, reflex and centrally evoked sympathetic vasomotor responses were abolished (Willette et al., 1983b).

The RVLM region contains a functionally and neurochemically heterogeneous population of neurons; some are involved in cardiovascular regulation such as sympathetic premotor neurons and supra-spinal interneurons; and some are considered non-cardiovascular, such as the extensive respiratory and chemoreceptive circuits that lie in adjacent and overlapping groups (Kanjhan et al., 1995, Sun et al., 1998, Mulkey et al., 2004, Stornetta et al., 2006, Gourine et al., 2010, Smith et al., 2012), as well as many other neurons with unidentified functions.

Putative cardiovascular RVLM neurons are defined as those with spontaneous activity that is modulated by sensory modalities that affect sympathetic nerve activity, particularly an inhibitory response to baroreceptor activation (Lipski et al., 1995a, McAllen and May, 1996). This population includes bulbospinal (i.e. sympathetic premotor neurons) and non-bulbospinal neurons (Caverson et al., 1983, Ross et al., 1984, Barman and Gebber, 1985, Brown and Guyenet, 1985, Tucker et al., 1987, Morrison et al., 1988, Granata and Kitai, 1992, Oshima et al., 2006). The response of cardiovascular bulbospinal neurons following the activation of supra-medullary (Lovick, 1992b, Verberne and Guyenet, 1992, Wang and Lovick, 1993, Verberne, 1996, Verberne et al., 1999a), somatic (Morrison and Reis, 1989, Zanzinger et al., 1994, McMullan et al., 2008) and visceral (Ermirio et al., 1993, Saita and Verberne, 2003) inputs is essentially identical to the response of peripheral vasomotor sympathetic outflow. Thus, cardiovascular sympathetic premotor neurons are thought to be directly involved in the regulation of sympathetic nerve activity, the modulation of SPN, and the maintenance of vasomotor tone.

Although bulbospinal neurons have received the greatest attention by researchers in this field, it is also worth pointing out that there is also a considerable non-bulbospinal barosensitive population, many of which can be antidromically activated by electrical

stimulation of the hypothalamus (Verberne et al., 1999c). These neurons may be differentiated anatomically from the bulbospinal group by their expression of neuropeptide Y (Minson et al., 1994, Stornetta et al., 1999), and may play a role in driving behavioural and cerebral vasomotor responses to acute brainstem hypoxia/ischaemia (Golanov et al., 2000, Golanov et al., 2001, Ilch and Golanov, 2004, Abbott et al., 2013) as well as effects on vasopressin release (Cunningham et al., 1990).

RVLM SYMPATHETIC PREMOTOR NEURONS: NEUROCHEMICAL PHENOTYPE

Figure 1.3, adapted from Pilowsky et al. (2002), shows the diverse neurochemical phenotypes of bulbospinal RVLM neurons which are almost uniformly excitatory, as indicated by the expression of vesicular glutamate transporter 2 (VGLUT2: Stornetta et al., 2002) and contain a diverse complement of amino acid and peptide neurotransmitters (reviewed by Stornetta, 2009). Nearly 70 % of sympathetic premotor neurons can be identified as members of the adrenergic C1 group by their expression of catecholaminergic enzymes: dopamine-β-hydroxylase (DβH), tyrosine hydroxylase (TH), or phenylethanolamine-N-methyltransferase (PNMT) (Hokfelt et al., 1973, Blessing et al., 1981, Ross et al., 1981, Goodchild et al., 1984, Schreihofer and Guyenet, 1997, Phillips et al., 2001, Stornetta et al., 2002). C1 neurons that project to the hypothalamus constitute more than 50 % of this population (Stornetta et al., 1999, Verberne et al., 1999b, Phillips et al., 2001). Most C1 cells are barosensitive (Sved et al., 1994, Sartor and Verberne, 2003); however, lesion of the C1 group or selective ablation of the bulbospinal subset has no significant effect on sympathetic nerve activity and merely reduces the arterial pressure by approximately 10 mmHg (Madden et al., 1999, Schreihofer et al., 2000, Madden and Sved, 2003b), suggesting that C1 neurons alone are not responsible for maintaining vasomotor function. Of the non-C1 group, preproenkephalin is expressed in 80 % of bulbospinal neurons (and 20 % of C1 bulbospinal neurons: Stornetta et al., 2001).

Peptide transmitters colocalized with catecholamine precursor enzymes in the RVLM include pituitary adenylyl cyclase activating polypeptide transporter (PACAP), which has been found in 84 % of C1 neurons in which 82 % were bulbospinal. PACAP has also been found in 10 % of non-C1 bulbospinal neurons (Farnham et al., 2008). Preprotachykinin, a substance P precursor, is expressed in 20 % of C1 bulbospinal neurons (Milner et al., 1988, Li et al., 2005). Neuropeptide-Y is absent in bulbospinal RVLM neurons but is expressed in 95 % of the C1

population projecting to the hypothalamus (Stornetta et al., 1999, Schreihofer et al., 2000). Catestatin (Gaede et al., 2009), cocaine- amphetamine-regulated transcript (Burman et al., 2004) and calbindin (Goodchild et al., 2000) also define a portion of bulbospinal and non-bulbospinal RVLM neurons. These neurons rarely express GABAergic or glycinergic precursors, and are therefore assumed to be uniformly excitatory (Stornetta et al., 2004). In contrast, a significant proportion of RVMM and raphé bulbospinal neurons are found to be GABAergic and glycinergic (Stornetta and Guyenet, 1999, Stornetta et al., 2004).

RVLM SYMPATHETIC PREMOTOR NEURONS: ELECTROPHYSIOLOGICAL PROPERTIES

Many bulbospinal neurons recorded *in vivo* are spontaneously active, with a firing rate of 1 - 40 spikes/s and a spinal conduction velocity of 1 – 30 m/s (Brown and Guyenet, 1984, 1985, Verberne et al., 1999c, McMullan et al., 2008, McMullan and Pilowsky, 2012). The spinal conduction velocities of barosensitive neurons are bimodal, composed of slowly conducting axons (unmyelinated: < 1m/s) and rapidly conducting axons (lightly myelinated, >1 m/s) (Morrison et al., 1988, Allen and Guyenet, 1993, Schreihofer and Guyenet, 1997). Baseline discharge rate and neurochemical phenotype correlated to a great extent with the axonal conduction velocity (Allen and Guyenet, 1993, Schreihofer and Guyenet, 1997, Sartor and Verberne, 2003). Neurons with rapidly conducting axons (3.1 ± 0.4 m/s) exhibit high spontaneous activity (19 ± 3 Hz, n = 23) and are equally likely to be C1 or non-C1 neurons, whereas neurons with slowly conducting axons group (0.6 ± 0.1 m/s) are less active (4 ± 1 Hz, n = 16) and uniformly catecholaminergic (Schreihofer and Guyenet, 1997). Both groups are equally barosensitive (Brown and Guyenet, 1985). However, relative contributions of myelinated versus unmyelinated bulbospinal barosensitive neurons in the control of sympathetic vasomotor tone are still unclear: given the rapidly-conducting group, which contains the non-C1 cells, is responsible for generating a greater volume of bulbospinal drive and is presumably responsible for maintaining sympathetic tone after depletion of C1 neurons (Madden et al., 1999, Schreihofer and Guyenet, 2000, Schreihofer et al., 2000, Guyenet et al., 2001), some authors have suggested that this population is predominantly responsible for the maintenance of sympathetic tone (Schreihofer and Guyenet, 2000, Madden and Sved, 2003a, Burke et al., 2011).

Bulbospinal RVLM neurons recorded in neonatal slices also exhibit spontaneous activity (Sun et al., 1988a, Sun et al., 1988b, Kangrga and Loewy, 1995, Li et al., 1995). As neither blood

pressure (Ito and Sved, 1997), sympathetic nerve activity (Sun and Guyenet, 1986), nor the firing of spinally projecting RVLM neurons *in vivo* (Sun et al., 1988a) or *in vitro* (Sun et al., 1988a, Li et al., 1995) is affected by blockade of RVLM glutamate receptors, some authors have interpreted the continued activity of these neurons as evidence of intrinsic autodepolarization. However, spontaneous activity is not apparent in acutely dissociated RVLM bulbospinal neurons (Lipski et al., 1998). Furthermore, the same group found that intracellularly recorded action potentials are always preceded by excitatory post-synaptic potentials *in vivo* (Lipski et al., 1996a), suggesting that (non-glutamatergic) transmission may be necessary for the generation of action potentials. As a result, it is now widely accepted that pacemaker currents play a minor role in the generation of spontaneous activity in these neurons *in vivo* (Coote, 2007), and that instead as yet unidentified extracellular signals drive activity in this population (Barman and Gebber, 1989, Guyenet, 2006, Coote, 2007).

This network interaction has been proposed by many researchers as a rhythmic driver of sympathetic nerves (Cohen and Gootman, 1970, Barman and Gebber, 1980, Zhong et al., 1992, McAllen et al., 2001) however, the source(s) of such drive remain unknown.

RVLM SYMPATHETIC PREMOTOR NEURONS: EFFERENT PROJECTIONS

The axonal arborizations of bulbospinal barosensitive neurons extend dorsomedially for nearly 1.5 – 2 mm before following their pathway to the spinal cord (Schreihofer and Guyenet, 1997). These arborizations project to different brainstem regions including the CVLM, RVLM, A5, and RVMM (Haselton and Guyenet, 1990, Lipski et al., 1995b). Non-bulbospinal barosensitive neurons follow the same trajectory before ultimately projecting in a rostral direction (Lipski et al., 1995b, Schreihofer and Guyenet, 1997).

Similar axonal projections of bulbospinal and non-bulbospinal C1 neurons have recently been reported by investigators using viral vectors that selectively drive reporter expression in catecholaminergic neurons (Card et al., 2006, Sevigny et al., 2008, Abbott et al., 2009b). Using this approach, Card et al. (2006) were also able to identify local synapses and varicosities formed by C1 neurons and demonstrate that they form close appositions with both C1 and non C1-neurons in the RVLM (Agassandian et al., 2012), suggesting that C1 RVLM neurons form a local synaptic network in addition to their supraspinal and reticulospinal projections. The participation of putative sympathetic premotor neurons in

local circuits is a recent discovery and an emergent topic of interest in this field; experiments investigating the prevalence of synaptic connections between pairs of bulbospinal RVLM neurons are described in Chapter 5.

RVLM SYMPATHETIC PREMOTOR NEURONS: NEUROPHARMACOLOGY

The RVLM is targeted by afferent projections from spinal, medullary, pontine and midbrain centres including the ipsi- and contralateral medulla, the inferior olive, RVMM, midline medulla, nucleus of the solitary tract (NTS), area postrema, dorsal motor nucleus of the vagus, caudal ventrolateral medulla (CVLM), nucleus ambiguus, periaqueductal grey (PAG), cuneiform nucleus, lateral parabrachial nucleus / kölliker-fuse, laterodorsal and pedunculopontine tegmental nuclei, and A5 (Dampney et al., 1987, Carrive et al., 1988, Yasui et al., 1990, Verberne, 1995, Koshiya and Guyenet, 1996, Horiuchi et al., 1999a, Padley et al., 2007, McMullan and Pilowsky, 2012, Bowman et al., 2013, Turner et al., 2013, Korim et al., 2014). In addition, the RVLM receives inputs from parts of the hypothalamus (lateral, perifornical, dorsomedial and paraventricular subnuclei), basal forebrain (central nucleus of the amygdala) and the cortex (insular and medial prefrontal cortex) (Shafton et al., 1998, Saha et al., 2005, Gabbott et al., 2007). Several neurotransmitter substances have been identified as having a direct effect on sympathetic nerve discharge and their pre- or post-synaptic receptors were found to be expressed in the RVLM. These include amino acids (GABA, glutamate and glycine), neuropeptides (angiotensin II, PACAP, orexin, opiates, substance P, galanin, somatostatin (SST) and cannabinoids), amines (acetylcholine, dopamine, serotonin, histamine, noradrenaline and adrenaline) and purines (ATP and adenosine) (Zanzinger et al., 1995, Stasinopoulos et al., 2000, Padley et al., 2003, Pimentel et al., 2003, Makeham et al., 2005, Padley et al., 2007, Abbott and Pilowsky, 2009). Unfortunately, a detailed connectomic map of sources of input to RVLM sympathetic premotor neurons and the neurotransmitters which evoke responses in the RVLM remain to be described. The following paragraphs represent a brief review of some of the metabotropic and ionotropic inputs which either supress or stimulate the RVLM and the sympathetic outflow, these neuromodulators will be linked to some functional and reflex roles played by the RVLM in later sections of this literature review.

<u>Amino Acids</u>

RVLM GABAergic drive plays an important role in the regulation of vasomotor activity: microinjection of the $GABA_A$ receptor antagonist bicuculline into the RVLM pressor region strongly increased sympathetic nerve activity and blood pressure (Willette et al., 1983b, Koshiya et al., 1993, Ito and Sved, 1997), and blocked inhibitory reflexes such as the baroreflex, abdominal vasodepressor and Bezold-jarisch reflexes (Willette et al., 1983a, Willette et al., 1983b, Koshiya et al., 1993). Smaller activation of these factors was recorded following blockade of $GABA_B$ or glycine (Ross et al., 1984, Guyenet et al., 1990, Li and Guyenet, 1995), suggesting that tonic activation of these receptors is less significant in the control of baselines sympathetic nerve activity. The likely sources of GABAergic transmission to the RVLM are widespread and include the nucleus of the solitary tract, area postrema, CVLM, midline raphe, ventrolateral periaqueductal gray, lateral hypothalamic area, central nucleus of the amygdala, sublenticular extended amygdala, interstitial nucleus of the posterior limb of the anterior commissure, bed nucleus of the stria terminals, and medial preoptic area (Cravo and Morrison, 1993, Bowman et al., 2013), but the physiological circumstances under which GABA is released from these structures is largely unknown.

Blockade of excitatory amino acidic inputs in the RVLM blocked the somatosympathetic reflex, the peripheral chemoreflex, and stimulation from higher brain regions such as the hypothalamus, PAG, and the cerebellum (Li and Lovick, 1985, McAllen, 1985, Koshiya et al., 1993, Kiely and Gordon, 1994, Miyawaki et al., 1996, Coote et al., 1998).

The major excitatory neurotransmitter examined within the RVLM is glutamate. It has been shown that glutamate RVLM microinjection caused a decrease in phrenic nerve frequency and an increase in heart rate, sympathetic nerve activity, arterial pressure and musculoskeletal vascular resistance (McAllen and Dampney, 1990, Miura et al., 1991, Tsuchihashi and Averill, 1993, Tsuchihashi et al., 1994). Some of the sources of glutamate in the RVLM include the contralateral RVLM, PVN, nucleus of the solitary tract (NTS), lateral parabrachial nucleus, kölliker-fuse, and central nucleus of the amygdala (Takayama and Miura, 1992). Excluding the NTS (Koshiya and Guyenet, 1996, Moraes et al., 2011), the glutamate-mediated effects played by these brain regions on the control of blood pressure is known. Following chemoactivation, AMPA/ kainate (Miyawaki et al., 1996) and NMDA (Kubo et al., 1993) receptors were found to be involved in the recorded sympathoexcitatory response. Furthermore, following sciatic nerve stimulation, non-NMDA receptors were

found to be involved in the recorded somatosympathetic response (Kiely and Gordon, 1993, Kiely and Gordon, 1994).

Neuropeptides and amines

While blockade of delta opioid receptors in the RVLM of anaesthetised rabbits causes an increase in arterial pressure and sympathetic nerve activity (Morilak et al., 1990) and blockade of muscarinic receptors causes large sympathoinhibition and hypotension in anaesthetised rats (Padley et al., 2007); for a large number of metabotropic neuromodulators such as: angiotensin I, NK1, cannabinoid 1, 5HT1A, P2X, PAC1 and SST_{2A} receptors, arterial pressure and sympathetic nerve activity in rats was not affected *in vivo* (Hirooka et al., 1997, Horiuchi et al., 1999b, Miyawaki et al., 2001, Padley et al., 2003, Makeham et al., 2005, Burke et al., 2008, Farnham et al., 2008). Blockade of baseline transmission of metabotropic neuromodulators such as angiotensin II (Head and Mayorov, 2001), NK1 (Makeham et al., 2005), cannabinoid 1 (Padley et al., 2003), 5HT1A , P2X (Horiuchi et al., 1999b), PAC1 (Farnham et al., 2008) and SST_{2A} receptors (Burke et al., 2008) is not associated with any change in arterial pressure or sympathetic nerve activity *in vivo*.

Although some of these transmitters have been associated with defined functional role such as orexinergic and cholinergic transmissions, which contribute to the regulation of the heart rate and arterial pressure following exercise and arousal (Padley et al., 2007, Furlong et al., 2009), the main physiological drivers of metabotropic neuromodulator release such as PACAP, SST and enkephalin are still unknown. In this thesis we test the direct effect of SST on sympathetic premotor RVLM neurons (see Chapter 4).

In summary, it seems that metabotropic neuromodulators potentially play an important role in the modulation of sympathoexcitatory neurons, but the functional roles of most neuromodulators is yet to be defined.

Purines

Exogenous ATP or ATP receptor agonist application has an excitatory effect on sympathetic premotor RVLM neurons (Sun et al., 1992b, Ralevic et al., 1999). In addition, increased arterial blood pressure, heart rate and renal sympathetic nerve activity were recorded following activation of ATP RVLM receptors (Sun et al., 1992b, Horiuchi et al., 1999b, Ralevic et al., 1999, Thomas et al., 2001).

The mechanisms responsible for oxygen sensing of RVLM neurons are unknown, but there is evidence suggesting an important role for ATP in mediating such sensitivity. First, ATP is released within the RVLM region following brainstem hypoxia (Gourine et al., 2005). Second, RVLM sympathetic premotor neurons are depolarized not only by exogenous ATP (Sun et al., 1992b, Horiuchi et al., 1999b, Ralevic et al., 1999, Zoccal et al., 2011) but also by glial ATP (Marina et al., 2013). Furthermore, glia are activated by hypoxia and in response to such signal they release ATP (for review, see Fields and Stevens-Graham, 2002, Aley et al., 2006, McDougal et al., 2013). In this thesis we tested whether glial ATP release plays a role in mediating hypoxic responses of RVLM bulbospinal neurons (see Chapter 2).

RVLM SYMPATHETIC PREMOTOR NEURONS: INVOLVEMENT IN AUTONOMIC REFLEX PATHWAYS

BARORECEPTOR REFLEX

The baroreceptor reflex, also referred to at the brainstem level as sympathetic baroreflex, is a negative feedback loop that buffers the response of the cardiovascular system to changes in the physiological state of the animal (i.e. exercise, stress, arousal) and postural and orthostatic changes to maintain arterial pressure within a narrow physiological range. Increased arterial pressure activates baroreceptors located in the walls of the aortic arch and carotid sinus. Signals are then transmitted via myelinated and unmyelinated fibres of the glossopharyngeal (IX) and vagal (X) nerves (Eyzaguirre and Uchizono, 1961, McDonald, 1983) or the aortic depressor nerve in rat, rabbit and mouse (Krieger and Marseillan, 1963, Devanandan, 1964, Fan and Andresen, 1998). Researchers have identified mainly glutamatergic baroreceptor afferent projections in the NTS using anterograde tracing techniques in the rat, cat and rabbit (Leone and Gordon, 1989, Seagard et al., 2000). The NTS is a large region in the dorsomedial medulla which has different first order cardiorespiratory reflex synapses including the peripheral chemoreflex and cardiovagal reflex in addition to the baroreflex (Finley and Katz, 1992, Kubin et al., 2006). Direct projections from the NTS to the CVLM have been found using retrograde and anterograde tracers (Ross et al., 1985), and electrophysiological experiments describe an excitatory baro-activated drive to the CVLM which in turn, was found to contain GABAergic neurons (Guyenet et al., 1987, Agarwal et al., 1990, Schreihofer and Guyenet, 2003), which are subsequently thought to inhibit

barosensitive presympathetic RVLM neurons (Cravo et al., 1991, Jeske et al., 1993, Jeske et al., 1995, Yu and Gordon, 1996, Schreihofer and Guyenet, 2003) (Figure 1.4).

The barosensitivity of RVLM sympathetic premotor neurons is one of their defining characteristics, and is the major functional criteria used to identify them *in vivo.* Bulbospinal RVLM neurons are inhibited by naturalistic changes in arterial pressure (Brown and Guyenet, 1985) or electrical stimulation of baroreceptor afferents (Lipski et al., 1995a). Furthermore, the sympathetic baroreflex, heart rate and plasma noradrenaline response to hydralazine were significantly attenuated following the depletion of bulbospinal C1 neurons by the application of anti-dopamine β-hydroxylase-saporin injected at the thoracic level of the spinal cord or in the RVLM. This highlights the important role played by C1 bulbospinal RVLM neurons in the control of the sympathetic baroreflex (Schreihofer and Guyenet, 2000, Madden et al., 2006).

One feature of the baroreflex is that it can be conditionally augmented depending on the physiological state of the animal. This is achieved by modulation of synaptic transmission at multiple points in the baroreflex arch, including the RVLM (reviewed by Pilowsky and Goodchild, 2002, Dampney et al., 2003a). During exercise for example, cholinergic projections are activated via a feed-forward mechanism from the pedunculopontine tegmental to the RVLM in order to increase baroreflex sensitivity and calibrate the arterial pressure (Padley et al., 2007). In addition, neurons in the locus coeruleus, A5 and hypothalamic regions do not directly subserve the baroreflex but may exhibit cardiac related rhythms or respond to baroreceptor activation (Guyenet, 1984, Guyenet and Byrum, 1985, Murase et al., 1994, Dampney et al., 2003b). More likely, these networks coordinate baroreceptive feedback with other blood pressure controllers in order to cope with behavioural responses to physiological changes.

CHEMORECEPTOR REFLEX

Peripheral chemoreceptor reflex

Hypoxia is detected as a change in partial pressure of oxygen (PaO_2) by peripheral chemoreceptors located within the carotid and aortic bodies (Marshall, 1994).

Chemoreceptor activation triggers a sympathoexcitatory reflex pathway that, via an excitatory relay in the NTS, increases the activity of RVLM sympathetic premotor neurons

and sympathetic nerve discharge, in order to maintain cerebral perfusion and counteract the vasodilatory effect of hypoxia by redistributing oxygenated blood to the brain and the heart (Marshall, 1994, Guyenet, 2000). The pathway involved in the sympathetic chemoreflex is illustrated in Figure 1.5. Activation of peripheral chemoreceptors by low O_2 and/or high CO_2/changes in pH causes the release of excitatory transmitters including ATP, acetylcholine and dopamine in order to activate chemosensory fibres of the carotid sinus nerve (Spyer et al., 2004, Nurse, 2005), which in turn activate second order neurons in the medial and commissural NTS (Mifflin, 1992). Chemosensitive NTS neurons then monosynaptically activate the RVLM region (Aicher et al., 1996, Koshiya and Guyenet, 1996), which may also be stimulated by synaptic relays from the RTN, ventral respiratory column VRC, CVLM, A5 and lateral parabrachial nucleus / Kölliker-Fuse (Takakura et al., 2006, Mandel and Schreihofer, 2009).

This reflex pathway is responsible for producing sympathoexcitation of sympathetic nerve discharge, but the level of excitation can also be influenced by several mechanisms such as synaptic inputs from pontine structure (Koshiya and Guyenet, 1994) and intrinsic hypoxia sensitivity of sympathetic premotor RVLM neurons (Sun and Reis, 1994c). Following central and peripheral chemoreceptor activation, galanin suppressed cardiovascular and ventilatory responses in the RVLM and Bötzinger complex respectively (Abbott et al., 2009a, Abbott and Pilowsky, 2009). However, opioids, serotonin and neuropeptide-Y inputs do not seem to affect RVLM modulation of the peripheral chemoreflex (Miyawaki et al., 2001, 2002, Kashihara et al., 2008). GABAergic inhibitory input to the RVLM from the CVLM during peripheral chemoreflex is well known. GABAergic CVLM neurons and presympathetic RVLM neurons are robustly activated by peripheral chemoreceptor stimulation. Increased central respiratory drive increases the activity of RVLM and CVLM neurons (Haselton and Guyenet, 1989, Kanjhan et al., 1995, Mandel and Schreihofer, 2006). Furthermore, during hypoxia, phasic inhibition of the respiratory-related splanchnic sympathetic nerve activity was abolished following the application of kynurenate (glutamate receptor antagonist) in the CVLM. However the splanchnic nerve amplitude was increased suggesting that the CVLM, in addition to its tonic sympathoinhibitory role, also has a respiratory modulation role to play (Mandel and Schreihofer, 2009). In addition, peptides, such as SST microinjected into the

RVLM attenuated the splanchnic sympathetic nerve activity response and abolished the pressor response to isocapnic anoxia (Burke et al., 2008).

Hypercapnia

Hypercapneic stimuli facilitate and redistribute blood flow, facilitate CO_2 clearance, and counteract the direct vasodilatory effects of CO_2.

Although peripheral chemoreceptors are activated following increases in CO_2 levels (Lahiri et al., 1979) and may play some role in driving sympathetic responses to hypercapnia, the activation of RVLM presympathetic neurons and sympathetic nerve discharge seems predominantly mediated by mechanisms that are insensitive to baro- and chemo- receptors denervation (Hanna et al., 1981, Haselton and Guyenet, 1989, Oikawa et al., 2005, Moreira et al., 2006). Central chemoreceptors responsible for driving autonomic and behavioural responses to elevated CO_2 are distributed throughout the brain, including the retrotrapezoid nucleus (RTN)(Mulkey et al., 2004, Guyenet et al., 2008), raphe obscurus (Depuy et al., 2011) pons and ventral respiratory column (Nattie and Li, 2009).

Central hypoxic chemoreceptor reflex

Perfusion of the subarachnoid space with artificial cerebrospinal fluid (aCSF) mixed with either NaCN or increasing CO_2 and H^+ led to immediate cardiovascular and respiratory changes suggesting that central chemoreceptors may be located in the ventrolateral surface of the medulla (Severinghaus et al., 1963). Further studies have shown that other brain regions such as: the preBötzinger complex, the locus coeruleus, the NTS and the caudal raphé may be involved in detecting and responding to changes in $PaCO_2$ and pH which suggests that central chemoreception may not be restricted to the ventral medulla (Pineda and Aghajanian, 1997, Solomon et al., 2000, Nattie and Li, 2002, da Silva et al., 2011). It does appear however that the RTN, residing in the ventral surface of the medulla, is one of the most critical sites for central CO2 sensing (Guyenet et al., 2005, Gourine et al., 2010, Marina et al., 2010)

In the absence of chemoafferent inputs, RVLM neurons can generate patterned responses to focal hypoxia consisting of cerebral vasodilation, an increase in cortical blood flow and sympathetic nerve activation that is mimicked by microinjection of cyanide into the RVLM (Sun et al., 1992a, Golanov and Reis, 1996, Reis et al., 1997). Iontophoresis of cyanide

directly excites presympathetic barosensitive RVLM neurons (but inhibits respiratory neurons) and does not affect non-bulbospinal barosensitive RVLM neurons (Sun and Reis, 1993, 1994a). Studies *in vitro* indicate that depolarization in response to hypoxia/cyanide persist in presympathetic RVLM neurons in the presence of the sodium channel blocker tetrodotoxin (TTX), suggesting that hypoxic responses are not secondary to activation of pre-synaptic neurons (Sun and Reis, 1994b). However, the cellular mechanisms that underlie O_2-sensing in RVLM neurons remain unclear. In Chapter 2 of this thesis I examine the contribution to RVLM hypoxia-sensing made by two mechanisms, the putative oxygen sensor Heme Oxygenase 2 (HO-2) (D'Agostino et al., 2009) and the role played by RVLM glia.

SOMATOSYMPATHETIC REFLEX

Stimulation of cutaneous or muscle Aδ (myelinated) and C (unmyelinated) afferent fibres evokes stereotypical sympathoexcitatory responses that result from activation of propriospinal and spino-RVLM-spinal pathways (Sato and Schmidt, 1971, Morrison and Reis, 1989, Stornetta et al., 1989, McMullan et al., 2008). Nociceptive afferents synapse in lamina I of the dorsal horn (Light and Perl, 1979) then these neurons project, via polysynaptic pathways, to SPNs in the thoracic and lumbar parts of the spinal cord bilaterally (Craig, 1993) then crosses the spinal cord before ascending to the ventrolateral medulla (Ammons, 1988) and other supraspinal nuclei (Craig, 1995, Craig and Dostrovsky, 2001).

Activation of somatic fibres results in distinctive phasic activation of sympathetic nerve fibres, composed of three distinct phases of activation (Burke et al., 2011). First, a short latency component (~20 ms) that is mediated by spinal pathways and normally suppressed in the intact preparation. Second, the 'first peak' of supraspinal sympathoexcitation, which occurs at ~100 ms, followed by a later 'second peak' that occurs ~100 ms later. This general pattern (without the spinal loop) is apparent in the activity of individual RVLM sympathetic premotor neurons (Morrison and Reis, 1989, McMullan et al., 2008), with recruitment of the first and second peaks occurring at different stimulus intensities, suggesting that the peaks correspond to recruitment of afferent fibres with different conduction velocities. Alternatively, some authors have argued that the different peaks apparent in peripheral sympathetic nerve recordings instead reflect simultaneous activation of bulbospinal RVLM neurons with rapid and slow conduction velocities, corresponding to non-C1 and C1 neurons respectively (Burke et al., 2011).

The somatosympathetic reflex is affected by different neurotransmitters such as: serotonin (Miyawaki et al., 2001), orexin (Shahid et al., 2012), substance P (Makeham et al., 2005), catestatin (Gaede and Pilowsky, 2010), enkephalin (Miyawaki et al., 2002) and SST (Burke et al., 2008), and the role played by these transmitters is well defined.

VISCEROSYMPATHETIC REFLEX

Deep pain triggers the viscerosympathetic reflex causing a reduction in sympathetic nerve activity, blood pressure and cardiac output (Keay and Bandler, 2002, Lumb, 2004). The role of the RVLM in mediating the viscerosympathetic reflex is unclear. In anaesthetized and vagotomized rabbits, Koganezawa et al. (2010) showed that most of RVLM barosensitive bulbospinal neurons responded to the stimulation of the greater splanchnic nerve showing in their responses inhibitory and excitatory components similar to the ones recorded in the reflex responses of the renal sympathetic activity following electrical stimulation of the greater splanchnic nerve. They also showed that GABAergic and glutamatergic transmission in the RVLM are related to the viscerosympathetic reflex; first, following bilateral microinjection of muscimol (a $GABA_A$ receptor agonist) into the RVLM the reflex responses were blocked. On the other hand, following bilateral microinjection of bicuculline (a $GABA_A$ receptor antagonist) the inhibitory component was significantly attenuated. Second, following kynurenic acid (a glutamate receptor antagonist) application the excitatory component was abolished.

The main sources of glutamatergic input to the RVLM that plays a role in the viscerosympathetic reflex remain unknown, however the NTS which sends excitatory inputs to the RVLM (Urbanski and Sapru, 1988, Aicher et al., 1996), is activated during visceral pain (Hammond et al., 1992). In addition, neuronal nitric oxide synthase mediate the pressor and sympathoexcitatory response to epicardial bradykinin (Guo et al., 2009) and may act as a facilitator of glutamatergic transmission (Wu et al., 2001). On the other hand, the main GABAergic input is mainly the CVLM (Masuda et al., 1992), since CVLM inhibition following activation of opioids activation or by glutamate antagonism application decreases the depressor response (Peng et al., 2002).

DIVING REFLEX

The stimuli that trigger the diving response are nasopharyngeal stimulation or immersion of the face in water (Gandevia et al., 1978), which evokes apnoea, bradycardia and sympathetic pressor responses (Campbell et al., 1969, de Burgh Daly et al., 1977, Drummond and Jones, 1979). Brain transection at the level of the midbrain (Gabbott and Jones, 1991), colliculus (Panneton et al., 2010) and pontomedullary border (Panneton et al., 2012) did not alter the diving response, suggesting that supramedullary centres are not involved in mediating autonomic components of the reflex. In contrast, an important role for the RVLM in driving such reflex was confirmed physiologically and anatomically. In conscious rabbit c-Fos expression in RVLM neurons is evoked by nasopharyngeal stimulation, of which 68% belong to the C1 group (Gieroba et al., 1994); similarly, in rats, underwater immersion activated 50% of C1 neurons (McCulloch and Panneton, 2003). Anterograde tracing from the anterior ethmoidal nerve, shown to be activated following nasal mucosa stimulation (Dutschmann and Herbert, 1997, McCulloch et al., 1999a), reveals dense labelling in the RVLM (Panneton et al., 2000). Furthermore, it has been shown by McCulloch et al. (1999b) that the activated RVLM neurons following nasal stimulation receive direct input from the medullary dorsal horn and that these excitatory inputs directly oppose barosensitive inhibitory inputs from the CVLM. Taken together, the RVLM is important for driving the diving reflex but neurotransmitters responsible for such role is unrevealed.

GLUCOPRIVATION RESPONSE

In order to maintain glucose homeostasis, physiological and behavioural responses are activated in response to glucoprivation. These include a decrease in insulin secretion, increases in glucagon, adrenaline, cortisol/corticosterone, growth hormone secretion, sweating, anxiety, hunger and tremor which trigger the ingestion of food (Yamaguchi, 1992, DeRosa and Cryer, 2004, Ritter et al., 2011, Beall et al., 2012). Extreme and prolonged glucoprivation causes the loss of cognitive function and in severe cases can cause death (Cryer, 2007).

Acute glucoprivation/hypoglycemia can be produced by 2-deoxy-D-glucose (2-DG), which stimulates glucose mobilization by interfering with glycolysis at the cellular level (Smith and Epstein, 1969, Kang and Hwang, 2006, Kurtoglu et al., 2007, Ritter et al., 2011). 2-DG is used experimentally to study glucoregulatory mechanisms in neurons (Borg et al., 1995, Sanders and Ritter, 2001, a, Andrew et al., 2007, Gonzalez et al., 2008).

Chemical excitation of RVLM neurons causes adrenaline release (McAllen, 1986) while disinhibition of the RVLM with bicuculline increases blood glucose which depends on the adrenal glands (Verberne and Sartor, 2010). Furthermore, a subpopulation of spinally projecting non-barosensitive C1 neurons are activated by 2-DG (Verberne et al., 1999a, Verberne and Sartor, 2010) suggesting that sympathetic premotor barosensitive neurons which respond to glucoprivation may be neurochemically distinct.

Sympathetic premotor RVLM neurons (Ritter et al., 1998, Verberne and Sartor, 2010) and orexinergic perifornical hypothalamus (PeH) neurons (Sakurai et al., 1998, Briski and Sylvester, 2001) are excited following systemic glucoprivation using 2-DG. Injection of neurotropic viruses into the adrenal gland label neurons in both the RVLM (Strack et al., 1989b) and PeH (Jansen et al., 1995). However, the factors responsible for excitation of RVLM adrenal premotor neurons in response to glucoprivation remain unknown and are considered in Chapter 3 of the current thesis.

AIMS AND OBJECTIVES

In the current thesis I examine intrinsic and extrinsic mechanisms that contribute to the excitability of sympathetic premotor neurons residing within the RVLM *in vitro*.

Since the molecular mechanisms that underlie the hypoxia-sensitivity of RVLM sympathetic premotor neurons remain elusive, In Chapter 2 I compare two rival mechanisms for which some evidence of involvement in RVLM oxygen-sensing exist. I first considered the role of the enzyme HO-2, an enzyme involved in the catabolism of heme, in driving excitatory neuronal responses to acute hypoxia. I then considered the hypothesis that responses to acute hypoxia may be secondary to local glial activation and subsequent release of excitatory transmitters, including ATP.

Systemic glucoprivation using 2-DG excites RVLM sympathetic premotor neurons. However, whether sympathetic premotor neurons are intrinsically glucose sensitive or whether their sensitivity to glucoprivation is secondary to activation of presynaptic inputs remains contentious. In Chapter 3 I directly examine the sensitivity of RVLM sympathetic premotor neurons to extracellular glucose concentration and examine their role in driving adrenaline release in response to acute glucoprivation, and find that orexinergic inputs from the hypothalamus play a key role in this pathway.

Activation of SST_{2A} receptors in the RVLM *in vivo* evokes powerful sympathoinhibition and reduces blood pressure to spinal levels. However, the distribution of SST_{2A} is restricted to a minority of bulbospinal neurons, suggesting that SST_{2A} expressing neurons are critically important for the maintenance of sympathetic vasomotor tone. A key caveat of this interpretation of the data is the assumption that SST_{2A} immunoreactivity closely correlates with SST sensitivity. In Chapter 4 we directly examine the sensitivity of RVLM sympathetic premotor neurons to SST, correlate SST sensitivity to SST receptor immunoreactivity, and map potential sources of SSTergic drive to the RVLM.

In vivo, the activities of sympathetic nerves and spinally projecting neurons in the RVLM display rhythmic bursting that is independent of baroreceptor input. Some investigators have proposed that such synchronisation represents reciprocal interaction between components of central brainstem circuits that co-ordinate spinal sympathetic outflow. Although many previous studies have focused on RVLM inputs from distant brain nuclei, the organisation of local RVLM microcircuits responsible for co-ordinating spinally projecting

outflows remains poorly characterised. Recent anatomical evidence indicates that many C1 neurons in the region receive inputs from other local C1 neurons, suggesting that RVLM sympathetic premotor neurons may provide drive to other sympathetic premotor neurons, providing a mechanism through which neuronal activity may feed back into cardiovascular control circuits. In Chapter 5 I investigate this hypothesis by examining functional coupling between pairs of RVLM spinally projecting neurons.

CHAPTER 1 FIGURES AND TABLES

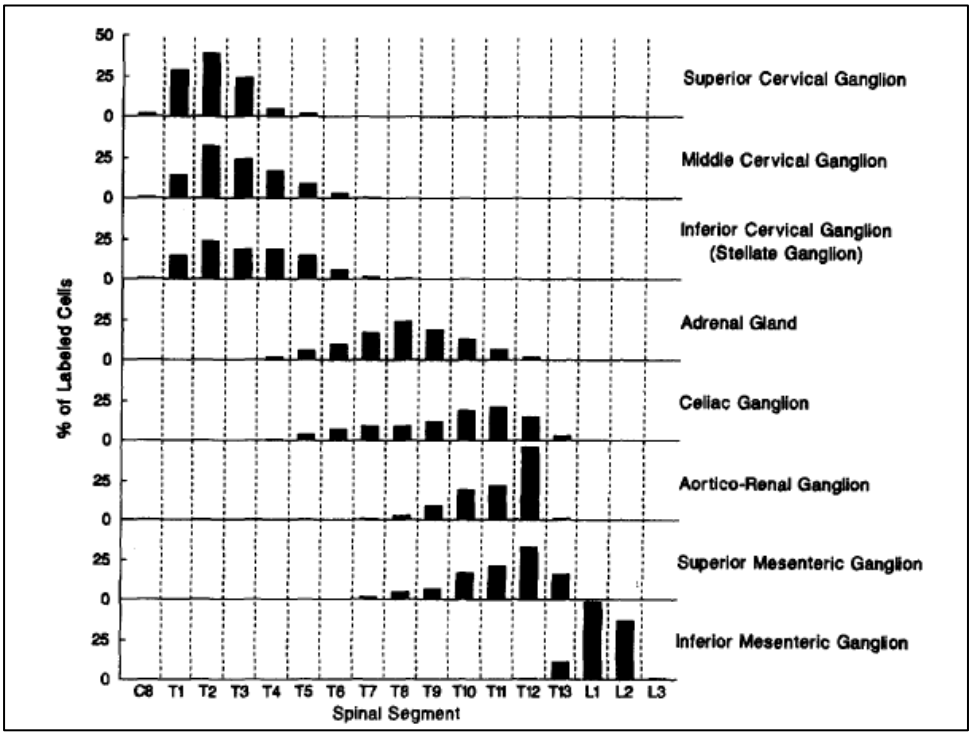

Figure 1.1: SPN distribution in the rat spinal cord. The histograms show the proportional distribution of SPNs following Fluorogold injections into different areas of the sympathetic ganglia and adrenal glands (on the right). Adapted from Strack et al. (1988).

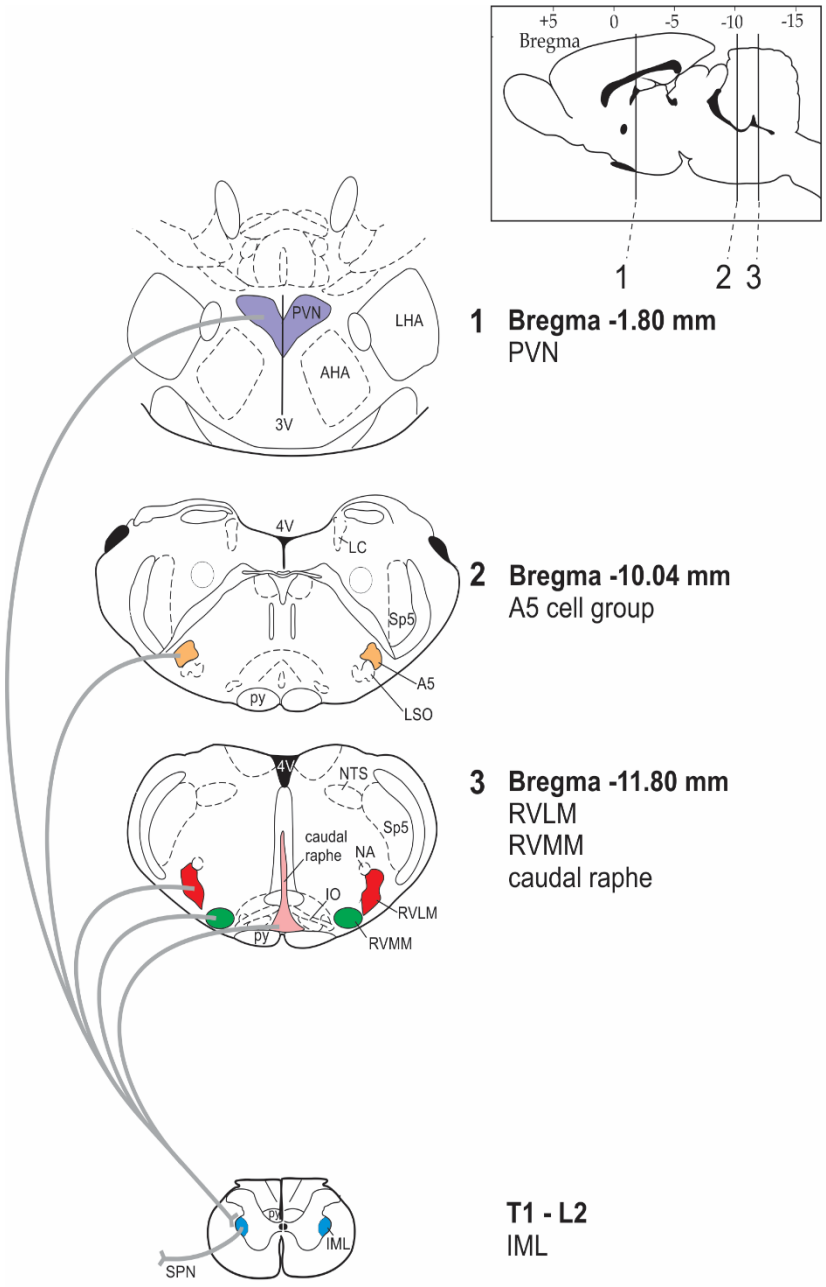

Figure 1.2: Sympathetic premotor neurons that project to the thoracic IML. The five main presympathetic inputs to IML SPNs are: the paraventricular hypothalamic nucleus (PVN), the A5 cell group in the pons, the rostral ventrolateral medulla (RVLM), the ventromedial medulla (RVMM), and the caudal raphé nuclei (MRN). Adapted from Strack et al. (1989a).

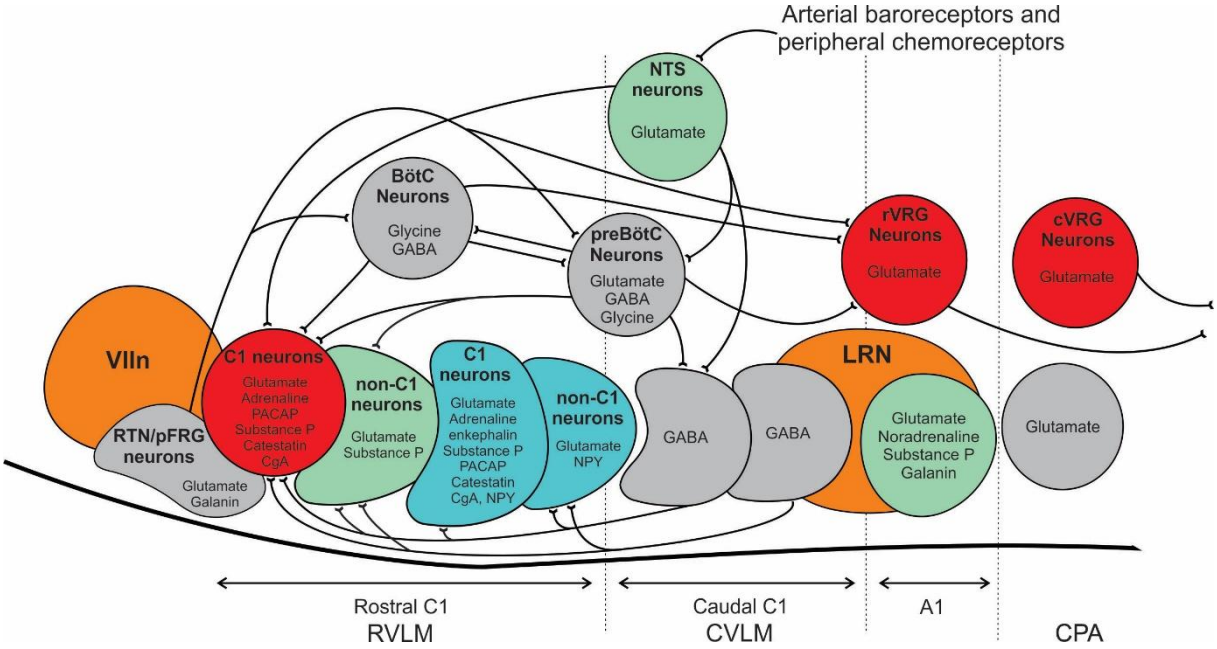

Figure 1.3: The neurochemical phenotype of neurons in the ventral medulla (Adapted from (Pilowsky et al., 2002)).

Intermedullary connections are indicated above, while neurons with spinal projections are identified in red, those with supramedullary projections are in blue and those that have both spinal and supramedullary projections are in green. Abbreviations: BötC, Bötzinger complex; CgA, Chromogranin A; CPA, caudal pressor area; CVLM, caudal ventrolateral medulla; cVRG, caudal ventral respiratory group; LRN, lateral reticular nucleus; NPY, neuropeptide Y; NTS, nucleus of the solitary tract; preBötC, pre-Bötzinger complex; RTN/pFRG, retrotrapezoid nucleus/parafacial respiratory group; RVLM, rostral ventrolateral medulla; rVRG, rostral ventral respiratory group; VIIn, facial nucleus.

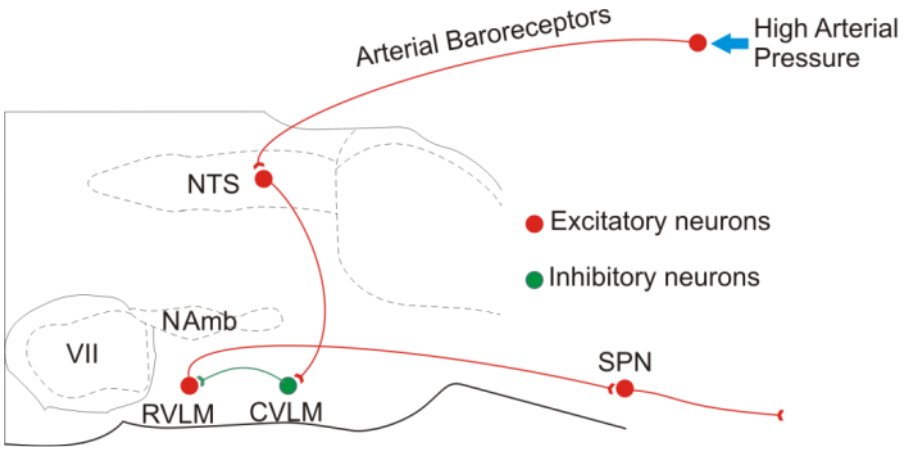

Figure 1.4: The sympathetic baroreflex. Afferent and efferent connections involved in the modulation of the baroreceptor reflex; including excitatory (in red) input from the NTS to GABAergic inhibitory CVLM neurons (in green) which in turn connects to excitatory bulbospinal RVLM neurons which project to SPNs that control the sympathetic outflow.

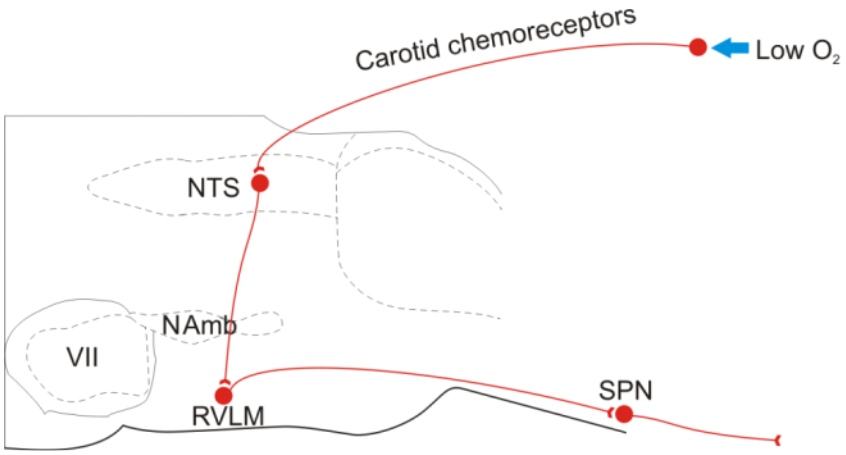

Figure 1.5: The hypoxic chemoreflex. Afferent and efferent connections involved in the modulation of the hypoxic chemoreflex; including excitatory (in red) input from the NTS to excitatory C1 and non-C1 bulbospinal RVLM neurons which project to SPNs that control the sympathetic outflow.

CHAPTER 2: GLIAL ATP RELEASE, BUT NOT ACTIVATION OF HEME OXYGENASE 2, CONTRIBUTES TO THE SENSITIVITY OF SYMPATHETIC PREMOTOR NEURONS IN THE ROSTRAL VENTROLATERAL MEDULLA TO CHEMICAL HYPOXIA

ABSTRACT

Sympathetic premotor neurons in the rostral ventrolateral medulla (RVLM) have an exaggerated sensitivity to local hypoxia compared to neighbouring non-bulbospinal neurons, but previous attempts to identify the cellular mechanisms responsible have been inconclusive. Here we investigate the contributions of two candidate mechanisms, activation of the putative oxygen sensor heme oxygenase 2 (HO-2) and glial ATP release.

The increased sensitivity of spinally projecting RVLM neurons to application of sodium cyanide (5 - 20 mM: NaCN) was first verified *in vitro:* bulbospinal neurons were labelled by microinjection of fluorescent tracer into the thoracic spinal cords of P7 – P25 rat pups and recorded in acute brainstem slices. Consistent with previous reports, the amplitudes of inward currents evoked by NaCN were dose-dependent, significantly greater in bulbospinal than unlabelled neurons, and were unaffected by tetrodotoxin. Bulbospinal and catecholaminergic RVLM neurons were then examined for HO-2 immunoreactivity. No evidence of HO-2 expression was found in putative sympathetic premotor neurons in adult or juvenile rats, or in bulbospinal RVLM neurons electrophysiologically verified as NaCN-sensitive.

In contrast, blockade of P2X receptors reduced the amplitudes of responses to NaCN, suggesting that extracellular ATP transmission contributes to hypoxic responses. Furthermore, pre-incubation of slices in a glial toxin, fluoroacetic acid, abolished responses to NaCN without altering any other electrophysiological property of recorded neurons or their sensitivity to iontophoretically applied ATP.

These data suggest a crucial role for RVLM astrocytes, but not HO-2, in driving sympathetic responses to acute brainstem hypoxia.

INTRODUCTION

The detection of hypoxemia is a fundamental homeostatic function that is subserved by both peripheral and central oxygen sensors. Although respiratory responses to systemic hypoxia are reversed by destruction of peripheral chemoreceptive nerves, sympathoexcitatory and vasomotor responses persist (Sun and Reis, 1993, 1994c, Niewinski et al., 2014), indicating a role for central oxygen sensors in the neural control of blood pressure.

Putative sympathetic premotor neurons in the rostral ventrolateral medulla (RVLM) play a key role in the generation of sympathetic vasomotor tone and elaboration of multiple sympathetic reflexes, including vasomotor responses to hypoxia (reviewed by Guyenet et al., 2013). Sympathoexcitatory and pressor responses to central hypoxia/ischaemia are abolished by electrolytic or chemical lesion of the RVLM (Dampney and Moon, 1980, Guyenet and Brown, 1986, Sun and Reis, 1996), and spinally-projecting RVLM neurons are excited by systemic hypoxia, even after destruction of peripheral chemoreceptors (Sun and Reis, 1993, 1994c, Koganezawa and Terui, 2006, Koganezawa and Paton, 2014), and by local histotoxic hypoxia evoked by sodium cyanide (NaCN) iontophoresis (Sun et al., 1992a, Sun and Reis, 1994c). Furthermore, spinally-projecting RVLM neurons show enhanced sensitivity to hypoxia compared to non-bulbospinal RVLM neurons *in vivo* (Sun and Reis, 1994c, 1996) and retain that sensitivity in acute slices *in vitro* (Wang et al., 2001). These observations are widely interpreted as evidence that RVLM sympathetic premotor neurons are intrinsically oxygen-sensitive (as reviewed by Dampney, 1994, Reis et al., 1997, Neubauer and Sunderram, 2004, Guyenet et al., 2013), but the cellular mechanisms that underlie this property remain elusive.

There are two major candidates for which supportive evidence can be identified. The first is the putative oxygen sensor heme oxygenase (HO: recently reviewed by Munoz-Sanchez and Chanez-Cardenas, 2014). There are three isoforms of HO; an inducible form, HO-1, which is largely absent from the brain under baseline conditions (Sun et al., 1990), but which may be upregulated by exposure to chronic hypoxia (Mazza et al., 2001, Sunderram et al., 2009), and two constitutively expressed forms, HO-2 and HO-3, of which HO-3 protein expression is low (Scapagnini et al., 2002) or undetectable (Hayashi et al., 2004) in the brain. Brain HO-2 immunoreactivity is, however, widespread (Ewing and Maines, 1992), and has been reported

in brainstem autonomic nuclei that are activated by hypoxia, including the nucleus of the solitary tract (Lo et al., 2006) and RVLM (Mazza et al., 2001, Dai et al., 2010). HO-2 is a candidate oxygen sensor in excitable cells: under hypoxic conditions HO-2 activity is suppressed, reducing the catabolism of heme to biliverdin and carbon monoxide, inactivating BK channels and subsequently depolarizing HO-expressing cells (Prabhakar et al., 1995, Maines, 1997, Adachi et al., 2004, Williams et al., 2004, Wu and Wang, 2005). In RVLM neurons maintained in dissociated cultures, hypoxia sensitivity is strongly correlated with HO-2 immunoreactivity, and is blocked by the HO-2 blocker tin protoporphyrin-IX (D'Agostino et al., 2009). However, no previous investigation has directly examined the expression of HO-2 in RVLM sympathetic premotor neurons.

The second candidate mechanism is the hypoxic activation of RVLM astrocytes, leading to the release of excitatory gliotransmitters such as ATP and subsequent excitation of adjacent sympathetic premotor neurons. Previous studies support key components of this arrangement: brainstem hypoxia drives the release of ATP within the RVLM region (Gourine et al., 2005), and RVLM sympathetic premotor neurons are depolarized by exogenous (Sun et al., 1992b, Horiuchi et al., 1999b, Ralevic et al., 1999, Zoccal et al., 2011) and glial ATP (Marina et al., 2013).

Critical evidence that directly assesses the role of HO-2 and/or glial activation in driving the responses of sympathetic premotor neurons to acute hypoxia is missing. Both hypotheses are tested in the current study. We first verified the enhanced sensitivity of spinally-projecting putative sympathetic premotor neurons versus non-spinal RVLM neurons to acute chemical hypoxia in brainstem slices prepared from neonatal rats. We then examined the distribution of HO-2 immunoreactivity in the adult and neonatal rat brainstem and in functionally verified hypoxia-sensitive RVLM sympathetic premotor neurons. Having established that HO-2 is not significantly expressed in spinally projecting neurons, we then determined that ATP transmission contributes to hypoxic responses in spinally projecting neurons. Finally, we show that disruption of glial activity attenuates responses to acute chemical hypoxia.

MATERIALS AND METHODS

All animal experiments were conducted in accordance with the *Australian code of practice for the care and use of animals for scientific purposes* and were approved by Macquarie University Animal Ethics Committee.

LABELLING OF BULBOSPINAL RVLM NEURONS

Sprague Dawley rat pups of either sex (P5 – P20) were anesthetized with intraperitoneal ketamine (7.5 mg/Kg, Parnell laboratories, Australia) mixed with medetomidine (0.05 mg/Kg, Pfizer animal health, Australia) and moved onto a heated pad. Adult rats (400 – 500 g) were anaesthetized with 75 mg/kg ketamine and 0.75 mg/kg medetomidine. Rats were treated with prophylactic analgesia (Carprofen, 2.5 mg/kg s.c. Norbrook Pharmaceuticals, Australia) and antibiotics (cefazolin sodium, 0.55 g/kg, i.m.; Mayne Pharma, Australia). A dorsal laminectomy was performed and the T2 spinal cord exposed. Fluorescently conjugated cholera toxin β subunit (CTB-Alexa 555, 0.5 %, Invitrogen) was injected (1 to 3 100 nl injections each side) bilaterally at co-ordinates corresponding to the intermediolateral cell column. After completion of microinjections, the wound was closed with cyanoacrylate glue (pups) or staples (adults) and anaesthesia was reversed with atipamazole (0.1 mg s.c., Pfizer animal health, Australia). Post-operative rats were monitored carefully for the duration of experiments and treated with additional analgesia when indicated.

IMMUNOHISTOCHEMISTRY

2 – 5 days after CTB injection rats were removed from their cages, euthanized with pentobarbital sodium (>100 mg/kg i.p.) and perfused transcardially with 300 ml of ice-cold Dulbecco's modified Eagle medium (Sigma-Aldrich, Australia) followed by 300 ml of ice-cold fixative (4 % paraformaldehyde/0.1 M phosphate buffer; pH 7.4; Sigma-Aldrich, Australia). The central nervous system was removed and post-fixed overnight. The following day coronal sections of the brainstem (40 µm thick) and spinal cord (100 µm thick) were prepared on a vibrating microtome. Spinal cord sections were mounted and immediately visualised to confirm tracer injection sites; every 5th brainstem section was collected for immunohistochemistry. Other sections from the same adult rats were used for a different study (Parker et al., 2013). Sections were permeabilized in PBS containing 0.1% Tween-20, and incubated in primary antibodies raised against HO-2 (Rabbit anti-HO-2, Tocris

bioscience, 1:1000) and tyrosine hydroxylase (TH: mouse anti-TH, Sigma Aldrich,1:2000) for 72 hours at 4 ^{o}C in 10% normal horse serum. Sections were washed and incubated in secondary antibodies (donkey anti-mouse 488, Jackson Immunoresearch, 1:500; donkey anti-rabbit Cy5, Jackson Immunoresearch, 1:500) with 5% horse serum overnight.

Cryoprotected brainstem slices containing biocytin-labelled neurons were processed using a different immunohistochemistry protocol (Gogolla et al., 2006). Sections were washed and permeabilized in PBS containing 0.5 % Triton X-100 for 12 hours at 4 ^{o}C, incubated in blocking solution (5 % bovine serum albumin, BSA) for 4 hours at room temperature followed by incubation with the same primary antibodies as above for 4 hours at room temperature in 5 % BSA. Sections were then washed and incubated in secondary antibodies (donkey anti-mouse 350 (Jackson Immunoresearch, 1:500; donkey anti-rabbit Cy5, Jackson Immunoresearch, 1:500) and ExtraAvidin FiTC (Jackson Immunoresearch, 1:500) with 5 % BSA for 4 hours at room temperature.

Sections were washed, mounted, coverslipped and imaged under confocal or epi-fluorescence with appropriate filter sets.

***IN VITRO* ELECTROPHYSIOLOGY**

Solutions (mM)

Cutting solution: 125 NaCl, 25 $NaHCO_3$, 3 KCl, 1.25 $NaH_2PO_4.H_2O$, 10 D-glucose, 1 $CaCl_2$, 6 $MgCl_2$; equilibrated with 95% O_2 – 5% CO_2.

Artificial cerebrospinal fluid (aCSF): 125 NaCl, 25 $NaHCO_3$, 3 KCl, 1.25 $NaH_2PO_4.H_2O$, 25 D-glucose, 2 $CaCl_2$, 1 $MgCl_2$; equilibrated with 95% O_2 – 5% CO_2.

Cesium chloride internal solution: 140 CsCl, 5 Hepes, 10 EGTA, 1 $MgCl_2$, 2 $CaCl_2$, 2 MgATP, 0.05% biocytin (pH = 7.3, 280 < Osmolarity < 285 mOsm).

Potassium gluconate internal solution: 125 K-gluconate, 10 Hepes, 11 EGTA, 15 NaCl, 1 $MgCl_2$, 2 MgATP, 0.25 NaGTP, 0.05% biocytin (pH = 7.3, 280 < Osmolality < 285).

ATP iontophoresis solution: 200 ATP, 160 NaCl (pH = 8.5).

<u>Whole-cell recordings from acute brainstem slices</u>

2-5 days after tracer microinjection pups (P7 – P25) were anaesthetized with isoflurane and quickly decapitated. The whole brain was rapidly removed and placed in ice cold oxygenated cutting solution. The brainstem was dissected, mounted in a vibratome, and 2-3 300 µm thick coronal sections from the region overlapping with the caudal pole of the facial nucleus were cut in ice-cold cutting solution and transferred to carbogen-bubbled aCSF at 34°C for at least 1 h before recording. Recordings were performed at room temperature in a 2 ml chamber superfused at 1.5 – 2 ml/min with carbogen-bubbled aCSF. Tracer-labelled neurons were viewed under epi-fluorescence: CTB-filled neurons lying ventral to nucleus ambiguus and lateral to the inferior olive were identified as putative sympathetic premotor neurons.

Whole-cell recordings were made from RVLM neurons using borosilicate pipettes with 1.5 - 2 µm tip diameters (pipette resistance: 3 – 6 MΩ). After formation of a gigaseal voltage-clamp (holding potential: -60 mV) or current-clamp recordings were obtained using Multiclamp 700B (Molecular Devices). Series resistance was compensated to 70-80 %. All recorded parameters were digitized using Spike 2 version 6.11 with a Power1401 mark II (Cambridge Electronic Design, UK). Voltage-clamp recordings were low-pass filtered at 200 Hz.

In some experiments recorded neurons were labelled by addition of 0.05 % biocytin to the internal solution. At the conclusion of recordings the pipette was withdrawn and slices were fixed overnight in 4% paraformaldehyde and then frozen in cryoprotectant until immunohistochemical processing.

Neuronal responses to acute hypoxia

Once holding current stabilized the extracellular perfusion was switched to carbogen-equilibrated aCSF containing 5, 10 or 20 mM NaCN (Sigma-Aldrich) until a response was observed or for a maximum of 60 seconds. Slices were then washed in normal aCSF for five minutes or until holding currents had recovered to baseline.

Responses to repeated 10 mM NaCN were compared in six bulbospinal neurons before and after addition of 1 - 10 µM tetrodotoxin (TTX, Jomar Bioscience) to the perfusion in order to determine whether responses were independent of activity in presynaptic neurons. Baseline responses to NaCN were recorded and allowed to recover for five minutes before 5 minutes incubation with TTX and re-exposure to NaCN.

The role played by ionotropic ATP receptors in driving responses to hypoxia was examined by comparing responses to repeated 10 mM NaCN before and after incubation with the P2X receptor antagonist pyridoxalphosphate-6-azophenyl-2', 4'-disulfonic acid (PPADS, 30 μM, Sigma-Aldrich) for five minutes. In six experiments the effect of PPADS on NaCN-evoked currents was examined using aCSF containing TTX; the remaining three experiments were conducted in the absence of TTX. The effect of PPADS on NaCN-evoked responses was similar in both groups, so the data were pooled.

The dependence of neuronal responses to chemical hypoxia on intact glial activity was examined by incubating sections for 30 – 60 minutes in aCSF containing a glial toxin, fluoroacetic acid (5 mM, Sigma Aldrich) prior to recordings of responses to 5, 10 and 20 mM NaCN.

In order to control for any potential effect of fluoroacetic acid on neuronal responses to exogenous ATP (independent of any effect on glia), responses to ATP iontophoresis were compared in neurons incubated in normal aCSF and aCSF containing fluoroacetic acid as described above. Neuronal activity was recorded in current clamp mode using potassium gluconate internal solution and ATP was iontophoretically applied (20 - 100 nA, 5 - 10 s) using a second pipette positioned within 10 μm of the recorded cell. ATP iontophoresis was controlled by an Axoclamp 900A (Molecular Devices); resistance of ATP-filled pipettes was 20 – 40 MΩ. A retaining current of -2 to -10 nA was applied between periods of drug ejection.

DATA ANALYSIS

Hypoxic responses were quantified by subtracting the holding current from the peak current evoked by NaCN perfusion. The sensitivities of bulbospinal and non-bulbospinal RVLM neurons to 5, 10 and 20 mM NaCN were compared by 2-way ANOVA. Repeated responses of bulbospinal neurons to NaCN following application of TTX or PPADS to the perfusate were normalized with respect to baseline responses; changes in median holding currents were assessed using Wilcoxon matched-pairs signed rank test (TTX) or 1-way ANOVA followed by Dunn's Multiple Comparison Test (PPADS). The magnitude of responses to 5, 10 and 20 mM NaCN recorded after incubation with fluoroacetic acid was compared to baseline responses using 2-way ANOVA. Effects of fluoroacetic acid on baseline electrophysiological properties

(holding current (voltage clamp mode; measured over 60 s prior to NaCN administration), synaptic current frequency (voltage clamp mode; measured over 30 s prior to NaCN administration), firing rate (current clamp mode; measured over 10 s of baseline), action potential rise time (averaged from spontaneous spikes occurring in 10 s of baseline activity, defined as the interval between the start of depolarization to peak membrane potential), action potential height (the total amplitude of the action potential), and the change in the firing rate following exogenous ATP iontophoresis (quantified by subtracting the baseline firing rate measured over 10 seconds prior to iontophoresis from the firing rate measured during iontophoresis) were assessed using an unpaired t-test. Parametric data are expressed as mean ± S.E.M. Non-parametric data are expressed as median (range). Differences were judged significant at $P<0.05$. In all figures *: $P<0.05$; **: $P<0.01$; ***: $P<0.001$. Statistical analyses were performed using Graphpad Prism 6.0.

RESULTS

BULBOSPINAL NEURONS WERE PREFERENTIALLY ACTIVATED BY NaCN

Responses to graded doses of NaCN were examined in 12 non-bulbospinal and 27 bulbospinal RVLM neurons from 28 animals. NaCN caused inward currents in all bulbospinal neurons examined and in most non-bulbospinal neurons (figure 2.1). Responses were dose-dependent (2-way ANOVA versus dose: $F_{2, 89} = 4.808$, $P = 0.0104$), reproducible, and in most cases reversible. Peak responses to 5, 10 and 20 mM NaCN in bulbospinal neurons were 83 ± 19, 548 ± 126 and 1030 ± 317 pA respectively, significantly greater than non-bulbospinal RVLM neurons (39 ± 4, 112 ± 14 and 169 ± 43 pA respectively, 2-way ANOVA: $F_{1, 89} = 9.94$, $P = 0.0022$ figure 2.1B). No outward currents were seen. Responses of bulbospinal neurons to 10 mM NaCN were unchanged by addition of TTX to the perfusate (87.1% (52 - 121.9%), Wilcoxon two-tailed P = 0.438, n = 6, data not shown: see figure 2.4 for example of response to NaCN under TTX). Intermittent short-lasting (< 3 ms) large (> 1 nA) inward currents, consistent with action current, were apparent on some recordings (e.g. figure 2.3). Such effects presumably resulted from action potentials propagating from the dendritic compartment, as they were abolished by TTX, and therefore considered space-clamp artefacts. Responses to NaCN in such cases appeared normal so the data were included.

RVLM SYMPATHETIC PREMOTOR NEURONS WERE NOT HO-2 IMMUNOREACTIVE

The RVLM was defined as the region of the ventral brainstem lying lateral to the inferior olive and ventral to nucleus ambiguus. Sections lying caudal to the main body of the facial nucleus and rostral to the emergence of the central canal into the fourth ventricle were considered to contain RVLM, equivalent to Bregma – 13.56 to –11.88 mm in the adult rat (Paxinos and Watson, 2007). Brainstem sections from 2 adult and 2 juvenile rats were examined were for colocalization of HO-2 immunoreactivity with TH immunoreactivity or CTB transported from the spinal cord. The expression pattern of HO-2 immunoreactivity was similar in adult and neonatal rats: expression was strong in the facial nucleus, moderate in the nucleus of the solitary tract, prepositus nucleus, ventral midline raphe, and ventromedial medulla, and weak at all rostrocaudal levels of the RVLM. In many cases RVLM HO-2 immunoreactivity was intermingled with, but never colocalized with, CTB labelling and TH-immunoreactivity (figure 2.2; some double-labelling of CTB and HO-2 immunoreactivity was

seen in the ventromedial medulla; such neurons were always medial to the main body of the TH positive cell group and were considered part of the rostral ventromedial medulla bulbospinal group. NaCN-sensitive biocytin-labelled bulbospinal neurons (n = 12) were examined for HO-2 immunoreactivity. Responses to NaCN were typical of bulbospinal neurons; all were identified as HO-2-negative (figure 2.3).

P2X RECEPTOR BLOCKADE ATTENUATED RESPONSES OF RVLM BULBOSPINAL NEURONS TO NaCN

Responses of bulbospinal RVLM neurons to 10 mM NaCN were significantly attenuated by superfusion with PPADS (1-way ANOVA P = 0.0006, figure 2.4). Median responses were reduced to 32.1% (4.9 % - 80.1 %) compared to control (Dunn's Multiple Comparison test: P < 0.001, n = 9) and in five neurons in which recordings were maintained median recovery was 97.2 % (17.4 % - 104.6 %).

INHIBITION OF GLIA DID NOT ALTER BASELINE ELECTROPHYSIOLOGICAL PARAMETERS OF BULBOSPINAL NEURONS

Baseline electrophysiological properties of bulbospinal neurons were unaffected by incubation in the glial toxin, fluoroacetic acid, for 30 – 60 minutes: in voltage clamp mode (CsCl internal solution), holding currents were unchanged compared to recordings obtained after incubation in normal aCSF (-142 ± 10 (n = 12) vs. -133 ± 14 pA respectively (n = 27), unpaired t-test: t = 0.42, df = 37, *two-tailed* P = 0.68), and no significant change in the frequency of spontaneous synaptic currents was recorded (1.8 ± 0.2 (n = 12) vs. 2.0 ± 0.1 Hz (n = 27), unpaired t-test: t = 0.9, df = 37, *two-tailed* P = 0.37, figure 2.5A). Bulbospinal neurons recorded in current clamp mode (K-gluconate internal solution) exhibited spontaneous action potentials that occurred at the same discharge rate in control (1.9 ± 0.8 Hz, n = 5) and fluoroacetic acid-incubated groups (1.4 ± 0.7 Hz, n = 5, unpaired t-test: t = 0.42, df = 8, *two-tailed* P = 0.68). Neither the height nor rise time of spontaneous action potentials were significantly different in control vs fluoroacetic acid-incubated groups (height: 93 ± 3 vs. 92 ± 3 mV, unpaired t-test: t = 0.31, df = 8, *two-tailed* P = 0.76; rise time: 1.9 ± 0.3 vs. 2.1 ± 0.3 ms, unpaired t-test: t = 0.36, df = 8, *two-tailed* P = 0.73, figure 2.5B).

GLIAL INHIBITION DID NOT ALTER RESPONSES TO ATP IONTOPHORESIS BUT SIGNIFICANTLY ATTENUATED RESPONSES TO NaCN

All five bulbospinal neurons examined were excited by iontophoretic application of ATP: ATP caused a dose-dependent increase in firing frequency within 1 - 2 s of the beginning of iontophoresis that was sustained for the duration of ATP application (figure 2.6). The same iontophoresis parameters caused no effect on neuronal discharge when applied via a pipette containing aCSF without ATP (*n* = 3, figure 2.6C). No difference in responses evoked by 100 nA ATP iontophoresis was detected in neurons incubated in aCSF compared to fluoroacetic acid (2.3 ± 0.7 vs. 2.8 ± 0.7 spikes/s respectively, *n* = 5 in each group, unpaired t-test: *t* = 0.52*, df* = 8, *two-tailed P* = 0.62, figure2.6D).

Responses of bulbospinal RVLM neurons to acute chemical hypoxia were significantly reduced after 30-60 minutes incubation in fluoroacetic acid (5 mM): in all cases, addition of NaCN to the perfusate failed to evoke large inward currents typical of baseline recordings (figure 2.7A). Mean responses to 5, 10 and 20 mM NaCN were 9.4 ± 3 (n = 10), 21.4 ± 6.7 (n = 12) and 20.6 ± 7.8 pA (n = 8) respectively in the fluoroacetic acid group (figure 2.7B), significantly smaller than those observed in control experiments (2-way ANOVA versus untreated bulbospinal neurons: $F_{1, 84}$ = 12.12*, P* = 0.0008).

DISCUSSION

The major findings of this study are firstly that, consistent with previous reports, RVLM sympathetic premotor neurons have an exaggerated dose-dependent response to acute chemical hypoxia (NaCN) compared to unlabelled and presumably non bulbospinal neighbouring neurons. Second, HO-2 immunoreactivity, although present in adjacent brainstem regions, was not detected in bulbospinal neurons within the C1 region of the RVLM or in electrophysiologically characterised hypoxia-sensitive sympathetic premotor neurons. Third, blockade of P2X receptors significantly attenuated, and selective disruption of glial metabolism virtually abolished, response of RVLM bulbospinal neurons to NaCN. These findings indicate that responses of RVLM sympathetic premotor neurons to acute chemical hypoxia *in vitro* are independent of HO-2 expression, and are secondary to exogenous ATP transmission that originates most likely from neighbouring glial cells. We conclude that brainstem glia appear to play a key role in driving sympathoexcitatory responses to local chemical hypoxia.

In the current study sodium cyanide was used to evoke experimental hypoxia. Salts of cyanide evoke histotoxic anoxia by inhibiting the mitochondrial oxygen chain (Way, 1984) and have been widely used as an experimental model of chemical hypoxia. In our study, cyanide was substituted for hypoxia in order to have a better control of timing and dosage (Goldberg et al., 1987). Furthermore, researchers previously used both chemical and hypoxic hypoxia and same effects were recorded for both stimuli (Sun and Reis, 1994b, Wang et al., 2001, D'Agostino et al., 2009).

The concentrations of NaCN used in the current protocol (5 - 20 mM) are based on those used by D'Agostino et al. (2009) (3 - 10 mM) and are moderately high (although the exposure time brief) compared to a number of similar studies (e.g. 5.4 mM, 20 min: Noma, 1983, 4 mM, 5 min: Jiang et al., 1994, 0.3 mM, 40 s: Sun and Reis, 1994b, 5 mM, 5 min: Hammarström and Gage, 1999), although it should be pointed out that NaCN concentration would not have reached equilibrium in our setup. The responses observed here likely reflect direct sensitivity to cellular oxygen availability, rather than effects mediated by the breakdown of ATP metabolism and subsequent depletion of cellular energy stores, as the

effects were rapid and we observed no comparable responses to acute glucoprivation (Korim et al., 2014).

Under baseline conditions inward currents were consistently evoked by brief exposure to NaCN; responses were rapid, dose-dependent, reproducible and reversible, and greater in bulbospinal neurons than neighbouring non-bulbospinal cells. Outward currents, corresponding to the hyperpolarizing responses to acute cyanide occasionally encountered by D'Agostino et al. (2009) and Wang et al. (2001), were never seen. Although the relative sensitivities of bulbospinal and non-bulbospinal RVLM neurons to graded chemical hypoxia have not previously been compared in voltage-clamp mode, these findings are consistent with previous reports *in vivo* (Sun and Reis, 1993, 1994c) and *in vitro* (Wang et al., 2001), and support a role for RVLM sympathetic premotor neurons as central oxygen sensors. Technically, recordings made at room temperature *in vitro* may alter neuronal properties such as the input resistance and action potential amplitude and width, and the data collected at higher temperatures may more closely resemble conditions *in vivo* (Graham et al., 2008). Although recordings reported here were made at room temperature, it is unlikely that temperature significantly influenced responses to hypoxia as they resembled previously collected data *in vivo* (Sun and Reis, 1993, 1994c). Furthermore, many studies did similar recordings at room temperature *in vitro* (Kawai et al., 1999, Wang et al., 2001) and data were consistent.

Responses to NaCN were unaffected by TTX at concentrations that suppress action potential generation. Similar findings in RVLM pacemaker neurons recorded in the presence of TTX *in vitro* (Sun and Reis, 1994b) or in barosensitive RVLM neurons recorded under blockade of fast neurotransmission *in situ* (Koganezawa and Paton, 2014) have been interpreted as evidence that sensitivity to acute hypoxia is an endogenous property of sympathetic premotor neurons, rather than the result of synaptic drive. However an important caveat to this reading of the current data is that cyanide can itself drive synaptic glutamate release in the absence of neuronal activity (Dong et al., 2012). We acknowledge that global glutamate exocytosis may contribute to the effects we report here, and indeed may underlie the inward currents and enhanced synaptic activity often seen in non-bulbospinal neurons. However, such effects are unlikely to account for the differences in responses seen in bulbospinal compared to non-bulbospinal neurons.

HO-2 activation does not appear to underlie the chemical hypoxia sensitivity of RVLM sympathetic premotor neurons

As reviewed in the introduction of this chapter, Maines et al. have described three forms of HO (Maines et al., 1986, McCoubrey et al., 1997). HO-2, which is a constitutive isoform expressed under homeostatic conditions (Maines et al., 1986) and is involved in hypoxic responses in dissociated cultured RVLM neurons (D'Agostino et al., 2009). Furthermore, following transient cerebral ischemia, HO-2 was found to be responsible for preventing neuronal death in brain cultures (Dore et al., 2000). In contrast, the other isoforms seem unlikely to mediate responses to hypoxia; HO-1 is not expressed under normal conditions, but is an inducible isoform that increases in response to oxidative stress; like hypoxia (Geddes et al., 1996, Nimura et al., 1996). HO-3 is reported to be catalytically inactive (McCoubrey et al., 1997), therefore suggesting that HO-2 should be the focus of this study.

HO-2 immunoreactivity has been reported in the RVLM region (Mazza et al., 2001) and, by the same group, in cultured RVLM neurons electrophysiologically confirmed as hypoxia-sensitive (D'Agostino et al., 2009). In that study responses to acute hypoxia were consistently blocked by application of the non-specific heme oxygenase inhibitor, tin protoporphyrin IX.

In the current study we observed no compelling evidence for involvement of HO-2 in mediating chemical hypoxia sensitivity in RVLM sympathetic premotor neurons. Consistent with previous reports (Ewing and Maines, 1992, Mazza et al., 2001), we saw robust HO-2 immunoreactivity in the facial nucleus, but sparse expression in the area that corresponds with the RVLM pressor region (Goodchild and Moon, 2009), and no colocalization of HO-2 immunoreactivity in spinally projecting or TH-immunoreactive RVLM neurons, widely accepted anatomical and phenotypic markers of sympathetic premotor neurons (Burke et al., 2008, Stornetta, 2009, Guyenet et al., 2013). Furthermore, no HO-2 immunoreactivity was detected in 12 biotin-labelled sympathetic premotor neurons that were electrophysiologically confirmed as hypoxia-sensitive.

As D'Agostino et al. (2009) did not discriminate between bulbospinal and non-bulbospinal neurons, the most parsimonious explanation for this discrepancy is that HO-2 may contribute to the hypoxia-sensitivity of non-bulbospinal neurons, which were not

investigated in detail in the current study, but does not appear to underlie the enhanced hypoxia-sensitivity of bulbospinal cells, which represent a small subpopulation of RVLM neurons. Alternatively it could be that HO-2 is not involved in generating hypoxic responses in acute preparations, but assumes a more significant role under the dissociated culture conditions used by D'Agostino et al. (2009).

Hypoxic responses are ATP-mediated

The relatively higher hypoxia-sensitivity of bulbospinal compared to non-bulbospinal RVLM neurons is not maintained in acutely dissociated preparations (Kawai et al., 1999). This key observation suggests that a component of the immediate extracellular environment is responsible for sensing hypoxia and providing excitatory drive to RVLM sympathetic premotor neurons. ATP is released in the ventral medulla in response to acute central hypoxia *in vivo* (Gourine et al., 2005) and is implicated in driving bradypnoeic responses to central hypoxia (Rong et al., 2003, Lorier et al., 2008, Huxtable et al., 2009, Zhang et al., 2012), but no previous study has investigated its role in generating sympathoexcitatory responses to acute hypoxia. In the current study blockade of ionotropic ATP receptors by PPADS reversibly attenuated responses to NaCN, indicating that responses are at least partially mediated by ATP signalling. This effect was observed in the presence of TTX, suggesting that hypoxic ATP release is independent of action potential generation, consistent with a non-synaptic release mechanism.

Astrocytes release transmitters including adenosine, ATP and glutamate in response to a range of metabolic stimuli, including acute hypoxia (for review, see Fields and Stevens-Graham, 2002, Aley et al., 2006, Martín et al., 2007, McDougal et al., 2013), and contribute to the regulation of neuronal excitability during acute (Oliva et al., 2013) and chronic ischaemia (Hines and Haydon, 2013), and are therefore a strong candidate as mediators of hypoxic ATP release in the RVLM. This proposal was investigated by examining responses of bulbospinal neurons to NaCN following incubation of slices in a glial toxin, fluoroacetic acid, for 30 - 60 minutes prior to recordings. In the present study, fluoroacetic acid potently blocked responses of bulbospinal neurons to NaCN, reducing NaCN-evoked currents by over 90% overall.

Fluoroacetic acid inhibits cell metabolism by blocking the tricarboxylic acid cycle. As the uptake of acetate (and fluoroacetate) is relatively higher in glia compared to neurons, fluoroacetic acid administration has been widely used by other researchers as a selective inhibitor of glial function (reviewed by: Fonnum et al., 1997, Goncharov et al., 2006). Although fluoroacetic acid has numerous effects on glial biology (Szerb and Issekutz, 1987, Swanson and Graham, 1994, Fonnum et al., 1997, Largo et al., 1997, Magistretti and Chatton, 2005, Goncharov et al., 2006), of particular relevance to the current study its inhibition of glial transmitter release including ATP (Koenig and Patel, 1970, Cremer-Lacuara et al., 1980, Accorsi-Mendonca et al., 2013) and glutamate (Hassel et al., 1994). A number of key studies suggest that fluoroacetic acid is specifically gliotoxic at the dose and the incubation time used here (20 mM, 30 min: Canals et al., 2008, 5 mM, 50 - 80 min: Parsons and Hirasawa, 2010), and, in accordance with the data presented here, confirm that effects on glia are observed in the absence of any changes in neuronal electrophysiological properties (Parsons and Hirasawa, 2010, Accorsi-Mendonca et al., 2013). Of particular relevance to the current study, Accorsi-Mendonca et al. (2013) found that a 20 minute perfusion with 1 mM fluoroacetic acid decreased spontaneous ATP release in NTS slices, but had no effect on the amplitude or half-width of spontaneous synaptic events of NTS neurons. In the current study we found no effect of fluoroacetic acid on baseline electrophysiological properties of recorded neurons or their sensitivity to exogenous ATP, suggesting a glial site of action of the toxin.

We therefore propose a critical role for RVLM astrocytes in mediating hypoxic responses in RVLM sympathetic premotor neurons, analogous to the role played by astrocytes in sensing pH in the neighbouring retrotrapezoid nucleus (Gourine et al., 2010, Kasymov et al., 2013). However, the mechanisms that underlie the relative sensitivity of bulbospinal compared to non-bulbospinal neurons remain enigmatic. One obvious possibility is that bulbospinal neurons may differentially express ATP receptors compared to non-bulbospinal neurons. P2X receptor immunoreactivity is detectable at moderate levels in the RVLM (Kanjhan et al., 1999, Yao et al., 2000, Yao et al., 2003, Zhang et al., 2012), including a high proportion of C1 neurons (at least 50%: Yao et al., 2000); similarly, 50% of RVLM neurons activated by the P2Y1 agonist MRS2365 are also found to be TH-immunoreactive (Wenker et al., 2013). Furthermore, as mentioned previously, glia release glutamate so we suggest that

glutamatergic transmission could underlie the remaining current recorded following P2X receptor blockade.

Functional Significance

The previously widespread view of glia as essentially supportive cells that play little role in the elaboration of complex brain functions has recently been challenged by parallel developments in diverse branches of neuroscience (Tsuda et al., 2003, Halassa et al., 2009, Gourine et al., 2010, Ferrini et al., 2013). The present study implicates glia as critical mediators of defensive cardiovascular responses to acute oxygen deprivation and complements recent work that implicates RVLM astrocytes in the pathophysiology of heart failure (Marina et al., 2013), a condition characterized by reduced cerebral perfusion (Gruhn et al., 2001, Alves et al., 2005) and sympathoexcitation (Hasking et al., 1985, Leimbach Jr et al., 1986). A key objective for future studies will be to directly compare the oxygen-sensitivity of RVLM glia to glia obtained from other brain regions, as performed for establishing the role of astrocytes as putative pH sensors in the retrotrapezoid nucleus (Kasymov et al., 2013).

CHAPTER 2 FIGURES AND TABLES

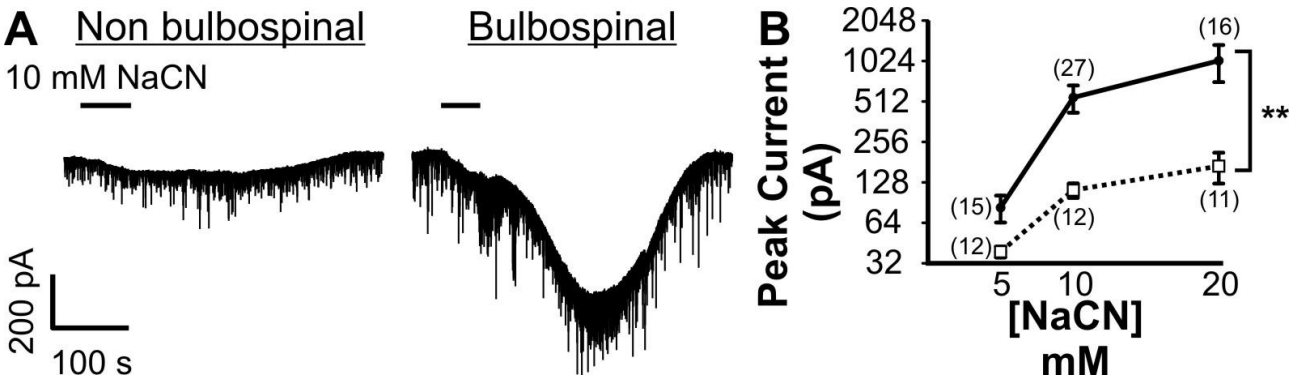

Figure 2.1: RVLM sympathetic premotor neurons have an exaggerated and dose-dependent response to sodium cyanide (NaCN) compared to neighbouring non-bulbospinal neurons. A. Raw data: Typical voltage-clamp responses to perfusion with NaCN. **B.** Pooled data: closed circles: bulbospinal RVLM neurons; open squares: unlabelled RVLM neurons, **: P<0.01. Numbers of neurons in parentheses.

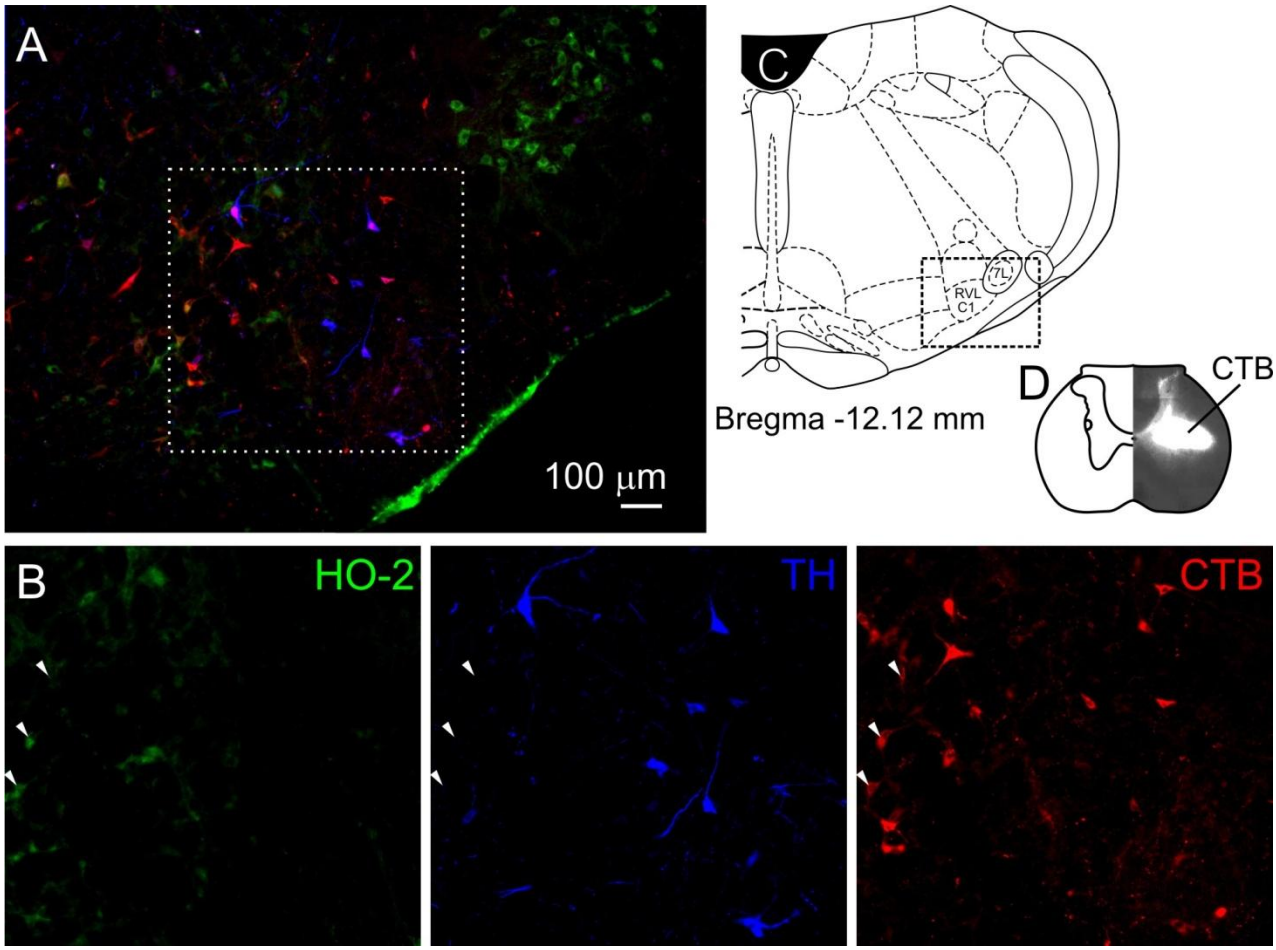

Figure 2.2: HO-2 immunoreactivity does not colocalize with markers of cardiovascular function in the RVLM. A. Low-power merged image showing HO-2 (green), TH (blue) and CTB (red) immunofluorescence in the ventrolateral medulla of the adult rat. HO-2 immunoreactivity is abundant in the facial nucleus (top right corner) but sparse elsewhere. **B.** Enlarged images of boxed area indicated in A. No colocalisation of HO-2 and TH immunoreactivity is seen, although HO-2 positive CTB-positive neurons (arrowheads) were consistently identified medial to the TH-positive cell group. **C.** Schematic diagram modified from Paxinos and Watson (2007) indicating the location of the photomicrograph shown in A. **D.** Schematic diagram (LHS) and corresponding histological section (RHS) showing CTB injection site in the thoracic spinal cord. Contrast, intensity and colour of images have been adjusted for optimal clarity.

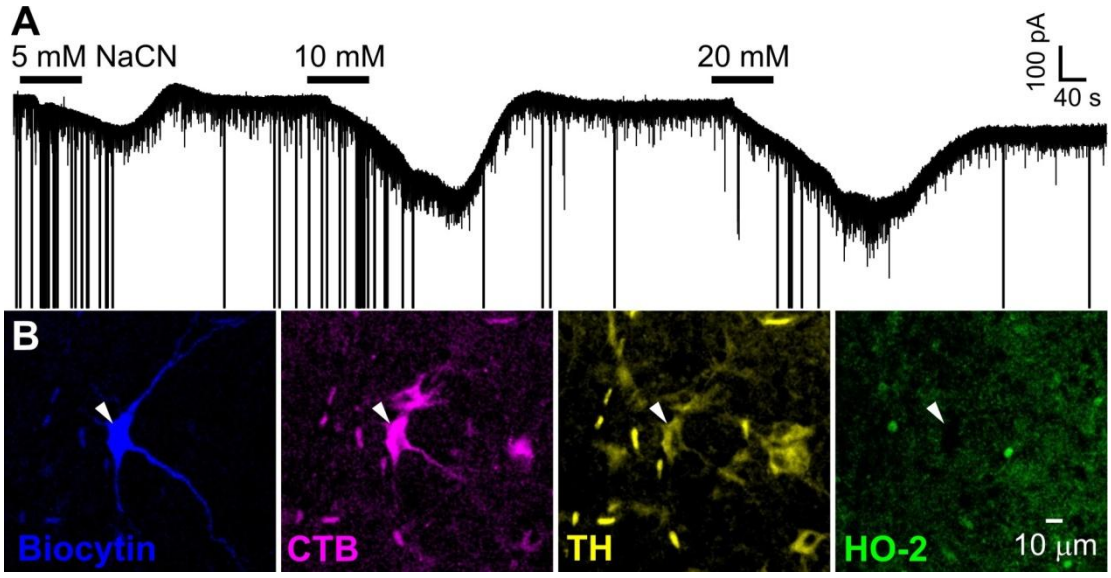

Figure 2.3: Hypoxia-sensitive sympathetic premotor neurons do not contain HO-2 immunoreactivity. A. Dose-dependent responses to NaCN in a bulbospinal RVLM neuron that was filled with biocytin during recording. **B.** Confocal images confirm the same neuron as bulbospinal (CTB) and catecholaminergic (TH), but HO-2 negative. Action currents in A have been truncated for clarity. Contrast, intensity and colour of images in B have been adjusted for optimal display.

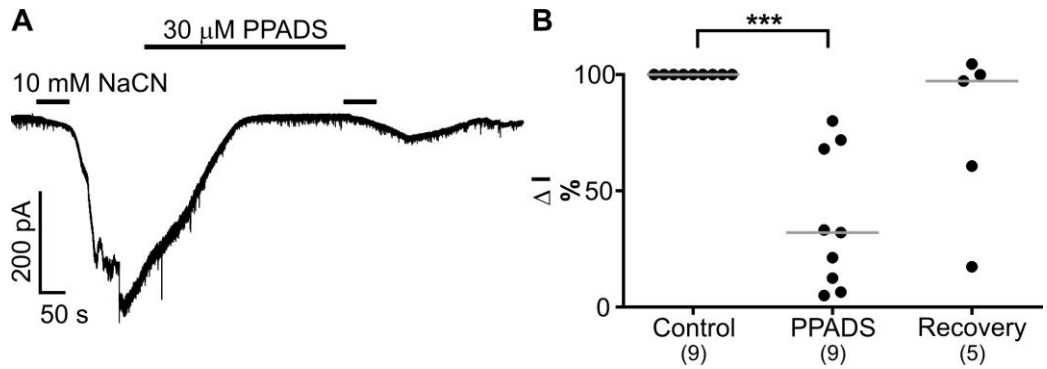

Figure 2.4: Blockade of ionotropic ATP receptors attenuates responses to 10 mM NaCN in RVLM sympathetic premotor neurons. A. Voltage-clamp recording of responses to acute chemical hypoxia before and after the addition of PPADS to the perfusion. Experiment conducted using aCSF containing TTX. **B.** Pooled data: *** $P < 0.001$, numbers of cells in parentheses. Grey horizontal line indicates median.

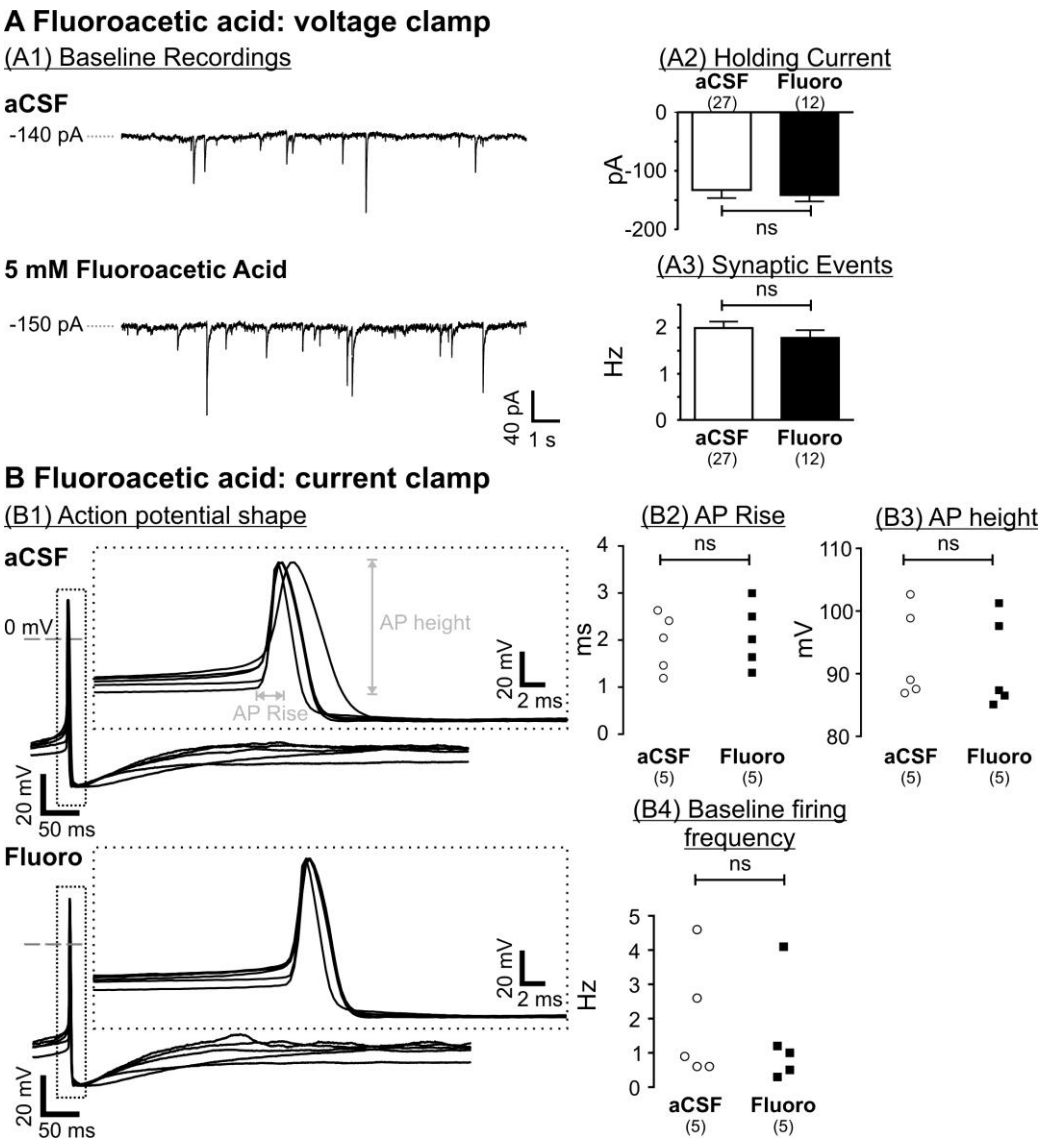

Figure 2.5: Incubation of slices in glial metabolic inhibitor fluoroacetic acid (5 mM) for 30 - 60 minutes has no measureable effect on baseline electrophysiological properties recorded in bulbospinal RVLM neurons. **A.** In voltage clamp mode there was no significant effect of fluoroacetic acid incubation on current (A1) or synaptic current frequency (A2). **B.** In current clamp there was no effect of fluoroacetic acid incubation on electrophysiological parameters measured from spontaneous action potentials. B1 shows superimposed action potentials recorded after incubation in aCSF (n = 5) holding or fluoroacetic acid (n = 5); insets show expanded detail of boxed portions and indicates measured variables. There was no measureable effect of fluoroacetic acid incubation on the duration of the rising phase of the action potential (AP Rise, B2), the height of spontaneous action potentials (AP height, B3), or the frequency of spontaneous action potentials (B4). Numbers of cells in parentheses.

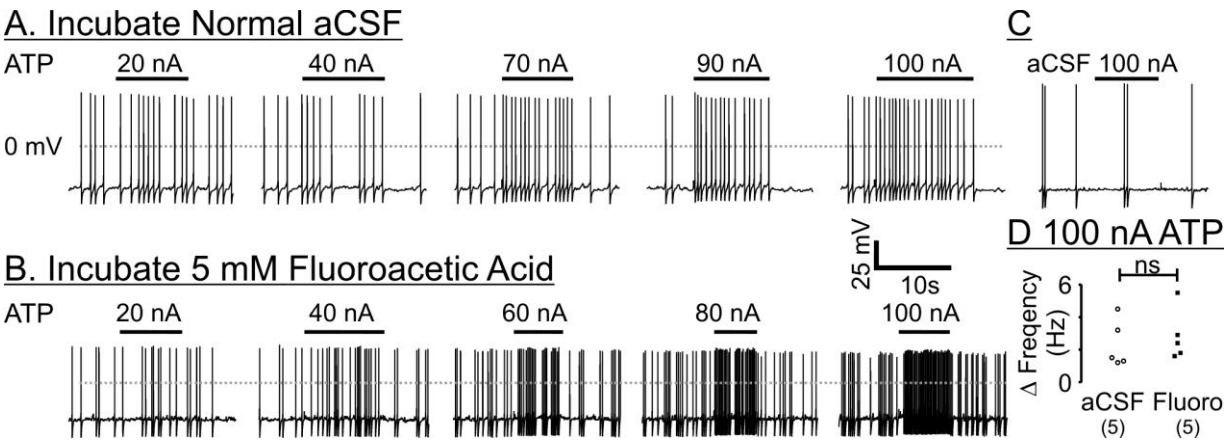

Figure 2.6: Neuronal firing in response to 20 – 100 nA ATP iontophoresis in bulbospinal RVLM neurons incubated for 30 - 60 minutes in **(A)** aCSF or **(B)** fluoroacetic acid. **C.** No firing was evoked by 100 nA delivered via a pipette containing aCSF without ATP. **D.** Pooled data of responses to 100 nA ATP iontophoresis.

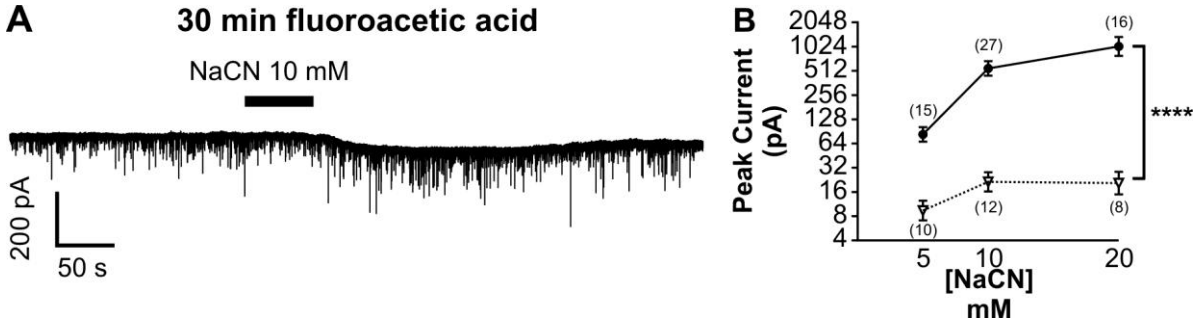

Figure 2.7: Incubation of slices in fluoroacetic acid abolished responses to NaCN in RVLM bulbospinal neurons. A. Response to 10 mM NaCN in a bulbospinal neuron after 30 minutes incubation in 5 mM fluoroacetic acid. **B.** Pooled data from bulbospinal neurons incubated for 30 - 60 minutes in fluoroacetic acid (open triangles) and bulbospinal neurons incubated in normal aCSF (same data as Figure 2.1, closed circles). Numbers of neurons in parentheses.

CHAPTER 3: OREXINERGIC ACTIVATION OF MEDULLARY PREMOTOR NEURONS MODULATES THE ADRENAL SYMPATHOEXCITATION TO HYPOTHALAMIC GLUCOPRIVATION

ABSTRACT

Glucoprivation activates neurons in the perifornical hypothalamus (PeH) and in the rostral ventrolateral medulla (RVLM), which results in release of adrenaline. The current study aimed to establish (i) whether neuroglucoprivation in the PeH or in the RVLM elicits adrenaline release *in vivo*; and (ii) whether direct activation by glucoprivation or orexin release in the RVLM modulates the adrenaline release. Neuroglucoprivation in the PeH or RVLM was elicited by microinjections of 2-deoxy-D-glucose or 5-thio-D-glucose in anesthetized, euglycemic, rats. We found that inhibition of neurons in the PeH abolished the increase in adrenal sympathetic nerve activity (ASNA) to systemic glucoprivation. Secondly, glucoprivation of neurons in the PeH increased ASNA. Thirdly, *in vivo* or *in vitro* glucoprivation did not affect the activity of RVLM adrenal premotor neurons. Finally, blockade of orexin receptors in the RVLM abolished the increase in ASNA to neuroglucoprivation in the PeH. The evoked changes in ASNA were directly correlated to levels of plasma metanephrine, but not to normetanephrine. These findings suggest that orexin release modulates the activation of adrenal presympathetic neurons in the RVLM.

INTRODUCTION

Glucoprivation is a metabolic challenge capable of eliciting adrenaline release, an important mechanism for restoration of normal blood sugar levels. Additionally, neuroglucoprivation produced by 2-deoxy-D-glucose (2-DG) is used as an experimental tool to study glucoregulatory neurons (Borg et al., 1995, Sanders and Ritter, 2001, Andrew et al., 2007, Gonzalez et al., 2008). Previous findings suggest that adrenaline release in response to glucoprivation involves activation of neurons in the perifornical hypothalamus (PeH) and rostral ventrolateral medulla (RVLM). Systemic glucoprivation using 2-DG excites RVLM sympathetic premotor neurons (Ritter et al., 1998, Verberne and Sartor, 2010) and orexinergic neurons (Sakurai et al., 1998) in the PeH (Briski and Sylvester, 2001). Additionally, neurotropic viruses injected into the adrenal gland trans-synaptically label neurons in both the RVLM (Strack et al., 1989b) and PeH (Jansen et al., 1995). Disinhibition of perifornical neurons produces an increase in endogenous glucose production in the liver, which is mediated by the autonomic nervous system (Yi et al., 2009). However, it remains unknown as to whether intrinsic glucose sensitivity or projections from hypothalamic glucose-sensitive neurons (Oomura et al., 1974, Burdakov et al., 2005, Gonzalez et al., 2008) plays an important role in the excitation of RVLM adrenal premotor neurons in response to glucoprivation. In particular, if the responses evoked in RVLM neurons are modulated by orexinergic inputs (De Lecea et al., 1998, Peyron et al., 1998).

In this study, we hypothesize that perifornical hypothalamic neurons respond to neuroglucoprivation, and elicit adrenaline release by orexinergic activation of sympathetic premotor neurons in the RVLM. To test this hypothesis, we used a combination of *in vivo* and *in vitro* electrophysiological techniques to first examine the role played by neurons in the PeH in driving adrenal sympathetic nerve activity (ASNA). We then demonstrate for the first time that these effects are independent of any intrinsic sensitivity of neurons in the RVLM to glucoprivation, and that the activation of orexin receptors in the RVLM modulates the adrenal sympathoexcitatory responses.

MATERIALS AND METHODS

Experiments were performed according to the "*Australian Code of Practice for the Care and Use of Animals for Scientific Purposes".* All experiments were approved by the Austin Health (2012/4764) and Macquarie University (2011/055) Animal Ethics Committees.

IN VIVO EXPERIMENTS

General procedures

Adult male Sprague-Dawley rats (250 - 350 g) were anesthetized with isoflurane (1.7 % in 100 % O_2). The left femoral vein and artery were cannulated for drug administration and arterial blood pressure (AP) recording, respectively. Body temperature was kept at 37 ± 0.5 ^{o}C by a thermocouple-controlled heating pad. The rats were tracheostomized, paralyzed (pancuronium bromide; 1 mg*kg^{-1}, i.v.; supplemented by 0.1 mg*kg^{-1}*h^{-1}), and artificially ventilated with oxygen-enriched air (3.5 ml, 70 cycles*min^{-1}). Following completion of surgery, isoflurane was replaced by urethane (1.2 g*kg^{-1}; i.v.). The level of anesthesia was monitored by hindpaw pinch and the corneal reflex; urethane was supplemented (0.2 g*kg^{-1} i.v.) as required. After neuromuscular blockade, anesthesia was maintained at a level in which paw pinch produced minimal changes in blood pressure (≤ 10 mmHg). Blood glucose was measured by withdrawing a drop of ar blood from the femoral artery and applied to a glucometer (Optium Xceed; Medisense; Abbott Laboratories, Bedford, USA), as previously described (Verberne and Sartor, 2010).

Adrenal sympathetic nerve recording

The right adrenal sympathetic nerve was prepared for recording via a retroperitoneal approach. Fibers emerging from the ganglion projecting towards the adrenal gland were carefully dissected free from connective tissue and fat. The fibers were tied together using 10 - 0 surgical nylon, cut distally, and mounted on bipolar silver wire electrodes. The nerve was covered with paraffin oil or embedded in a silicone elastomer (Kwik-Cast Sealant, WPI, Sarasota, FL, USA). Adrenal sympathetic nerve activity (ASNA) was amplified (x 10000; Grass 7P5B, Quincy, MA, USA) filtered (100 Hz - 3 kHz), and sampled at 6 kHz using a CED Power1401 (Cambridge Electronic Design, UK) with Spike2 v7.02 software. ASNA was rectified and integrated (τ = 1s) prior to analysis. All neurograms were normalized with reference to the resting level prior to stimulus (100 %) after subtraction of the noise (0 %),

determined *post mortem* or after clonidine (200 µg*kg^{-1}, i.v.; Sigma-Aldrich). Experiments were not included for analysis if the ratio of pre-/post- ganglionic ASNA was higher than 50 %, verified by intravenous hexamethonium (40 mg*kg^{-1}, Sigma-Aldrich) at the end of the experiments.

Measurement of blood catecholamines

Due to the rapid degradation of catecholamines, we measured plasma levels of metanephrines (Lenders et al., 2002). Plasma (0.2 ml) was extracted from blood (0.5 ml), withdrawn from the femoral arterial cannula, to determine the levels of metanephrine and normetanephrine. Plasma metanephrines were assayed by liquid chromatography tandem mass spectrometry, modified from the method of Whiting (2009). Heparinized plasma samples had deuterated internal standards for each analyte that were added prior to solid phase extraction using weak cation exchange. Extracted samples were evaporated to dryness, reconstituted and derivatised using cyanoborohydride and acetaldehyde prior to chromatographic separation and mass spectrometric detection using multiple reactions monitoring (model 6460 Agilent Technologies, Mulgrave, Australia).

Location of the PeH and RVLM

The perifornical hypothalamus (PeH) was located using stereotaxic coordinates (Paxinos and Watson, 1998). These were: 2.9 - 3.4 mm caudal to Bregma, 1.1 - 1.3 mm lateral to the midline, 8.6 - 8.7 mm ventral to the dorsal surface.

RVLM adrenal sympathetic premotor neurons are mingled with cardiovascular premotor neurons (Verberne and Sartor, 2010). Hence, the RVLM was identified by extracellular recording of cardiovascular sympathetic premotor neurons, which were inhibited by phenylephrine (10 µg*kg^{-1}; i.v.; Sigma-Aldrich - Supplementary figure 3.1) (Brown and Guyenet, 1985, a, Verberne and Sartor, 2010). These neurons were identified following antidromic field potential mapping of the facial nucleus, elicited by electrical stimulation (0.5 Hz, 0.1 ms, 0.5 - 1.0 mA) of the facial nerve. Extracellular recordings were made using glass microelectrodes (2 mm OD, 5 - 9 MΩ) filled with 2 % Pontamine Sky Blue in 0.5 M sodium acetate. Extracellular potentials were recorded using a window discriminator and amplifier (x 10000; 400 - 4000 Hz; Fintronics, Orange, USA). RVLM sympathetic premotor neurons

were found at: + 0.1 rostral to - 0.3mm caudal, 0.1 - 0.3 mm medial, and 0.1 - 0.3 mm ventral to the caudal pole of the facial nucleus.

Glucoprivation and microinjections

All experimental procedures were conducted following establishment of a euglycemic baseline (4.8 - 7.0 mM; average: 6.1 ± 0.1 mM, n = 60). Systemic glucoprivation was produced by 2DG (250 mg*kg-1, i.v.; Sigma-Aldrich). Microinjections were performed using multibarrel micropipettes. All drugs were diluted in a solution of latex fluorescent beads 2 % (Invitrogen) in artificial cerebrospinal fluid (aCSF (in mM): NaCl, 128; KCl, 2.6; NaH2PO4, 1.3; NaHCO3, 2; CaCl2, 1.3; MgCl2, 0.9). All microinjections were 50 nl. Neuroglucoprivation was elicited by microinjections of 2DG (0.2 - 20 mM) or 5-thio-D-glucose (5-TG; 0.6 - 600 mM; Sigma-Aldrich), using doses based on previous reports (Shiraishi and Simpson, 1987, Andrew et al., 2007). Perifornical neurons were permanently inhibited by the GABAA agonist muscimol (4 mM; Sigma-Aldrich) or disinhibited by the GABAA antagonist bicuculline (1 mM; Sigma-Aldrich). Note that these agents were used primarily to inhibit or activate hypothalamic neurons, and also to determine the role of their respective GABAergic inputs in glucose homeostasis. Orexin A (0.1 - 10 mM; Sigma-Aldrich) was microinjected into the RVLM using doses based on a previous study (Shahid et al., 2012). Orexin receptors in the RVLM were blocked using the non-selective antagonist TCS1102 (5 mM; Tocris), diluted in 50 % dimethyl sulfoxide (DMSO, Sigma-Aldrich) using a dose based on a previous report (Hsiao et al., 2012).

Histology

At the end of the experiments, animals were perfused with NaCl 0.9 % w/v followed by 10 % formalin. Brains were removed, fixed in formalin overnight, and cut with a vibratome in 100 µm coronal sections. Sections were mounted onto gelatin-subbed slides for identification of the injection sites. Sections were examined under epi-fluorescence to locate the fluorescent bead deposits. The center of the injections were photographed (Sony DXC-9100P; Tokyo, Japan), and plotted (Supplementary figure 3.1) with reference to a rat brain atlas (Paxinos and Watson, 1998).

***IN VITRO* EXPERIMENTS**

Voltage-clamp recordings from putative rvlm sympathetic premotor neurons

Sprague Dawley rat pups (P5 – P20) were anesthetized with 2 - 5% isoflurane (Veterinary Companies of Australia) in oxygen and moved onto a heated pad. A dorsal laminectomy was performed and the T2 spinal cord exposed. Fluorescently conjugated cholera toxin β subunit (CTB-Alexa 555, 0.5 – 1 %, Invitrogen) was injected bilaterally at co-ordinates corresponding to the intermediolateral cell column (100 nl injections each side). After completion of microinjections the wound was closed with cyanoacrylate glue and anesthesia discontinued. Pups were allowed to recover on a warm pad until ambulatory and were then returned to the cage with their mother and littermates. Post-operative rats were carefully monitored and treated with additional analgesia when indicated (Carprofen, 2 mg/kg s.c. Norbrook pharmaceuticals, Australia).

Whole-cell recordings from RVLM medullospinal neurons

Solutions (mM):

Cutting solution: 118 NaCl, 25 $NaHCO_3$, 3 KCl, 1.2 $NaH_2PO_4.H_2O$, 10 D-glucose, 1.5 $CaCl_2$, 1 $MgCl_2$; equilibrated with 95 % O_2 – 5 % CO_2 (Burdakov and Ashcroft, 2002).

aCSF: 125 NaCl, 21 $NaHCO_3$, 2.5 KCl, 1.2 $NaH_2PO_4.H_2O$, 2 D-glucose, 2 $CaCl_2$, 2 $MgCl_2$; equilibrated with 95 % O_2 – 5 % CO_2 (pH = 7.35).

Potassium gluconate internal solution: 125 K-gluconate, 10 Hepes, 11 EGTA, 15 NaCl, 1 $MgCl_2$, 2 MgATP, 0.25 NaGTP, 0.05% biocytin (pH = 7.3, 280 < Osmolarity < 285 mOsm).

2 - 5 days after tracer microinjection pups were anaesthetized with isoflurane and quickly decapitated. The whole brain was quickly removed and dissected in ice cold oxygenated cutting solution; the brainstem was mounted in a vibratome and 300 µm thick coronal sections were cut under ice-cold carbogen-bubbled cutting solution. 3-4 sections from the region immediately caudal the facial nucleus were retained and transferred to carbogen-bubbled aCSF containing 2 mM glucose at 34 ^{o}C for at least 1h. Recordings were performed at room temperature in the recording chamber of an Olympus microscope superfused at 1.5 – 2 ml/min with carbogen-bubbled aCSF.

Tracer-labeled neurons were identified under epi-fluorescence: CTB-filled neurons lying ventral to nucleus ambiguus and lateral to the inferior olive were identified as RVLM putative sympathetic premotor neurons. Whole-cell recordings were made in voltage - or

current-clamp modes using borosilicate pipettes with 1.5 - 2 µm tip diameters (3 – 6 MΩ). After formation of a gigaseal, recordings were obtained using a Multiclamp 700B patch clamp amplifier (Molecular Devices, USA). Baseline recordings were made for 300 seconds prior to 2DG administration. Series resistance compensation of 70 - 80 % was used in voltage clamp recordings. Recorded parameters were digitized using Spike2 with a Power 1401 mark II (Cambridge Electronic Design, UK). Data from 3 neurons recorded with the addition of 1 µM tetrodotoxin (TTX, Jomar Bioscience) to the aCSF were included in the dataset. At the conclusion of recordings the pipette was withdrawn and slices were fixed overnight in 4 % paraformaldehyde and then frozen in cryoprotectant prior to immunohistochemical processing for biocytin and tyrosine hydroxylase immunoreactivity.

Immunohistochemistry

Sections containing biocytin-labelled neurons were removed from cryoprotectant, washed, and permeabilized in PBS with 0.5 % Triton X- 100 for 12 hours at 4 ^{o}C. The sections were incubated in blocking solution (5 % bovine serum albumin, BSA, in PBS) for 4 hours at room temperature followed by incubation in mouse anti-tyrosine hydroxylase primary antibodies (TH - 1:2000, Sigma-Aldrich) for 4 hours at room temperature in 5 % BSA. Sections were then washed and incubated in secondary antibodies (Cy5 Donkey anti-Mouse and ExtrAvidin FITC (both 1:500, Jackson Immunoresearch) with 5 % BSA for 4 hours at room temperature, then washed, mounted and coverslipped. Sections were visualized and photographed using a Zeiss Z1 microscope (Carl Zeiss, USA), under epi-fluorescence with appropriate filter sets.

Data analysis

The effects of 2-DG were assessed by comparing the holding current and the synaptic current frequency, averaged over 50 seconds prior to drug administration (baseline), to the mean over the last 50 seconds of drug perfusion (drug). The dose of 2-DG (5 mM) was selected based on previous reports (Burdakov et al., 2005, Gonzalez et al., 2008).

D'Agostino & Pearson omnibus test was performed to verify normal distribution of the data. Changes in ASNA are presented as mean±S.E.M., determined from a 60 second window average, compared along time. Student's *t*-test, one-way ANOVA, and two-way ANOVA with the Bonferroni corrections were used for group comparisons. Correlations were determined by the Pearson or Spearman tests for parametric and non-parametric samples, respectively;

with linear regression to determine confidence intervals. Data that fit a normal distribution are presented as mean±SEM; non-parametric data are expressed as median (range). Statistical significance was determined when $P < 0.05$. All tests were performed using the GraphPad Prism 5.0.

EXPERIMENTAL PROTOCOLS

1. ASNA was plotted against levels of circulating metanephrines to establish the relationship between nerve discharge and adrenaline release. Two samples were taken per experiment: during the resting condition when ASNA recordings had been stable for 10 minutes and ~ 6 - 10 minutes after intravenous injection of 2-DG.

2. ASNA responses to intravenous 2-DG were tested after microinjection of muscimol or bicuculline into the PeH to determine the role of GABAergic drive to perifornical neurons in adrenal sympathetic responses to glucoprivation. 2-DG was also microinjected after bicuculline to determine its pharmacological effect in the absence of inhibitory tone to perifornical neurons. Lumbar sympathetic nerve activity (LSNA) and ASNA were recorded to determine if sympathetic responses to glucoprivation are differentially regulated.

3. The effects of focal PeH neuroglucoprivation on ASNA were determined by bilateral microinjections of 2-DG or 5-TG, according to previous reports (Shiraishi and Simpson, 1987, Andrew et al., 2007).

4. ASNA was compared before and after bilateral microinjections of 2-DG into the RVLM to determine whether adrenal RVLM sympathetic premotor neurons were responsive to glucoprivation *in vivo*. Subsequent intravenous injection of 2-DG confirmed that the ASNA responses were not dependent on a direct effect on RVLM neurons.

5. The intrinsic sensitivity of RVLM sympathetic premotor neurons to glucoprivation was also tested *in vitro*. Following the establishment of stable recordings in aCSF containing 2 mM glucose slices were perfused for 300 s in aCSF containing 5 mM 2-DG (Burdakov et al., 2005, Gonzalez et al., 2008). The effect of glucoprivation on membrane potential and spontaneous discharge frequency was assessed by comparing measurements made over the final 50 s of the control period to the final 50 s of 2-DG application. Membrane resistance was monitored by measuring changes in membrane potential evoked by hyperpolarizing currents (- 40 pA, 1

s) every 30 seconds and calculated using Ohm's Law (Gonzalez et al., 2008). The average membrane resistance measured over the final 3 steps of the control period was compared to data measured at the corresponding periods of 2-DG administration. Neuronal excitability was assessed by comparing the number of action potentials generated by depolarizing current pulses (20 pA, 3 s) every 60 seconds (Burdakov et al., 2005). As described above data were averaged from the final 3 consecutive depolarizing steps in the control and 2-DG periods. Voltage clamp ramps from 0 to - 140 mV from a holding potential of - 60 mV were performed to assess current-voltage relationships (Gonzalez et al., 2008).

6. These experiments determined whether orexinergic activation of premotor neurons in the RVLM mediates the adrenal sympathoexcitatation to glucoprivation. Orexin receptors were activated using microinjections of orexin A at different doses before and after microinjection of the antagonist TCS1102. Adrenal sympathoexcitation in response to microinjection of 2-DG into the PeH was also tested following microinjections of TCS1102 or vehicle into the RVLM.

RESULTS

CORRELATION OF ASNA AND PLASMA METANEPHRINES

At rest, the levels of blood glucose were 6.0 ± 0.1 mM (n = 8); systemic glucoprivation (2-DG, 250 mg/kg) increased the concentration of plasma metanephrine (3.4 ± 0.7 vs. 18.4 ± 4.4 pmol*l^{-1}, P = 0.008, n = 8), a methylated metabolite of adrenaline, in direct proportion to the increase in ASNA (P < 0.001, Spearman r = 0.79, n = 15; figure 3.1). In contrast, 2-DG failed to change the levels of normetanephrine (49.1 ± 9.9 vs. 44.3 ± 5.6 pmol*l^{-1}, P = 0.583, n = 8), a methylated metabolite of noradrenaline. Hence, changes in the levels of normetanephrine were not correlated with ASNA (P = 0.849, Spearman r = - 0.05, n = 15).

ROLE OF PERIFORNICAL NEURONS IN DRIVING SYMPATHETIC RESPONSES TO GLUCOPRIVATION

ASNA responses to systemic 2-DG (250mg/kg) in intact rats were compared to those measured following inhibition of perifornical neurons with microinjections of muscimol (4 mM). Prior to 2-DG administration, blood glucose was at 6.0 ± 0.2 mM (n = 14). Systemic glucoprivation increased ASNA (165 ± 12 %, P < 0.001, n = 17), which peaked at ~ 6 min (figure 3.2. A & B). Bilateral microinjections of muscimol into the PeH abolished the ASNA increase to systemic 2-DG (88 ± 9 %, P < 0.001, n = 6; figure 3.2. C & D). By contrast, following establishment of a stable glucose baseline (6.0 ± 0.2 mM; n = 8) unilateral microinjection of bicuculline (1 mM) into the PeH increased ASNA (199 ± 14 %, P < 0.001, n = 8) while subsequent microinjection of 2-DG reduced ASNA (143 ± 12 %, P < 0.001, n = 8; figure 3.2. E & F). Systemic glucoprivation (2-DG; 250mg/kg) selectively increased ASNA (162 ± 9%, P < 0.001, n = 6), but did not affect LSNA (101 ± 6 %, P = 0.22, n = 6). By contrast, elevation of blood pressure (phenylephrine, 10 µg*kg^{-1}) or blockade of sympathetic ganglionic transmission (hexamethonium, 40 mg*kg^{-1}) reduced only LSNA (figure 3.2. G & H).

EFFECTS OF NEUROGLUCOPRIVATION IN THE PeH

Perifornical focal microinjection of 2-DG or 5-TG evoked adrenal sympathoexcitation (figure 3.3). Resting levels of blood glucose prior to 2-DG and 5-TG administration were 6.6 ± 0.3 mM (n = 10) and 6.7 ± 0.1 mM (n = 6), respectively. Bilateral microinjections of 2-DG into the PeH (Shiraishi and Simpson, 1987) dose-dependently augmented ASNA (175 ± 10 %, P <

0.001, n = 10). Bilateral 5-TG also increased ASNA (145 ± 11 %, $P < 0.01$, n = 6). The increases in ASNA in response to either 2-DG or 5-TG were similar in magnitude ($P > 0.05$, n = 6), and correlated with the increases in arterial blood glucose (figure 3.3. D & F).

GLUCOPRIVATION OF RVLM SYMPATHETIC PREMOTOR NEURONS IN *VIVO*

At a blood glucose baseline of 6.4 ± 0.2 mM (n = 6), bilateral microinjections of 2-DG (2 mM) into the RVLM evoked no effect on ASNA (90 ± 12 %, $P = 0.33$, n = 6; figure 3.4). Subsequent systemic injection of 2-DG (250 mg/kg; i.v.) increased ASNA (162 ± 18 %, $P < 0.001$, n = 6).

GLUCOPRIVATION OF RVLM SYMPATHETIC PREMOTOR NEURONS *IN VITRO*

16 sympathetic premotor neurons were recorded in 11 brainstem slices from 5 rats (Figure 3.5). In all but three cases current- and voltage-clamp data were obtained from the same neurons. In no case did 2-DG evoke any clear effect on any parameter recorded. In current clamp the resting membrane potential was -52.7 ± 1.6 mV (n = 15 including 3 neurons recorded with TTX), with spontaneous action potentials occurring at 3.7 ± 0.8 Hz (n = 12). At the end of the 2-DG superfusion the membrane potential (-53.3 ± 1.6 mV, $P = 0.55$, n = 15), spontaneous discharge frequency (3.6 ± 0.8 Hz, $P = 0.46$, n = 12) and input resistance (335 ± 38 vs 327 ± 41 MΩ, $P = 0.35$, n = 14) were unchanged from baseline values. There was no significant change in the number of action potentials evoked by depolarizing current pulses by addition of 2DG to the perfusate (11.8 ± 1.7 vs 10.9 ± 1.6 spikes, $P = 0.48$, n = 12, figure 4.5. D). In voltage clamp mode no changes in holding current (-54.4 ± 7.5 vs -55.9 ± 7.4 pA, $P = 0.54$, n = 13) or response to voltage ramps were noted following addition of 2-DG to the perfusion fluid.

BLOCKADE OF OREXIN RECEPTORS IN THE RVLM DURING NEUROGLUCOPRIVATION OF THE PeH

Microinjection of orexin A into the RVLM produced an increase in ASNA (162 ± 16 %, $P < 0.001$, n = 6) that was blocked by the non-selective antagonist TCS 1102 (99 ± 3 %, $P < 0.001$, n = 6; figure 3.6. A-D). Bilateral microinjections of 2-DG (2 mM) into the PeH increased ASNA (151 ± 16 %, $P < 0.01$, n = 6), following microinjections of vehicle into the RVLM. By contrast, TCS 1102 in the RVLM abolished the increase in ASNA (95 ± 5 %, $P < 0.001$, n = 6) produced by microinjection of 2-DG into the PeH (figure 3.6. E-G).

DISCUSSION

The principal finding in this study is that orexin modulates the activity of RVLM adrenal sympathetic premotor neurons resulting in excitation of adrenal chromaffin cells. We showed that local glucoprivation or disinhibition of PeH neurons increased ASNA while inhibition of PeH neurons abolished the ASNA response following systemic glucoprivation. Conversely, glucoprivation of perifornical neurons subsequent to activation by the $GABA_A$ antagonist bicuculline reduced the adrenal sympathoexcitatory response. In addition, local neuroglucoprivation in the RVLM failed to activate premotor neurons *in vivo* or *in vitro* suggesting that RVLM neurons are not intrinsically glucose sensitive. Finally, ASNA was directly correlated with plasma metanephrine levels but not normetanephrine levels confirming that adrenal sympathoexcitation coincides with adrenaline release into the circulation. The ASNA, noradrenaline, and adrenaline responses to glucoprivation noted in our study were consistent with previous reports of the effects of glucoprivation on sympathetic preganglionic neurons (Morrison and Cao, 2000).

In this study, microinjection of 2-DG/5-TG or bicuculline into the PeH increased ASNA, whereas microinjection of the $GABA_A$ agonist muscimol into the PeH abolished the ASNA response to systemic injection of 2-DG. Reports by others have shown that 2-DG exerts a glucomimetic inhibition of orexinergic and GABAergic perifornical neurons (Burdakov et al., 2005, Gonzalez et al., 2008, Karnani et al., 2013). Thus, direct excitation of perifornical neurons by 2-DG in our study is unlikely to be the mechanism underlying the increase in ASNA. Alternatively, adrenal sympathoexcitation could result from disinhibition of perifornical neurons that receive GABAergic drive (Yi et al., 2009). Orexinergic neurons express GABA receptors (Alam et al., 2005), and may receive inhibitory inputs from adjacent interneurons (Karnani et al., 2013) or from the ventromedial hypothalamus (Chan et al., 2006, Chan et al., 2011). In our study, microinjection of 2-DG into the PeH decreased the ASNA response evoked by prior administration of bicuculline into the same site, confirming the glucomimetic inhibitory effect of 2-DG seen *in vitro* (Burdakov et al., 2005, Gonzalez et al., 2008, Karnani et al., 2013). One interpretation of this result is that 2-DG acts at some location adjacent to the PeH. If so, this could explain the onset (~1min) of the ASNA response to microinjection of 2-DG into the PeH. Consistent with this notion, are previous observations that injection of 2-DG into the ventromedial hypothalamus (Borg et al., 1995)

or into the ventrolateral portion of the lateral hypothalamus (Yoshimatsu et al., 1991) elicits glucoprivic effects resulting in adrenaline release and adrenal sympathoexcitation, respectively. While we have demonstrated that 2-DG can exert inhibitory effects on PeH neurons, consistent with previous observations *in vitro* (Burdakov et al., 2005, Gonzalez et al., 2008, Karnani et al., 2013), the inevitable conclusion is that in our *in vivo* study an excitatory response predominates.

Blockade of orexin receptors in the RVLM by microinjection of TCS1102 eliminated the adrenal sympathoexcitatory response to injections of 2-DG into the PeH. The dose of the orexin antagonist used was sufficient to block the effects of microinjection of orexin into the RVLM on ASNA. Based on the density of the extracellular milieu (Nicholson, 1985) and histology, our injections extended for ~ 400 µm, and so targeted the majority of C1 neurons (Ritter et al., 1998). The ASNA response to microinjection of orexin into the RVLM concurs with previous observations (Shahid et al., 2012). Glucoprivation activates slow-conducting (<1 m/s) RVLM adrenal premotor neurons, which are intermingled with the cardiovascular premotor neurons (Verberne and Sartor, 2010). The slow-conducting axons suggest that they are C1 catecholaminergic cells (Schreihofer and Guyenet, 1997). Glucoprivation also elicits Fos expression (Ritter et al., 1998) and phosphorylation (Damanhuri et al., 2012) in C1 neurons. Orexinergic neurons project to the C1 region of the RVLM (De Lecea et al., 1998, Peyron et al., 1998) and their terminals make close appositions with C1 neurons (Puskas et al., 2010). Moreover, neurotoxic ablation of C1 neurons eliminates the glucoregulatory response to 2-DG (Ritter et al., 2001). Together, the evidence suggests that orexinergic activation of adrenal sympathetic premotor neurons modulates the adrenal sympathoexcitatory response to glucoprivation. Although previous studies (DiRocco and Grill, 1979, Ritter et al., 1981) have shown that selective glucoprivation of hindbrain neurons increases blood glucose; local application of 2-DG failed to activate the RVLM adrenal premotor neurons. Thus, hindbrain glucose-sensitive neurons (Ritter et al., 1998, Dunn-Meynell et al., 2002) are presumably located outside the RVLM, but project to (Aicher et al., 1996) and excite the adrenal C1 neurons.

Whether orexinergic neurons are directly glucose sensitive or they respond to glucoprivation-evoked drive from either glial or neuronal input remains unknown. Researchers have described an important role for glia in driving glucoprivic responses in

other brain systems: first, the existence of central glucose sensors requiring glucose transporter type 2 expression in glial cells in the NTS and the dorsal motor nucleus of the vagus has been identified (Marty et al., 2005). Second, increases in gastric motility recorded following glucoprivation depends on intact hindbrain astrocytes (McDougal et al., 2013, Hermann et al., 2014). Finally, Ainscow and colleagues showed that hypothalamic glia respond to increases in extracellular glucose (Ainscow et al. 2002); so addressing whether hypothalamic astrocytes activates the glucose sensing pathway of orexinergic neurons is a plausible hypothesis that should be investigated.

The present study has explored the neural pathway(s) that relay the adrenal sympathoexcitatory response to neuroglucoprivation. We used 2-DG as a glucoprivic agent *in vivo* because it allows the investigator to produce localized glucoprivation when injected into the brain parenchyma and *in vitro* because it's a non-metabolizable glucose analogue that competes with glucose, depleting available energy, and is easy to use and control. Importantly, systemic 2-DG produces secretion of adrenaline, glucagon, cortisol, and growth hormone (Goldsmith et al., 1970, Ritter et al., 1995). Since 2-DG is also detected by most glucometers, we were unable to determine blood glucose changes after systemic 2-DG. Nonetheless, glucoprivation elicits hyperglycemia via activation of glycogenolysis and gluconeogenesis in the liver (Sanders and Ritter, 2001, Watt et al., 2001, Yi et al., 2009). General anesthesia was essential for measurement of ASNA and eliminated the influence of stress, respiration, or body temperature (Ehrentheil et al., 1967, Shah et al., 1977, Guenther et al., 2012). Anesthesia can alter neural metabolism and modulate glycemia and it is known that intraperitoneal urethane causes hyperglycemia (Reinert, 1964). However, under the conditions of our experiment we found that urethane produced normoglycemic animals (~ 6.1 mM). Comparison of different methods for determining catecholamine levels indicated that plasma metanephrines determined by mass spectrometry is the most reliable method (Lenders et al., 2002). In addition, the age of rat pups used the *in vitro* experiments correspond to previous electrophysiological studies (Cotero and Routh, 2009) and the catecholaminergic neurons are likely to be mature and functional (Roux et al., 2003).

In conclusion, our findings suggest a key role for orexin in modulating the sympathetic drive to the adrenal chromaffin cells during glucoprivation. It is possible that during arousal orexin changes the electrophysiological properties of adrenal premotor neurons facilitating

adrenaline release in response to glucopenia – a mechanism that may be compromised when hypoglycemia unawareness develops in response to recurrent glucoprivation (Sanders and Ritter, 2001).

CHAPTER 3 FIGURES AND TABLES

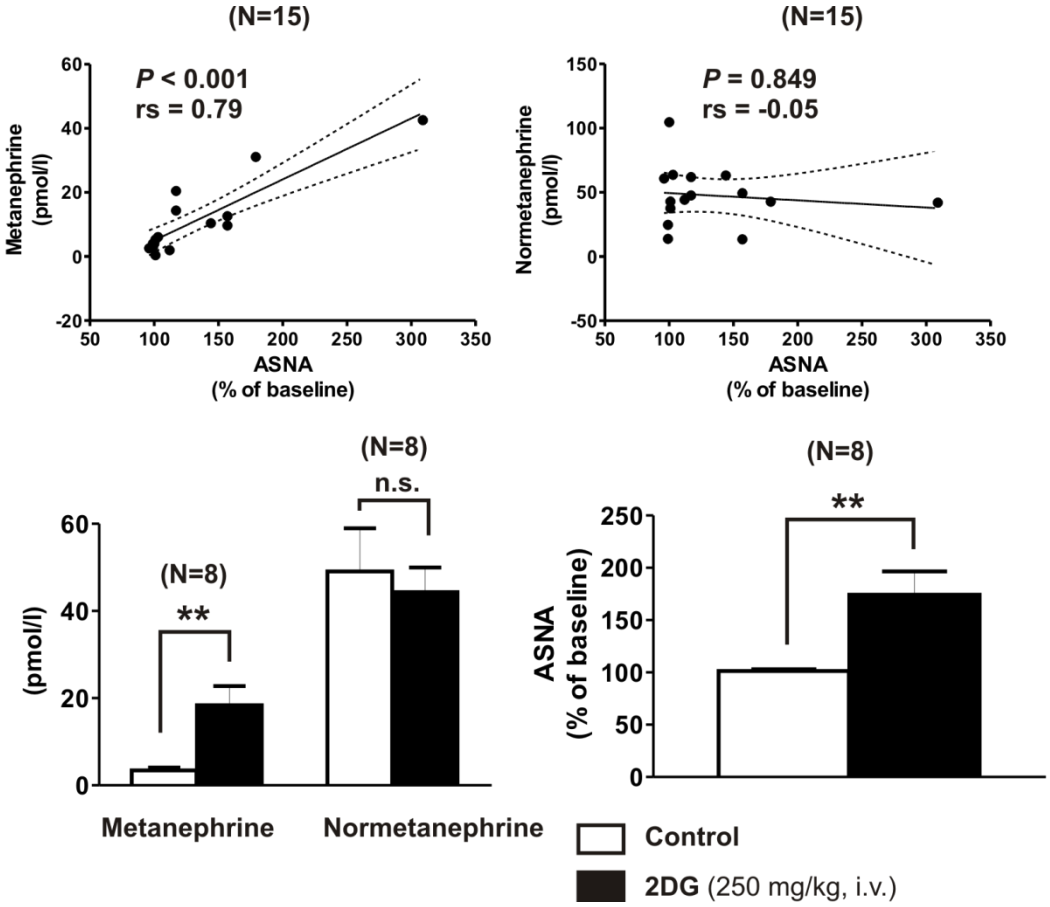

Figure 3.1: Glucoprivation elicits increases in ASNA correlated with the levels of metanephrines. Systemic injection of 2-DG increased adrenal sympathetic nerve activity (ASNA). The increase in ASNA correlated with plasma levels of metanephrine, a methylated metabolite of adrenaline. However, 2-DG failed to alter the levels of normetanephrine, the corresponding methylated metabolite of noradrenaline. All data are presented as mean ± S.E.M. ** $P < 0.01$; n.s. non-significant.

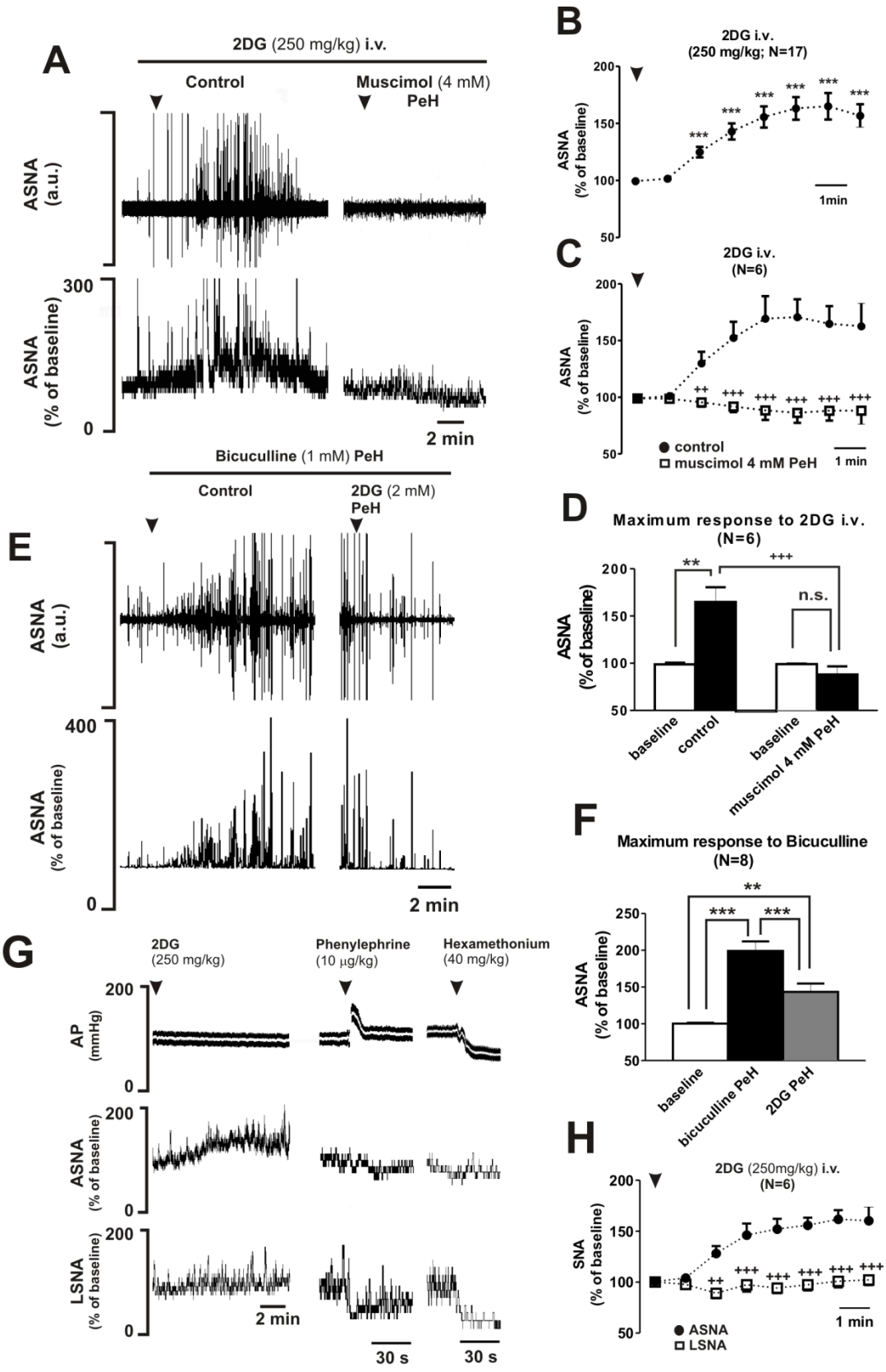

Figure 3.2: Selective effects of glucoprivation on ASNA depends on perifornical neurons. A. Neurograms of adrenal sympathetic nerve activity (ASNA), top: arbitrary units (a.u.) bottom: rectified, integrated, and normalized to % of baseline. Systemic glucoprivation with 2-deoxy-

D-glucose (2-DG) increased ASNA, which was abolished by bilateral microinjections of muscimol into the perifornical hypothalamus (PeH). **B.** Pooled increases in ASNA following 2-DG. **C.** Group data of the response to 2-DG after inhibition of the PeH. **D.** Muscimol in the PeH reduced the maximum increase in ASNA to systemic 2-DG in the group. **E.** Microinjection of bicuculline into the PeH increased ASNA, and subsequent microinjection of 2DG reduced the evoked increase in ASNA. **F.** Group data of maximum ASNA increases to microinjection of bicuculline and 2-DG into the PeH. **G.** Systemic 2-DG increased only ASNA, but did not affect lumbar sympathetic nerve activity (LSNA). **H.** The differential sympathetic response to 2-DG replicated within the group. All data are presented as mean ± S.E.M. ***** $P < 0.05$, ****** $P < 0.01$, ******* $P < 0.001$ to baseline; ++ $P < 0.01$, +++ $P < 0.001$ to control group; n.s. non-significant. AP, arterial blood pressure.

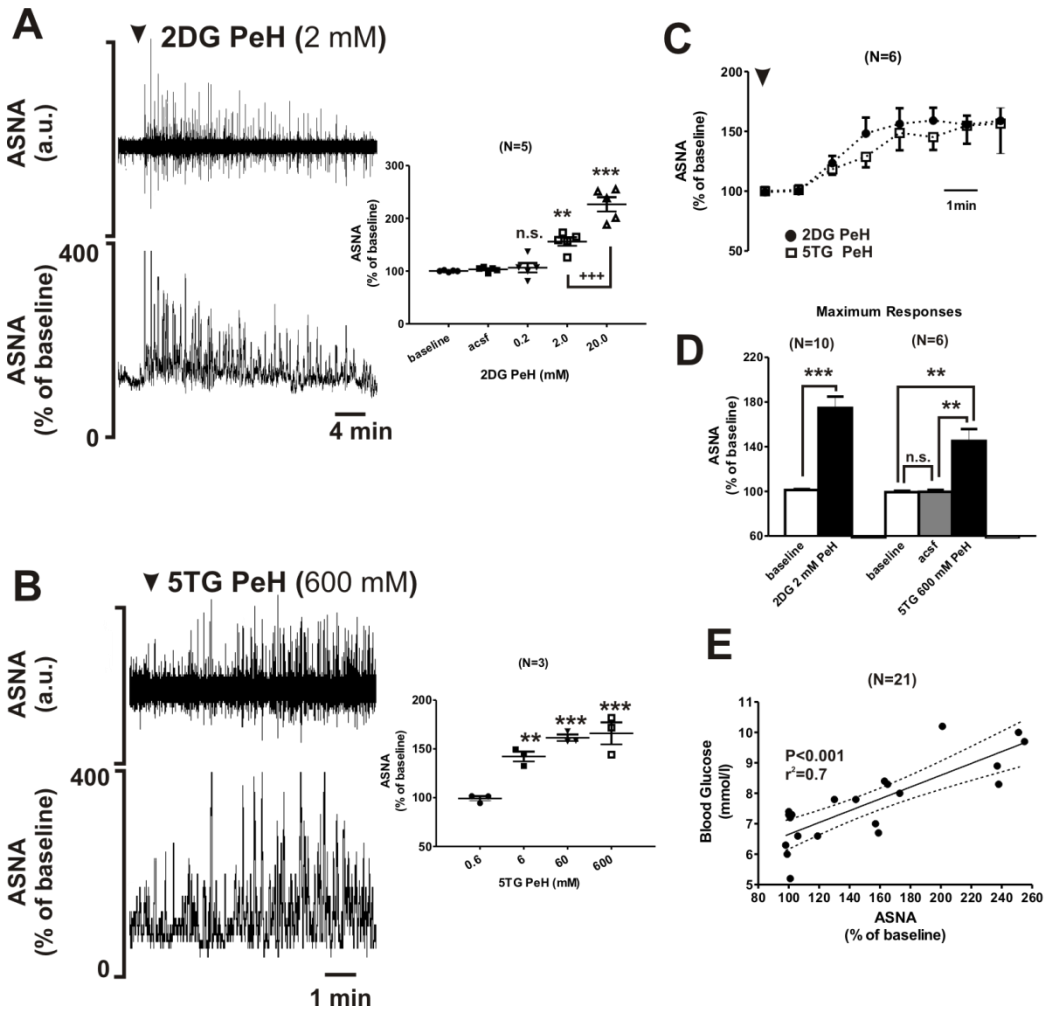

Figure 3.3: Glucoprivation in the PeH increases ASNA. A. Neurograms of raw and rectified, smoothed, and normalized adrenal sympathetic nerve activity (ASNA). Bilateral microinjections of 2-deoxy-D-glucose (2-DG) into the perifornical hypothalamus (PeH) elicited dose-dependent increases in ASNA. **B.** Bilateral microinjections of 5-thio-D-glucose (5-TG) into the PeH also augmented ASNA. **C.** Group data of sympathetic responses to microinjections of 2-DG and 5-TG. **D.** Pooled data of maximum increases in ASNA to 2-DG or 5-TG into the PeH. **E.** Increases in ASNA in response to microinjections of 2-DG and 5-TG into the PeH were directly correlated with levels of blood glucose. All data are presented as mean ± S.E.M. ** $P < 0.01$, *** $P < 0.001$ to baseline; +++ $P < 0.001$ to 2-DG (2 mM); n.s. non-significant. aCSF, artificial cerebrospinal fluid.

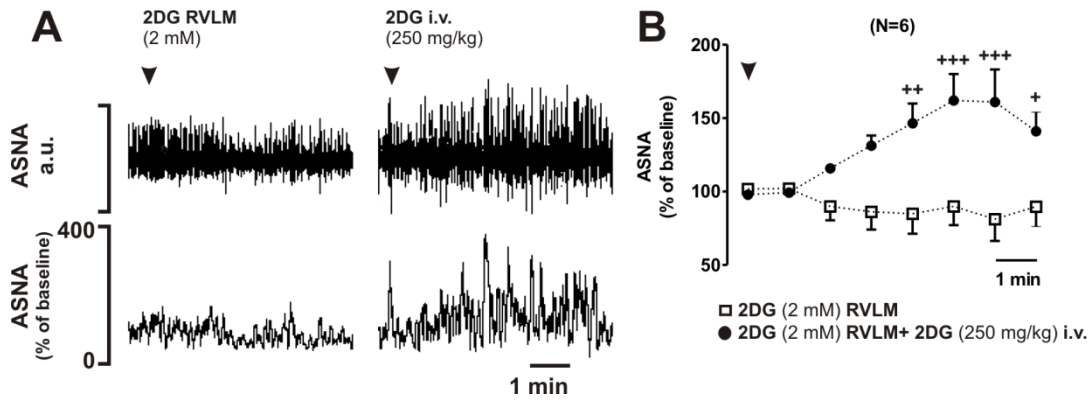

Figure 3.4: RVLM neurons are not glucose-sensitive *in vivo*. A. Neurograms of raw and rectified, smoothed, and normalized (% of baseline) adrenal sympathetic nerve activity (ASNA). Bilateral microinjections of 2-deoxy-D-glucose (2-DG) into the rostral ventrolateral medulla (RVLM), where premotor neurons are found, did not alter ASNA. However, subsequent intravenous injection of 2-DG in the same animal increased ASNA. **B.** Group data of ASNA responses to microinjections of 2-DG into the RVLM, followed by systemic 2-DG. All data are presented as mean ± S.E.M. + $P < 0.05$, ++ $P < 0.01$, +++ $P < 0.001$ to 2-DG into the RVLM; n.s. non-significant.

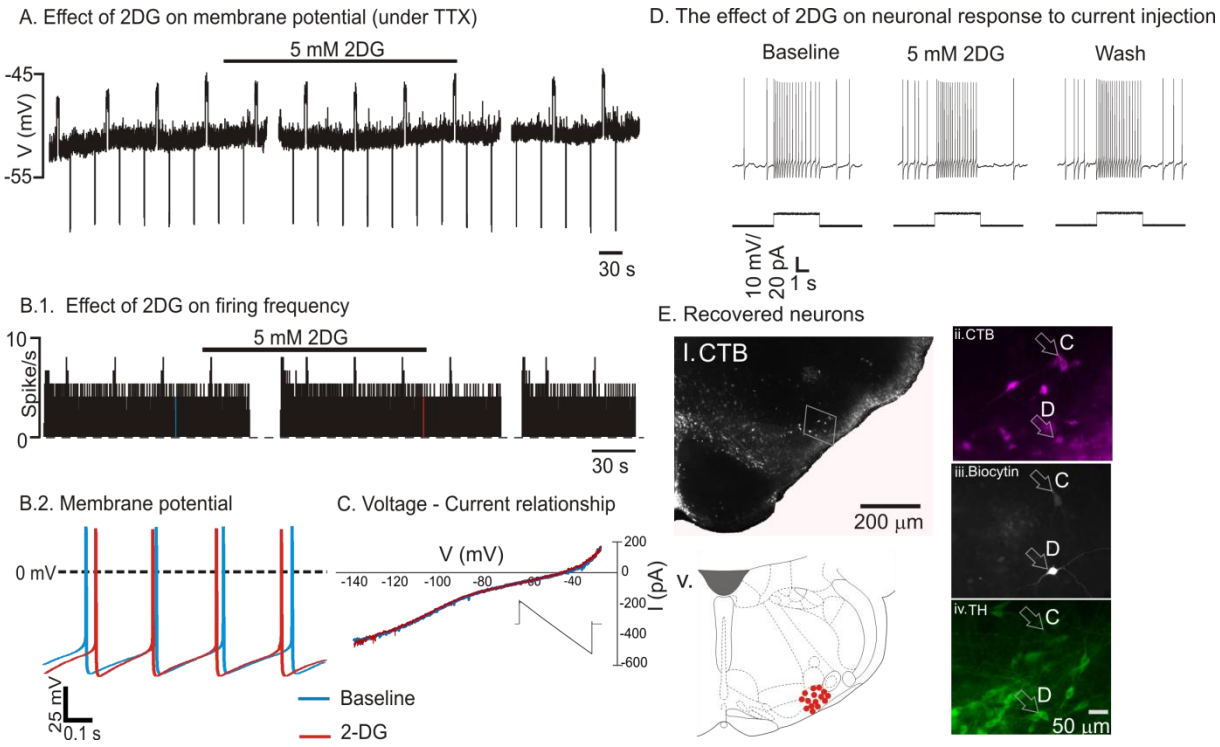

Figure 3.5: 2-DG exerts no direct effect on medullospinal RVLM neurons recorded *in vitro*. **A.** Whole-cell current clamp recording performed in the presence of TTX: bath application of 2-DG exerts no effect on resting membrane potential or resistance. Deflections indicate responses to current injection. **B1.** Current clamp recording showing effect of 2-DG on spontaneous discharge of medullospinal RVLM neuron. Regular increases in firing frequency indicate responses to depolarizing current injections. Breaks in recordings in panels A and B1 indicate recording mode switch. **B2.** Raw data excerpts at points denoted (arrows) in panel B1. **C.** 2-DG exerted no effect on current-voltage relationships recorded in voltage clamp mode. **D.** 2-DG exerted no effect on responsiveness to depolarizing currents (see also panel B1). **E.** In some cases neurons were filled with biocytin during recording and subsequently examined histologically. i. Low power photomicrograph showing distribution of CTB labeling. Field of view of high powered images denoted by box. ii. Two neurons were recorded and recovered in the experiment shown; raw data from each is shown in panels C & D. Both were CTB-labeled (iii) and under close examination C was lightly TH-positive whereas D was TH-negative (iv). v. Schematic diagram showing locations of recorded neurons.

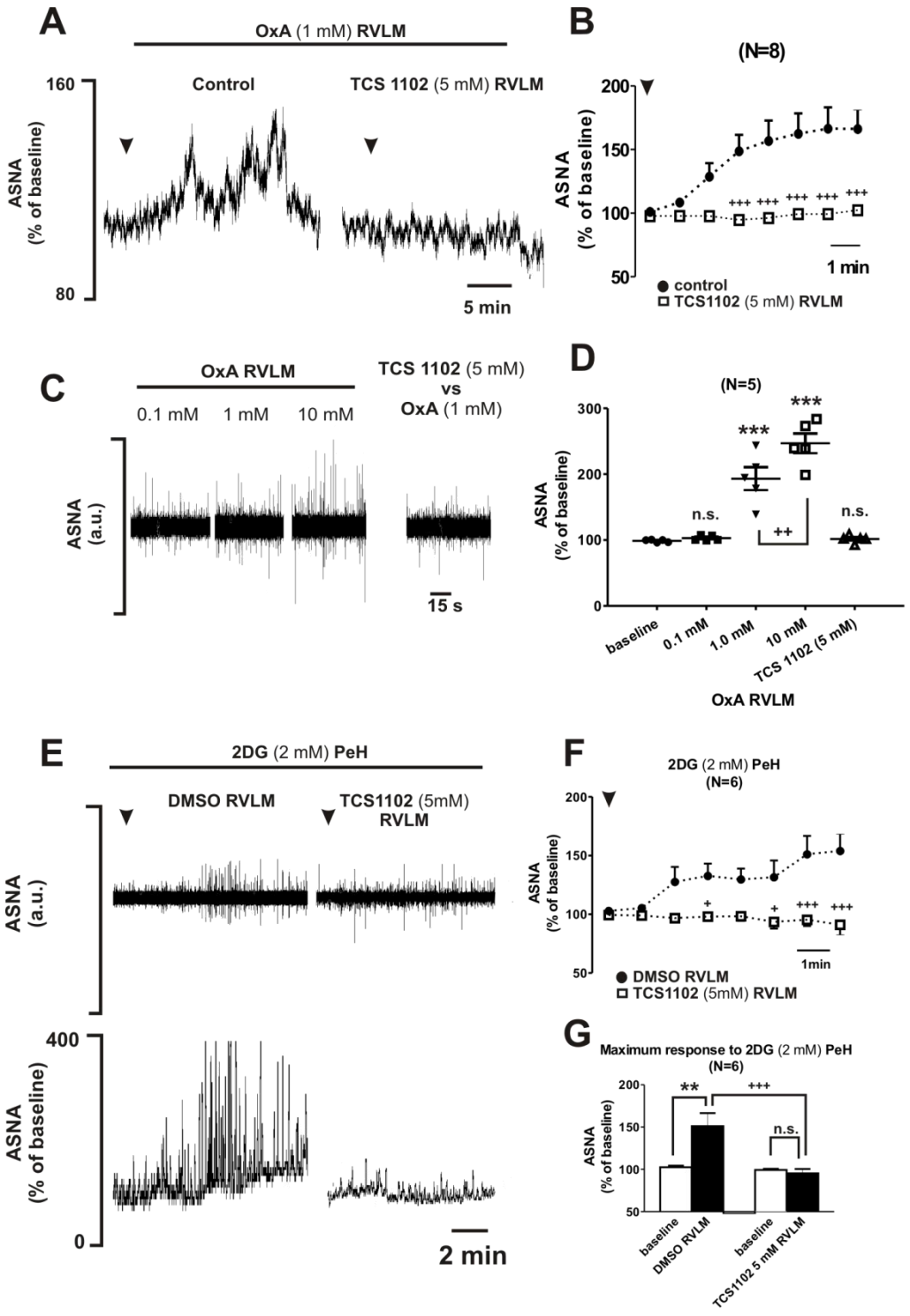

Figure 3.6: Orexin in the RVLM mediates the ASNA increase to glucoprivation. A. Neurograms of rectified, smoothed, and normalized (% of baseline) adrenal sympathetic nerve activity (ASNA). Microinjection of orexin A (OxA) into the rostral ventrolateral medulla (RVLM) produced sympathoexcitation, which was blocked by the non-selective antagonist TCS1102. **B.** The blockade of the response replicated in a group of animals. **C.** Neurograms of raw ASNA. OxA into the RVLM evoked a dose-dependent increase in ASNA that was

antagonized by TCS1102. **D.** The dose-response effect replicated in a group of animals. **E.** Neurograms of raw (Top) and rectified, smoothed, and normalized (Bottom) ASNA. Bilateral microinjections of 2-DG into the perifornical hypothalamus (PeH), following vehicle (50% dimethyl sulfoxide; DMSO) microinjection into the rostral ventrolateral medulla (RVLM), increased ASNA. However, bilateral injections of the antagonist TCS1102 into the RVLM abolished the rise elicited by 2DG in the PeH. **F.** Blockade of the ASNA response replicated in a group of animals. **G.** Grouped data of maximum increases in ASNA to 2-DG in the PeH, subsequent to DMSO or TCS1102 in the RVLM. All data are presented as mean ± S.E.M. ****** $P<0.01$, ******* $P < 0.001$ to baseline; + $P < 0.05$, +++ $P < 0.001$ to control group; ++ $P < 0.01$ to OxA (1mM); n.s. non-significant.

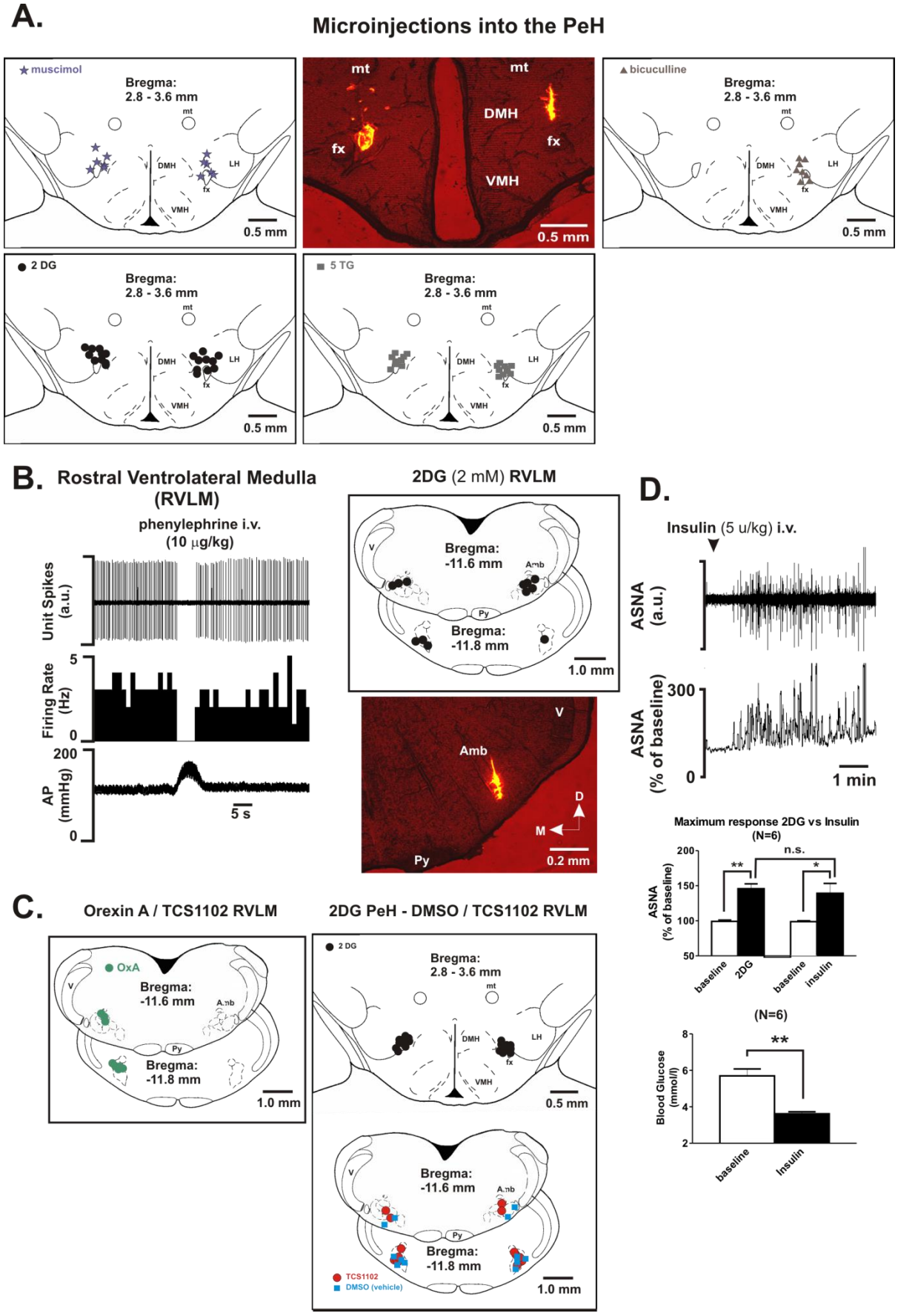

Supplementary Figure 3.1.

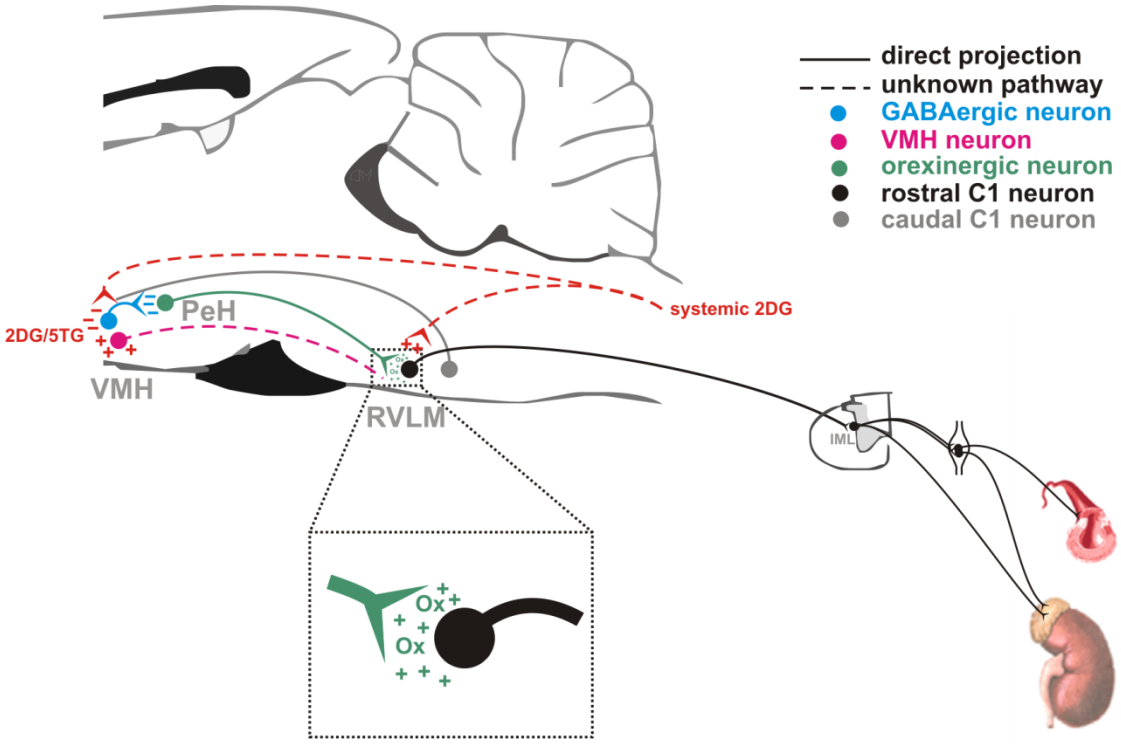

Supplementary Figure 3.2.

CHAPTER 4: SOMATOSTATIN IN THE RAT ROSTRAL VENTROLATERAL MEDULLA: ORIGINS AND MECHANISM OF ACTION

ABSTRACT

Somatostatin (SST) or agonists of the SST-2 receptor (sst_2) in the rostral ventrolateral medulla (RVLM) lower sympathetic nerve activity, arterial pressure and heart rate, or when administered within the Bötzinger region, evoke apneusis. Our aims were to describe the mechanisms responsible for the sympathoinhibitory effects of SST on bulbospinal neurons and to identify likely sources of RVLM SST release. Patch clamp recordings were made from bulbospinal RVLM neurons (n = 31) in brainstem slices prepared from juvenile rat pups. 55% of neurons responded to SST, displaying an increase in conductance that reversed at -93 mV, indicative of an inwardly rectifying potassium channel (GIRK) mechanism. Blockade of sst_2 abolished this effect, but application of tetrodotoxin did not, indicating that the SST effect is independent of presynaptic activity. Fourteen bulbospinal RVLM neurons were recovered for immunohistochemistry; nine were SST insensitive and did not express sst_{2A}. Three out of five responsive neurons were sst_{2A} immunoreactive. Neurons that contained preprosomatostatin mRNA and cholera-toxin-B retrogradely transported from the RVLM were detected in: paratrigeminal nucleus, lateral parabrachial nucleus, Kölliker-Fuse nucleus, ventrolateral periaqueductal grey area , central nucleus of the amygdala , sublenticular extended amygdala , interstitial nucleus of the posterior limb of the anterior commissure nucleus and bed nucleus of the stria terminalis. Thus, those brain regions likely contribute to the sympathoinhibition exerted via sst_2 in the RVLM to mediate sympathoinhibition and/or apneusis.

INTRODUCTION

The inhibitory peptide somatostatin (SST) is expressed widely throughout the brain; its two isoforms, SST-14 and SST-28, act on six receptors, $sst_{1\text{-}5}$ (Bruno et al., 1992, O'Carroll et al., 1992, Vanetti et al., 1992, Yasuda et al., 1992, Hoyer et al., 1995), with sst_2 receptors present in two subtypes, sst_{2A} and sst_{2B} (Vanetti et al., 1992, Vanetti et al., 1994).

The expression of SST and its receptors within the rostral ventrolateral medulla (RVLM), and the functional consequences of SST transmission in this region, has emerged as a topic of considerable interest in both the fields of central respiratory and central cardiovascular control. The medullary distribution of SST partially overlaps with putative markers of respiratory rhythm-generating neurons in the pre-Bötzinger Complex (Stornetta et al., 2003, Gray et al., 2010, Tupal et al., 2014), and pharmacogenetic silencing of SSTergic neurons in and around the pre-Bötzinger Complex causes apnoea *in vivo* (Tan et al., 2008), leading to the proposal that SST may be a marker of pre-Bötzinger complex pacemaker neurons (Gray et al., 2010). Furthermore, microinjection of SST into the Bötzinger region, one target of pre-Bötzinger Complex SSTergic neurons (Tan et al., 2010), evokes apneusis, a gasping breathing pattern characterized by a lengthened inspiratory phase and a shortened expiratory period (Burke et al., 2010).

SST also causes dose-dependent sympathoinhibition, hypotension and bradycardia, as well as attenuation of chemo- and somatosympathetic reflexes, when microinjected into the pressor region of the RVLM (Burke et al., 2008). A direct effect of SST agonists on RVLM sympathetic premotor neurons is presumed to underlie this effect, as sst_{2A} receptors are the predominant receptor subtype expressed in the region and are widely expressed on RVLM C1 and non-C1 neurons (Burke et al., 2008, Spary et al., 2008), including those with bulbospinal projections (Burke et al., 2008). Involvement of other receptor subtypes is unlikely, as sst_5 mRNA is absent from the VLM, and isoforms 1, 2b and 4 are expressed at low levels (Spary et al., 2008, Ramírez-Jarquín et al., 2012). Similarly, we and others have reported pronounced VLM expression of sst_{2a} immunoreactivity, weak expression of sst_4, and no consistent neuronal expression of any other subtype (Burke et al., 2008, Spary et al., 2008). Finally, pre-treatment with the sst_2 selective antagonist BIM-23627 abolishes

cardiovascular responses evoked by both SST and the sst_2 agonist lanreotide (Burke et al., 2008).

The cellular mechanisms that underlie the inhibitory effects of RVLM SST receptor activation, the sources of RVLM SST release, and the circumstances under which SST is released in the RVLM, are unknown. In general, the cellular responses evoked by SST receptor activation are wide ranging, modulating multiple second messenger systems. These include G-protein modulation of adenylate cyclase, Ca^{2+} and K^+ channels, phospholipases, MAP kinase and phosphotyrosine protein phosphatases (Patel, 1999). When sst_{2-5} receptors were co-expressed with a GIRK subunit in oocytes, sst_2 receptors were the most efficient in activating a GIRK mediated current (Kreienkamp et al., 1997). Similarly, whole cell patch clamp recordings of neurons in the periaqueductal grey (Connor et al., 2004) or the substantia gelatinosa of the spinal cord (Nakatsuka et al., 2008) show that SST application evokes a large outward current mediated by K^+ channels consistent with GIRK characteristics, although calcium currents may also be activated (Connor et al., 2004).

Regions innervating the RVLM are well described and widely distributed (Hopkins and Holstege, 1978, Ross et al., 1985, Dampney et al., 1987, Carrive et al., 1988, M'Hamed et al., 1993, Padley et al., 2007, Bowman et al., 2013), as is the brain-wide distribution of neurons expressing SST-immunoreactivity or preprosomatostatin (PPS) mRNA (De León et al., 1992, Gray and Magnuson, 1992, Smith et al., 1994). However, whether or not RVLM-projecting neurons synthesize SST is largely unknown.

Therefore the aims of this study are, firstly, to determine the cellular mechanisms responsible for the inhibition of RVLM sympathetic premotor neurons by SST, using whole cell patch clamp in acute brainstem slices and, secondly, to define likely sources of SST by identifying RVLM-projecting neurons that contain PPS mRNA using a combination of retrograde tracing and *in situ* hybridization.

MATERIALS AND METHODS

All experiments were approved by the Macquarie University Animal Ethics Committee and performed in accordance with the Australian Code of Practice for the Care and Use of Animals for Scientific Purposes.

IN VITRO ELECTROPHYSIOLOGY

Labelling of bulbospinal RVLM neurons

Sprague Dawley rat pups (P5 – P25) were anaesthetized with 2-5% isoflurane (Veterinary Companies of Australia, Pty) in oxygen and moved onto a heated pad. A dorsal laminectomy was performed and the T2 spinal cord exposed. Fluorescently conjugated cholera toxin β subunit (CTB-Alexa 555, 0.5 - 1%, Invitrogen) was injected bilaterally at co-ordinates corresponding to the interomediolateral cell column (1 to 3 100 nl injections each side). After completion of microinjections the wound was closed with cyanoacrylate glue and anesthesia discontinued. Pups were allowed to recover on a warm pad until ambulatory and were then placed back in the cage with their mother and littermates. Post-operative rats were carefully monitored for the duration of experiments and treated with additional analgesia when indicated (Carprofen, 2 mg/kg s.c. Norbrook pharmaceuticals, Australia).

Solutions (mM):

Cutting solution: 125 NaCl, 25 $NaHCO_3$, 3 KCl, 1.25 $NaH_2PO_4.H_2O$, 10 D-glucose, 1 $CaCl_2$, 6 $MgCl_2$; equilibrated with 95% O_2 – 5% CO_2.

Artificial cerebrospinal fluid (aCSF): 125 NaCl, 25 $NaHCO_3$, 3 KCl, 1.25 $NaH_2PO_4.H_2O$, 25 D-glucose, 2 $CaCl_2$, 1 $MgCl_2$; equilibrated with 95% O_2 – 5% CO_2 (pH = 7.35).

Potassium gluconate internal solution: 125 K-gluconate, 10 Hepes, 11 EGTA, 15 NaCl, 1 $MgCl_2$, 2 MgATP, 0.25 NaGTP, 0.05% biocytin (pH = 7.3, Osmolarity 280 - 285 mOsm).

Whole-cell recordings

Two to five days following tracer injection pups (P8 – P28) were anaesthetized with isoflurane and decapitated. The brain was rapidly removed and placed in ice-cold oxygenated cutting solution. The brainstem was isolated, mounted in a vibratome, and immersed in ice-cold aCSF solution. Coronal sections of 300 µm thickness were taken from

the region immediately caudal to the caudal pole of the facial nucleus and transferred to continuously oxygenated (aCSF) at 36 °C and left for at least 1 hr before recordings in an oxygenated aCSF-filled chamber maintained at room temperature. Tracer-labelled neurons were viewed under epifluorescence: CTB-labelled neurons ventral to nucleus ambiguus and lateral to the inferior olive were identified as putative RVLM premotor neurons and targeted.

Whole-cell recordings were obtained from RVLM neurons in voltage clamp mode using borosilicate pipettes with 1.5 - 2 µm tip diameters (pipette resistance: 3 - 6 MΩ when filled with internal solution). After formation of a gigaseal, voltage clamp recordings were obtained using a Multiclamp 700B (Molecular Devices). Once the holding current (I) and input resistance (R_i) stabilized, baseline recordings were made for at least five minutes prior to commencement of the experimental protocol. Series resistance (R_s) was compensated by 70-80%. All recorded parameters were digitized using Spike 2 version 6.11 with a Power 1401 mark II digitizer (Cambridge Electronic Design, UK). In some experiments two neurons were simultaneously recorded from the same slice.

Recorded neurons were labelled using 0.05% biocytin contained in the internal solution. At the conclusion of experiments slices were briefly fixed in 4% paraformaldehyde and cryoprotected until immunohistochemical processing.

Experimental protocol

The effect of SST on bulbospinal RVLM neurons was determined by superfusing slices with 300 nM SST (Auspep, Australia) as described previously for midbrain slices (Connor et al., 2004) in carbogen-equilibrated aCSF for up to 100 s which was then washed out until recovery to baseline was achieved. Membrane currents were evoked by voltage command steps from -60 to -130 mV in 10 mV increments and 250 ms duration before, during and after drug infusion. In order to confirm the hyperpolarizing effect of SST slices were perfused with 10 µM Baclofen (Sigma Aldrich) for 100 s and washed out until recovery to baseline.

In order to assess whether the inhibition seen following SST application was mediated by SST_2 receptor activation, the effects of repeated SST application were compared before and after the addition of the sst_2 receptor antagonist cyanamid to the perfusate (CYN-154806, 300 nM, Tocris, UK). Baseline responses to 300 or 50 nM SST were assessed as described

above; once a response to SST was detected sections were washed in aCSF for 1000 s then CYN-154806 was perfused for 500 s before the second application of SST.

To determine whether responses to SST were dependent on activity in putative presynaptic neurons we compared responses to 100 nM SST before and after addition of 10 µM tetrodotoxin (TTX, Jomar Bioscience) to the perfusion. This concentration blocked electrically-evoked synaptic currents in pilot experiments (data not shown) and exceeds that generally used elsewhere (Kawai et al., 1999, Kawashima et al., 2013). Baseline responses to SST were recorded and allowed to recover for 1000 s before incubation with TTX for 5 min and re-exposure to SST.

Data analysis

Responses to SST were quantified by measuring the peak change in holding current recorded immediately following SST application. The current-voltage relationship was calculated by plotting membrane current against holding potential (Connor et al., 2004). Repeated responses of bulbospinal neurons to SST following application of TTX or cyanamid to the perfusate were compared using Student's paired t-test. Grouped data are expressed as mean ± SEM for parametric series or median (range) for non-parametric series. Differences were judged significant at $p < 0.05$. Statistical analyses were performed using Graphpad Prism 6.0.

Immunohistochemical processing and analysis of recorded neurons

All slices were fixed overnight in 4% paraformaldehyde in phosphate buffer (0.1 M, pH 7.4) then frozen in cryoprotectant (30% sucrose plus glycerol). Slices were then processed for sst_{2A} receptor immunoreactivity using a protocol based on that described by Gogolla et al. (2006).

Free-floating slices were washed in 20 ml pots for 10 min in 0.01 M PBS and incubated overnight at 4 °C in 0.5% Triton X-100 in 0.01 M PBS. Then slices underwent a blocking step in 5% bovine serum albumin (BSA) in 0.01 M PBS for 4 hr at room temperature. Primary antibody (rabbit anti-sst_{2A} receptor, 1:100, #SS-800, Biotrend, Germany) was added to 5% BSA/0.01 M PBS for a 4 hr incubation at room temperature then washed off with 30 min TPBS. Slices were then incubated at 4 °C overnight in 5% BSA/0.01 M PBS containing secondary antibody for detection of sst_{2A} receptor expression (AlexaFluor 647 donkey anti-

rabbit, 1:250, #711-605-152 Jackson ImmunoResearch, USA) and biocytin-filled cells (ExtraAvidin-FITC, 1:500, #E2761 Sigma-Aldrich, USA). Antibodies were washed off with TPBS for 30 min. Slices were wet-mounted on glass slides, coverslipped and viewed under epifluorescence to confirm labelling before mounting with DAKO fluorescent mounting medium. Fourteen slices contained intact recovered neurons and were imaged using an AxioImager Z2 microscope with ZEISS Efficient Navigation software (2012 version, Carl Zeiss).

RETROGRADE TRACING OF SST-ERGIC NEURONS

Animal surgery

Experiments were performed on male Sprague Dawley rats (n = 10); 14-15 weeks old, 400-550 g) from the Animal Resources Centre, Perth, Western Australia. The retrograde tracing and combined *in situ* hybridization and immunohistochemistry methods used here have been previously published (Kumar et al., 2009). In brief, rats were anaesthetized with ketamine (Parnell Laboratories, Australia) mixed with medetomidine hydrochloride (Pfizer Animal Health, 75 and 0.5 mg/kg respectively, i.p.) and administered preoperative analgesia (carprofen, 5 mg/kg s.c.) and prophylactic antibiotics (cephazolin, 20 mg/kg i.m., Mayne Pharma, Australia). A flat skull approach was used to microinject the retrograde tracer cholera toxin subunit B (CTB, 1% in 200 nl saline; List Biological, Campbell, CA, USA) unilaterally into the RVLM. After conducting a small craniotomy through the occipital bone and incision through the dura, antidromic facial field potentials were evoked by stimulation of the facial nerve. CTB microinjections were made 0.3 mm caudal to the facial nucleus, 1.7-2.1 mm lateral to midline and 0.3 mm deep to the ventral margin of the facial field (that is, 8.8 - 9.2 mm from the dorsal surface of the brain). After withdrawal of the pipette, the wound was closed and 5 ml of physiological saline was administered i.p. Rats were then administered sedative reversal agent atipamezole hydrochloride (Pfizer Animal Health, Australia, 0.75 mg, 0.15 ml s.c.) and allowed to recover for 2-3 days under close monitoring.

Tissue preparation

Animals were deeply anaesthetized with sodium pentobarbitone (>100 mg/kg i.p.) and perfused transcardially with 250 ml heparinized 0.9% sodium chloride followed by 250 ml 4% paraformaldehyde in phosphate buffer (0.1 M, pH 7.4). The brain was removed, the medulla dissected and fixed overnight at 4 °C. Brains were sectioned coronally at 40 µm into four series using a vibrating microtome (VT1200S; Leica, Germany). Sections in each series were

thus separated by 160 µm. Fluorescent immunohistochemical detection of CTB was conducted using a rabbit anti-CTB primary antibody (1:5000, #7927, ViroStat, Portland, ME, US) and a Dylight 488-conjugated donkey anti-rabbit IgG secondary antibody (1:500, Jackson Immunoresearch Laboratories) alongside detection of mRNA using digoxigenin (DIG)-labelled riboprobes targeting PPS mRNA as described previously (Burke et al., 2008). Both anti-sense and sense probes were synthesized, with RNA polymerase T7 and SP6 promoters attached to the 5' end of the reverse and forward oligonucleotide primers respectively (primers listed below in lowercase with promoter attached in uppercase). PCR amplified cDNA template was then *in vitro* transcribed using T7 (AmpliScribe™ T7-Flash™ Transcription Kit, #ASF 3257, Epicentre Biotechnologies, Madison, WI) or SP6 (RiboMAX large scale RNA production system, #P1280, Promega, Madison, WI) *in vitro* transcription kits. Digoxigenin-11-UTP (Roche Applied Sciences, Mannheim, Germany) was incorporated into the riboprobes during *in vitro* transcription.

PPS Forward: GGATCCATTTAGGTGACACTATAGAAGctcaagctcggctgtctgag

PPS Reverse: GAATTCTAATACGACTCACTATAGGGAGAggaggagagggatcagaggt

Free floating brain sections were processed using the protocol described by Li et al. (2005). No labelling in any brain region was seen using sense probes.

Cell counts and analysis

Tissue sections were mounted on glass slides, coverslipped (Vectashield Hardset, Vector Laboratories, USA) and viewed and imaged using a Zeiss AxioImager Z1 microscope under epifluorescence. Images were acquired with Zeiss Axiovision software (Version 4.8). In each whole brain, sections separated by 160 µm were analyzed from Bregma level 5.16 mm to -15.24 mm. Six of the ten brains injected with CTB were selected for quantitative analysis, with every region quantified in at least three brains and confirmation assessed qualitatively in all other cases. Brains were selected due to their small CTB injection sites centered in the RVLM with little impingement on surrounding regions.

Each brain region containing CTB labelled neurons was assessed for expression of PPS mRNA. A neuron was considered CTB immunoreactive (-ir) when the cell body contained Dylight-488 labelling within the cytoplasm and/or in the proximal dendrites. When a region was

found to contain double-labelled neurons, the section that contained the most CTB labelling was selected for counting, and, dependent upon the rostrocaudal extent of the region, a second and third section was also assessed for double labelling (> 300 µm apart).

Using these counts, the percentage of CTB-ir neurons that colocalized with PPS in that brain region, combining all sampled rostrocaudal levels, was determined for 3 - 4 animals and the mean ± SEM was calculated.

In addition, in order to describe those regions which provided the greatest number of retrogradely traced neurons containing PPS mRNA, the number of double-labelled neurons in each region (combining the selected rostrocaudal levels) was determined as a proportion of all double-labelled neurons and the results expressed as the mean percentage.

RESULTS

IN VITRO ELECTROPHYSIOLOGY

Superfusion of 300 nM SST produced an outward current (I_{SST}) in 18/31 (58 %) bulbospinal neurons tested. The mean value of I_{SST} was 40.7 ± 4.8 pA (figure 4.1). Subsequent application of $GABA_B$ agonist baclofen (10 µM) produced an outward current in SST-responsive (49.3 ± 5. 9 pA, *n* = 4, figure 4.1A) and SST-insensitive neurons (42.6 ± 4.3 pA, *n* = 5, figure 4.1B).

SST-sensitive neurons displayed desensitization to repeated application of 50 [*n* = 2], 100 [n = 2] or 300 nM [*n* = 1] SST. Responses to 50, 100 or 300 nM SST were reduced by 20.0 %, 32.4 %, or 43.8 % respectively: pooled responses were 36.6 ± 5.5 vs 24.8 ± 2.4 pA, Paired t-test *t* = 3.4, *df* = 4, 2-tailed *p* = 0.027, figure 4.2A. A similar reduction of response amplitude following repeated 100 nM SST application was observed following addition of TTX to the perfusate between SST trials (39.7 ± 4.9 vs 25.9 ± 4.6 pA, Paired t-test *t* = 15.4, *df* = 4, 2-tailed *p* = 0.0001, *n* = 5, figure 4.2B).

In order to assess whether sst_2-receptor activation underlies responses of bulbospinal neurons to SST, we reapplied SST to neurons previously shown to be SST-sensitive in the presence of the sst_2 antagonist cyanamid (300 nM). Baseline responses to 300 nM (*n* = 2) or 50 nM (*n* = 3) SST were of 40.15 ± 3.5 pA (300 nM) or 25.12 ± 2.9 pA (50 nM) respectively. Cyanamid reduced the amplitude of SST-evoked responses from 31.1 ± 4.1 pA to 2.8 ± 0.6 pA (Paired-t-test *t* = 6.7, *df* = 4, 2-tailed *p* = 0.0025, *n* = 5, figure 4.3).

In 17 bulbospinal neurons in which SST induced an outward current at a holding potential of -60 mV, the resting membrane conductance showed inward rectification (figure 4.4). SST activated a conductance that was greater at more negative currents and had a reversal potential of -93 ± 6 mV in responsive neurons (figure 4.4ii) which was not detected in SST-insensitive neurons.

<u>Sst2A receptor expression on electrophysiologically characterized bulbospinal neurons</u>

Fourteen biocytin-labelled bulbospinal neurons were recovered for histological processing. No sst_{2A} immunoreactivity was ever identified on SST-insensitive neurons (*n* = 9, figure 4.5A). SST evoked responses of 42.3 ± 7.9 pA in the remaining 5 neurons: 3/5 were subsequently identified as sst_{2a}-positive (figure 4.5).

RETROGRADE TRACING OF SSTERGIC NEURONS

CTB injection sites were located in the RVLM and extended 0.7- 1.1 mm caudal to the facial nucleus (Bregma -11.64 mm) with the core of the injection sites centred between Bregma -11.8 and -12.3 mm (figure 4.6).

The majority of brain regions that contained CTB-labelled neurons also contained neurons expressing PPS mRNA. Table 4.1 presents the distribution and relative density of cells containing CTB and/ or PPS mRNA in all brain regions that contained CTB labelled neurons.

Colocalization of PPS mRNA with CTB immunoreactivity was restricted to 8 brain regions: the paratrigeminal nucleus (Pa5), lateral parabrachial nucleus (LPB), Kölliker-Fuse nucleus (KF), ventrolateral periaqueductal grey area (VLPAG), central nucleus of the amygdala (CeA), sublenticular extended amygdala (SLEA), interstitial nucleus of the posterior limb of the anterior commissure nucleus (IPAC) and bed nucleus of the stria terminalis (BNST). Figure 4.7 shows examples of double labelling in the Pa5, VLPAG, CeA and BNST.

The proportion of CTB-labelled neurons that contain PPS mRNA within each region is shown in figure 4.8. Of the eight brain regions, CTB-labelled cells in Pa5 contained the highest PPS-expression (40 ± 3%, 73/173 CTB-ir cells, *n* = 4), followed closely by the SLEA (34 ± 6%, 65/180, *n* = 3). The IPAC possessed a small, variable population of double-labelled cells across animals (26 ± 10%, 20/68 CTB-ir cells, *n* = 3). The VLPAG contained PPS mRNA expression in approximately one fifth of its RVLM-projecting cell population (22 ± 3%), however this region also exhibited the highest number of double labelled cells of all regions analyzed (158/791, *n* = 4). Retrogradely traced populations of the LPB and BNST contained similar proportions of PPS (13 ± 1%, 47/369, *n* = 4 and 12 ± 2%, 48/406, *n* = 3 respectively), followed by the KF (10 ± 0.5%, 14/137, *n* = 4) which furthermore contained the lowest number of double labelled cells of all RVLM-projecting populations. Despite the CeA possessing the lowest percentage of double labelled neurons (10 ± 1%), it contained a relatively large number of PPS-expressing CTB labelled cells (110/713 cells, *n* = 3), which was only overshadowed by the size of the VLPAG projection.

DISCUSSION

The main findings are: firstly, that SST evoked an outward current suggestive of activation of an inwardly rectifying potassium channel in approximately half of RVLM bulbospinal neurons. Second, this effect is most likely due to activation of sst_2 receptors, as SST-activated currents were blocked by cyanamid and sst_{2A} receptor expression was identified on SST-sensitive neurons. Thirdly, putative sources of SSTergic drive to the RVLM were identified in 8 distinct brain regions: the Pa5, KF, LPB, VLPAG, CeA, SLEA, IPAC and BNST.

SST hyperpolarizes spinally-projecting RVLM neurons via GIRK channels

SST hyperpolarized about 50% of bulbospinal neurons in acute brain slices from young rats. 300 nM SST has been reported to evoke approximately 75% maximal inhibitory effect on spontaneously firing locus coeruleus neurons recorded in acute brain slices (Chessell et al., 1996) and 95% inhibition of calcium current in dissociated periaqueductal grey neurons (Connor et al., 2004). The SST-evoked responses were effectively blocked by cyanamid, a selective antagonist of sst_2 receptors (Nunn et al., 2003), suggesting specific involvement of sst_2 receptors in mediating the response in bulbospinal neurons. Addition of TTX to the perfusate did not alter outward currents evoked by SST, indicating that the evoked currents were mediated by postsynaptic rather than presynaptic mechanisms. The proportion of SST-sensitive neurons in the current study is consistent with the proportion of bulbospinal (35%) and C1 neurons (50%) that were previously identified as sst_{2A}-immunoreactive in adult animals (Burke et al., 2008), although higher than the proportion of biotin-labelled bulbospinal neurons identified as sst_{2A}-immunoreactive in the current study (21%). Dialysis of sst_{2A} from the recording pipette, and difficulties in discriminating lightly immunoreactive neurons in thick slices from electrophysiology experiments may contribute to this lower than expected result.

The outward current evoked by SST resulted from an increase in inwardly rectifying potassium conductance, since at more negative potentials SST activated a greater conductance and had a reversal potential approaching the Nernst potential calculated for a potassium (-93 mV). This is in keeping with data indicating that sst_2 couples efficiently to GIRK1, examined by comparing dose-response curves and the maximum currents obtained by the five different rat SST receptor subtypes (sst_1 – sst_5) that were co-expressed with GIRK1

(Kreienkamp et al., 1997). Our results are consistent with the effects of SST on inwardly rectifying potassium conductance in neurons in other brainstem regions including the locus coeruleus (Inoue et al., 1988) and PAG (Connor et al., 2004). In addition, in different brain regions such as the superior cervical ganglion (Shapiro and Hille, 1993), amygdala (Viana and Hille, 1996) and PAG (Connor et al., 2004), SST directly activates potassium conductance and inhibits GABA release via a presynaptic calcium dependent mechanism. Such experiments should be carried to test these effects on RVLM sympathetic premotor neurons.

Of the five recovered neurons that responded to SST, only three clearly expressed sst_{2A} immunoreactivity, whereas all 9 non-responsive neurons were sst_{2A} negative. In the neurons that expressed sst_{2A} it seems likely that the SST-evoked response was mediated via this receptor, although our data does not eliminate the possibility that other receptor subtypes could also have contributed. In neurons that responded to SST but did not express sst_{2A} it is possible that sst_{2A} expression was too low for detection by fluorescence immunohistochemistry, although it may also have been that sst_{2A} receptors had internalized following stimulation and were not re-expressed (Waser et al., 2009). However we cannot eliminate the possibility that other SST receptors were expressed on these cell bodies or their dendrites.

In the current study, repeated application of SST evoked hyperpolarizing responses that showed considerable desensitization. Following long exposure to agonists, G-protein coupled receptors mediate a signal that triggers receptor dephosphorylation (Premont et al., 1995, Bohm et al., 1997, Lefkowitz, 1998, Horie and Insel, 2000). Desensitization of the SST receptors has been reported in rat hippocampal and neocortical neurons (Wang et al., 1990, Priestley, 1992, Young Shim et al., 2006, Yin et al., 2009), and, of particular relevance to the current study, Liu et al. (2008) found that SST_2 receptors internalize and desensitize following agonist stimulation within minutes.

The current study also identified the expression of a hyperpolarization-activated inward current (I_h) in 6 out of 18 SST-sensitive bulbospinal RVLM neurons. Although not studied in detail, the time-course and reversal potential of this current were consistent with the distinctive profile of hyperpolarization and cyclic nucleotide channel-mediated I_h (reviewed by Robinson and Siegelbaum, 2003). I_h has not previously been demonstrated on RVLM

sympathetic premotor neurons. Although I_h has been implicated in the generation of spontaneous pacemaker activity in other cell types (recently reviewed by He et al., 2014), it is not thought to play a critical role in driving autodepolarization in RVLM, as its blockade by ZD7288 evokes no significant effect on sympathetic nerve activity or blood pressure (Miyawaki et al., 2003).

Technical limitations

Electrophysiological recordings were confined to brain slices made from 8 -28 days old rats. As global SST binding and brain-wide sst receptor expression undergo some lability in the neonatal period in rats (Gonzalez et al., 1989, Thoss et al., 1995), it is possible that changes in the relative expression of sst receptor isoforms in the brainstem could complicate interpretation of the current data. No developmental study has yet described the relative expression of sst isoforms in the brainstem over the neonatal period. However, the expression of sst_{2a} in putative TH-positive neurons containing the Lmx1b and Phox2b transcription factors is already established by birth (Gray, 2013). Furthermore, the gross pattern of sst expression, including sst_{2a}, in P5 rats is similar to that observed in adults (Thoss et al., 1995). Although the quality of sst_{2a} labelling in thick brain slices reported here is inferior to that observed in conventional thin sections (Burke et al., 2008), sst_{2A}–like immunoreactivity was detected on all slices tested and the general pattern of expression was similar to that seen in adult rats, suggesting that sst2a expression in juveniles is likely to be representative of older animals.

In common with many other studies using conventional retrograde tracers, interpretation of our anatomical study should be tempered with three caveats. First, CTB may be taken up by any fiber that passes through the site of tracer deposition. We cannot therefore determine whether retrogradely labelled neurons form synaptic terminals within the RVLM or simply represent fibers of passage. Second, assuming some CTB-labelled neurons do actually form terminals within the RVLM, we cannot determine the function or phenotype of their post-synaptic targets. Finally, significant numbers of neurons in the ventrolateral medulla express somatostatin and project to the ipsi- and contralateral RVLM (Tan et al., 2010). However, discrimination of local SSTergic neurons was confounded by the tracer injection site; we therefore cannot exclude local interneurons as a potential source of SST release.

PPS mRNA is found in select groups of neurons projecting to the RVLM

The paratrigeminal nucleus

Distinct clusters of PPS mRNA-expressing neurons were found in the Pa5 in the current study, as previously noted (Kiyama and Emson, 1990). Both anterograde and retrograde studies have revealed projections from the Pa5 to the RVLM (Caous et al., 2001, de Sousa Buck et al., 2001), however this is the first study to describe a somatostatinergic phenotype in just under half the RVLM-projecting neurons in the region. Enkephalin, calbindin, and nNOS have been detected in Pa5 neurons that project to the dorsal motor nucleus of the vagus (Armstrong and Hopkins, 1998); these groups may also overlap with the PPS containing population described here. Pa5 microinjection of bradykinin evokes pressor effects (Lindsey et al., 1997) via direct activation of barosensitive RVLM neurons (Caous et al., 2004). Many (60-80%) Pa5 neurons are themselves barosensitive, increasing their firing rate in response to phenylephrine administration (Balan Jr et al., 2004, Sousa and Lindsey, 2009b), while bilateral Pa5 ablation reduces cardiac barosensitivity (Sousa and Lindsey, 2009a). Whether SST participates in mediating such reflex modulation in the RVLM is unknown.

The Kölliker-Fuse and lateral parabrachial nuclei

Together, the KF and LPB form the pontine respiratory group, and while PPS expression has been explicitly demonstrated in the LPB (Kiyama and Emson, 1990), reporting of its localization in the KF has been overlooked prior to the current study (Kiyama and Emson, 1990, Giehl and Mestres, 1995). Projections from both KF and LPB to the RVLM region have been described (Smith et al., 1989). Although cardiovascular responses to chemical stimulation of parabrachial nuclei have been examined, they are inconsistent, brief and/ or small (Ward, 1988, Chamberlin and Saper, 1994, Lara et al., 1994), and the region's function in respiratory control is certainly better understood (Smith et al., 1989, Morschel and Dutschmann, 2009). At LPB/ KF sites corresponding to the location of PPS-expressing, RVLM projecting neurons detected in the current study, glutamate microinjection elicits inspiratory facilitation resembling apneusis (Chamberlin and Saper, 1994).

The ventrolateral periaqueductal grey (VLPAG)

PPS mRNA expression was observed in the VLPAG as previously described (Smith et al., 1994), and in neurons projecting to the raphe magnus (Beitz et al., 1983). Although

projections from the VLPAG to the RVLM have been described (Carrive and Bandler, 1991), this is the first study to attribute a somatostatinergic phenotype to some elements of the pathway. Depressor responses associated with reductions in renal vascular resistance are evoked chiefly by stimulation of the caudal VLPAG (Carrive and Bandler, 1991), which overlaps anatomically with the PPS-expressing RVLM projecting neurons identified in the current study. On the other hand stimulation of the VLPAG also evokes vasodilation in the hindlimb (Lovick, 1992a) and this has been attributed to a raphe-mediated pathway (Wang and Lovick, 1993). It is possible that raphe and RVLM projections arise from discrete regions of the VLPAG, as changes in iliac or renal blood flow are associated with different rostrocaudal levels of the VLPAG and corresponding RVLM termination sites (Carrive and Bandler, 1991). The caudal VLPAG has also been implicated in hemorrhage as the activity of neurons in the region increase during the decompensatory or hypotensive phase (Cavun and Millington, 2001).

The central nucleus of the amygdala (CeA) and the extended amygdala

Somatostatinergic neurons have been described in the CeA (Vincent et al., 1985) and these project to the PAG (Gray and Magnuson, 1992) and/ or dorsal vagal complex, in particular the NTS (Veening et al., 1984, Gray and Magnuson, 1987, Saha et al., 2002). The present study however, is the first to demonstrate a dense PPS-expressing projection to the RVLM. Both coronal transection caudal to, or sagittal transection medial to the CeA reduce the amount of SST-ir fibers in the ventrolateral medulla (Kawai et al., 1982) supporting our findings. Furthermore the CeA also contains a glutamatergic population which projects to the RVLM (Takayama and Miura, 1991), and terminals arising from cells in the CeA appose barosensitive C1 neurons and non-C1 neurons (Cassell and Gray, 1989, Saha et al., 2005). Therefore it is possible that the PPS expressing neurons in the CeA described in the present study also contain glutamate.

The functional role of these neurons is more difficult to ascribe. Low frequency stimulation of CeA in the awake animal promotes inspiration, even respiratory entrainment (Harper et al., 1984). At higher frequencies (>10 Hz), phrenic nerve frequency is increased (Cox et al., 1987) and a prolonged period of inspiration occurs (Harper et al., 1984), while mostly pressor and some depressor effects have been reported (Stock et al., 1978, Frysinger et al., 1984, Harper et al., 1984, Gelsema et al., 1987, Iwata et al., 1987). It also appears that the

responses evoked are state dependent, with sleep and anesthesia either dampening or reversing cardiorespiratory effects (Stock et al., 1978, Frysinger et al., 1984, Harper et al., 1984, Cox et al., 1987, Gelsema et al., 1987, Iwata et al., 1987). As the CeA forms a crucial link in the coordination of autonomic and behavioral responses to stress such as conditioned fear (LeDoux et al., 1988, Paré et al., 2004, Wilensky et al., 2006), it is possible that the somatostatinergic pathway identified in the current study may be involved in recovery responses such as the return of mean arterial pressure to baseline levels following freezing responses to conditioned fear (Carrive, 2000, Dielenberg et al., 2001) or the suppression of sympathetic responses during passive versus active coping (Sherwood et al., 1990, Roozendaal et al., 1991).

Extending dorsomedially from rostral parts of the CeA, the SLEA also contained a population of PPS-expressing RVLM-projecting neurons which has otherwise only been referred to briefly in studies of the developing and adult rodent brain (Real et al., 2009, deCampo and Fudge, 2013). Prior to this study knowledge of the SLEA's descending projections was restricted to the NTS/DMV and parabrachial complex (Grove, 1988; Sun et al., 1994; Waraczynski, 2006). Chemical stimulation of the SLEA elicits depressor responses (Gelsema et al., 1993). Although a respiratory relationship is associated with the SLEA, it is somewhat complex, as SLEA activity is normally synchronized with the onset of spontaneous breathing but suppressed during cognitive tasks which drive respiration (Evans et al., 2009). Activation of the SLEA is evident in subjects experiencing dyspnea, and is associated with the unpleasant emotional processing that occurs during a dyspneic episode (von Leupoldt et al., 2008). It is possible that the PPS-expressing pathway to the RVLM from the SLEA may be part of a complex circuit linking emotional state to cardiovascular and respiratory outflows.

The interstitial nucleus of the posterior limb of the anterior commissure (IPAC) expresses PPS mRNA in neurons projecting to the RVLM however very little is known about its function except for its role in reward and motivational processes (Waraczynski, 2003). Perhaps, as with other components of the extended amygdala, the IPAC is involved in the integration of emotional processing and autonomic outflows.

We have identified PPS-expressing neurons in the BNST that project to the RVLM despite the fact that such neurons have been found previously to project to the LPB, the PAG and dorsal

vagal complex (Gray and Magnuson, 1987, Moga et al., 1989, Gray and Magnuson, 1992), and furthermore, neurochemically undefined neurons are known to project to the lateral tegmental field (Holstege et al., 1985). Although ablation of the region does not affect baseline arterial pressure or heart rate (Crestani et al., 2006), both chemical and electrical stimulation of the lateral subdivisions of BNST (where many PPS neurons in the present study were located) evoke a depressor response (Dunn and Williams, 1995). As PPS neurons projecting to the LPB and NTS are involved in feeding related responses (Smith et al., 2005, Li and Cho, 2006, Saggu and Lundy, 2008, Panguluri et al., 2009) it is possible that the projection identified here has a corresponding role. Alternatively, the BNST modulates MAP and HR during exercise (Alves et al., 2011), so whether the bradycardic and depressor responses evoked by SST microinjection in the RVLM (Burke et al., 2008) are simulating this function remains to be determined.

Conclusion

This study reveals that a discrete subset of brain regions provides somatostatinergic projections to the RVLM: the Pa5, KF, LPB, VLPAG, CeA, SLEA, IPAC and BNST, and we have provided evidence-based speculation as to the roles of these projections. The projection from the KF and LPB most likely has a respiratory function, however the role of the other pathways suggested remains to be tested. Nevertheless it is clear that SST activates G-protein coupled sst_2 (most likely sst_{2A}) receptors whereby GIRK channels are activated that serve to hyperpolarize neurons in the RVLM, but the role of endogenously released SST in determining the RVLM activity and its cardiovascular reflexes remains to be determined.

CHAPTER 4 FIGURES AND TABLES

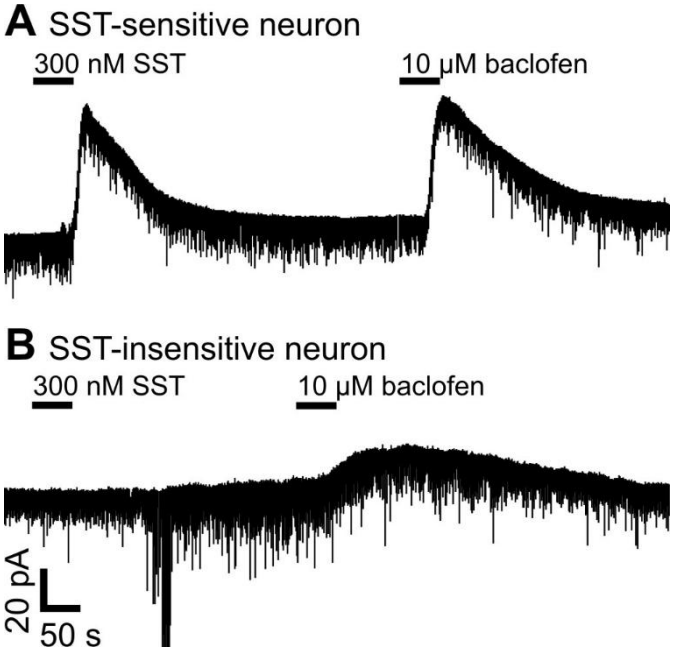

Figure 4.1: Responses of bulbospinal RVLM neurons to SST. A. SST and baclofen (black horizontal bars indicate time of application) produced outward currents in sst-sensitive bulbospinal RVLM neurons. **B.** baclofen still produced outward currents in sst-insensitive bulbospinal RVLM neurons.

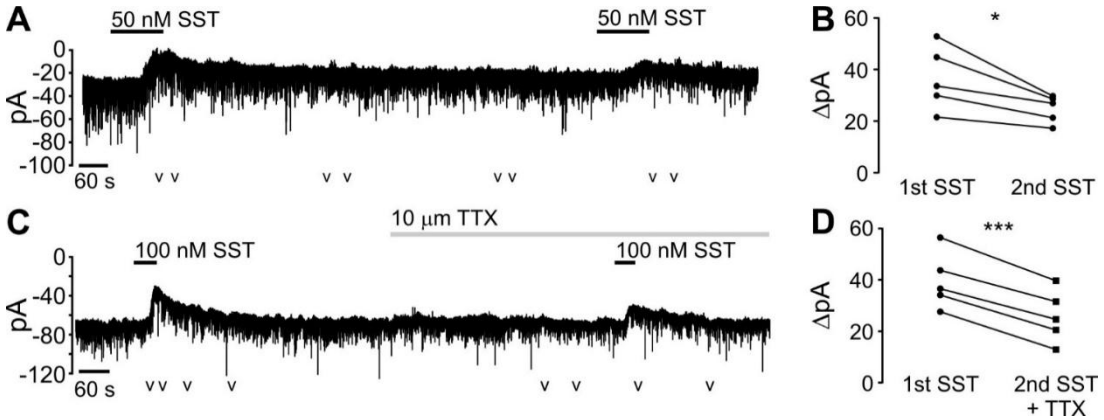

Figure 4.2: Responses of bulbospinal RVLM neurons to SST application exhibited desensitization. A. Raw data showing desensitization to repeated application of 50 nM SST ('v' denotes where voltage steps were performed; steps have been removed from traces to aid clarity). **B.** Pooled data; responses to 50, 100 and 300 nM SST have been combined. **C.** raw data demonstrating that responses to repeated SST were unaffected by tetrodotoxin

(TTX). **D.** pooled data of responses to 100 nM SST before and after addition of TTX to the perfusate.

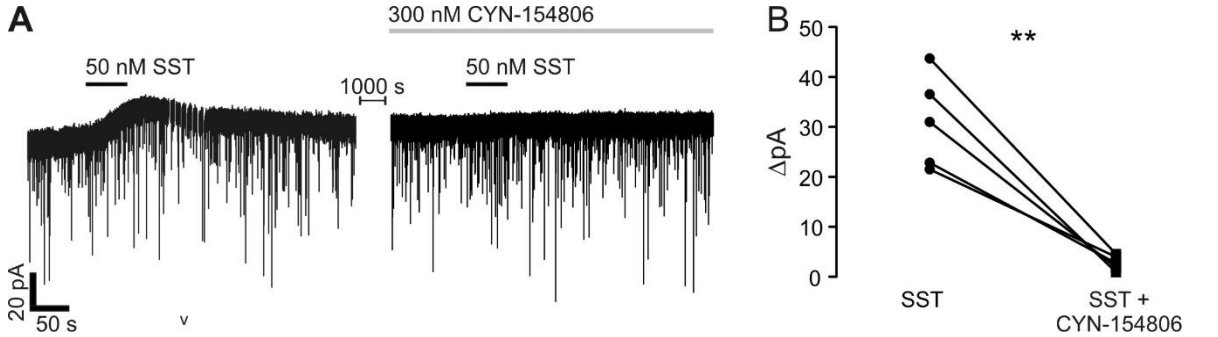

Figure 4.3: SST_2 blockade abolished sst-induced outward currents. **A.** raw data showing responses to SST application before and after superfusion with the sst_2 blocker cyn-154806 ('v' denotes where voltage steps were performed). **B.** pooled data.

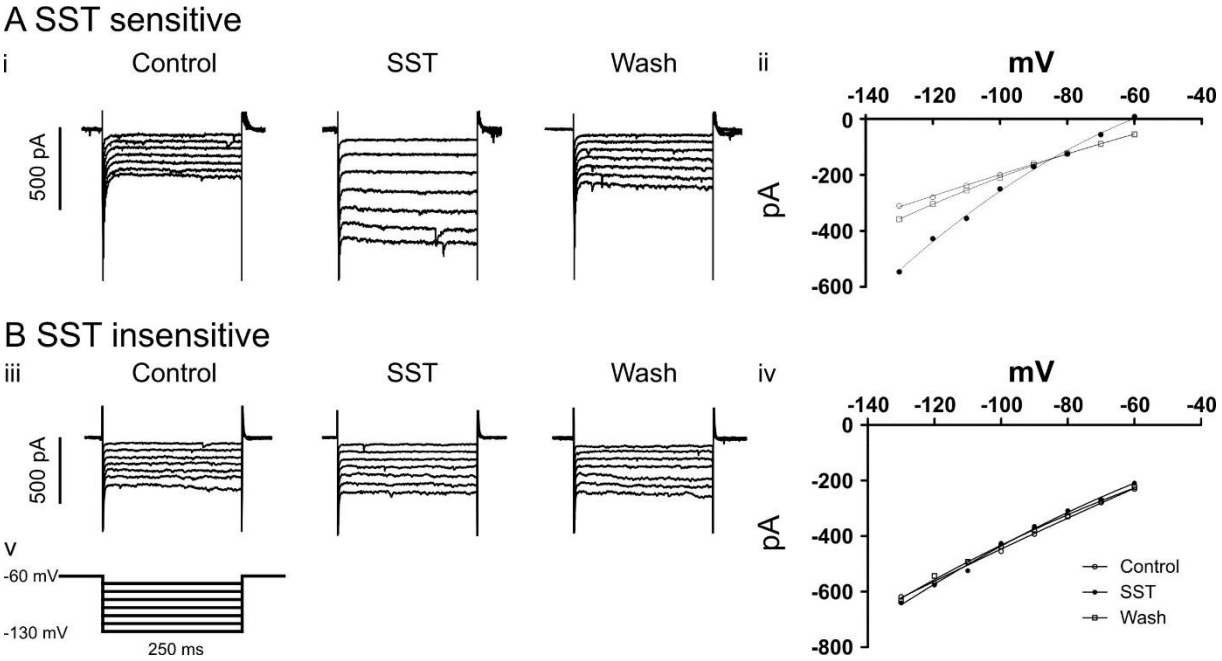

Figure 4.4: Current-voltage relationship of sst-sensitive (A) and sst-insensitive (B) bulbospinal RVLM neurons. Examples of membrane currents evoked by voltage steps before, during and after 300 nm sst superfusion; raw data shown in i and iii, i-v plots shown in ii and iv. 250 ms command voltages were stepped from -60 to -130 mv in 10 mv increments (v).

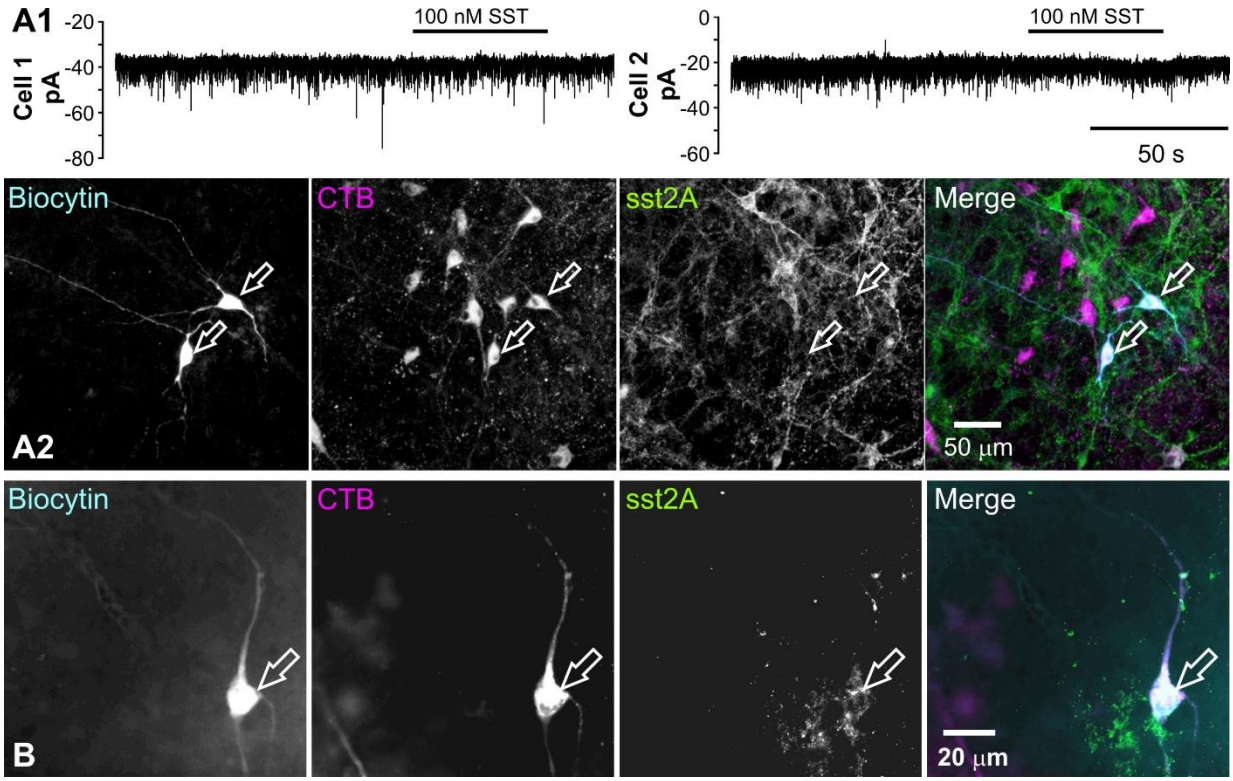

Figure 4.5: Immunohistochemical recovery of electrophysiologically characterised rvlm bulbospinal neurons. A1. Simultaneous recordings from two bulbospinal RVLM neurons; neither responded to 100 nm SST. **A2.** Histological recovery of the same neurons; both were confirmed as CTB-positive and sst2a-negative. **B.** Weakly sst2a-positive bulbospinal neuron recorded in a different experiment; electrophysiological response to SST is shown in Figure 4.1A.

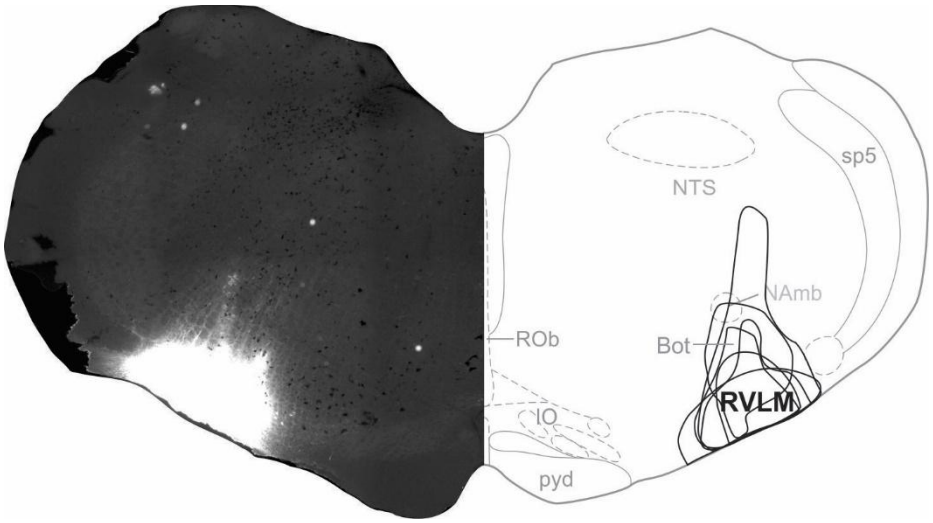

Figure 4.6: CTB injection sites targeting the RVLM. The left coronal hemisection shows the CTB injection site from one animal. The right hemisection shows schematically the extents of six injection sites in animals used for quantitative analysis.

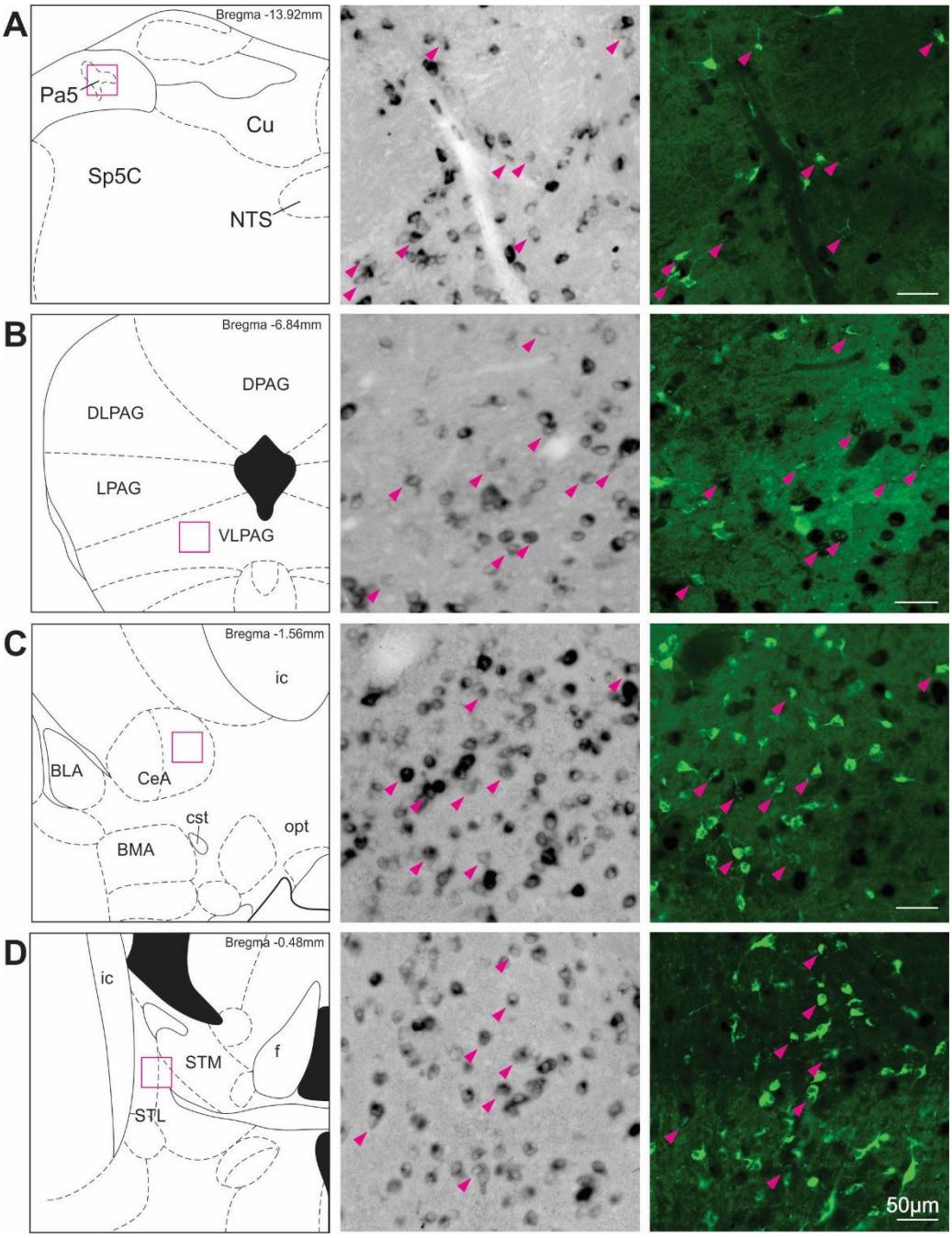

Figure 4.7: Brain regions (bregma levels indicated) showing neurons retrogradely labelled from the RVLM (CTB-ir, green) that express PPS mRNA. The magenta box shown in the left hand schematic panel is the site depicted in the central panel showing neurons expressing PPS mRNA (black) and in the right hand panel showing CTB labelling (green). Double-labelled cells are indicated by magenta arrowheads. **A.** paratrigeminal (pa5) **B.** ventrolateral periaqueductal grey (VLPAG) **C.** central nucleus of the amygdala (CeA) **D.** bed nucleus of the stria terminalis lateral and medial divisions (STL and STM respectively). Scale bars = 50µm. schematic diagrams adapted from Paxinos and Watson (2007).

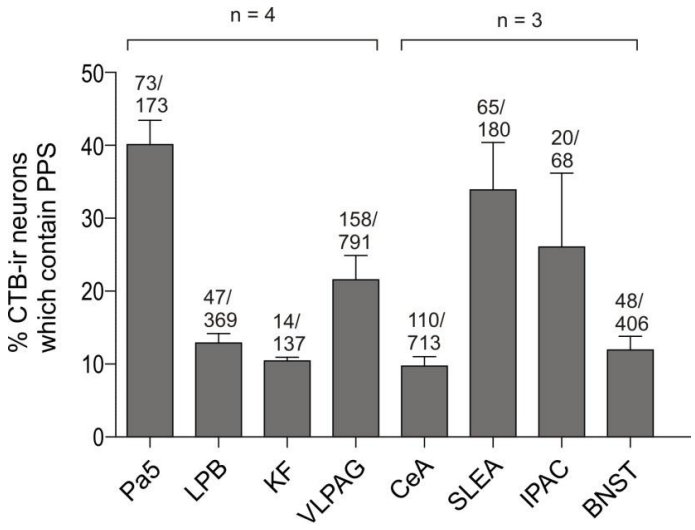

Figure 4.8: Brain regions containing RVLM projecting (CTB-ir) neurons that express PPS mRNA.

Table 4.1: Relative abundance of neurons containing CTB-ir and/ or PPS mRNA in each brain region projecting to the RVLM. Scattered (+) labelling refers to sparsely distributed cells (<5 per region) light (++) labelling indicates coverage of less than one third of the defined region. Moderate (+++) labelling indicates a range of labelling from approximately one to two thirds coverage of the cell group while dense (++++) labelling describes an area containing a high number of labelled cells which cover more than two thirds of the anatomically defined region.

LOCATION	SUBREGION	LATERALITY OF CTB	CTB	PPS
Cortical	Motor Cortex (MC)	Bi	++	+++
	Sensory Cortex (SC)	Bi	++	++
	Infralimbic Cortex (IL)	Bi	+++	+++
	Prelimbic Cortex (PrL)	Bi	++	+++
	Insular Cortex (IC)	Bi	++	++
Subcortical	Vascular Organ, Lamina Terminalis	-	++	+
	Medial Preoptic Area (MPA)	bi	++	+
	Bed Nucleus, Stria Terminalis (BNST)	bi	+++	++++
	Interstitial Nucleus of Posterior Limb, Anterior Commissure (IPAC)	ipsi	++	+++
	Sublenticular Extended Amygdala (SLEA)	ipsi	+++	+++
	Paraventricular Nucleus, Hypothalamus (PVN)	bi	++++	++
	Ventromedial Hypothalamus (VMH)	Bi	+	+++
	Central Nucleus of the Amygdala (CeA)	Ipsi	++++	+++

	Dorsomedial Hypothalamus (DMH)	bi	++	++
	Zona Incerta (ZI)	bi	++	
	Lateral Hypothalamic Area (LHA)	Bi	+++	++
Midbrain	Lateral PAG (LPAG)	Bi	+	++
	Ventrolateral PAG (VLPAG)	bi	+++	+++
	Dorsomedial PAG (DMPAG)	Bi	+++	++
	Oculomotor Nucleus, Parvicellular (3PC)	contra	+	++++
	Intermediate White Layer, Superior Colliculus (InWh)	contra	+	+
	Inferior Colliculus (InC)	bi	++	+++
	Dorsal Raphe, Caudal Part (DRC)	-	++	-
	Retrorubral Field (RRF)	Bi	++	+
Pons	Pedunculopontine Tegmental Area (PPTg)	Bi	++	+
	Lateral Parabrachial Nucleus (LPB)	Bi	+++	+++
	Medial Parabrachial Nucleus (MPB)	Bi	++	++
	Kölliker Fuse (KF)	Bi	+++	++++
	Locus Coeruleus (LC)	Ipsi	++	+
	Subcoeruleus (SubC)	ipsi	++	-
	A5 region	Bi	++	+
Medulla	Midline Raphe	-	+++	++
	Vestibular Nucleus	Bi	++	+++

Gigantocellular Reticular Nucleus (Gi)	Bi	+	+
Caudal Ventrolateral Medulla (CVLM)	bi	+++	++
Intermediate Reticular Nucleus	bi	+	+
Nucleus of the Solitary Tract (NTS)	bi	++++	++
Area Postrema (AP)	-	++++	-
Paratrigeminal Nucleus (Pa5)	bi	+	+++
A1 region/ Retro Ambiguus	Bi	++	+

CHAPTER 5: EXAMINATION OF RVLM MICROCIRCUITS THAT CONTROL SYMPATHETIC NERVE ACTIVITY

ABSTRACT

Sympathetic premotor neurons within the rostral ventrolateral medulla (RVLM) are thought to drive the activity of sympathetic nerves and therefore contribute to the maintenance of blood pressure. *In vivo*, the activities of sympathetic nerves and spinally projecting RVLM neurons display rhythmic bursting that is independent of baroreceptor input. We have previously proposed that such synchronisation could result from functional coupling between spinally projecting neurons.

In this study we directly test that hypothesis by examining the prevalence of functional synapses linking pairs of RVLM sympathetic premotor neurons, identified by retrograde transport of a fluorescent tracer microinjected into the spinal cord.

Whole-cell patch clamp recordings were performed on pairs of bulbospinal neurons in acute brainstem slices prepared from P8 – P28 rats. By simultaneously recording membrane current in a putative post-synaptic cell and driving trains of action potentials in the 'pre-synaptic' cell, the prevalence of functional synapses linking bulbospinal neurons within close proximity to one another was examined.

Averages of 'post-synaptic' membrane currents, triggered by 'pre-synaptic' action potentials, were generated from 38 pairs of spinally projecting RVLM neurons. In no case was any evidence of a temporal relationship between the occurrence of synaptic currents in the post-synaptic cell and the timing of action potentials in the pre-synaptic neuron observed. We conclude that direct links between bulbospinal neurons are rarely, if ever, present in juvenile rats and are unlikely to contribute significantly to the synchronization of sympathetic nerve activity.

INTRODUCTION

The spinal sympathetic preganglionic neurons (SPN) that give rise to sympathetic nerves are critically dependent on supraspinal drive for their spontaneous activity (Morrison et al., 1991, Deuchars et al., 1995, Deuchars et al., 1997, Lewis and Coote, 2008). Although multiple brain regions contain neurons that synapse with SPN (see Dampney, 1994), disruption of neuronal activity within the rostral ventrolateral medulla (RVLM) is alone sufficient to largely abolish baseline sympathetic nerve activity and reduce blood pressure to spinal levels (Guertzenstein and Silver, 1974, Dampney and Moon, 1980). Putative sympathetic premotor neurons within the RVLM project to the thoracic spinal cord, are spontaneously active, and are sensitive to multiple afferent sensory modalities and inputs from higher centres that modulate sympathetic nerve activity, and have phasic bursting patterns coinciding with sympathetic nerve activity (Morrison et al., 1988, see Guyenet, 2006). Given the strong correlation between the functional properties of these neurons and the activity of vasomotor sympathetic nerves, unravelling the factors that underlie their spontaneous activity is a major research goal (Coote, 2007).

Putative sympathetic premotor neurons from juvenile animals exhibit spontaneous depolarisations that are independent of excitatory synaptic inputs *in vitro* (Sun et al., 1988b, Guyenet et al., 1989, Kangrga and Loewy, 1995, Li et al., 1995) and *in situ* (Koganezawa and Paton, 2014). These data were initially interpreted as evidence that RVLM sympathetic premotor neurons have a capacity for auto-depolarization. However, the 'pacemaker' hypothesis has been undermined by two critical observations. First, acutely dissociated sympathetic premotor RVLM neurons are not spontaneously active despite the presence of sodium and calcium conductances (Lipski et al., 1998). Second, action potentials in sympathetic premotor neurons recorded from adult rats *in vivo* are always preceded by excitatory synaptic potentials (Lipski et al., 1996a). As a result, the 'pacemaker' hypothesis has been largely superseded by a 'network' hypothesis, which proposes that tonic vasomotor tone is produced by the summation of many excitatory and inhibitory synaptic inputs within the RVLM, or a hybrid pacemaker-network arrangement, in which autonomously active neurons play a minor role (Lipski et al., 1996a, Lipski et al., 1996b, Ito and Sved, 1997, Lipski et al., 1998, Lipski et al., 2002, Dampney et al., 2003a, Koganezawa and Paton, 2014).

Although RVLM sympathetic premotor neurons appear to receive tonic inhibitory control from the caudal ventrolateral medulla (Cravo and Morrison, 1993) and contralateral RVLM (McMullan and Pilowsky, 2012), little progress has been made in identifying other sources of tonic drive to RVLM sympathetic premotor neurons, and in particular no source of tonic excitatory input has yet been identified. One intriguing possibility is that RVLM premotor neurons may themselves participate in reciprocal local microcircuits. Such an arrangement would allow percolation of activity generated by active units across networks of synaptically linked neurons, potentially contributing to the excitability of other sympathetic premotor neurons and synchronising activity across the network. Anatomical observations are supportive of such an arrangement: RVLM C1 neurons form multiple local arborisations that target C1 and non-C1 RVLM neurons (Patrick Card et al., 2010), and catecholaminergic synapses that originate in the RVLM have been identified on many RVLM C1 neurons (Agassandian et al., 2012). However, functional evidence for such an arrangement is inconclusive: one previous study has examined cross-correlograms of spike timing recorded from pairs of sympathetic premotor neurons *in vivo* (McAllen et al., 2001). Although no evidence of monosynaptic coupling was identified in that study, technical limitations associated with the cross-correlation technique hampers interpretation of those results since the technique may miss weakly coupled neurons and is dependent on the recording of large blocks of activity (Shannon et al., 2000, Oshima et al., 2006).

The paired whole-cell patch clamp technique provides a more powerful tool for the study of neuronal circuitry, as it allows the identification of sub-threshold synaptic events or inhibitory synaptic currents (Miles and Poncer, 1996, Debanne et al., 2008) and is less dependent on huge datasets for reliable detection of events.

The objective of the current study was to use the paired whole-cell patch clamp technique to examine whether pairs of spinally projecting RVLM neurons form functional synapses *in vitro*. By examining whether action potentials in one neuron lead to time-locked synaptic currents in the other, we have directly examined the evidence for microcircuit participation in these neurons.

MATERIALS AND METHODS

All animal experiments were conducted in accordance with the *Australian code of practice for the care and use of animals for scientific purposes* and were approved by Macquarie University Animal Ethics Committee.

ANATOMY

Labelling of bulbospinal RVLM neurons

Sprague Dawley rat pups (P5 – P25) were anaesthetized with 2-5% isoflurane (Veterinary Companies of Australia, Pty) in oxygen and moved onto a heated pad. A dorsal laminectomy was performed and the T2 spinal cord exposed. Fluorescently conjugated cholera toxin β subunit (CTB-Alexa 555, 0.5 - 1%, Invitrogen) was injected bilaterally at co-ordinates corresponding to the intermediolateral cell column (1 to 3 100 nl injections each side). After completion of microinjections the wound was closed with cyanoacrylate glue and anaesthesia discontinued. Pups were allowed to recover on a warm pad until ambulatory and were then placed back in the cage with their mother and littermates. Post-operative rats were carefully monitored for the duration of experiments and treated with analgesia when indicated (Carprofen, 2 mg/kg s.c. Norbrook pharmaceuticals, Australia).

***IN VITRO* ELECTROPHYSIOLOGY**

SOLUTIONS (mM)

Cutting solution: 125 NaCl, 25 $NaHCO_3$, 3 KCl, 1.25 $NaH_2PO_4.H_2O$, 10 D-glucose, 1 $CaCl_2$, 6 $MgCl_2$; equilibrated with 95% O_2 – 5% CO_2.

Artificial cerebrospinal fluid (aCSF): 125 NaCl, 25 $NaHCO_3$, 3 KCl, 1.25 $NaH_2PO_4.H_2O$, 25 D-glucose, 2 $CaCl_2$, 1 $MgCl_2$; equilibrated with 95% O_2 – 5% CO_2 (pH = 7.35).

Potassium gluconate internal solution: 125 K-gluconate, 10 Hepes, 11 EGTA, 15 NaCl, 1 $MgCl_2$, 2 MgATP, 0.25 NaGTP, 0.05% biocytin (pH = 7.3, 280 < Osmolarity < 285 mOsm).

Cesium chloride internal solution: 140 CsCl, 5 Hepes, 10 EGTA, 1 $MgCl_2$, 2 $CaCl_2$, 2 MgATP, 0.05% biocytin (pH = 7.3, 280 < Osmolarity < 285 mOsm).

Whole-cell recordings from acute brainstem slices

2-5 days after tracer microinjection, pups (P8 – P28) were anaesthetized with isoflurane and quickly decapitated. The whole brain was rapidly removed and placed in ice cold oxygenated cutting solution. The brainstem was dissected, mounted in a vibratome, and 2 - 3 300 µm thick coronal sections from the region overlapping the caudal pole of the facial nucleus were cut in ice-cold cutting solution, transferred to carbogen-bubbled aCSF at 34°C and rested for at least 1 h before recording. Recordings were performed at room temperature in a 2 ml chamber superfused at 1.5 – 2 ml/min with carbogen-bubbled aCSF. Tracer-labelled neurons were viewed under epi-fluorescence: CTB-filled neurons lying ventral to nucleus ambiguus and lateral to the inferior olive were identified as putative sympathetic premotor neurons.

Whole-cell recordings were made from labelled RVLM neurons using borosilicate glass pipettes with 1.5 - 2 µm tip diameters (pipette resistance: 3 – 6 MΩ). After formation of a gigaseal, voltage clamp recordings were obtained using Multiclamp 700B (Molecular Devices). Series resistance was compensated to 70 - 80 %. All recorded parameters were digitized using Spike 2 version 6.11 with a Power1401 mark II (Cambridge Electronic Design, UK).

In some cases recorded neurons were labelled by addition of 0.05 % biocytin to the internal solution. At the conclusion of recordings the pipette was withdrawn, slices were fixed overnight in 4% paraformaldehyde and then frozen in cryoprotectant until immunohistochemical processing.

EXPERIMENTAL PROTOCOL

Simultaneous recordings from pairs of bulbospinal neurons

Simultaneous recordings of membrane voltage and current were performed in pairs of bulbospinal RVLM neurons recorded in close proximity to one another (< 100 µm between cells). The ‘pre-synaptic’ neuron was held in current clamp mode, whereas the ‘post-synaptic’ cell was held in voltage clamp at a holding potential of -60 mV. Stable recordings were established for up to 25 minutes, over which spontaneous or evoked action potentials (pre-synaptic cell) and synaptic currents (post-synaptic cell) were recorded. In neurons in which spontaneous action potentials were infrequent or absent depolarizing currents were injected to increase neuronal excitability. If recordings remained stable the recording modes

were switched so that the 'pre-synaptic' neuron became the 'post-synaptic' cell, and the recording protocol was repeated, allowing examination of any reciprocal connections.

Control experiments

As a control experiment, we tested our ability to detect constant-latency synaptic events evoked by electrical stimulation of presynaptic neurons or axons. Intermittent monopolar stimulation (0 to 800 µA, 0.2 ms, 0.5 – 2 Hz) was delivered via a borosilicate pipette (10 µm outer diameter) filled with aCSF. The stimulating electrode was placed on the contralateral side of the RVLM between the ventral surface of the slice and the nucleus ambiguous or in close proximity to the recorded neuron. Control experiments were performed using CsCl internal solution; all paired recordings were performed using K-gluconate internal solutions.

DATA ANALYSIS

In order to ensure that identification of a synaptic connection was not confused with spontaneous currents (it is possible to fail to detect weak synapses of 10 pA in the recording noise: Debanne et al. (2008)); trains of 102 to 1658 action potentials were used to trigger waveform averages of holding current as previously described (Barman, 1990, Chen and Toney, 2003, Stocker and Toney, 2005, 2007, Boudkkazi et al., 2011). Negative controls for each recording were made by processing the same block of data triggered by a "dummy" channel with an average frequency equal to that of the current-clamped neuron. Spike-triggered averages were 100 ms long with a 50 ms pre-trigger offset. The acceptance criteria for evidence of a synaptic connection was the presence of a constant latency synaptic current (> 5 pA) in the spike-triggered average of the 'post-synaptic' neuron within 50 ms of action potential generation in the 'presynaptic' cell (Debanne et al., 2008). The amplitude of a putative synaptic current should also exceed twice the standard deviation of data triggered by the dummy channel. All the data in the current study are expressed as mean ± SEM. Statistical analysis was performed using Spike 2 (Cambridge Electronic Design, UK), Excel (Microsoft, USA) and Prism 6.0 (Graphpad Software, Inc, USA).

IMMUNOHISTOCHEMISTRY

Some sections containing biocytin-labelled neurons were removed from cryoprotectant, washed, and permeabilized in phosphate buffered solution (PBS) with 0.5% Triton X-100 for 12 hours at 4 ^{o}C. Sections were incubated in blocking solution (5% bovine serum albumin,

BSA, in PBS) for 4 hours at room temperature followed by incubation in secondary antibodies (ExtraAvidin FITC 1:500, Jackson Immunoresearch) with 5 % BSA for 4 hours at room temperature, washed, mounted and coverslipped. Sections were examined and photographed under epi-fluorescence with appropriate filter sets.

RESULTS

ELECTROPHYSIOLOGICAL CHARACTERISTICS OF RECORDED NEURONS

38 pairs of neurons were simultaneously recorded from 46 CTB-labelled RVLM neurons. The average length of each recording was 478 ± 28 seconds, the average number of spikes recorded in current clamped neurons was 619 ± 64 and the frequency of synaptic events of the neurons recorded in voltage clamp mode was 1.98 ± 0.13 Hz.

As a positive control, we were able to detect constant-latency synaptic events recorded from bulbospinal RVLM neurons evoked by electrical stimulation of the contralateral brainstem in 7 cases (average latency = 7.32 ± 0.51 ms, the evoked synaptic current amplitude varied from 42.2 pA to 141.4 pA. The stimulation threshold ranged from 20 µA to 380 µA, figure 5.1).

EVIDENCE FOR SYNAPTIC CONNECTIONS BETWEEN RECORDED CELLS

Simultaneous recordings were made from 38 pairs of RVLM neurons. In no instance did we encounter evidence of synaptic currents in the 'post-synaptic' cell that were time-locked to action potentials in the 'pre-synaptic' neuron (figures 5.2 and 5.3). An example of a pair biocytin-filled bulbospinal RVLM neurons is shown in figure 5.4.

DISCUSSION

The aim of this study was to electrophysiologically examine the hypothesis that collateral axons from RVLM sympathetic premotor neurons provide synaptic drive to local bulbospinal neurons. Although long and stable recordings of neuronal activity was maintained, sufficient to permit robust statistical examination of our hypothesis, no evidence for connections between pairs of spinally projecting neurons was encountered. We therefore conclude that connections between RVLM sympathetic premotor neurons are either non-existent, so sparse as to be unlikely to fulfil any significant functional role, or undetectable using the approaches employed here. These findings are consistent with a study by McAllen et al. (2001), in which pairs of bulbospinal barosensitive RVLM neurons were recorded in anaesthetised cats and examined for evidence of synaptic coupling, but at odds with neuroanatomical evidence suggesting that RVLM sympathetic premotor neurons and C1 neurons contribute to local neuronal networks. Reconstructions of single RVLM sympathetic premotor neurons filled intracellularly with lucifer yellow and visualised after diaminobenzidine immunohistochemistry indicate extensive colateralisation of axons and with local varicosities and terminals (Lipski et al., 1995b). These findings are supported by recent imaging data obtained following infection of RVLM C1 neurons with a lentiviral vector that drives the expression of a green fluorescent reporter (Card et al., 2006, Agassandian et al., 2012). Using this technology, Card et al. (2006) were able to map the efferent projections of C1 neurons and identified axonal varicose arborizations that form close appositions with other neurons residing in close proximity to the C1 population, confirmed as synapses in subsequent electron microscopy studies (Agassandian et al., 2012). Agassandian et al. (2012) also demonstrated the presence of reporter-filled synapses on C1 and non-C1 cells throughout the rostrocaudal extent of the C1 cell column. These data are consistent to some extent with previous work from our laboratory that shows that small numbers of C1 and bulbospinal neurons are retrogradely labelled from the contralateral RVLM pressor region (Turner et al., 2013) and therefore likely to participate in local RVLM circuits in addition to their well-defined bulbospinal and rostral projections. Although we did not observe changes in post-synaptic holding current in response to current injection in the pre-synaptic neuron, the possibility of electrical coupling was not systematically investigated, and therefore remains plausible (Alvarez et al., 2002, Mancilla et al., 2007).

Technical considerations

Antidromic activation of neurons following electrical stimulation of the spinal cord is the gold-standard for evidence of bulbospinal projection, whereas sensitivity to stimuli known to modulate sympathetic nerve activity (e.g. activation of the baroreflex) are used to functionally identify these neurons *in vivo* (Brown and Guyenet, 1984, Lipski et al., 1995a). Conformity to both sets of criteria are required for the confident interpretation of electrophysiological recordings obtained *in vivo.* In the slice preparation identification of bulbospinal neurons by retrograde transport of fluorescent dyes is straightforward, but functional classification of neurons is impossible, so we consider the data described here as coming from putative sympathetic premotor neurons. Assuming that most of these neurons represent sympathetic premotor neurons, it seems that there is little or no connectivity between cells.

A major limitation of the current study is that that preparation of brain slices reduces connectivity, as by definition many axons and dendrites are damaged during slicing (Debanne et al., 2008). In order to minimise tissue damage we glued the brainstem block with the ventral surface of the brain facing the blade and supported the dorsal surface with an agar block, and advanced the vibratome blade at speed that minimised brain compression and tissue displacement. Using ice, we kept the slicing chamber cool throughout the entire procedure and the tissue was exposed to aCSF saturated with carbogen before slicing and carbogen bubbling was maintained in order to keep the tissue alive. A balance of care and speed was used in order to minimise the amount of time needed to slice a block of tissue and to keep it healthy at the same time. We also limited recordings to pairs of neurons recorded in close proximity to each other and away from the surface of the slice. Finally, coronal sections may truncate connections if the neuronal organization is rostral-caudally oriented.

Conclusions

Excitatory synaptic drive plays a crucial role in generating baseline activity in RVLM sympathetic premotor neurons in healthy animals, and synaptic plasticity in the RVLM is thought to drive pathophysiological changes in baselines sympathetic nerve activity characteristic of many cardiovascular diseases. However, identifying the interneurons that

contribute to their baseline activity remains incomplete. In the current study we investigated the hypothesis that sympathetic premotor neurons in the RVLM are one source of synaptic drive to other nearby sympathetic premotor neurons. We did not find any sign of bulbospinal to bulbospinal microcircuit formation within the RVLM. New technologies, such as restricted trans-synaptic tracing techniques (Marshel et al., 2010) coupled with the dual patch clamp method or optogenetic techniques could be used to unambiguously identify the networks that drive RVLM sympathetic premotor neurons in the future.

CHAPTER 5 FIGURES AND TABLES

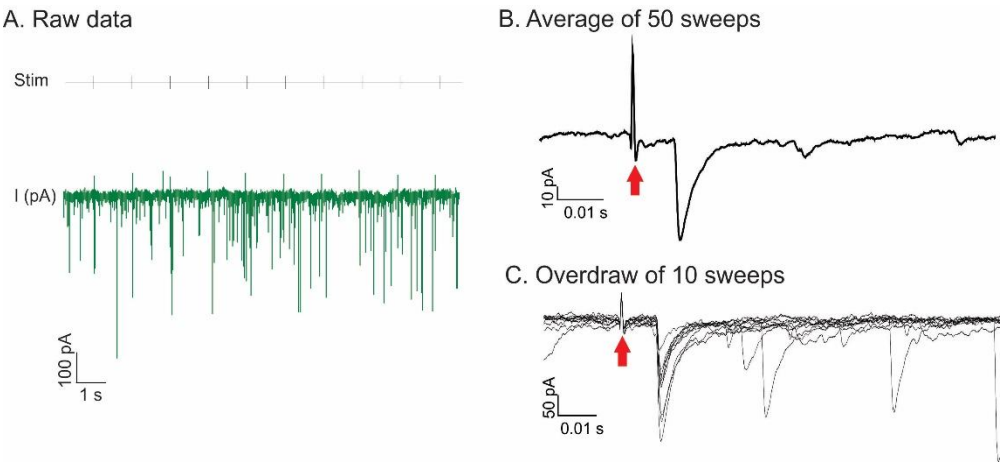

Figure 5.1: Evoked post synaptic current following electrical stimulation. A. Raw data recorded from a sympathetic premotor RVLM neuron and showing inward current evoked by electrical stimulation of pre-synaptic neurons. **B.** Average evoked responses of 50 sweeps following electrical stimulation with a shock intensity of 50 µA. **C.** shows overdraw of 10 evoked responses. Recording performed using CsCl internal solution.

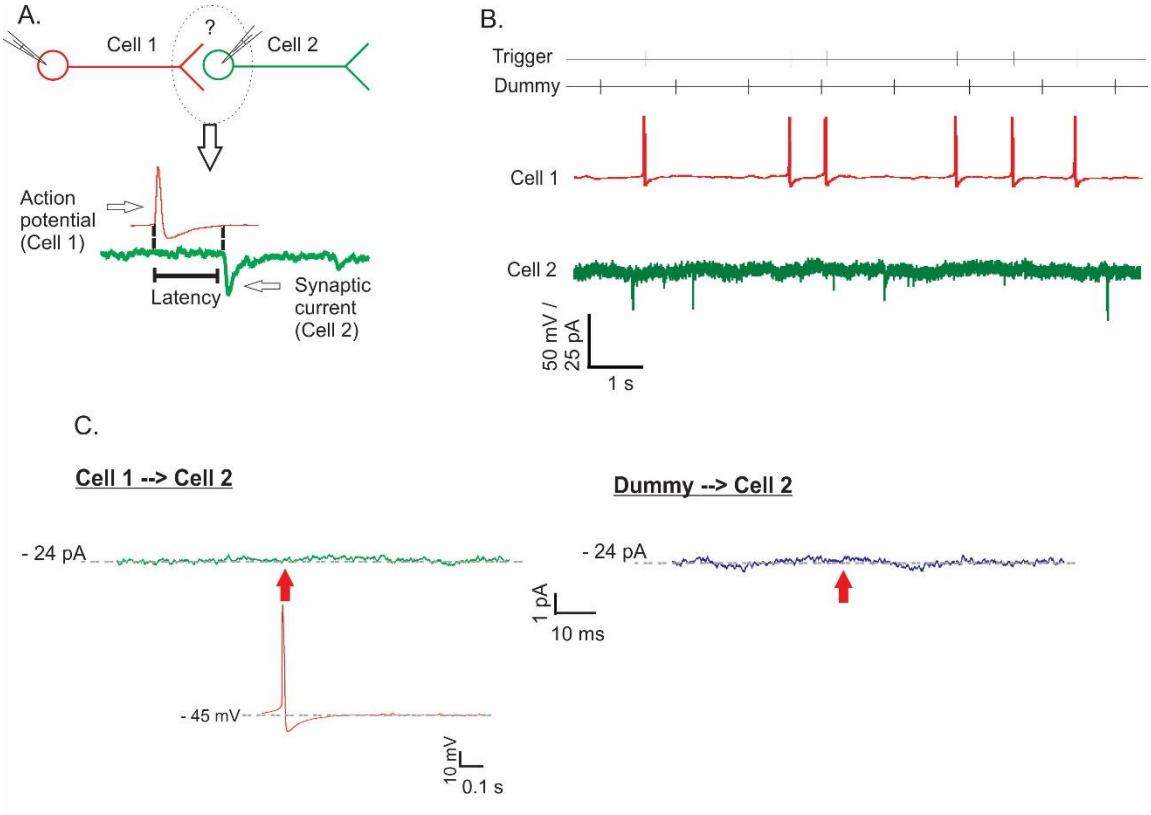

Figure 5.2: Conceptual overview of experiment. A. Schematic diagram showing a connected pair of neurons and expected relationship between presynaptic action potential and time-locked post-synaptic currents. **B.** Raw data showing action potentials recorded in current clamp mode in cell 1 and membrane currents recorded in voltage clamp mode in cell 2. Note 'trigger' channel, derived from action potential timing, and 'dummy' channel, derived from a clock running at the same average frequency as cell 1. **C.** Average of membrane currents recorded in cell 2 triggered by trigger (136 sweeps, top trace) or dummy channel (199 sweeps). Red arrows indicate the trigger.

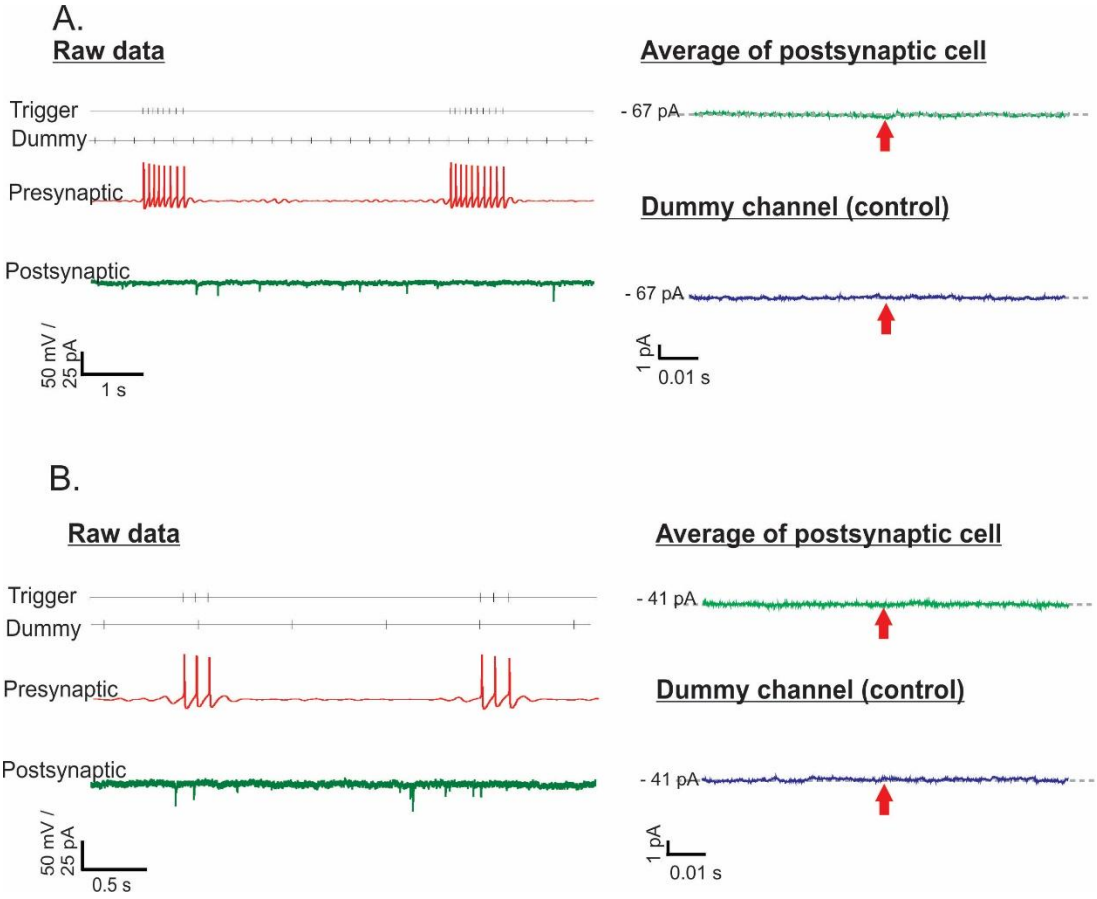

Figure 5.3: More examples of paired recordings of bulbospinal RVLM neurons. A & B. shows two different examples of tested pairs recorded from bulbospinal neurons. Connections between the pairs were not found. The red arrows show the action potential / trigger point recorded from the presynaptic neuron.

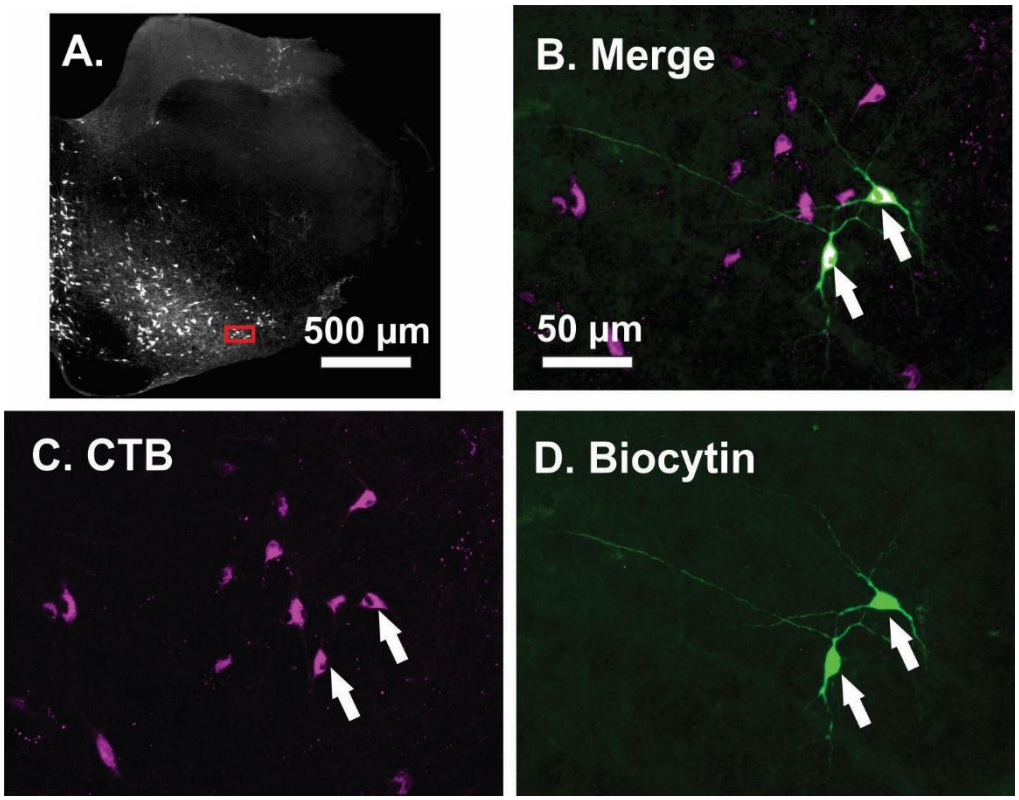

Figure 5.4: Histologically recovered recorded bulbospinal neurons. Biotin-filled neurons (white arrow) from a paired recording experiment (raw data: Figure 5.3A). **A.** Brainstem hemisection showing position of recovered neurons (red box). **B.** Merged high-power image of region denoted by red box showing adjacent biotin-labelled CTB positive neurons (arrows). **C and D.** individual CTB and biotin channels.

CHAPTER 6: SUMMARY OF FINDINGS

The RVLM is a small area of the brainstem that is essential for the generation of sympathetic vasomotor tone and elaboration of multiple homeostatic reflexes. These properties arise from the continuous activity of sympathetic premotor RVLM neurons, which is modulated by a combination of ascending and descending inputs. The functional profile of these neurons emerges from the integration of intrinsic (membrane) properties, synaptic drive, and the activity of glia in their immediate vicinity.

The main objectives of the studies conducted in the current thesis were:

1. To investigate the hypoxia-sensitivity of sympathetic premotor RVLM neurons and its probable mediators.
2. To determine the role played by RVLM bulbospinal neurons in driving adrenaline release in response to acute glucoprivation.
3. To determine the cellular mechanisms responsible for sympathoinhibition caused by somatostatin.
4. To examine whether there is any functional evidence of direct synaptic connections between pairs of spinally projecting RVLM.

Chapter 2: summary, perspectives and future directions

In chapter 2 of this thesis I investigated the cellular mechanisms that underlie the hypoxia-sensitivity of bulbospinal RVLM neurons *in vitro*. Consistent with previous reports, I found that brief cyanide application evoked dose-dependent inward currents that were relatively greater in bulbospinal RVLM neurons compared to randomly selected non bulbospinal RVLM neurons and were unaffected by TTX application, supporting a role of bulbospinal neurons as acute hypoxia sensors.

I first eliminated one candidate mediator for the RVLM hypoxic response, Heme-Oxygenase 2 (HO-2). Consistent with Mazza et al. (2001), we found that HO-2 was densely expressed in the adjacent facial nucleus, but that HO-2 immunoreactivity was sparse in the RVLM. Colocalization of HO-2 immunoreactivity was never detected in putative RVLM sympathetic premotor neurons, including those functionally verified as hypoxia-sensitive, suggesting that HO-2 is unlikely to play an important role in determining hypoxia-sensitivity in this population.

I then investigated glial ATP release as a candidate mediator of this effect, since it has been shown by Gourine et al. (2005) that during hypoxia ATP is released from the ventral surface of the medulla. I found that P2X receptor blockade reversibly attenuated the hypoxia sensitivity in bulbospinal RVLM neurons, suggesting that ATP release is a key component of this response. Furthermore, I also found that hypoxia sensitivity was essentially abolished by incubation in a glia inhibitor, fluoroacetate. Taken together, these findings support a strong role for RVLM glia in mediating responses to acute brainstem hypoxia.

Limitations of this study were, first, that HO-2 immunoreactivity may not be sufficiently sensitive to identify low levels of HO-2 expression that may be functionally significant. Second, our case for a role for glia in mediating hypoxic responses is based on inductive reasoning, rather than direct examination of glia. Third, it is unclear whether the mechanisms identified here *in vitro* play a functionally significant role *in vivo*. Finally, it would also be interesting to examine whether these mechanisms play a role in disease states characterised by chronic or repeated hypoxia or brainstem hypoperfusion.

Future directions that could address these limitations would be to pharmacologically block HO-2 activity and then examine neuronal responses to hypoxia, comprehensively eliminating any role for HO-2 in mediating these responses, to test the role played by glutamate released by glia in testing its effect on the remaining current following P2X receptor blockade and to directly record glial responses to hypoxia using electrophysiological or optical recordings. The question of whether the same mechanisms play an important role *in vivo*, and whether glial ATP release contributes to pathophysiological conditions, could be addressed by using viral vectors to either block gliotransmitter release or metabolise extracellular ATP.

Chapter 3: summary, perspectives and future directions

In chapter 3 of this thesis I investigated the role of sympathetic premotor RVLM neurons in driving adrenaline release in response to acute glucoprivation. *In vivo*, we found that ASNA increases following local glucoprivation or disinhibition of PeH neurons and following systemic glucoprivation and that ASNA correlated with plasma metanephrine levels but not normetanephrine levels. This effect was abolished by inhibition of the PeH. Then we demonstrated that the adrenal sympathoexcitatory response was reduced by the

glucoprivation of perifornical neurons subsequent to activation by bicuculline, a $GABA_A$ antagonist. *In vitro* we showed that local neuroglucoprivation in the RVLM failed to activate sympathetic premotor neurons.

C1 cells seem to play an important role in hyperglycemic responses to glucoprivation; first, these neurons express Fos following 2-DG application (Ritter et al., 1998). Second, adrenaline is released from the adrenal medulla following glucoprivation (Sun et al., 1979, Rappaport et al., 1982, Storlien et al., 1985, Matsunaga et al., 1989). Third, C1 neurons project to preganglionic cells that innervate the adrenal gland (Strack et al., 1989b). Fourth, following RVLM stimulation the 2-DG sensitive sympathetic preganglionic neurons are activated with a slow conducting velocity (Morrison et al., 1988) corresponding to that of C1 neurons (Schreihofer and Guyenet, 1997). So, it has been suggested that C1 neurons project to sympathetic preganglionic neurons which in turn innervate adrenal chromaffin cells.

In our study we found that orexin modulates the activity of RVLM adrenal sympathetic premotor neurons resulting in excitation of adrenal chromaffin cells and we also found that bulbospinal RVLM neurons are not intrinsically glucose sensitive. In order to confirm the glucose-sensing pathway described in this study, the next step should be testing the sensitivity of RVLM neurons to orexin.

Further studies to determine the function of glucose sensing neurons and to identify glucose-sensing cells that control counter-regulatory responses are crucial. In order to specifically target C1 neurons and test their responses to glucoprivation, we can use viral vectors that specifically infect C1 neurons. In addition, for a full understanding of energy homeostasis it is very important to determine the role played by hindbrain counter-regulatory systems in response to glucose homeostasis under non-glucoprivic conditions.

Chapter 4: summary, perspectives and future directions

In chapter 4 of this thesis I investigated the cellular mechanisms responsible for the inhibition of RVLM sympathetic premotor neurons by SST and its probable sources. I showed that SST evoked an outward current in 50% of RVLM sympathetic premotor neurons. The SSTergic responses were blocked by Cyanamid, an sst_2 receptor blocker and sst_{2A} receptor was identified on SST-sensitive recorded neurons. We also identified 8 distinct brain regions

as sources of SSTergic input to the RVLM. The study conducted here examined the effect of SST on neurons that play a key role in the regulation of the sympathetic vasomotor tone.

The role of SST in the ventrolateral medulla is mainly depressor. In cats and rats, SST evokes hypotension when it is locally injected in the ventrolateral medulla (Yamamoto et al., 1988, Chen et al., 1990). Most relevant to this thesis is the study made by Burke et al. (2008), who proved that SST causes a dramatic splanchnic sympathoinhibition, bradycardia and hypotension when injected bilaterally into the RVLM. These effects were dose-dependent and reversible; in addition it has been shown that the reflex control of sympathetic nerve activity was less affected.

SST is involved in many disease states such as sudden infant death where the victims express an abnormally high level of SST receptor expression in the ventrolateral medulla and other brainstem areas (Chigr et al., 1992, Carpentier et al., 1998). However, the mechanisms that control the release of SST under physiological conditions have not yet been described.

Limitations of this study were, first, we cannot confirm that CTB labelled neurons form synaptic terminals within the RVLM or simply represent fibres of passage, since CTB labels all fibres that cross the injection site. Second, CTB-labelled SSTergic neurons do not necessarily indicate the presence of an SSTergic input to RVLM bulbospinal neurons. Third, we cannot exclude local interneurons as a potential source of SST release. Fourth, we are using rat pups, SST receptors may not be fully developed on the recorded neurons which could complicate interpretation of our data.

Future directions that could address these limitations would be to use new technologies such as restricted trans-synaptic tracing techniques that will link us to the exact SSTergic inputs to the RVLM. In addition, patch clamp recordings can also be performed on slices collected from adult rats which is much harder to perform but feasible.

Chapter 5: summary, perspectives and future directions

In chapter 5 of this thesis I investigated whether or not bulbospinal RVLM neurons form a local network *in vitro*. I used the paired-patch clamp technique in order to record simultaneously from pairs of neuron; links between recorded bulbospinal RVLM neurons were not found, suggesting that the local network that may be formed by bulbospinal RVLM

neurons does not significantly contribute to the activity of these cells. We found a discrepancy in the data since anatomical studies had indicated that connection may be present. Consistent with our finding, McAllen et al. (2001) showed, using extracellular recordings in cats, that there is little synchronicity between pairs of RVLM neurons and no evidence of synaptic interconnections between the pairs was presented. Hence, RVLM neurons, known to be a group of premotor units driving rhythmic discharge of sympathetic nerves, do not appear to contribute synaptic drive to other sympathetic premotor neurons. These neurons appear to be rhythmically entrained by common afferent inputs. Roles for angiotensin and glutamatergic inputs have been postulated as they tonically excite RVLM cells (Dampney et al., 2005, Stocker et al., 2006); but the sources of these inputs are still unclear.

Limitations of this study were, first, we used fresh prepared brainstem slices, even though I was very careful in preparing the slices some connections (axons and dendrites) might be cut during slicing. Second, I used rat pups in which axons may not be fully developed.

Future directions that could address these limitations would be to either pair patch RVLM bulbospinal neurons *in vivo*, and this is very complicated to perform since the RVLM is a deep brain area, or to use restricted trans-synaptic tracing techniques coupled with the dual patch clamp method used in this study in order to map the network of these neurons.

Closing remarks

Within the hypothalamus and lower brainstem resides the neural circuit that underlies circulation and breathing functions. From birth, this circuit is constructed in a way to respond to homeostatic challenges that are essential for survival such as: blood loss, injury, infection, hypoxia and hypotension. Hence, identifying the mechanisms that regulate the activity of the cardiovascular and respiratory networks are primordial. In this thesis we studied some of the intrinsic characteristics and network organisation of sympathetic premotor RVLM neurons.

Guyenet et al. (2013), in their recent review, described C1 neurons as the body's "emergency medical technicians", since these cells are implicated in autonomic, metabolic, and neuroendocrine responses that help survival. However, many fundamental characteristics regarding C1 neurons remain unclear: first, are C1 and non-C1 sympathetic premotor

neurons developmentally related? Second, from where does the mysterious excitatory drive, thought to generate spontaneous activity in these neurons, arise? Third, do factors, such as gliotransmitters, have a more prerequisite role in regulating the activity of these neurons? Fourth, what other undiscovered functional subsets of sympathetic premotor neurons remain to be discovered?

REFERENCES

Abbott SB, Burke PG, Pilowsky PM (2009a) Galanin microinjection into the PreBotzinger or the Botzinger Complex terminates central inspiratory activity and reduces responses to hypoxia and hypercapnia in rat. Respir Physiol Neurobiol 167:299-306.

Abbott SB, Coates MB, Stornetta RL, Guyenet PG (2013) Optogenetic stimulation of c1 and retrotrapezoid nucleus neurons causes sleep state-dependent cardiorespiratory stimulation and arousal in rats. Hypertension 61:835-841.

Abbott SB, Pilowsky PM (2009) Galanin microinjection into rostral ventrolateral medulla of the rat is hypotensive and attenuates sympathetic chemoreflex. American journal of physiology Regulatory, integrative and comparative physiology 296:R1019-1026.

Abbott SB, Stornetta RL, Fortuna MG, Depuy SD, West GH, Harris TE, Guyenet PG (2009b) Photostimulation of retrotrapezoid nucleus phox2b-expressing neurons in vivo produces long-lasting activation of breathing in rats. The Journal of neuroscience : the official journal of the Society for Neuroscience 29:5806-5819.

Abbott SB, Stornetta RL, Socolovsky CS, West GH, Guyenet PG (2009c) Photostimulation of channelrhodopsin-2 expressing ventrolateral medullary neurons increases sympathetic nerve activity and blood pressure in rats. J Physiol 587:5613-5631.

Accorsi-Mendonca D, Zoccal DB, Bonagamba LG, Machado BH (2013) Glial cells modulate the synaptic transmission of NTS neurons sending projections to ventral medulla of Wistar rats. Physiological reports 1:e00080.

Adachi T, Ishikawa K, Hida W, Matsumoto H, Masuda T, Date F, Ogawa K, Takeda K, Furuyama K, Zhang Y, Kitamuro T, Ogawa H, Maruyama Y, Shibahara S (2004) Hypoxemia and blunted hypoxic ventilatory responses in mice lacking heme oxygenase-2. Biochemical and Biophysical Research Communications 320:514-522.

Agarwal SK, Gelsema AJ, Calaresu FR (1990) Inhibition of rostral VLM by baroreceptor activation is relayed through caudal VLM. The American journal of physiology 258:R1271-1278.

Agassandian K, Shan Z, Raizada M, Sved AF, Card JP (2012) C1 catecholamine neurons form local circuit synaptic connections within the rostroventrolateral medulla of rat. Neuroscience 227:247-259.

Aicher SA, Saravay RH, Cravo S, Jeske I, Morrison SF, Reis DJ, Milner TA (1996) Monosynaptic projections from the nucleus tractus solitarii to C1 adrenergic neurons in the rostral ventrolateral medulla: comparison with input from the caudal ventrolateral medulla. The Journal of comparative neurology 373:62-75.

Ainscow, E. K., Mirshamsi, S., Tang, T., Ashford, M. L. & Rutter, G. A. 2002 Dynamic imaging of free cytosolic ATP concentration during fuel sensing by rat hypothalamic neurones: evidence for ATP-independent control of ATP-sensitive KC channels. J. Physiol. 544, 429–445.

Alam MN, Kumar S, Bashir T, Suntsova N, Methippara MM, Szymusiak R, McGinty D (2005) GABA-mediated control of hypocretin- but not melanin-concentrating hormone-immunoreactive neurones during sleep in rats. J Physiol (Lond) 563:569-582.

Aley PK, Murray HJ, Boyle JP, Pearson HA, Peers C (2006) Hypoxia stimulates Ca2+ release from intracellular stores in astrocytes via cyclic ADP ribose-mediated activation of ryanodine receptors. Cell Calcium 39:95-100.

Allen AM, Guyenet PG (1993) Alpha 2-adrenoceptor-mediated inhibition of bulbospinal barosensitive cells of rat rostral medulla. The American journal of physiology 265:R1065-1075.

Alvarez VA, Chow CC, Van Bockstaele EJ, Williams JT (2002) Frequency-dependent synchrony in locus ceruleus: role of electrotonic coupling. Proc Natl Acad Sci U S A 99:4032-4036.

Alves F, Resstel L, Correa F, Crestani C (2011) Bed nucleus of the stria terminalis α1 and 2-adrenoceptors differentially modulate the cardiovascular responses to exercise in rats. Neuroscience 177:74-83.

Alves TCTF, Rays J, Fráguas Jr R, Wajngarten M, Meneghetti JC, Prando S, Busatto GF (2005) Localized cerebral blood flow reductions in patients with heart failure: A study using 99mTc-HMPAO SPECT. Journal of Neuroimaging 15:150-156.

Amendt K, Czachurski J, Dembowsky K, Seller H (1979) Bulbospinal projections to the intermediolateral cell column: a neuroanatomical study. Journal of the autonomic nervous system 1:103-107.

Ammons WS (1988) Renal and somatic input to spinal neurons antidromically activated from the ventrolateral medulla. Journal of Neurophysiology 60:1967-1981.

Andrew SF, Dinh TT, Ritter S (2007) Localized glucoprivation of hindbrain sites elicits corticosterone and glucagon secretion. American journal of physiology Regulatory, integrative and comparative physiology 292:R1792-R1798.

Armstrong CL, Hopkins DA (1998) Neurochemical organization of paratrigeminal nucleus projections to the dorsal vagal complex in the rat. Brain research 785:49-57.

Balan Jr A, Caous CA, Yu YG, Lindsey CJ (2004) Barosensitive neurons in the rat tractus solitarius and paratrigeminal nucleus: A new model for medullary, cardiovascular reflex regulation. Canadian journal of physiology and pharmacology 82:474-484.

Barman SM (1990) Descending projections of hypothalamic neurons with sympathetic nerve-related activity. J Neurophysiol 64:1019-1032.

Barman SM, Gebber GL (1980) Sympathetic nerve rhythm of brain stem origin. The American journal of physiology 239:R42-47.

Barman SM, Gebber GL (1985) Axonal projection patterns of ventrolateral medullospinal sympathoexcitatory neurons. J Neurophysiol 53:1551-1566.

Barman SM, Gebber GL (1989) Basis for the naturally occurring activity of rostral ventrolateral medullary sympathoexcitatory neurons. Progress in brain research 81:117-129.

Beall C, Ashford ML, McCrimmon RJ (2012) The physiology and pathophysiology of the neural control of the counterregulatory response. American journal of physiology Regulatory, integrative and comparative physiology 302:R215-223.

Beitz AJ, Shepard RD, Wells WE (1983) The periaqueductal gray-raphe magnus projection contains somatostatin, neurotensin and serotonin but not cholecystokinin. Brain research 261:132-137.

Blessing WW, Goodchild AK, Dampney RA, Chalmers JP (1981) Cell groups in the lower brain stem of the rabbit projecting to the spinal cord, with special reference to catecholamine-containing neurons. Brain research 221:35-55.

Bohm SK, Grady EF, Bunnett NW (1997) Regulatory mechanisms that modulate signalling by G-protein-coupled receptors. The Biochemical journal 322 (Pt 1):1-18.

Borg WP, Sherwin RS, During MJ, Borg MA, Shulman GI (1995) Local ventromedial hypothalamus glucopenia triggers counterregulatory hormone release. Diabetes 44:180-184.

Boudkkazi S, Fronzaroli-Molinieres L, Debanne D (2011) Presynaptic action potential waveform determines cortical synaptic latency. J Physiol 589:1117-1131.

Bowman BR, Kumar NN, Hassan SF, McMullan S, Goodchild AK (2013) Brain sources of inhibitory input to the rat rostral ventrolateral medulla. The Journal of comparative neurology 521:213-232.

Briski KP, Sylvester PW (2001) Hypothalamic orexin-A-immunpositive neurons express Fos in response to central glucopenia. Neuroreport 12:531-534.

Brown DL, Guyenet PG (1984) Cardiovascular neurons of brain stem with projections to spinal cord. The American journal of physiology 247:R1009-1016.

Brown DL, Guyenet PG (1985) Electrophysiological study of cardiovascular neurons in the rostral ventrolateral medulla in rats. Circ Res 56:359-369.

Bruno JF, Xu Y, Song J, Berelowitz M (1992) Molecular cloning and functional expression of a brain-specific somatostatin receptor. Proceedings of the National Academy of Sciences 89:11151-11155.

Burdakov D, Ashcroft FM (2002) Cholecystokinin tunes firing of an electrically distinct subset of arcuate nucleus neurons by activating A-Type potassium channels. The Journal of neuroscience : the official journal of the Society for Neuroscience 22:6380-6387.

Burdakov D, Gerasimenko O, Verkhratsky A (2005) Physiological changes in glucose differentially modulate the excitability of hypothalamic melanin-concentrating hormone and

orexin neurons in situ. The Journal of neuroscience : the official journal of the Society for Neuroscience 25:2429-2433.

Burke PG, Abbott SB, McMullan S, Goodchild AK, Pilowsky PM (2010) Somatostatin selectively ablates post-inspiratory activity after injection into the Botzinger complex. Neuroscience 167:528-539.

Burke PG, Li Q, Costin ML, McMullan S, Pilowsky PM, Goodchild AK (2008) Somatostatin 2A receptor-expressing presympathetic neurons in the rostral ventrolateral medulla maintain blood pressure. Hypertension 52:1127-1133.

Burke PG, Neale J, Korim WS, McMullan S, Goodchild AK (2011) Patterning of somatosympathetic reflexes reveals nonuniform organization of presympathetic drive from C1 and non-C1 RVLM neurons. American journal of physiology Regulatory, integrative and comparative physiology 301:R1112-1122.

Burman KJ, Sartor DM, Verberne AJ, Llewellyn-Smith IJ (2004) Cocaine- and amphetamine-regulated transcript in catecholamine and noncatecholamine presympathetic vasomotor neurons of rat rostral ventrolateral medulla. The Journal of comparative neurology 476:19-31.

Campbell LB, Gooden BA, Horowitz JD (1969) Cardiovascular responses to partial and total immersion in man. J Physiol 202:239-250.

Canals S, Larrosa B, Pintor J, Mena MA, Herreras O (2008) Metabolic challenge to glia activates an adenosine-mediated safety mechanism that promotes neuronal survival by delaying the onset of spreading depression waves. Journal of cerebral blood flow and metabolism : official journal of the International Society of Cerebral Blood Flow and Metabolism 28:1835-1844.

Cao WH, Morrison SF (2003) Disinhibition of rostral raphe pallidus neurons increases cardiac sympathetic nerve activity and heart rate. Brain research 980:1-10.

Caous CA, Balan A, Lindsey CJ (2004) Bradykinin microinjection in the paratrigeminal nucleus triggers neuronal discharge in the rat rostroventrolateral reticular nucleus. Canadian journal of physiology and pharmacology 82:485-492.

Caous CA, Buck HdS, Lindsey CJ (2001) Neuronal connections of the paratrigeminal nucleus: a topographic analysis of neurons projecting to bulbar, pontine and thalamic nuclei related to cardiovascular, respiratory and sensory functions. Autonomic Neuroscience 94:14-24.

Card JP, Sved JC, Craig B, Raizada M, Vazquez J, Sved AF (2006) Efferent projections of rat rostroventrolateral medulla C1 catecholamine neurons: Implications for the central control of cardiovascular regulation. The Journal of comparative neurology 499:840-859.

Carpentier V, Vaudry H, Mallet E, Laquerriere A, Leroux P (1998) Increased density of somatostatin binding sites in respiratory nuclei of the brainstem in sudden infant death syndrome. Neuroscience 86:159-166.

Carrive P (2000) Conditioned fear to environmental context: cardiovascular and behavioral components in the rat. Brain research 858:440-445.

Carrive P, Bandler R (1991) Viscerotopic organization of neurons subserving hypotensive reactions within the midbrain periaqueductal grey: a correlative functional and anatomical study. Brain research 541:206-215.

Carrive P, Bandler R, Dampney RA (1988) Anatomical evidence that hypertension associated with the defence reaction in the cat is mediated by a direct projection from a restricted portion of the midbrain periaqueductal grey to the subretrofacial nucleus of the medulla. Brain research 460:339-345.

Cassell MD, Gray TS (1989) The amygdala directly innervates adrenergic (C1) neurons in the ventrolateral medulla in the rat. Neuroscience letters 97:163-168.

Caverson MM, Ciriello J, Calaresu FR (1983) Direct pathway from cardiovascular neurons in the ventrolateral medulla to the region of the intermediolateral nucleus of the upper thoracic cord: an anatomical and electrophysiological investigation in the cat. Journal of the autonomic nervous system 9:451-475.

Cavun S, Millington WR (2001) Evidence that hemorrhagic hypotension is mediated by the ventrolateral periaqueductal gray region. American journal of physiology Regulatory, integrative and comparative physiology 281:R747-R752.

Chamberlin N, Saper C (1994) Topographic organization of respiratory responses to glutamate microstimulation of the parabrachial nucleus in the rat. The Journal of Neuroscience 14:6500-6510.

Chan O, Paranjape S, Czyzyk D, Horblitt A, Zhu W, Ding Y, Fan X, Seashore M, Sherwin R (2011) Increased GABAergic output in the ventromedial hypothalamus contributes to impaired hypoglycemic counterregulation in diabetic rats. Diabetes 60:1582-1589.

Chan O, Zhu W, Ding Y, McCrimmon RJ, Sherwin RS (2006) Blockade of GABA(A) receptors in the ventromedial hypothalamus further stimulates glucagon and sympathoadrenal but not the hypothalamo-pituitary-adrenal response to hypoglycemia. Diabetes 55:1080-1107.

Chen QH, Toney GM (2003) Identification and characterization of two functionally distinct groups of spinal cord-projecting paraventricular nucleus neurons with sympathetic-related activity. Neuroscience 118:797-807.

Chen ZB, Hedner T, Hedner J (1990) Local application of somatostatin in the rat ventrolateral brain medulla induces apnea. Journal of applied physiology 69:2233-2238.

Chigr F, Jordan D, Najimi M, Denoroy L, Sarrieau A, de Broca A, Rostene W, Epelbaum J, Kopp N (1992) Quantitative autoradiographic study of somatostatin and neurotensin binding sites in medulla oblongata of SIDS. Neurochemistry international 20:113-118.

Christou H, Morita T, Hsieh CM, Koike H, Arkonac B, Perrella MA, Kourembanas S (2000) Prevention of hypoxia-induced pulmonary hypertension by enhancement of endogenous heme oxygenase-1 in the rat. Circ Res 86:1224-1229.

Cohen MI, Gootman PM (1970) Periodicities in efferent discharge of splanchnic nerve of the cat. The American journal of physiology 218:1092-1101.

Connor M, Bagley EE, Mitchell VA, Ingram SL, Christie MJ, Humphrey PP, Vaughan CW (2004) Cellular actions of somatostatin on rat periaqueductal grey neurons in vitro. British journal of pharmacology 142:1273-1280.

Coote JH (2007) Landmarks in understanding the central nervous control of the cardiovascular system. Experimental physiology 92:3-18.

Coote JH, Yang Z, Pyner S, Deering J (1998) Control of sympathetic outflows by the hypothalamic paraventricular nucleus. Clinical and experimental pharmacology & physiology 25:461-463.

Cornish KG, Barazanji MW, Iaffaldano R (1990) Neural and hormonal control of blood pressure in conscious monkeys. The American journal of physiology 258:H107-112.

Cotero VE, Routh VH (2009) Insulin blunts the response of glucose-excited neurons in the ventrolateral-ventromedial hypothalamic nucleus to decreased glucose. American journal of physiology Endocrinology and metabolism 296:E1101-E1109.

Cox GE, Jordan D, Paton JF, Spyer KM, Wood LM (1987) Cardiovascular and phrenic nerve responses to stimulation of the amygdala central nucleus in the anaesthetized rabbit. J Physiol 389:541-556.

Craig AD (1993) Propriospinal input to thoracolumbar sympathetic nuclei from cervical and lumbar lamina I neurons in the cat and the monkey. Journal of Comparative Neurology 331:517-530.

Craig AD (1995) Distribution of brainstem projections from spinal lamina I neurons in the cat and the monkey. The Journal of comparative neurology 361:225-248.

Craig AD, Dostrovsky JO (2001) Differential Projections of Thermoreceptive and Nociceptive Lamina I Trigeminothalamic and Spinothalamic Neurons in the Cat. Journal of Neurophysiology 86:856-870.

Cravo SL, Morrison SF (1993) The caudal ventrolateral medulla is a source of tonic sympathoinhibition. Brain research 621:133-136.

Cravo SL, Morrison SF, Reis DJ (1991) Differentiation of two cardiovascular regions within caudal ventrolateral medulla. The American journal of physiology 261:R985-994.

Cremer-Lacuara MG, Lacuara JL, Fiol de Cuneo M, Ruiz RD (1980) Substrate supply and function of isolated venous smooth muscle under anoxia and metabolic inhibition. Canadian journal of physiology and pharmacology 58:723-730.

Crestani CC, Alves FHF, Resstel LBM, CorrÃªa FMdA (2006) The bed nucleus of the stria terminalis modulates baroreflex in rats. Neuroreport 17:1531-1535

Cryer PE (2007) Hypoglycemia, functional brain failure, and brain death. The Journal of clinical investigation 117:868-870.

Cunningham ET, Jr., Bohn MC, Sawchenko PE (1990) Organization of adrenergic inputs to the paraventricular and supraoptic nuclei of the hypothalamus in the rat. The Journal of comparative neurology 292:651-667.

D'Agostino D, Mazza E, Jr., Neubauer JA (2009) Heme oxygenase is necessary for the excitatory response of cultured neonatal rat rostral ventrolateral medulla neurons to hypoxia. American journal of physiology Regulatory, integrative and comparative physiology 296:R102-118.

da Silva GS, Giusti H, Benedetti M, Dias MB, Gargaglioni LH, Branco LG, Glass ML (2011) Serotonergic neurons in the nucleus raphe obscurus contribute to interaction between central and peripheral ventilatory responses to hypercapnia. Pflugers Archiv : European journal of physiology 462:407-418.

Dai KY, Chan SH, Chang AY (2010) Heme oxygenase-1 plays a pro-life role in experimental brain stem death via nitric oxide synthase I/protein kinase G signaling at rostral ventrolateral medulla. Journal of biomedical science 17:72.

Damanhuri HA, Burke PG, Ong LK, Bobrovskaya L, Dickson PW, Dunkley PR, Goodchild AK (2012) Tyrosine hydroxylase phosphorylation in catecholaminergic brain regions: a marker of activation following acute hypotension and glucoprivation. PLoS ONE 7:e50535.

Dampney RA (1994) Functional organization of central pathways regulating the cardiovascular system. Physiological reviews 74:323-364.

Dampney RA, Czachurski J, Dembowsky K, Goodchild AK, Seller H (1987) Afferent connections and spinal projections of the pressor region in the rostral ventrolateral medulla of the cat. Journal of the autonomic nervous system 20:73-86.

Dampney RA, Goodchild AK, Robertson LG, Montgomery W (1982) Role of ventrolateral medulla in vasomotor regulation: a correlative anatomical and physiological study. Brain research 249:223-235.

Dampney RA, Horiuchi J, Killinger S, Sheriff MJ, Tan PS, McDowall LM (2005) Long-term regulation of arterial blood pressure by hypothalamic nuclei: some critical questions. Clinical and experimental pharmacology & physiology 32:419-425.

Dampney RA, Horiuchi J, Tagawa T, Fontes MA, Potts PD, Polson JW (2003a) Medullary and supramedullary mechanisms regulating sympathetic vasomotor tone. Acta physiologica Scandinavica 177:209-218.

Dampney RA, Moon EA (1980) Role of ventrolateral medulla in vasomotor response to cerebral ischemia. The American journal of physiology 239:H349-358.

Dampney RA, Polson JW, Potts PD, Hirooka Y, Horiuchi J (2003b) Functional organization of brain pathways subserving the baroreceptor reflex: studies in conscious animals using immediate early gene expression. Cell Mol Neurobiol 23:597-616.

de Burgh Daly M, Elsner R, Angell-James JE (1977) Cardiorespiratory control by carotid chemoreceptors during experimental dives in the seal. American Journal of Physiology - Heart and Circulatory Physiology 232:H508-H516.

De Lecea L, Kilduff TS, Peyron C, Gao XB, Foye PE, Danielson PE, Fukuhara C, Battenberg ELF, Gautvik VT, Bartlett Ii FS, Frankel WN, Van Den Pol AN, Bloom FE, Gautvik KM, Sutcliffe JG (1998) The hypocretins: Hypothalamus-specific peptides with neuroexcitatory activity. Proc Natl Acad Sci U S A 95:322-327.

De León M, Coveñas R, Narváez JA, Tramu G, Aguirre JA, González-Barón S (1992) Distribution of somatostatin-28 (1–12) in the cat brainstem: an immunocytochemical study. Neuropeptides 21:1-11.

de Sousa Buck H, Caous CA, Lindsey CJ (2001) Projections of the paratrigeminal nucleus to the ambiguus, rostroventrolateral and lateral reticular nuclei, and the solitary tract. Autonomic Neuroscience 87:187-200.

Debanne D, Boudkkazi S, Campanac E, Cudmore RH, Giraud P, Fronzaroli-Molinieres L, Carlier E, Caillard O (2008) Paired-recordings from synaptically coupled cortical and hippocampal neurons in acute and cultured brain slices. Nature protocols 3:1559-1568.

deCampo DM, Fudge JL (2013) Amygdala projections to the lateral bed nucleus of the stria terminalis in the macaque: Comparison with ventral striatal afferents. Journal of Comparative Neurology 521:3191-3216.

Depuy SD, Kanbar R, Coates MB, Stornetta RL, Guyenet PG (2011) Control of breathing by raphe obscurus serotonergic neurons in mice. The Journal of neuroscience : the official journal of the Society for Neuroscience 31:1981-1990.

DeRosa MA, Cryer PE (2004) Hypoglycemia and the sympathoadrenal system: neurogenic symptoms are largely the result of sympathetic neural, rather than adrenomedullary, activation. American journal of physiology Endocrinology and metabolism 287:E32-41.

Deuchars SA, Morrison SF, Gilbey MP (1995) Medullary-evoked EPSPs in neonatal rat sympathetic preganglionic neurones in vitro. J Physiol 487 (Pt 2):453-463.

Deuchars SA, Spyer KM, Gilbey MP (1997) Stimulation within the rostral ventrolateral medulla can evoke monosynaptic GABAergic IPSPs in sympathetic preganglionic neurons in vitro. J Neurophysiol 77:229-235.

Devanandan MS (1964) A Study of the Myelinated Fibres of the Aortic Nerve of Cats. J Physiol 171:361-367.

Dielenberg RA, Carrive P, McGregor IS (2001) The cardiovascular and behavioral response to cat odor in rats: unconditioned and conditioned effects. Brain research 897:228-237.

DiRocco RJ, Grill HJ (1979) The forebrain is not essential for sympathoadrenal hyperglycemic response to glucoprivation. Science 204:1112-1114.

Dong Y, Zhang W, Lai B, Luan WJ, Zhu YH, Zhao BQ, Zheng P (2012) Two free radical pathways mediate chemical hypoxia-induced glutamate release in synaptosomes from the prefrontal cortex. Biochim Biophys Acta 1823:493-504.

Dore S, Goto S, Sampei K, Blackshaw S, Hester LD, Ingi T, Sawa A, Traystman RJ, Koehler RC, Snyder SH (2000) Heme oxygenase-2 acts to prevent neuronal death in brain cultures and following transient cerebral ischemia. Neuroscience 99:587-592.

Drummond PC, Jones DR (1979) The initiation and maintenance of bradycardia in a diving mammal, the muskrat, Ondatra zibethica. J Physiol 290:253-271.

Dunn-Meynell AA, Routh VH, Kang L, Gaspers L, Levin BE (2002) Glucokinase is the likely mediator of glucosensing in both glucose-excited and glucose-inhibited central neurons. Diabetes 51:2056-2065.

Dunn JD, Williams TJ (1995) Cardiovascular responses to electrical stimulation of the bed nucleus of the stria terminalis. The Journal of comparative neurology 352:227-234.

Dutschmann M, Herbert H (1997) Fos expression in the rat parabrachial and Kölliker-Fuse nuclei after electrical stimulation of the trigeminal ethmoidal nerve and water stimulation of the nasal mucosa. Experimental brain research 117:97-110.

Ehrentheil OF, Reyna LJ, Adams CJ, Giovanniello TJ, Chen ET (1967) Studies in stress glycosuria. II. Glycosuria and blood sugar elevation in alloxanized subdiabetic white rats subjected to electric shock stress. Diabetes 16:319-324.

Ermirio R, Ruggeri P, Molinari C, Weaver LC (1993) Somatic and visceral inputs to neurons of the rostral ventrolateral medulla. The American journal of physiology 265:R35-40.

Esler M (2000) The sympathetic system and hypertension. American journal of hypertension 13:99S-105S.

Evans KC, Dougherty DD, Schmid AM, Scannell E, McCallister A, Benson H, Dusek JA, Lazar SW (2009) Modulation of spontaneous breathing via limbic/paralimbic-bulbar circuitry: an event-related fMRI study. NeuroImage 47:961-971.

Ewing JF, Maines MD (1992) In situ hybridization and immunohistochemical localization of heme oxygenase-2 mRNA and protein in normal rat brain: Differential distribution of isozyme 1 and 2. Mol Cell Neurosci 3:559-570.

Eyzaguirre C, Uchizono K (1961) Observations on the fibre content of nerves reaching the carotid body of the cat. J Physiol 159:268-281.

Fan W, Andresen MC (1998) Differential frequency-dependent reflex integration of myelinated and nonmyelinated rat aortic baroreceptors. The American journal of physiology 275:H632-640.

Farnham MM, Li Q, Goodchild AK, Pilowsky PM (2008) PACAP is expressed in sympathoexcitatory bulbospinal C1 neurons of the brain stem and increases sympathetic nerve activity in vivo. American journal of physiology Regulatory, integrative and comparative physiology 294:R1304-1311.

Feldberg W, Guertzenstein PG (1972) A vasodepressor effect of pentobarbitone sodium. J Physiol 224:83-103.

Feldberg W, Guertzenstein PG (1976) Vasodepressor effects obtained by drugs acting on the ventral surface of the brain stem. J Physiol 258:337-355.

Ferrini F, Trang T, Mattioli TAM, Laffray S, Del'Guidice T, Lorenzo LE, Castonguay A, Doyon N, Zhang W, Godin AG, Mohr D, Beggs S, Vandal K, Beaulieu JM, Cahill CM, Salter MW, De Koninck Y (2013) Morphine hyperalgesia gated through microglia-mediated disruption of neuronal Cl-homeostasis. Nature Neuroscience 16:183-192.

Fields RD, Stevens-Graham B (2002) New insights into neuron-glia communication. Science 298:556-562.

Finley JC, Katz DM (1992) The central organization of carotid body afferent projections to the brainstem of the rat. Brain research 572:108-116.

Fonnum F, Johnsen A, Hassel B (1997) Use of fluorocitrate and fluoroacetate in the study of brain metabolism. Glia 21:106-113.

Frysinger RC, Marks JD, Trelease RB, Schechtman VL, Harper RM (1984) Sleep states attenuate the pressor response to central amygdala stimulation. Experimental neurology 83:604-617.

Furlong TM, Vianna DM, Liu L, Carrive P (2009) Hypocretin/orexin contributes to the expression of some but not all forms of stress and arousal. The European journal of neuroscience 30:1603-1614.

Gabbott GRJ, Jones DR (1991) The effect of brain transection on the response to forced submergence in ducks. Journal of the autonomic nervous system 36:65-74.

Gabbott PL, Warner T, Busby SJ (2007) Catecholaminergic neurons in medullary nuclei are among the post-synaptic targets of descending projections from infralimbic area 25 of the rat medial prefrontal cortex. Neuroscience 144:623-635.

Gaede AH, Lung MS, Pilowsky PM (2009) Catestatin attenuates the effects of intrathecal nicotine and isoproterenol. Brain research 1305:86-95.

Gaede AH, Pilowsky PM (2010) Catestatin in rat RVLM is sympathoexcitatory, increases barosensitivity, and attenuates chemosensitivity and the somatosympathetic reflex. American Journal of Physiology - Regulatory, Integrative and Comparative Physiology 299:R1538-R1545.

Gandevia SC, McCloskey DI, Potter EK (1978) Reflex bradycardia occurring in response to diving, nasopharyngeal stimulation and ocular pressure, and its modification by respiration and swallowing. The Journal of Physiology 276:383-394.

Geddes JW, Pettigrew LC, Holtz ML, Craddock SD, Maines MD (1996) Permanent focal and transient global cerebral ischemia increase glial and neuronal expression of heme oxygenase-1, but not heme oxygenase-2, protein in rat brain. Neurosci Lett 210:205-208.

Gelsema AJ, Copeland NE, Drolet G, Bachelard H (1993) Cardiovascular effects of neuronal activation of the extended amygdala in rats. Brain research 626:156-166.

Gelsema AJ, McKitrick DJ, Calaresu FR (1987) Cardiovascular responses to chemical and electrical stimulation of amygdala in rats. The American journal of physiology 253:R712-718.

Giehl K, Mestres P (1995) Somatostatin-mRNA expression in brainstem projections into the medial preoptic nucleus. Experimental brain research 103:344-354.

Gieroba ZJ, Yu Y-H, Blessing WW (1994) Vasoconstriction induced by inhalation of irritant vapour is associated with appearance of Fos protein in C1 catecholamine neurons in rabbit medulla oblongata. Brain research 636:157-161.

Gogolla N, Galimberti I, DePaola V, Caroni P (2006) Staining protocol for organotypic hippocampal slice cultures. Nature protocols 1:2452-2456.

Golanov EV, Christensen JRC, Reis DJ (2001) Neurons of a limited subthalamic area mediate elevations in cortical cerebral blood flow evoked by hypoxia and excitation of neurons of the rostral ventrolateral medulla. J Neurosci 21:4032-4041.

Golanov EV, Reis DJ (1996) Contribution of oxygen-sensitive neurons of the rostral ventrolateral medulla to hypoxic cerebral vasodilatation in the rat. J Physiol 495 (Pt 1):201-216.

Golanov EV, Ruggiero DA, Reis DJ (2000) A brainstem area mediating cerebrovascular and EEG responses to hypoxic excitation of rostal ventrolateral medulla in rat. Journal of Physiology 529:413-429.

Goldberg MP, Weiss JH, Pham PC, Choi DW (1987) N-methyl-D-aspartate receptors mediate hypoxic neuronal injury in cortical culture. J Pharmacol Exp Ther 243:784-791.

Goldsmith SJ, Yalow RS, Berson SA (1970) Effects of 2-deoxy-D-glucose on insulin-secretory responses to intravenous glucose, glucagon, tolbutamide and arginine in man. Diabetes 19:453-457.

Goncharov NV, Jenkins RO, Radilov AS (2006) Toxicology of fluoroacetate: a review, with possible directions for therapy research. Journal of applied toxicology : JAT 26:148-161.

Gonzalez BJ, Leroux P, Bodenant C, Laquerriere A, Coy DH, Vaudry H (1989) Ontogeny of somatostatin receptors in the rat brain: biochemical and autoradiographic study. Neuroscience 29:629-644.

Gonzalez JA, Jensen LT, Fugger L, Burdakov D (2008) Metabolism-independent sugar sensing in central orexin neurons. Diabetes 57:2569-2576.

Goodchild AK, Dampney RA, Bandler R (1982) A method for evoking physiological responses by stimulation of cell bodies, but not axons of passage, within localized regions of the central nervous system. Journal of neuroscience methods 6:351-363.

Goodchild AK, Llewellyn-Smith IJ, Sun QJ, Chalmers J, Cunningham AM, Pilowsky PM (2000) Calbindin-immunoreactive neurons in the reticular formation of the rat brainstem: catecholamine content and spinal projections. The Journal of comparative neurology 424:547-562.

Goodchild AK, Moon EA (2009) Maps of cardiovascular and respiratory regions of rat ventral medulla: focus on the caudal medulla. J Chem Neuroanat 38:209-221.

Goodchild AK, Moon EA, Dampney RAL, Howe PRC (1984) Evidence That Adrenaline Neurons in the Rostral Ventrolateral Medulla Have a Vasopressor Function. Neuroscience letters 45:267-272.

Gourine AV, Kasymov V, Marina N, Tang F, Figueiredo MF, Lane S, Teschemacher AG, Spyer KM, Deisseroth K, Kasparov S (2010) Astrocytes control breathing through pH-dependent release of ATP. Science 329:571-575.

Gourine AV, Llaudet E, Dale N, Spyer KM (2005) Release of ATP in the ventral medulla during hypoxia in rats: role in hypoxic ventilatory response. J Neurosci 25:1211-1218.

Graham BA, Brichta AM, Callister RJ (2008) Recording temperature affects the excitability of mouse superficial dorsal horn neurons, in vitro. J Neurophysiol 99:2048-2059.

Granata AR, Kitai ST (1992) Intracellular analysis in vivo of different barosensitive bulbospinal neurons in the rat rostral ventrolateral medulla. The Journal of neuroscience : the official journal of the Society for Neuroscience 12:1-20.

Gray PA (2013) Transcription factors define the neuroanatomical organization of the medullary reticular formation. Frontiers in neuroanatomy 7:7.

Gray PA, Hayes JA, Ling GY, Llona I, Tupal S, Picardo MC, Ross SE, Hirata T, Corbin JG, Eugenin J, Del Negro CA (2010) Developmental origin of preBotzinger complex respiratory neurons. The Journal of neuroscience : the official journal of the Society for Neuroscience 30:14883-14895.

Gray TS, Magnuson DJ (1987) Neuropeptide neuronal efferents from the bed nucleus of the stria terminalis and central amygdaloid nucleus to the dorsal vagal complex in the rat. The Journal of comparative neurology 262:365-374.

Gray TS, Magnuson DJ (1992) Peptide immunoreactive neurons in the amygdala and the bed nucleus of the stria terminalis project to the midbrain central gray in the rat. Peptides 13:451-460.

Grisk O (2005) Sympatho-renal interactions in the determination of arterial pressure: role in hypertension. Experimental physiology 90:183-187.

Gruhn N, Larsen FS, Boesgaard S, Knudsen GM, Mortensen SA, Thomsen G, Aldershvile J (2001) Cerebral blood flow in patients with chronic heart failure before and after heart transplantation. Stroke 32:2530-2533.

Guenther MA, Bruder ED, Raff H (2012) Effects of body temperature maintenance on glucose, insulin, and corticosterone responses to acute hypoxia in the neonatal rat. American journal of physiology Regulatory, integrative and comparative physiology 302:R627-R633.

Guertzenstein PG, Silver A (1974) Fall in blood pressure produced from discrete regions of the ventral surface of the medulla by glycine and lesions. Journal of Physiology 242:489-503.

Guo Z-L, Tjen-A-Looi SC, Fu L-W, Longhurst JC (2009) Nitric oxide in rostral ventrolateral medulla regulates cardiac-sympathetic reflexes: role of synthase isoforms. American Journal of Physiology - Heart and Circulatory Physiology 297:H1478-H1486.

Guyenet PG (1984) Baroreceptor-mediated inhibition of A5 noradrenergic neurons. Brain research 303:31-40.

Guyenet PG (2000) Neural structures that mediate sympathoexcitation during hypoxia. Respir Physiol 121:147-162.

Guyenet PG (2006) The sympathetic control of blood pressure. Nat Rev Neurosci 7:335-346.

Guyenet PG, Brown DL (1986) Unit activity in nucleus paragigantocellularis lateralis during cerebral ischemia in the rat. Brain research 364:301-314.

Guyenet PG, Byrum CE (1985) Comparative effects of sciatic nerve stimulation, blood pressure, and morphine on the activity of A5 and A6 pontine noradrenergic neurons. Brain research 327:191-201.

Guyenet PG, Cabot JB (1981) Inhibition of sympathetic preganglionic neurons by catecholamines and clonidine: mediation by an alpha-adrenergic receptor. The Journal of neuroscience : the official journal of the Society for Neuroscience 1:908-917.

Guyenet PG, Darnall RA, Riley TA (1990) Rostral ventrolateral medulla and sympathorespiratory integration in rats. The American journal of physiology 259:R1063-1074.

Guyenet PG, Filtz TM, Donaldson SR (1987) Role of excitatory amino acids in rat vagal and sympathetic baroreflexes. Brain research 407:272-284.

Guyenet PG, Haselton JR, Sun MK (1989) Sympathoexcitatory neurons of the rostroventrolateral medulla and the origin of the sympathetic vasomotor tone. Progress in brain research 81:105-116.

Guyenet PG, Schreihofer AM, Stornetta RL (2001) Regulation of sympathetic tone and arterial pressure by the rostral ventrolateral medulla after depletion of C1 cells in rats. Annals of the New York Academy of Sciences 940:259-269.

Guyenet PG, Stornetta RL, Bayliss DA (2008) Retrotrapezoid nucleus and central chemoreception. J Physiol 586:2043-2048.

Guyenet PG, Stornetta RL, Bayliss DA, Mulkey DK (2005) Retrotrapezoid nucleus: a litmus test for the identification of central chemoreceptors. Experimental physiology 90:247-253; discussion 253-247.

Guyenet PG, Stornetta RL, Bochorishvili G, Depuy SD, Burke PG, Abbott SB (2013) C1 neurons: the body's EMTs. American journal of physiology Regulatory, integrative and comparative physiology 305:R187-204.

Halassa MM, Florian C, Fellin T, Munoz JR, Lee SY, Abel T, Haydon PG, Frank MG (2009) Astrocytic modulation of sleep homeostasis and cognitive consequences of sleep loss. Neuron 61:213-219.

Hammarström AKM, Gage PW (1999) Nitric oxide increases persistent sodium current in rat hippocampal neurons. Journal of Physiology 520:451-461.

Hammond DL, Presley R, Gogas KR, Basbaum AI (1992) Morphine or U-50,488 suppresses Fos protein-like immunoreactivity in the spinal cord and nucleus tractus solitarii evoked by a noxious visceral stimulus in the rat. The Journal of comparative neurology 315:244-253.

Hanna BD, Lioy F, Polosa C (1981) Role of carotid and central chemoreceptors in the CO2 response of sympathetic preganglionic neurons. Journal of the autonomic nervous system 3:421-435.

Harper RM, Frysinger RC, Trelease RB, Marks JD (1984) State-dependent alteration of respiratory cycle timing by stimulation of the central nucleus of the amygdala. Brain research 306:1-8.

Haselton JR, Guyenet PG (1989) Central respiratory modulation of medullary sympathoexcitatory neurons in rat. The American journal of physiology 256:R739-750.

Haselton JR, Guyenet PG (1990) Ascending collaterals of medullary barosensitive neurons and C1 cells in rats. The American journal of physiology 258:R1051-1063.

Hasking GJ, Esler MD, Jennings GL (1985) Sympathetic tone in congestive heart failure. The American journal of cardiology 56:912.

Hassel B, Sonnewald U, Unsgard G, Fonnum F (1994) NMR spectroscopy of cultured astrocytes: effects of glutamine and the gliotoxin fluorocitrate. Journal of neurochemistry 62:2187-2194.

Hayashi S, Omata Y, Sakamoto H, Higashimoto Y, Hara T, Sagara Y, Noguchi M (2004) Characterization of rat heme oxygenase-3 gene. Implication of processed pseudogenes derived from heme oxygenase-2 gene. Gene 336:241-250.

He C, Chen F, Li B, Hu Z (2014) Neurophysiology of HCN channels: from cellular functions to multiple regulations. Prog Neurobiol 112:1-23.

Head GA, Mayorov DN (2001) Central angiotensin and baroreceptor control of circulation. Annals of the New York Academy of Sciences 940:361-379.

Hermann GE, Viard E, Rogers RC (2014) Hindbrain glucoprivation effects on gastric vagal reflex circuits and gastric motility in the rat are suppressed by the astrocyte inhibitor fluorocitrate. The Journal of neuroscience : the official journal of the Society for Neuroscience 34:10488-10496.

Hines DJ, Haydon PG (2013) Inhibition of a SNARE-sensitive pathway in astrocytes attenuates damage following stroke. J Neurosci 33:4234-4240.

Hirooka Y, Potts PD, Dampney RA (1997) Role of angiotensin II receptor subtypes in mediating the sympathoexcitatory effects of exogenous and endogenous angiotensin peptides in the rostral ventrolateral medulla of the rabbit. Brain research 772:107-114.

Hokfelt T, Fuxe K, Goldstein M, Johansson O (1973) Evidence for adrenaline neurons in the rat brain. Acta physiologica Scandinavica 89:286-288.

Holstege G, Meiners L, Tan K (1985) Projections of the bed nucleus of the stria terminalis to the mesencephalon, pons, and medulla oblongata in the cat. Experimental brain research 58:379-391.

Hopkins DA, Holstege G (1978) Amygdaloid projections to the mesencephalon, pons and medulla oblongata in the cat. Experimental brain research 32:529-547.

Horie K, Insel PA (2000) Retrovirally mediated transfer of a G protein-coupled receptor kinase (GRK) dominant-negative mutant enhances endogenous calcitonin receptor signaling in Chinese hamster ovary cells. GRK inhibition enhances expression of receptors and receptor mRNA. The Journal of biological chemistry 275:29433-29440.

Horiuchi J, Potts PD, Polson JW, Dampney RA (1999a) Distribution of neurons projecting to the rostral ventrolateral medullary pressor region that are activated by sustained hypotension. Neuroscience 89:1319-1329.

Horiuchi J, Potts PD, Tagawa T, Dampney RA (1999b) Effects of activation and blockade of P2x receptors in the ventrolateral medulla on arterial pressure and sympathetic activity. Journal of the autonomic nervous system 76:118-126.

Hoyer D, Bell GI, Berelowitz M, Epelbaum J, Feniuk W, Humphrey PPA, O'Carroll AM, Patel YC, Schonbrunn A, Taylor JE, Reisine T (1995) Classification and nomenclature of somatostatin receptors. Trends in Pharmacological Sciences 16:86-88.

Hsiao YT, Jou SB, Yi PL, Chang FC (2012) Activation of GABAergic pathway by hypocretin in the median raphe nucleus (MRN) mediates stress-induced theta rhythm in rats. Behavioural brain research 233:224-231.

Huxtable AG, Zwicker JD, Poon BY, Pagliardini S, Vrouwe SQ, Greer JJ, Funk GD (2009) Tripartite purinergic modulation of central respiratory networks during perinatal development: the influence of ATP, ectonucleotidases, and ATP metabolites. The Journal of neuroscience : the official journal of the Society for Neuroscience 29:14713-14725.

Ilch CP, Golanov EV (2004) Cerebrovasodilation evoked by stimulation of subthalamic vasodilator area and hypoxia depends upon the integrity of cortical neurons in the rat. Neuroscience letters 368:92-95.

Inokuchi H, Yoshimura M, Polosa C, Nishi S (1993) Tachykinins depress a calcium-dependent potassium conductance in sympathetic preganglionic neurons. Regulatory peptides 46:367-369.

Inoue M, Nakajima S, Nakajima Y (1988) Somatostatin induces an inward rectification in rat locus coeruleus neurones through a pertussis toxin-sensitive mechanism. Journal of Physiology 407:177-198.

Ito S, Sved AF (1997) Tonic glutamate-mediated control of rostral ventrolateral medulla and sympathetic vasomotor tone. The American journal of physiology 273:R487-494.

Iwata J, Chida K, LeDoux JE (1987) Cardiovascular responses elicited by stimulation of neurons in the central amygdaloid nucleus in awake but not anesthetized rats resemble conditioned emotional responses. Brain research 418:183-188.

Janig W, Habler HJ (2003) Neurophysiological analysis of target-related sympathetic pathways--from animal to human: similarities and differences. Acta physiologica Scandinavica 177:255-274.

Jansen ASP, Van Nguyen X, Karpitskiy V, Mettenleiter TC, Loewy AD (1995) Central command neurons of the sympathetic nervous system: Basis of the fight-or-flight response. Science 270:644-646.

Jeske I, Morrison SF, Cravo SL, Reis DJ (1993) Identification of baroreceptor reflex interneurons in the caudal ventrolateral medulla. The American journal of physiology 264:R169-178.

Jeske I, Reis DJ, Milner TA (1995) Neurons in the barosensory area of the caudal ventrolateral medulla project monosynaptically on to sympathoexcitatory bulbospinal neurons in the rostral ventrolateral medulla. Neuroscience 65:343-353.

Jiang C, Sigworth FJ, Haddad GG (1994) Oxygen deprivation activates an ATP-inhibitable K+ channel in substantia nigra neurons. J Neurosci 14:5590-5602.

Kang HT, Hwang ES (2006) 2-Deoxyglucose: an anticancer and antiviral therapeutic, but not any more a low glucose mimetic. Life sciences 78:1392-1399.

Kangrga IM, Loewy AD (1995) Whole-cell recordings from visualized C1 adrenergic bulbospinal neurons: ionic mechanisms underlying vasomotor tone. Brain research 670:215-232.

Kanjhan R, Housley GD, Burton LD, Christie DL, Kippenberger A, Thorne PR, Luo L, Ryan AF (1999) Distribution of the P2X2 receptor subunit of the ATP-gated ion channels in the rat central nervous system. The Journal of comparative neurology 407:11-32.

Kanjhan R, Lipski J, Kruszewska B, Rong W (1995) A comparative study of pre-sympathetic and Botzinger neurons in the rostral ventrolateral medulla (RVLM) of the rat. Brain research 699:19-32.

Karnani MM, Szabó G, Erdélyi F, Burdakov D (2013) Lateral hypothalamic GAD65 neurons are spontaneously firing and distinct from orexin- and melanin-concentrating hormone neurons. J Physiol (Lond) 591:933-953.

Kashihara K, McMullan S, Lonergan T, Goodchild AK, Pilowsky PM (2008) Neuropeptide Y in the rostral ventrolateral medulla blocks somatosympathetic reflexes in anesthetized rats. Autonomic neuroscience : basic & clinical 142:64-70.

Kasymov V, Larina O, Castaldo C, Marina N, Patrushev M, Kasparov S, Gourine AV (2013) Differential sensitivity of brainstem versus cortical astrocytes to changes in pH reveals functional regional specialization of astroglia. J Neurosci 33:435-441.

Kawai Y, Inagaki S, Shiosaka S, Senba E, Hara Y, Sakanaka M, Takatsuki K, Tohyama M (1982) Long descending projections from amygdaloid somatostatin-containing cells to the lower brain stem. Brain research 239:603-607.

Kawai Y, Qi J, Comer AM, Gibbons H, Win J, Lipski J (1999) Effects of cyanide and hypoxia on membrane currents in neurones acutely dissociated from the rostral ventrolateral medulla of the rat. Brain research 830:246-257.

Kawashima T, Kitamura K, Suzuki K, Nonaka M, Kamijo S, Takemoto-Kimura S, Kano M, Okuno H, Ohki K, Bito H (2013) Functional labeling of neurons and their projections using the synthetic activity-dependent promoter E-SARE. Nature Methods 10:889-895.

Keay K, Bandler R (2002) Distinct central representations of inescapable and escapable pain: observations and speculation. Experimental physiology 87:275-279.

Kiely JM, Gordon FJ (1993) Non-NMDA receptors in the rostral ventrolateral medulla mediate somatosympathetic pressor responses. Journal of the autonomic nervous system 43:231-239.

Kiely JM, Gordon FJ (1994) Role of rostral ventrolateral medulla in centrally mediated pressor responses. The American journal of physiology 267:H1549-1556.

Kiyama H, Emson PC (1990) Distribution of somatostatin mRNA in the rat nervous system as visualized by a novel non-radioactive in situ hybridization histochemistry procedure. Neuroscience 38:223-244.

Koenig H, Patel A (1970) Biochemical basis for fluorouracil neurotoxicity. The role of Krebs cycle inhibition by fluoroacetate. Archives of neurology 23:155-160.

Koganezawa T, Paton JF (2014) Intrinsic chemosensitivity of RVLM sympathetic premotor neurons in the in situ arterially perfused preparation of rats. Experimental physiology.

Koganezawa T, Shimomura Y, Terui N (2010) The viscerosympathetic response in rabbits is mediated by GABAergic and glutamatergic inputs into the sympathetic premotor neurons of the rostral ventrolateral medulla. Experimental physiology 95:1061-1070.

Koganezawa T, Terui N (2006) Differential responsiveness of RVLM sympathetic premotor neurons to hypoxia in the rabbit. American journal of physiology Heart and circulatory physiology.

Korim WS, Bou Farah L, McMullan S, Verberne AJ (2014) Orexinergic activation of medullary premotor neurons modulates the adrenal sympathoexcitation to hypothalamic glucoprivation. Diabetes 63:1895-1906.

Koshiya N, Guyenet PG (1994) Role of the pons in the carotid sympathetic chemoreflex. The American journal of physiology 267:R508-518.

Koshiya N, Guyenet PG (1996) NTS neurons with carotid chemoreceptor inputs arborize in the rostral ventrolateral medulla. The American journal of physiology 270:R1273-1278.

Koshiya N, Huangfu D, Guyenet PG (1993) Ventrolateral medulla and sympathetic chemoreflex in the rat. Brain research 609:174-184.

Kreienkamp H-J, Hönck H-H, Richter D (1997) Coupling of rat somatostatin receptor subtypes to a G-protein gated inwardly rectifying potassium channel (GIRK1). FEBS Letters 419:92-94.

Krieger EM, Marseillan RF (1963) Aortic Depressor Fibers in the Rat: An Electrophysiological Study. The American journal of physiology 205:771-774.

Kubin L, Alheid GF, Zuperku EJ, McCrimmon DR (2006) Central pathways of pulmonary and lower airway vagal afferents. Journal of applied physiology 101:618-627.

Kubo T, Amano M, Asari T (1993) N-Methyl-d-aspartate receptors but not non-N-methyl-d-aspartate receptors mediate hypertension induced by carotid body chemoreceptor stimulation in the rostral ventrolateral medulla of the rat. Neuroscience letters 164:113-116.

Kumar NN, Ferguson J, Padley JR, Pilowsky PM, Goodchild AK (2009) Differential muscarinic receptor gene expression levels in the ventral medulla of spontaneously hypertensive and

Wistar-Kyoto rats: role in sympathetic baroreflex function. Journal of hypertension 27:1001-1008.

Kurtoglu M, Gao N, Shang J, Maher JC, Lehrman MA, Wangpaichitr M, Savaraj N, Lane AN, Lampidis TJ (2007) Under normoxia, 2-deoxy-D-glucose elicits cell death in select tumor types not by inhibition of glycolysis but by interfering with N-linked glycosylation. Molecular cancer therapeutics 6:3049-3058.

L Bou-Farah and BR Bowman PB, S Karim, S Le, AK Goodchild , S McMullan (2015) Somatostatin in the rat rostral ventrolateral medulla: origins and mechanism of action Journal of Comparative Neurology.

Lahiri S, Mulligan E, Nishino T, Mokashi A (1979) Aortic body chemoreceptor responses to changes in PCO2 and PO2 in the cat. Journal of applied physiology: respiratory, environmental and exercise physiology 47:858-866.

Lara JP, Parkes MJ, Silva-Carvhalo L, Izzo P, Dawid-Milner MS, Spyer KM (1994) Cardiovascular and respiratory effects of stimulation of cell bodies of the parabrachial nuclei in the anaesthetized rat. The Journal of Physiology 477:321-329.

Largo C, Ibarz JM, Herreras O (1997) Effects of the gliotoxin fluorocitrate on spreading depression and glial membrane potential in rat brain in situ. J Neurophysiol 78:295-307.

LeDoux J, Iwata J, Cicchetti P, Reis D (1988) Different projections of the central amygdaloid nucleus mediate autonomic and behavioral correlates of conditioned fear. The Journal of Neuroscience 8:2517-2529.

Lefkowitz RJ (1998) G protein-coupled receptors. III. New roles for receptor kinases and beta-arrestins in receptor signaling and desensitization. The Journal of biological chemistry 273:18677-18680.

Leimbach Jr WN, Wallin BG, Victor RG, Aylward PE, Sundlöf G, Mark AL (1986) Direct evidence from intraneural recordings for increased central sympathetic outflow in patients with heart failure. Circulation 73:913-919.

Lenders JW, Pacak K, Walther MM, Linehan WM, Mannelli M, Friberg P, Keiser HR, Goldstein DS, Eisenhofer G (2002) Biochemical diagnosis of pheochromocytoma: which test is best? Jama 287:1427-1434.

Leone C, Gordon FJ (1989) Is L-glutamate a neurotransmitter of baroreceptor information in the nucleus of the tractus solitarius? The Journal of pharmacology and experimental therapeutics 250:953-962.

Lewis DI, Coote JH (2008) Electrophysiological characteristics of vasomotor preganglionic neurons and related neurons in the thoracic spinal cord of the rat: an intracellular study in vivo. Neuroscience 152:534-546.

Li C-S, Cho YK (2006) Efferent projection from the bed nucleus of the stria terminalis suppresses activity of taste-responsive neurons in the hamster parabrachial nuclei. American Journal of Physiology - Regulatory, Integrative and Comparative Physiology 291:R914-R926.

Li P, Lovick TA (1985) Excitatory projections from hypothalamic and midbrain defense regions to nucleus paragigantocellularis lateralis in the rat. Experimental neurology 89:543-553.

Li Q, Goodchild AK, Seyedabadi M, Pilowsky PM (2005) Pre-protachykinin A mRNA is colocalized with tyrosine hydroxylase-immunoreactivity in bulbospinal neurons. Neuroscience 136:205-216.

Li YW, Bayliss DA, Guyenet PG (1995) C1 neurons of neonatal rats: intrinsic beating properties and alpha 2-adrenergic receptors. The American journal of physiology 269:R1356-1369.

Li YW, Guyenet PG (1995) Neuronal inhibition by a GABAB receptor agonist in the rostral ventrolateral medulla of the rat. The American journal of physiology 268:R428-437.

Light AR, Perl ER (1979) Spinal termination of functionally identified primary afferent neurons with slowly conducting myelinated fibers. The Journal of comparative neurology 186:133-150.

Lindsey CJ, Buck HS, Fior-Chadi DR, Lapa RC (1997) Pressor effect mediated by bradykinin in the paratrigeminal nucleus of the rat. J Physiol 502 (Pt 1):119-129.

Lipski J, Kanjhan R, Kruszewska B, Rong W (1996a) Properties of presympathetic neurones in the rostral ventrolateral medulla in the rat: an intracellular study "in vivo'. J Physiol 490 (Pt 3):729-744.

Lipski J, Kanjhan R, Kruszewska B, Rong WF (1995a) Criteria for intracellular identification of pre-sympathetic neurons in the rostral ventrolateral medulla in the rat. Clinical and experimental hypertension 17:51-65.

Lipski J, Kanjhan R, Kruszewska B, Rong WF, Smith M (1996b) Pre-sympathetic neurones in the rostral ventrolateral medulla of the rat: electrophysiology, morphology and relationship to adjacent neuronal groups. Acta Neurobiol Exp (Wars) 56:373-384.

Lipski J, Kanjhan R, Kruszewska B, Smith M (1995b) Barosensitive neurons in the rostral ventrolateral medulla of the rat in vivo: morphological properties and relationship to C1 adrenergic neurons. Neuroscience 69:601-618.

Lipski J, Kawai Y, Qi J, Comer A, Win J (1998) Whole cell patch-clamp study of putative vasomotor neurons isolated from the rostral ventrolateral medulla. The American journal of physiology 274:R1099-1110.

Lipski J, Lin J, Teo MY, van Wyk M (2002) The network vs. pacemaker theory of the activity of RVL presympathetic neurons--a comparison with another putative pacemaker system. Autonomic neuroscience : basic & clinical 98:85-89.

Liu Q, Dewi DA, Liu W, Bee MS, Schonbrunn A (2008) Distinct phosphorylation sites in the SST2A somatostatin receptor control internalization, desensitization, and arrestin binding. Mol Pharmacol 73:292-304.

Lo WC, Lu PJ, Ho WY, Hsiao M, Tseng CJ (2006) Induction of heme oxygenase-1 is involved in carbon monoxide-mediated central cardiovascular regulation. Journal of Pharmacology and Experimental Therapeutics 318:8-16.

Lorier AR, Lipski J, Housley GD, Greer JJ, Funk GD (2008) ATP sensitivity of preBotzinger complex neurones in neonatal rat in vitro: mechanism underlying a P2 receptor-mediated increase in inspiratory frequency. J Physiol 586:1429-1446.

Lovick TA (1992a) Inhibitory modulation of the cardiovascular defence response by the ventrolateral periaqueductal grey matter in rats. Experimental brain research 89:133-139.

Lovick TA (1992b) Midbrain influences on ventrolateral medullo-spinal neurones in the rat. Experimental brain research 90:147-152.

Lumb BM (2004) Hypothalamic and Midbrain Circuitry That Distinguishes Between Escapable and Inescapable Pain. Physiology 19:22-26.

M'Hamed S, B., Sequeira H, Poulain P, Bennis M, Roy JC (1993) Sensorimotor cortex projections to the ventrolateral and the dorsomedial medulla oblongata in the rat. Neuroscience letters 164:195-198.

Madden CJ, Ito S, Rinaman L, Wiley RG, Sved AF (1999) Lesions of the C1 catecholaminergic neurons of the ventrolateral medulla in rats using anti-DbetaH-saporin. The American journal of physiology 277:R1063-1075.

Madden CJ, Stocker SD, Sved AF (2006) Attenuation of homeostatic responses to hypotension and glucoprivation after destruction of catecholaminergic rostral ventrolateral medulla neurons. American journal of physiology Regulatory, integrative and comparative physiology 291:R751-759.

Madden CJ, Sved AE (2003a) Rostral ventrolateral medulla C1 neurons and cardiovascular regulation. Cell Mol Neurobiol 23:739-749.

Madden CJ, Sved AF (2003b) Cardiovascular regulation after destruction of the C1 cell group of the rostral ventrolateral medulla in rats. American journal of physiology Heart and circulatory physiology 285:H2734-2748.

Magistretti PJ, Chatton JY (2005) Relationship between L-glutamate-regulated intracellular Na+ dynamics and ATP hydrolysis in astrocytes. Journal of neural transmission 112:77-85.

Maines MD, Trakshel GM, Kutty RK (1986) Characterization of two constitutive forms of rat liver microsomal heme oxygenase. Only one molecular species of the enzyme is inducible. J Biol Chem 261:411-419.

Maines MD (1997) The heme oxygenase system: a regulator of second messenger gases. Annual review of pharmacology and toxicology 37:517-554.

Makeham JM, Goodchild AK, Pilowsky PM (2005) NK1 receptor activation in rat rostral ventrolateral medulla selectively attenuates somato-sympathetic reflex while antagonism attenuates sympathetic chemoreflex. American journal of physiology Regulatory, integrative and comparative physiology 288:R1707-1715.

Malpas SC (2010) Sympathetic nervous system overactivity and its role in the development of cardiovascular disease. Physiological reviews 90:513-557.

Mancia G, Grassi G, Parati G, Zanchetti A (1997) The sympathetic nervous system in human hypertension. Acta physiologica Scandinavica Supplementum 640:117-121.

Mancilla JG, Lewis TJ, Pinto DJ, Rinzel J, Connors BW (2007) Synchronization of electrically coupled pairs of inhibitory interneurons in neocortex. The Journal of neuroscience : the official journal of the Society for Neuroscience 27:2058-2073.

Mandel DA, Schreihofer AM (2006) Central respiratory modulation of barosensitive neurones in rat caudal ventrolateral medulla. J Physiol 572:881-896.

Mandel DA, Schreihofer AM (2009) Modulation of the sympathetic response to acute hypoxia by the caudal ventrolateral medulla in rats. J Physiol 587:461-475.

Marina N, Abdala AP, Korsak A, Simms AE, Allen AM, Paton JF, Gourine AV (2011) Control of sympathetic vasomotor tone by catecholaminergic C1 neurones of the rostral ventrolateral medulla oblongata. Cardiovasc Res.

Marina N, Abdala AP, Trapp S, Li A, Nattie EE, Hewinson J, Smith JC, Paton JF, Gourine AV (2010) Essential role of Phox2b-expressing ventrolateral brainstem neurons in the chemosensory control of inspiration and expiration. The Journal of neuroscience : the official journal of the Society for Neuroscience 30:12466-12473.

Marina N, Tang F, Figueiredo M, Mastitskaya S, Kasimov V, Mohamed-Ali V, Roloff E, Teschemacher AG, Gourine AV, Kasparov S (2013) Purinergic signalling in the rostral ventro-lateral medulla controls sympathetic drive and contributes to the progression of heart failure following myocardial infarction in rats. Basic Research in Cardiology 108.

Marshall JM (1994) Peripheral chemoreceptors and cardiovascular regulation. Physiological reviews 74:543-594.

Marshel JH, Mori T, Nielsen KJ, Callaway EM (2010) Targeting single neuronal networks for gene expression and cell labeling in vivo. Neuron 67:562-574.

Martín ED, Fernández M, Perea G, Pascual O, Haydon PG, Araque A, Ceña V (2007) Adenosine released by astrocytes contributes to hypoxia-induced modulation of synaptic transmission. Glia 55:36-45.

Marty N, Dallaporta M, Foretz M, Emery M, Tarussio D, Bady I, Binnert C, Beermann F, Thorens B (2005) Regulation of glucagon secretion by glucose transporter type 2 (glut2) and astrocyte-dependent glucose sensors. The Journal of clinical investigation 115:3545-3553.

Masuda N, Ootsuka Y, Terui N (1992) Neurons in the caudal ventrolateral medulla mediate the somato-sympathetic inhibitory reflex response via GABA receptors in the rostral ventrolateral medulla. Journal of the autonomic nervous system 40:91-98.

Matsumoto M, Takayama K, Miura M (1994) Distribution of glutamate- and GABA-immunoreactive neurons projecting to the vasomotor center of the intermediolateral nucleus of the lower thoracic cord of Wistar rats: a double-labeling study. Neuroscience letters 174:165-168.

Matsunaga H, Iguchi A, Yatomi A, Uemura K, Miura H, Gotoh M, Mano T, Sakamoto N (1989) The relative importance of nervous system and hormones to the 2-deoxy-D-glucose-induced hyperglycemia in fed rats. Endocrinology 124:1259-1264.

Mazza E, Thakkar-Varia S, Tozzi CA, Neubauer JA (2001) Expression of heme oxygenase in the oxygen-sensing regions of the rostral ventrolateral medulla. J Appl Physiol 91:379-385.

McAllen RM (1985) Mediation of the fastigial pressor response and a somatosympathetic reflex by ventral medullary neurones in the cat. J Physiol 368:423-433.

McAllen RM (1986) Action and specificity of ventral medullary vasopressor neurones in the cat. Neuroscience 18:51-59.

McAllen RM, Dampney RA (1990) Vasomotor neurons in the rostral ventrolateral medulla are organized topographically with respect to type of vascular bed but not body region. Neuroscience letters 110:91-96.

McAllen RM, May CN (1996) Brainstem neurones and postganglionic sympathetic nerves: Does correlation mean connection? Acta Neurobiologiae Experimentalis 56:129-135.

McAllen RM, Trevaks D, Allen AM (2001) Analysis of firing correlations between sympathetic premotor neuron pairs in anesthetized cats. J Neurophysiol 85:1697-1708.

McCoubrey WK, Jr., Huang TJ, Maines MD (1997) Isolation and characterization of a cDNA from the rat brain that encodes hemoprotein heme oxygenase-3. Eur J Biochem 247:725-732.

McCulloch PF, Faber KM, Panneton WM (1999a) Electrical stimulation of the anterior ethmoidal nerve produces the diving response. Brain research 830:24-31.

McCulloch PF, Panneton WM (2003) Activation of brainstem catecholaminergic neurons during voluntary diving in rats. Brain research 984:42-53.

McCulloch PF, Panneton WM, Guyenet PG (1999b) The rostral ventrolateral medulla mediates the sympathoactivation produced by chemical stimulation of the rat nasal mucosa. The Journal of Physiology 516:471-484.

McDonald DM (1983) Morphology of the rat carotid sinus nerve. I. Course, connections, dimensions and ultrastructure. Journal of neurocytology 12:345-372.

McDougal DH, Viard E, Hermann GE, Rogers RC (2013) Astrocytes in the hindbrain detect glucoprivation and regulate gastric motility. Autonomic Neuroscience: Basic and Clinical 175:61-69.

McMullan S, Pathmanandavel K, Pilowsky PM, Goodchild AK (2008) Somatic nerve stimulation evokes qualitatively different somatosympathetic responses in the cervical and splanchnic sympathetic nerves in the rat. Brain research 1217:139-147.

McMullan S, Pilowsky PM (2012) Sympathetic premotor neurones project to and are influenced by neurones in the contralateral rostral ventrolateral medulla of the rat in vivo. Brain research 1439:34-43.

Meckler RL, Weaver LC (1985) Splenic, renal, and cardiac nerves have unequal dependence upon tonic supraspinal inputs. Brain research 338:123-135.

Mifflin SW (1992) Arterial chemoreceptor input to nucleus tractus solitarius. The American journal of physiology 263:R368-375.

Miles R, Poncer JC (1996) Paired recordings from neurones. Curr Opin Neurobiol 6:387-394.

Milner TA, Pickel VM, Abate C, Joh TH, Reis DJ (1988) Ultrastructural characterization of substance P-like immunoreactive neurons in the rostral ventrolateral medulla in relation to neurons containing catecholamine-synthesizing enzymes. The Journal of comparative neurology 270:427-445, 402-425.

Minson JB, Arnolda LF, Llewellyn-Smith IJ (2002) Neurochemistry of nerve fibers apposing sympathetic preganglionic neurons activated by sustained hypotension. The Journal of comparative neurology 449:307-318.

Minson JB, Llewellyn-Smith IJ, Pilowsky PM, Chalmers JP (1994) Bulbospinal neuropeptide Y-immunoreactive neurons in the rat: comparison with adrenaline-synthesising neurons. Journal of the autonomic nervous system 47:233-243.

Miura M, Takayama K, Okada J (1991) Difference in sensitivity of cardiovascular and respiratory control neurons in the subretrofacial nucleus to glutamate receptor subtype agonists in SHR, WKY and cats. Journal of the autonomic nervous system 36:1-12.

Miyawaki T, Goodchild AK, Pilowsky PM (2001) Rostral ventral medulla 5-HT1A receptors selectively inhibit the somatosympathetic reflex. American Journal of Physiology - Regulatory Integrative and Comparative Physiology 280:R1261-R1268.

Miyawaki T, Goodchild AK, Pilowsky PM (2002) Activation of mu-opioid receptors in rat ventrolateral medulla selectively blocks baroreceptor reflexes while activation of delta opioid receptors blocks somato-sympathetic reflexes. Neuroscience 109:133-144.

Miyawaki T, Goodchild AK, Pilowsky PM (2003) Maintenance of sympathetic tone by a nickel chloride-sensitive mechanism in the rostral ventrolateral medulla of the adult rat. Neuroscience 116:455-464.

Miyawaki T, Minson J, Arnolda L, Llewellyn-Smith I, Chalmers J, Pilowsky P (1996) AMPA/kainate receptors mediate sympathetic chemoreceptor reflex in the rostral ventrolateral medulla. Brain research 726:64-68.

Moga MM, Saper CB, Gray TS (1989) Bed nucleus of the stria terminalis: cytoarchitecture, immunohistochemistry, and projection to the parabrachial nucleus in the rat. The Journal of comparative neurology 283:315-332.

Molkov YI, Zoccal DB, Moraes DJA, Paton JFR, Machado BH, Rybak IA (2011) Intermittent hypoxia-induced sensitization of central chemoreceptors contributes to sympathetic nerve activity during late expiration in rats. Journal of Neurophysiology 105:3080-3091.

Moraes DJA, Bonagamba LGH, Zoccal DB, Machado BH (2011) Modulation of respiratory responses to chemoreflex activation by l-glutamate and ATP in the rostral ventrolateral medulla of awake rats. American Journal of Physiology - Regulatory, Integrative and Comparative Physiology 300:R1476-R1486.

Moraes DJA, Zoccal DB, Machado BH (2012) Sympathoexcitation during chemoreflex active expiration is mediated by L-glutamate in the RVLM/Bötzinger complex of rats. Journal of Neurophysiology 108:610-623.

Moreira TS, Takakura AC, Colombari E, Guyenet PG (2006) Central chemoreceptors and sympathetic vasomotor outflow. J Physiol 577:369-386.

Morilak DA, Drolet G, Chalmers J (1990) Cardiovascular effects of opioid antagonist naloxone in rostral ventrolateral medulla of rabbits. The American journal of physiology 258:R325-331.

Morrison SF (1999) RVLM and raphe differentially regulate sympathetic outflows to splanchnic and brown adipose tissue. The American journal of physiology 276:R962-973.

Morrison SF (2001) Differential control of sympathetic outflow. American journal of physiology Regulatory, integrative and comparative physiology 281:R683-698.

Morrison SF, Callaway J, Milner TA, Reis DJ (1991) Rostral ventrolateral medulla: a source of the glutamatergic innervation of the sympathetic intermediolateral nucleus. Brain research 562:126-135.

Morrison SF, Cao WH (2000) Different adrenal sympathetic preganglionic neurons regulate epinephrine and norepinephrine secretion. American journal of physiology Regulatory, integrative and comparative physiology 279:R1763-R1775.

Morrison SF, Milner TA, Reis DJ (1988) Reticulospinal vasomotor neurons of the rat rostral ventrolateral medulla: relationship to sympathetic nerve activity and the C1 adrenergic cell group. The Journal of neuroscience : the official journal of the Society for Neuroscience 8:1286-1301.

Morrison SF, Reis DJ (1989) Reticulospinal vasomotor neurons in the RVL mediate the somatosympathetic reflex. The American journal of physiology 256:R1084-1097.

Morschel M, Dutschmann M (2009) Pontine respiratory activity involved in inspiratory/expiratory phase transition. Philos Trans R Soc Lond B Biol Sci 364:2517-2526.

Mulkey DK, Stornetta RL, Weston MC, Simmons JR, Parker A, Bayliss DA, Guyenet PG (2004) Respiratory control by ventral surface chemoreceptor neurons in rats. Nat Neurosci 7:1360-1369.

Munoz-Sanchez J, Chanez-Cardenas ME (2014) A Review on Hemeoxygenase-2: Focus on Cellular Protection and Oxygen Response. Oxidative medicine and cellular longevity 2014:604981.

Murase S, Inui K, Nosaka S (1994) Baroreceptor inhibition of the locus coeruleus noradrenergic neurons. Neuroscience 61:635-643.

Nagata O, Li WM, Sato A (1995) Glutamate N-methyl-D-aspartate (NMDA) and non-NMDA receptor antagonists administered into the brain stem depress the renal sympathetic reflex discharges evoked by single shock of somatic afferents in anesthetized rats. Neuroscience letters 201:111-114.

Nakatsuka T, Fujita T, Inoue K, Kumamoto E (2008) Activation of GIRK channels in substantia gelatinosa neurones of the adult rat spinal cord: a possible involvement of somatostatin. The Journal of Physiology 586:2511-2522.

Nattie E, Li A (2009) Central chemoreception is a complex system function that involves multiple brain stem sites. Journal of applied physiology 106:1464-1466.

Nattie EE, Li A (2002) CO2 dialysis in nucleus tractus solitarius region of rat increases ventilation in sleep and wakefulness. Journal of applied physiology 92:2119-2130.

Neubauer JA, Sunderram J (2004) Oxygen-sensing neurons in the central nervous system. Journal of applied physiology 96:367-374.

Nicholson C (1985) Diffusion from an injected volume of a substance in brain tissue with arbitrary volume fraction and tortuosity. Brain research 333:325-329.

Niewinski P, Janczak D, Rucinski A, Tubek S, Engelman ZJ, Jazwiec P, Banasiak W, Sobotka PA, Hart ECJ, Paton JFR, Ponikowski P (2014) Dissociation between blood pressure and heart rate response to hypoxia after bilateral carotid body removal in men with systolic heart failure. Experimental physiology 99:552-561.

Nimura T, Weinstein PR, Massa SM, Panter S, Sharp FR (1996) Heme oxygenase-1 (HO-1) protein induction in rat brain following focal ischemia. Brain Res Mol Brain Res 37:201-208.

Noma A (1983) ATP-regulated K+ channels in cardiac muscle. Nature 305:147-148.

Nunn C, Schoeffter P, Langenegger D, Hoyer D (2003) Functional characterisation of the putative somatostatin sst2 receptor antagonist CYN 154806. Naunyn-Schmiedeberg's archives of pharmacology 367:1-9.

Nurse CA (2005) Neurotransmission and neuromodulation in the chemosensory carotid body. Autonomic neuroscience : basic & clinical 120:1-9.

O'Carroll AM, Lolait SJ, König M, Mahan LC (1992) Molecular cloning and expression of a pituitary somatostatin receptor with preferential affinity for somatostatin-28. Molecular Pharmacology 42:939-946.

Oikawa S, Hirakawa H, Kusakabe T, Nakashima Y, Hayashida Y (2005) Autonomic cardiovascular responses to hypercapnia in conscious rats: the roles of the chemo- and baroreceptors. Autonomic neuroscience : basic & clinical 117:105-114.

Oliva I, Fernández M, Martín ED (2013) Dopamine release regulation by astrocytes during cerebral ischemia. Neurobiology of Disease 58:231-241.

Oomura Y, Ooyama H, Sugimori M, Nakamura T, Yamada Y (1974) Glucose inhibition of the glucose-sensitive neurone in the rat lateral hypothalamus. Nature 247:284-286.

Oshima N, Kumagai H, Onimaru H, Kawai A, Pilowsky PM, Iigaya K, Takimoto C, Hayashi K, Saruta T, Itoh H (2008) Monosynaptic excitatory connection from the rostral ventrolateral medulla to sympathetic preganglionic neurons revealed by simultaneous recordings. Hypertension research : official journal of the Japanese Society of Hypertension 31:1445-1454.

Oshima N, McMullan S, Goodchild AK, Pilowsky PM (2006) A monosynaptic connection between baroinhibited neurons in the RVLM and IML in Sprague-Dawley rats. Brain research 1089:153-161.

Padley JR, Kumar NN, Li Q, Nguyen TB, Pilowsky PM, Goodchild AK (2007) Central command regulation of circulatory function mediated by descending pontine cholinergic inputs to sympathoexcitatory rostral ventrolateral medulla neurons. Circ Res 100:284-291.

Padley JR, Li Q, Pilowsky PM, Goodchild AK (2003) Cannabinoid receptor activation in the rostral ventrolateral medulla oblongata evokes cardiorespiratory effects in anaesthetised rats. British journal of pharmacology 140:384-394.

Panguluri S, Saggu S, Lundy R (2009) Comparison of somatostatin and corticotrophin-releasing hormone immunoreactivity in forebrain neurons projecting to taste-responsive and non-responsive regions of the parabrachial nucleus in rat. Brain research 1298:57-69.

Panneton WM, Gan Q, Juric R (2010) The rat: a laboratory model for studies of the diving response. Journal of applied physiology 108:811-820.

Panneton WM, Gan Q, Sun DW (2012) Persistence of the nasotrigeminal reflex after pontomedullary transection. Respir Physiol Neurobiol 180:230-236.

Panneton WM, McCulloch PF, Sun W (2000) Trigemino-autonomic connections in the muskrat: the neural substrate for the diving response. Brain research 874:48-65.

Paré D, Quirk GJ, Ledoux JE (2004) New Vistas on Amygdala Networks in Conditioned Fear. Journal of Neurophysiology 92:1-9.

Parker LM, Kumar NN, Lonergan T, McMullan S, Goodchild AK (2013) Distribution and neurochemical characterization of neurons in the rat ventrolateral medulla activated by glucoprivation. Brain structure & function.

Parsons MP, Hirasawa M (2010) ATP-sensitive potassium channel-mediated lactate effect on orexin neurons: implications for brain energetics during arousal. The Journal of neuroscience : the official journal of the Society for Neuroscience 30:8061-8070.

Patel YC (1999) Somatostatin and Its Receptor Family. Frontiers in Neuroendocrinology 20:157-198.

Patrick Card J, Lois J, Sved AF (2010) Distribution and phenotype of Phox2a-Containing neurons in the adult Sprague-Dawley rat. Journal of Comparative Neurology 518:2202-2220.

Paxinos G, Watson C (1998) The rat brain in stereotaxic coordinates. San Diego: 4 ed. Academic Press, Inc.

Paxinos G, Watson C (2007) The Rat Brain in Stereotaxic Coordinates: Elsevier.

Peng Y-J, Wang N, Gong Q-L, Li P (2002) Caudal ventrolateral medulla mediates the depressor response elicited by the greater splanchnic nerve afferent stimulation in rats. Neuroscience letters 325:134-138.

Peyron C, Tighe DK, Van Den Pol AN, De Lecea L, Heller HC, Sutcliffe JG, Kilduff TS (1998) Neurons containing hypocretin (orexin) project to multiple neuronal systems. The Journal of neuroscience : the official journal of the Society for Neuroscience 18:9996-10015.

Phillips JK, Goodchild AK, Dubey R, Sesiashvili E, Takeda M, Chalmers J, Pilowsky PM, Lipski J (2001) Differential expression of catecholamine biosynthetic enzymes in the rat ventrolateral medulla. The Journal of comparative neurology 432:20-34.

Pilowsky P, West M, Chalmers J (1985) Renal sympathetic nerve responses to stimulation, inhibition and destruction of the ventrolateral medulla in the rabbit. Neuroscience letters 60:51-55.

Pilowsky PM, Goodchild AK (2002) Baroreceptor reflex pathways and neurotransmitters: 10 years on. Journal of hypertension 20:1675-1688.

Pimentel FF, Bonagamba LG, Machado BH (2003) Pressor response to chemoreflex activation before and after microinjection of glycine into the NTS of awake rats. American journal of physiology Regulatory, integrative and comparative physiology 284:R1000-1009.

Pineda J, Aghajanian GK (1997) Carbon dioxide regulates the tonic activity of locus coeruleus neurons by modulating a proton- and polyamine-sensitive inward rectifier potassium current. Neuroscience 77:723-743.

Prabhakar NR, Dinerman JL, Agani FH, Snyder SH (1995) Carbon monoxide: a role in carotid body chemoreception. Proc Natl Acad Sci U S A 92:1994-1997.

Premont RT, Inglese J, Lefkowitz RJ (1995) Protein kinases that phosphorylate activated G protein-coupled receptors. FASEB journal : official publication of the Federation of American Societies for Experimental Biology 9:175-182.

Priestley T (1992) The effect of baclofen and somatostatin on neuronal activity in the rat ventromedial hypothalamic nucleus in vitro. Neuropharmacology 31:103-109.

Puskas N, Papp RS, Gallatz K, Palkovits M (2010) Interactions between orexin-immunoreactive fibers and adrenaline or noradrenaline-expressing neurons of the lower brainstem in rats and mice. Peptides 31:1589-1597.

Rahn KH (1999) The sympathetic nervous system in the pathogenesis of hypertension. Journal of Hypertension, Supplement 17.

Ralevic V, Thomas T, Burnstock G, Spyer KM (1999) Characterization of P2 receptors modulating neural activity in rat rostral ventrolateral medulla. Neuroscience 94:867-878.

Ramírez-Jarquín JO, Lara-Hernández S, López-Guerrero JJ, Aguileta MA, Rivera-Angulo AJ, Sampieri A, Vaca L, Ordaz B, Peña-Ortega F (2012) Somatostatin modulates generation of inspiratory rhythms and determines asphyxia survival. Peptides 34:360-372.

Rappaport EB, Young JB, Landsberg L (1982) Effects of 2-deoxy-D-glucose on the cardiac sympathetic nerves and the adrenal medulla in the rat: further evidence for a dissociation of sympathetic nervous system and adrenal medullary responses. Endocrinology 110:650-656.

Rathner JA, McAllen RM (1999) Differential control of sympathetic drive to the rat tail artery and kidney by medullary premotor cell groups. Brain research 834:196-199.

Real MA, Heredia R, del Carmen Labrador M, Dávila JC, Guirado S (2009) Expression of somatostatin and neuropeptide Y in the embryonic, postnatal, and adult mouse amygdalar complex. The Journal of comparative neurology 513:335-348.

Reinert H (1964) Urethane Hyperglycaemia and Hypothalamic Activation. Nature 204:889-891.

Reis DJ, Golanov EV, Galea E, Feinstein DL (1997) Central neurogenic neuroprotection: central neural systems that protect the brain from hypoxia and ischemia. Annals of the New York Academy of Sciences 835:168-186.

Reis DJ, Ross CA, Ruggiero DA, Granata AR, Joh TH (1984) Role of adrenaline neurons of ventrolateral medulla (the C1 group) in the tonic and phasic control of arterial pressure. Clinical and experimental hypertension Part A, Theory and practice 6:221-241.

Ritter RC, Slusser PG, Stone S (1981) Glucoreceptors controlling feeding and blood glucose: Location in the hindbrain. Science 213:451-453.

Ritter S, Bugarith K, Dinh TT (2001) Immunotoxic destruction of distinct catecholamine subgroups produces selective impairment of glucoregulatory responses and neuronal activation. The Journal of comparative neurology 432:197-216.

Ritter S, Li AJ, Wang Q, Dinh TT (2011) Minireview: The value of looking backward: the essential role of the hindbrain in counterregulatory responses to glucose deficit. Endocrinology 152:4019-4032.

Ritter S, Llewellyn-Smith I, Dinh TT (1998) Subgroups of hindbrain catecholamine neurons are selectively activated by 2-deoxy-D-glucose induced metabolic challenge. Brain research 805:41-54.

Ritter S, Scheurink A, Singer LK (1995) 2-Deoxy-D-glucose but not 2-mercaptoacetate increases Fos-like immunoreactivity in adrenal medulla and sympathetic preganglionic neurons. Obesity research 729S-734S.

Robinson RB, Siegelbaum SA (2003) Hyperpolarization-activated cation currents: from molecules to physiological function. AnnuRevPhysiol 65:453.

Rong W, Gourine AV, Cockayne DA, Xiang Z, Ford APDW, Spyer KM, Burnstock G (2003) Pivotal Role of Nucleotide P2X2 Receptor Subunit of the ATP-Gated Ion Channel Mediating Ventilatory Responses to Hypoxia. J Neurosci 23:11315-11321.

Roozendaal B, Koolhaas JM, Bohus B (1991) Central amygdala lesions affect behavioral and autonomic balance during stress in rats. Physiology & Behavior 50:777-781.

Ross CA, Armstrong DM, Ruggiero DA, Pickel VM, Joh TH, Reis DJ (1981) Adrenaline neurons in the rostral ventrolateral medulla innervate thoracic spinal cord: a combined immunocytochemical and retrograde transport demonstration. Neuroscience letters 25:257-262.

Ross CA, Ruggiero DA, Park DH, Joh TH, Sved AF, Fernandez-Pardal J, Saavedra JM, Reis DJ (1984) Tonic vasomotor control by the rostral ventrolateral medulla: effect of electrical or chemical stimulation of the area containing C1 adrenaline neurons on arterial pressure, heart rate, and plasma catecholamines and vasopressin. The Journal of neuroscience : the official journal of the Society for Neuroscience 4:474-494.

Ross CA, Ruggiero DA, Reis DJ (1985) Projections from the nucleus tractus solitarii to the rostral ventrolateral medulla. The Journal of comparative neurology 242:511-534.

Roux JC, Mamet J, Perrin D, Peyronnet J, Royer C, Cottet-Emard JM, Pequignot JM, Dalmaz Y (2003) Neurochemical development of the brainstem catecholaminergic cell groups in rat. Journal of neural transmission 110:51-65.

Saggu S, Lundy RF (2008) Forebrain neurons that project to the gustatory parabrachial nucleus in rat lack glutamic acid decarboxylase. American Journal of Physiology - Regulatory, Integrative and Comparative Physiology 294:R52-R57.

Saha S, Drinkhill MJ, Moore JP, Batten TF (2005) Central nucleus of amygdala projections to rostral ventrolateral medulla neurones activated by decreased blood pressure. The European journal of neuroscience 21:1921-1930.

Saha S, Henderson Z, Batten TFC (2002) Somatostatin immunoreactivity in axon terminals in rat nucleus tractus solitarii arising from central nucleus of amygdala: coexistence with GABA and postsynaptic expression of sst2A receptor. Journal of Chemical Neuroanatomy 24:1-13.

Saita M, Verberne AJ (2003) Roles for CCK1 and 5-HT3 receptors in the effects of CCK on presympathetic vasomotor neuronal discharge in the rat. British journal of pharmacology 139:415-423.

Sakurai T, Amemiya A, Ishii M, Matsuzaki I, Chemelli RM, Tanaka H, Williams SC, Richarson JA, Kozlowski GP, Wilson S, Arch JR, Buckingham RE, Haynes AC, Carr SA, Annan RS, McNulty DE, Liu WS, Terrett JA, Elshourbagy NA, Bergsma DJ, Yanagisawa M (1998) Orexins and orexin receptors: a family of hypothalamic neuropeptides and G protein-coupled receptors that regulate feeding behavior. Cell 92:573-585.

Sanders NM, Ritter S (2001) Acute 2DG-induced glucoprivation or dexamethasone abolishes 2DG-induced glucoregulatory responses to subsequent glucoprivation. Diabetes 50:2831-2836.

Sartor DM, Verberne AJ (2003) Phenotypic identification of rat rostroventrolateral medullary presympathetic vasomotor neurons inhibited by exogenous cholecystokinin. The Journal of comparative neurology 465:467-479.

Sato A, Schmidt RF (1971) Spinal and supraspinal components of the reflex discharges into lumbar and thoracic white rami. The Journal of Physiology 212:839-850.

Scapagnini G, D'Agata V, Calabrese V, Pascale A, Colombrita C, Alkon D, Cavallaro S (2002) Gene expression profiles of heme oxygenase isoforms in the rat brain. Brain research 954:51-59.

Schreihofer AM, Guyenet PG (1997) Identification of C1 presympathetic neurons in rat rostral ventrolateral medulla by juxtacellular labeling in vivo. The Journal of comparative neurology 387:524-536.

Schreihofer AM, Guyenet PG (2000) Sympathetic reflexes after depletion of bulbospinal catecholaminergic neurons with anti-DbetaH-saporin. American journal of physiology Regulatory, integrative and comparative physiology 279:R729-742.

Schreihofer AM, Guyenet PG (2003) Baro-activated neurons with pulse-modulated activity in the rat caudal ventrolateral medulla express GAD67 mRNA. J Neurophysiol 89:1265-1277.

Schreihofer AM, Stornetta RL, Guyenet PG (2000) Regulation of sympathetic tone and arterial pressure by rostral ventrolateral medulla after depletion of C1 cells in rat. J Physiol 529 Pt 1:221-236.

Seagard JL, Dean C, Hopp FA (2000) Neurochemical transmission of baroreceptor input in the nucleus tractus solitarius. Brain research bulletin 51:111-118.

Severinghaus JW, Mitchell RA, Richardson BW, Singer MM (1963) Respiratory Control at High Altitude Suggesting Active Transport Regulation of Csf Ph. J Appl Physiol 18:1155-1166.

Sevigny CP, Bassi J, Teschemacher AG, Kim KS, Williams DA, Anderson CR, Allen AM (2008) C1 neurons in the rat rostral ventrolateral medulla differentially express vesicular monoamine transporter 2 in soma and axonal compartments. The European journal of neuroscience 28:1536-1544.

Shafton AD, Ryan A, Badoer E (1998) Neurons in the hypothalamic paraventricular nucleus send collaterals to the spinal cord and to the rostral ventrolateral medulla in the rat. Brain research 801:239-243.

Shah JH, Wongsurawat N, Aran PP, Motto GS, Bowser EN (1977) A method for studying acute insulin secretion and glucose tolerance in unanesthetized and unrestrained rats. The effect of mild stress on carbohydrate metabolism. Diabetes 26:1-6.

Shahid IZ, Rahman AA, Pilowsky PM (2012) Orexin A in rat rostral ventrolateral medulla is pressor, sympatho-excitatory, increases barosensitivity and attenuates the somato-sympathetic reflex. Br J Pharmacol 165:2292-2303.

Shannon R, Baekey DM, Morris KF, Li Z, Lindsey BG (2000) Functional connectivity among ventrolateral medullary respiratory neurones and responses during fictive cough in the cat. J Physiol 525 Pt 1:207-224.

Shapiro MS, Hille B (1993) Substance P and somatostatin inhibit calcium channels in rat sympathetic neurons via different G protein pathwavs. Neuron 10:11-20.

Share L, Crofton JT (1984) The role of vasopressin in hypertension. Federation proceedings 43:103-106.

Sherwood A, Dolan CA, Light KC (1990) Hemodynamics of Blood Pressure Responses During Active and Passive Coping. Psychophysiology 27:656-668.

Shiraishi T, Simpson A (1987) Central control of gastric acid secretion by extralateralhypothalamic nuclei. Brain research bulletin 18:309-314.

Smith DV, Ye M-K, Li C-S (2005) Medullary Taste Responses are Modulated by the Bed Nucleus of the Stria Terminalis. Chemical Senses 30:421-434.

Smith GP, Epstein AN (1969) Increased feeding in response to decreased glucose utilization in the rat and monkey. The American journal of physiology 217:1083-1087.

Smith GST, Savery D, Marden C, Costa JJL, Averill S, Priestley JV, Rattray M (1994) Distribution of messenger RNAs encoding enkephalin, substance P, somatostatin, galanin, vasoactive intestinal polypeptide, neuropeptide Y, and calcitonin gene-related peptide in the midbrain periaqueductal grey in the rat. The Journal of comparative neurology 350:23-40.

Smith JC, Abdala AP, Borgmann A, Rybak IA, Paton JF (2012) Brainstem respiratory networks: building blocks and microcircuits. Trends in neurosciences.

Smith JC, Morrison DE, Ellenberger HH, Otto MR, Feldman JL (1989) Brainstem projections to the major respiratory neuron populations in the medulla of the cat. The Journal of comparative neurology 281:69-96.

Smith PA, Graham LN, Mackintosh AF, Stoker JB, Mary DASG (2004) Relationship between central sympathetic activity and stages of human hypertension. American journal of hypertension 17:217-222.

Solomon IC, Edelman NH, Neubauer JA (2000) Pre-Botzinger complex functions as a central hypoxia chemosensor for respiration in vivo. J Neurophysiol 83:2854-2868.

Sousa LO, Lindsey CJ (2009a) Cardiovascular and baroreceptor functions of the paratrigeminal nucleus for pressor effects in non-anaesthetized rats. Autonomic Neuroscience 147:27-32.

Sousa LO, Lindsey CJ (2009b) Discharge rate profiles of paratrigeminal nucleus neurons throughout a pressor event in non-anaesthetized rats. Autonomic Neuroscience 147:20-26.

Spary EJ, Maqbool A, Batten TF (2008) Expression and localisation of somatostatin receptor subtypes sst1-sst5 in areas of the rat medulla oblongata involved in autonomic regulation. J Chem Neuroanat 35:49-66.

Spyer KM, Dale N, Gourine AV (2004) ATP is a key mediator of central and peripheral chemosensory transduction. Experimental physiology 89:53-59.

Stasinopoulos T, Goodchild AK, Christie MJ, Chalmers J, Pilowsky PM (2000) Delta opioid receptor immunoreactive boutons appose bulbospinal CI neurons in the rat. Neuroreport 11:887-891.

Stock G, Schlör KH, Heidt H, Buss J (1978) Psychomotor behaviour and cardiovascular patterns during stimulation of the amygdala. Pflugers Archiv : European journal of physiology 376:177-184.

Stocker SD, Simmons JR, Stornetta RL, Toney GM, Guyenet PG (2006) Water deprivation activates a glutamatergic projection from the hypothalamic paraventricular nucleus to the rostral ventrolateral medulla. The Journal of comparative neurology 494:673-685.

Stocker SD, Toney GM (2005) Median preoptic neurones projecting to the hypothalamic paraventricular nucleus respond to osmotic, circulating Ang II and baroreceptor input in the rat. J Physiol 568:599-615.

Stocker SD, Toney GM (2007) Vagal afferent input alters the discharge of osmotic and ANG II-responsive median preoptic neurons projecting to the hypothalamic paraventricular nucleus. Brain research 1131:118-128.

Storlien LH, Grunstein HS, Smythe GA (1985) Guanethidine blocks the 2-deoxy-D-glucose-induced hypothalamic noradrenergic drive to hyperglycemia. Brain research 335:144-147.

Stornetta RL (2009) Neurochemistry of bulbospinal presympathetic neurons of the medulla oblongata. J Chem Neuroanat 38:222-230.

Stornetta RL, Akey PJ, Guyenet PG (1999) Location and electrophysiological characterization of rostral medullary adrenergic neurons that contain neuropeptide Y mRNA in rat medulla. The Journal of comparative neurology 415:482-500.

Stornetta RL, Guyenet PG (1999) Distribution of glutamic acid decarboxylase mRNA-containing neurons in rat medulla projecting to thoracic spinal cord in relation to monoaminergic brainstem neurons. The Journal of comparative neurology 407:367-380.

Stornetta RL, McQuiston TJ, Guyenet PG (2004) GABAergic and glycinergic presympathetic neurons of rat medulla oblongata identified by retrograde transport of pseudorabies virus and in situ hybridization. The Journal of comparative neurology 479:257-270.

Stornetta RL, Moreira TS, Takakura AC, Kang BJ, Chang DA, West GH, Brunet JF, Mulkey DK, Bayliss DA, Guyenet PG (2006) Expression of Phox2b by brainstem neurons involved in chemosensory integration in the adult rat. The Journal of neuroscience : the official journal of the Society for Neuroscience 26:10305-10314.

Stornetta RL, Morrison SF, Ruggiero DA, Reis DJ (1989) Neurons of rostral ventrolateral medulla mediate somatic pressor reflex. The American journal of physiology 256:R448-462.

Stornetta RL, Rosin DL, Wang H, Sevigny CP, Weston MC, Guyenet PG (2003) A group of glutamatergic interneurons expressing high levels of both neurokinin-1 receptors and somatostatin identifies the region of the pre-Botzinger complex. Journal of Comparative Neurology 455:499-512.

Stornetta RL, Schreihofer AM, Pelaez NM, Sevigny CP, Guyenet PG (2001) Preproenkephalin mRNA is expressed by C1 and non-C1 barosensitive bulbospinal neurons in the rostral ventrolateral medulla of the rat. The Journal of comparative neurology 435:111-126.

Stornetta RL, Sevigny CP, Guyenet PG (2002) Vesicular glutamate transporter DNPI/VGLUT2 mRNA is present in C1 and several other groups of brainstem catecholaminergic neurons. The Journal of comparative neurology 444:191-206.

Strack AM, Sawyer WB, Hughes JH, Platt KB, Loewy AD (1989a) A general pattern of CNS innervation of the sympathetic outflow demonstrated by transneuronal pseudorabies viral infections. Brain research 491:156-162.

Strack AM, Sawyer WB, Marubio LM, Loewy AD (1988) Spinal origin of sympathetic preganglionic neurons in the rat. Brain research 455:187-191.

Strack AM, Sawyer WB, Platt KB, Loewy AD (1989b) CNS cell groups regulating the sympathetic outflow to adrenal gland as revealed by transneuronal cell body labeling with pseudorabies virus. Brain research 491:274-296.

Sun CL, Thoa NB, Kopin IJ (1979) Comparison of the effects of 2-deoxyglucose and immobilization on plasma levels of catecholamines and corticosterone in awake rats. Endocrinology 105:306-311.

Sun MK, Guyenet PG (1986) Hypothalamic glutamatergic input to medullary sympathoexcitatory neurons in rats. The American journal of physiology 251:R798-810.

Sun MK, Hackett JT, Guyenet PG (1988a) Sympathoexcitatory neurons of rostral ventrolateral medulla exhibit pacemaker properties in the presence of a glutamate-receptor antagonist. Brain research 438:23-40.

Sun MK, Jeske IT, Reis DJ (1992a) Cyanide excites medullary sympathoexcitatory neurons in rats. The American journal of physiology 262:R182-189.

Sun MK, Reis DJ (1993) Differential responses of barosensitive neurons of rostral ventrolateral medulla to hypoxia in rats. Brain research 609:333-337.

Sun MK, Reis DJ (1994a) Central neural mechanisms mediating excitation of sympathetic neurons by hypoxia. Prog Neurobiol 44:197-219.

Sun MK, Reis DJ (1994b) Hypoxia-activated Ca2+ currents in pacemaker neurones of rat rostral ventrolateral medulla in vitro. J Physiol 476:101-116.

Sun MK, Reis DJ (1994c) Hypoxia selectively excites vasomotor neurons of rostral ventrolateral medulla in rats. The American journal of physiology 266:R245-256.

Sun MK, Reis DJ (1996) Medullary vasomotor activity and hypoxic sympathoexcitation in pentobarbital-anesthetized rats. American Journal of Physiology - Regulatory Integrative and Comparative Physiology 270:R348-R355.

Sun MK, Wahlestedt C, Reis DJ (1992b) Action of externally applied ATP on rat reticulospinal vasomotor neurons. European journal of pharmacology 224:93-96.

Sun MK, Young BS, Hackett JT, Guyenet PG (1988b) Reticulospinal pacemaker neurons of the rat rostral ventrolateral medulla with putative sympathoexcitatory function: an intracellular study in vitro. Brain research 442:229-239.

Sun QJ, Goodchild AK, Chalmers JP, Pilowsky PM (1998) The pre-Botzinger complex and phase-spanning neurons in the adult rat. Brain research 809:204-213.

Sun Y, Rotenberg MO, Maines MD (1990) Developmental expression of heme oxygenase isozymes in rat brain. Two HO-2 mRNAs are detected. Journal of Biological Chemistry 265:8212-8217.

Sunderram J, Semmlow J, Thakker-Varia S, Bhaumik M, Hoang-Le O, Neubauer JA (2009) Heme oxygenase-1-dependent central cardiorespiratory adaptations to chronic hypoxia in mice. American Journal of Physiology - Regulatory Integrative and Comparative Physiology 297.

Sved AF, Mancini DL, Graham JC, Schreihofer AM, Hoffman GE (1994) PNMT-containing neurons of the C1 cell group express c-fos in response to changes in baroreceptor input. The American journal of physiology 266:R361-367.

Swanson RA, Graham SH (1994) Fluorocitrate and fluoroacetate effects on astrocyte metabolism in vitro. Brain research 664:94-100.

Szerb JC, Issekutz B (1987) Increase in the stimulation-induced overflow of glutamate by fluoroacetate, a selective inhibitor of the glial tricarboxylic cycle. Brain research 410:116-120.

Takakura AC, Moreira TS, Colombari E, West GH, Stornetta RL, Guyenet PG (2006) Peripheral chemoreceptor inputs to retrotrapezoid nucleus (RTN) CO2-sensitive neurons in rats. J Physiol 572:503-523.

Takayama K, Miura M (1991) Glutamate-immunoreactive neurons of the central amygdaloid nucleus projecting to the subretrofacial nucleus of SHR and WKY rats: A double-labeling study. Neuroscience letters 134:62-66.

Takayama K, Miura M (1992) Difference in distribution of glutamate-immunoreactive neurons projecting into the subretrofacial nucleus in the rostral ventrolateral medulla of SHR and WKY: a double-labeling study. Brain research 570:259-266.

Tan W, Janczewski WA, Yang P, Shao XM, Callaway EM, Feldman JL (2008) Silencing preBotzinger complex somatostatin-expressing neurons induces persistent apnea in awake rat. Nat Neurosci 11:538-540.

Tan W, Pagliardini S, Yang P, Janczewski WA, Feldman JL (2010) Projections of preBotzinger complex neurons in adult rats. The Journal of comparative neurology 518:1862-1878.

Thomas T, Ralevic V, Bardini M, Burnstock G, Spyer KM (2001) Evidence for the involvement of purinergic signalling in the control of respiration. Neuroscience 107:481-490.

Thoss VS, Ferez J, Duc D, Hoyer D (1995) Embryonic and postnatal mRNA distribution of five somatostatin receptor subtypes in the rat brain. Neuropharmacology 34:1673-1688.

Tsuchihashi T, Abe I, Fujishima M (1994) Role of metabotropic glutamate receptors in ventrolateral medulla of hypertensive rats. Hypertension 24:648-652.

Tsuchihashi T, Averill DB (1993) Metabotropic glutamate receptors in the ventrolateral medulla of rats. Hypertension 21:739-744.

Tsuda M, Shigemoto-Mogami Y, Koizumi S, Mizokoshi A, Kohsaka S, Salter MW, Inoue K (2003) P2X4 receptors induced in spinal microglia gate tactile allodynia after nerve injury. Nature 424:778-783.

Tucker DC, Saper CB, Ruggiero DA, Reis DJ (1987) Organization of central adrenergic pathways: I. Relationships of ventrolateral medullary projections to the hypothalamus and spinal cord. The Journal of comparative neurology 259:591-603.

Tupal S, Rieger MA, Ling GY, Park TJ, Dougherty JD, Goodchild AK, Gray PA (2014) Testing the role of preBotzinger Complex somatostatin neurons in respiratory and vocal behaviors. The European journal of neuroscience.

Turner A, Kumar N, Farnham M, Lung M, Pilowsky P, McMullan S (2013) Rostroventrolateral medulla neurons with commissural projections provide input to sympathetic premotor neurons: anatomical and functional evidence. The European journal of neuroscience 38:2504-2515.

Urbanski RW, Sapru HN (1988) Evidence for a sympathoexcitatory pathway from the nucleus tractus solitarii to the ventrolateral medullary pressor area. Journal of the autonomic nervous system 23:161-174.

Vanetti M, Kouba M, Wang X, Vogt G, Höllt V (1992) Cloning and expression of a novel mouse somatostatin receptor (SSTR2B). FEBS Letters 311:290-294.

Vanetti M, Ziolkowska B, Wang X, Horn G, Hollt V (1994) mRNA distribution of two isoforms of somatostatin receptor 2 (mSSTR2A and mSSTR2B) in mouse brain. Brain research Molecular brain research 27:45-50.

Veening JG, Swanson LW, Sawchenko PE (1984) The organization of projections from the central nucleus of the amygdala to brainstem sites involved in central autonomic regulation: A combined retrograde transport-immunohistochemical study. Brain research 303:337-357.

Verberne AJ (1995) Cuneiform nucleus stimulation produces activation of medullary sympathoexcitatory neurons in rats. The American journal of physiology 268:R752-758.

Verberne AJ (1996) Medullary sympathoexcitatory neurons are inhibited by activation of the medial prefrontal cortex in the rat. The American journal of physiology 270:R713-719.

Verberne AJ, Guyenet PG (1992) Midbrain central gray: influence on medullary sympathoexcitatory neurons and the baroreflex in rats. The American journal of physiology 263:R24-33.

Verberne AJ, Sartor DM (2010) Rostroventrolateral medullary neurons modulate glucose homeostasis in the rat. American journal of physiology Endocrinology and metabolism 299:E802-E807.

Verberne AJ, Sartor DM, Berke A (1999a) Midline medullary depressor responses are mediated by inhibition of RVLM sympathoexcitatory neurons in rats. The American journal of physiology 276:R1054-1062.

Verberne AJ, Stornetta RL, Guyenet PG (1999b) Properties of C1 and other ventrolateral medullary neurones with hypothalamic projections in the rat. J Physiol 517 (Pt 2):477-494.

Verberne AJ, Stornetta RL, Guyenet PG (1999c) Properties of C1 and other ventrolateral medullary neurones with hypothalamic projections in the rat. Journal of Physiology 517 (Pt 2):477-494.

Viana F, Hille B (1996) Modulation of High Voltage-Activated Calcium Channels by Somatostatin in Acutely Isolated Rat Amygdaloid Neurons. The Journal of Neuroscience 16:6000-6011.

Vincent SR, McIntosh CHS, Buchan AMJ, Brown JC (1985) Central somatostatin systems revealed with monoclonal antibodies. The Journal of comparative neurology 238:169-186.

von Leupoldt A, Sommer T, Kegat S, Baumann HJr, Klose H, Dahme B, BÃ¼chel C (2008) The Unpleasantness of Perceived Dyspnea Is Processed in the Anterior Insula and Amygdala. American Journal of Respiratory and Critical Care Medicine 177:1026-1032.

Wang G, Zhou P, Repucci MA, Golanov EV, Reis DJ (2001) Specific actions of cyanide on membrane potential and voltage-gated ion currents in rostral ventrolateral medulla neurons in rat brainstem slices. Neuroscience letters 309:125-129.

Wang HL, Dichter M, Reisine T (1990) Lack of cross-desensitization of somatostatin-14 and somatostatin-28 receptors coupled to potassium channels in rat neocortical neurons. Mol Pharmacol 38:357-361.

Wang WH, Lovick TA (1993) The inhibitory effect of the ventrolateral periaqueductal grey matter on neurones in the rostral ventrolateral medulla involves a relay in the medullary raphe nuclei. Experimental brain research 94:295-300.

Waraczynski M (2003) Lidocaine inactivation demonstrates a stronger role for central versus medial extended amygdala in medial forebrain bundle self-stimulation. Brain research 962:180-198.

Ward DG (1988) Stimulation of the parabrachial nuclei with monosodium glutamate increases arterial pressure. Brain research 462:383-390.

Waser B, Tamma ML, Cescato R, Maecke HR, Reubi JC (2009) Highly efficient in vivo agonist-induced internalization of sst2 receptors in somatostatin target tissues. Journal of nuclear medicine : official publication, Society of Nuclear Medicine 50:936-941.

Watt MJ, Howlett KF, Febbraio MA, Spriet LL, Hargreaves M (2001) Adrenaline increases skeletal muscle glycogenolysis, pyruvate dehydrogenase activation and carbohydrate oxidation during moderate exercise in humans. J Physiol (Lond) 534:269-278.

Way JL (1984) Cyanide intoxication and its mechanism of antagonism. Annual review of pharmacology and toxicology 24:451-481.

Wenker IC, Sobrinho CR, Takakura AC, Mulkey DK, Moreira TS (2013) P2Y1 Receptors Expressed by C1 Neurons Determine Peripheral Chemoreceptor Modulation of Breathing, Sympathetic Activity, and Blood Pressure. Hypertension 62:263-273.

Whiting MJ (2009) Simultaneous measurement of urinary metanephrines and catecholamines by liquid chromatography with tandem mass spectrometric detection. Annals of clinical biochemistry 46:129-136.

Wilensky AE, Schafe GE, Kristensen MP, LeDoux JE (2006) Rethinking the Fear Circuit: The Central Nucleus of the Amygdala Is Required for the Acquisition, Consolidation, and Expression of Pavlovian Fear Conditioning. The Journal of Neuroscience 26:12387-12396.

Willette RN, Barcas PP, Krieger AJ, Sapru HN (1983a) Vasopressor and depressor areas in the rat medulla. Identification by microinjection of L-glutamate. Neuropharmacology 22:1071-1079.

Willette RN, Krieger AJ, Barcas PP, Sapru HN (1983b) Medullary gamma-aminobutyric acid (GABA) receptors and the regulation of blood pressure in the rat. The Journal of pharmacology and experimental therapeutics 226:893-899.

Williams SEJ, Wootton P, Mason HS, Bould J, Iles DE, Riccardi D, Peers C, Kemp PJ (2004) Hemoxygenase-2 is an oxygen sensor for a calcium-sensitive potassium channel. Science 306:2093-2097.

Wu L, Wang R (2005) Carbon monoxide: Endogenous production, physiological functions, and pharmacological applications. Pharmacological Reviews 57:585-630.

Wu WC, Wang Y, Su CK, Chai CY (2001) The nNOS/cGMP signal transducing system is involved in the cardiovascular responses induced by activation of NMDA receptors in the rostral ventrolateral medulla of cats. Neuroscience letters 310:121-124.

Yamaguchi N (1992) Sympathoadrenal system in neuroendocrine control of glucose: mechanisms involved in the liver, pancreas, and adrenal gland under hemorrhagic and hypoglycemic stress. Canadian journal of physiology and pharmacology 70:167-206.

Yamamoto Y, Runold M, Prabhakar N, Pantaleo T, Lagercrantz H (1988) Somatostatin in the control of respiration. Acta physiologica Scandinavica 134:529-533.

Yao ST, Barden JA, Finkelstein DI, Bennett MR, Lawrence AJ (2000) Comparative study on the distribution patterns of P2X(1)-P2X(6) receptor immunoreactivity in the brainstem of the rat and the common marmoset (Callithrix jacchus): association with catecholamine cell groups. The Journal of comparative neurology 427:485-507.

Yao ST, Gourine AV, Spyer KM, Barden JA, Lawrence AJ (2003) Localisation of P2X2 receptor subunit immunoreactivity on nitric oxide synthase expressing neurones in the brain stem and hypothalamus of the rat: a fluorescence immunohistochemical study. Neuroscience 121:411-419.

Yasuda K, Rens-Domiano S, Breder CD, Law SF, Saper CB, Reisine T, Bell GI (1992) Cloning of a novel somatostatin receptor, SSTR3, coupled to adenylylcyclase. Journal of Biological Chemistry 267:20422-20428.

Yasui Y, Cechetto DF, Saper CB (1990) Evidence for a cholinergic projection from the pedunculopontine tegmental nucleus to the rostral ventrolateral medulla in the rat. Brain research 517:19-24.

Yi CX, Serlie MJ, Ackermans MT, Foppen E, Buijs RM, Sauerwein HP, Fliers E, Kalsbeek A (2009) A major role for perifornical orexin neurons in the control of glucose metabolism in rats. Diabetes 58:1998-2005.

Yin H, Lee KE, Park SA, Bhattarai JP, Suh BJ, Jeon JG, Kim BG, Park SJ, Han SK (2009) Inhibitory effects of somatostatin on the substantia gelatinosa neurons of trigeminal subnucleus caudalis via somatostatin type 2 receptors in juvenile mice. Brain research 1304:49-56.

Yoshimatsu H, Egawa M, Bray GA (1991) Adrenal sympathetic nerve activity in response to hypothalamic injections of 2-deoxy-D-glucose. American journal of physiology Regulatory, integrative and comparative physiology 261:R875-R881.

Yoshimura M, Polosa C, Nishi S (1986) Noradrenaline modifies sympathetic preganglionic neuron spike and afterpotential. Brain research 362:370-374.

Young Shim E, Jung Kim H, Kim MJ, Rhie DJ, Jo YH, Kim MS, June Hahn S, Lee MY, Yoon SH (2006) Desensitization of somatostatin-induced inhibition of low extracellular magnesium concentration-induced calcium spikes in cultured rat hippocampal neurons. Brain research 1111:61-71.

Yu D, Gordon FJ (1996) Anatomical evidence for a bi-neuronal pathway connecting the nucleus tractus solitarius to caudal ventrolateral medulla to rostral ventrolateral medulla in the rat. Neuroscience letters 205:21-24.

Zakhary R, Gaine SP, Dinerman JL, Ruat M, Flavahan NA, Snyder SH (1996) Heme oxygenase 2: endothelial and neuronal localization and role in endothelium-dependent relaxation. Proc Natl Acad Sci U S A 93:795-798.

Zanzinger J, Czachurski J, Offner B, Seller H (1994) Somato-sympathetic reflex transmission in the ventrolateral medulla oblongata: spatial organization and receptor types. Brain research 656:353-358.

Zanzinger J, Czachurski J, Seller H (1995) Effects of nitric oxide on sympathetic baroreflex transmission in the nucleus tractus solitarii and caudal ventrolateral medulla in cats. Neuroscience letters 197:199-202.

Zhang L, Wang H, Li Q, Zhan R, Yu SY (2012) Purinergic modulation of hypoxic regulation via the rostral ventral lateral medulla in rats. Respir Physiol Neurobiol 184:48-54.

Zhong S, Barman SM, Gebber GL (1992) Effects of brain stem lesions on 10-Hz and 2- to 6-Hz rhythms in sympathetic nerve discharge. The American journal of physiology 262:R1015-1024.

Zoccal DB, Huidobro-Toro JP, Machado BH (2011) Chronic intermittent hypoxia augments sympatho-excitatory response to ATP but not to L-glutamate in the RVLM of rats. Autonomic neuroscience : basic & clinical 165:156-16.

APPENDIX I: PUBLISHED WORK

Willian S. Korim,[1] Lama Bou Farah,[2] Simon McMullan,[2] and Anthony J.M. Verberne[1]

Orexinergic Activation of Medullary Premotor Neurons Modulates the Adrenal Sympathoexcitation to Hypothalamic Glucoprivation

Diabetes 2014;63:1895–1906 | DOI: 10.2337/db13-1073

Glucoprivation activates neurons in the perifornical hypothalamus (PeH) and in the rostral ventrolateral medulla (RVLM), which results in the release of adrenaline. The current study aimed to establish *1*) whether neuroglucoprivation in the PeH or in the RVLM elicits adrenaline release in vivo and *2*) whether direct activation by glucoprivation or orexin release in the RVLM modulates the adrenaline release. Neuroglucoprivation in the PeH or RVLM was elicited by microinjections of 2-deoxy-D-glucose or 5-thio-D-glucose in anesthetized, euglycemic rats. Firstly, inhibition of neurons in the PeH abolished the increase in adrenal sympathetic nerve activity (ASNA) to systemic glucoprivation. Secondly, glucoprivation of neurons in the PeH increased ASNA. Thirdly, in vivo or in vitro glucoprivation did not affect the activity of RVLM adrenal premotor neurons. Finally, blockade of orexin receptors in the RVLM abolished the increase in ASNA to neuroglucoprivation in the PeH. The evoked changes in ASNA were directly correlated to levels of plasma metanephrine but not to normetanephrine. These findings suggest that orexin release modulates the activation of adrenal presympathetic neurons in the RVLM.

Glucoprivation is a metabolic challenge capable of eliciting adrenaline release, an important mechanism for the restoration of normal blood glucose levels. Additionally, neuroglucoprivation produced by 2-deoxy-D-glucose (2DG) is used as an experimental tool to study glucoregulatory neurons (1–4). Previous findings suggest that adrenaline release in response to glucoprivation involves activation of neurons in the perifornical hypothalamus (PeH) and rostral ventrolateral medulla (RVLM). Systemic glucoprivation using 2DG excites RVLM sympathetic premotor neurons (5,6) and orexinergic neurons (7) in the PeH (8). Additionally, neurotropic viruses injected into the adrenal gland transsynaptically label neurons in the RVLM (9) and PeH (10). Disinhibition of perifornical neurons produces an increase in endogenous glucose production in the liver, which is mediated by the autonomic nervous system (11). However, it remains unknown whether intrinsic glucose sensitivity or projections from hypothalamic glucose-sensitive neurons (4,12,13) play an important role in the excitation of RVLM adrenal premotor neurons in response to glucoprivation; in particular, whether the responses evoked in RVLM neurons are modulated by orexinergic inputs (14,15).

In this study, we hypothesized that PeH neurons respond to neuroglucoprivation and elicit adrenaline release by orexinergic activation of sympathetic premotor neurons in the RVLM. To test this hypothesis, we used a combination of in vivo and in vitro electrophysiological techniques to first examine the role played by neurons in the PeH in driving adrenal sympathetic nerve activity (ASNA). We then demonstrate for the first time that these effects are independent of any intrinsic sensitivity

[1]Clinical Pharmacology and Therapeutics Unit, Department of Medicine, Austin Health, University of Melbourne, Heidelberg, Victoria, Australia
[2]Australian School of Advanced Medicine, Macquarie University, Sydney, New South Wales, Australia
Corresponding author: Willian S. Korim, willian.korim@unimelb.edu.au.

Received 15 July 2013 and accepted 10 February 2014.
This article contains Supplementary Data online at http://diabetes.diabetesjournals.org/lookup/suppl/doi:10.2337/db13-1073/-/DC1.

of neurons in the RVLM to glucoprivation and that the activation of orexin receptors in the RVLM modulates the adrenal sympathoexcitatory responses.

RESEARCH DESIGN AND METHODS

Experiments were performed according to the *Australian Code of Practice for the Care and Use of Animals for Scientific Purposes*. All experiments were approved by the Austin Health (2012/4764) and Macquarie University (2011/055) Animal Ethics Committees.

In Vivo Experiments

General Procedures

Adult male Sprague-Dawley rats (250–350 g) were anesthetized with isoflurane (1.7% in 100% O_2). The left femoral vein and artery were cannulated for drug administration and arterial blood pressure recording, respectively. Body temperature was kept at 37° ± 0.5°C by a thermocouple-controlled heating pad. The rats were tracheostomized, paralyzed (pancuronium bromide; 1 mg/kg i.v.; supplemented by 0.1 mg/kg/h), and artificially ventilated with oxygen-enriched air (3.5 mL, 70 cycles/min). After completion of surgery, isoflurane was replaced by urethane (1.2 g/kg i.v.). The level of anesthesia was monitored by hind paw pinch and the corneal reflex; urethane was supplemented (0.2 g/kg i.v.) as required. After neuromuscular blockade, anesthesia was maintained at a level in which paw pinch produced minimal changes in blood pressure (≤10 mmHg). Blood glucose was measured by withdrawing a drop of blood from the femoral artery and applying it to a glucometer (Optium Xceed; Medisense; Abbott Laboratories, Bedford, MA), as previously described (5).

Adrenal Sympathetic Nerve Recording

The right adrenal sympathetic nerve was prepared for recording via a retroperitoneal approach. Fibers emerging from the ganglion projecting toward the adrenal gland were carefully dissected free from connective tissue and fat. The fibers were tied together using 10-0 surgical nylon, cut distally, and mounted on bipolar silver wire electrodes. The nerve was covered with paraffin oil or embedded in a silicone elastomer (Kwik-Cast Sealant; WPI, Sarasota, FL). ASNA was amplified ×10,000 (7P5B; Grass Instruments, Quincy, MA) filtered (100 Hz–3 kHz), and sampled at 6 kHz using a CED Power1401 (Cambridge Electronic Design LTD, Cambridge, U.K.) with Spike2 v7.02 software. ASNA was rectified and integrated (τ = 1 s) before analysis. All neurograms were normalized with reference to the resting level before stimulus (100%) after subtraction of the noise (0%), determined postmortem or after clonidine (200 μg/kg i.v.; Sigma-Aldrich). Experiments were not included for analysis if the ratio of pre-to-postganglionic ASNA was higher than 50%, verified by intravenous hexamethonium (40 mg/kg; Sigma-Aldrich) at the end of the experiments.

Measurement of Blood Catecholamines

Owing to the rapid degradation of catecholamines, we measured plasma levels of metanephrines (16). Plasma (0.2 mL) was extracted from blood (0.5 mL) withdrawn from the femoral arterial cannula to determine the levels of metanephrine and normetanephrine. Plasma metanephrines were assayed by liquid chromatography tandem mass spectrometry, modified from the method of Whiting (17). Heparinized plasma samples had deuterated internal standards for each analyte that were added before solid-phase extraction using weak cation exchange. Extracted samples were evaporated to dryness, reconstituted, and derivatized using cyanoborohydride and acetaldehyde before chromatographic separation and mass spectrometric detection using multiple reactions monitoring (model 6460; Agilent Technologies, Mulgrave, Victoria, Australia).

Location of the PeH and RVLM

The PeH was located using stereotaxic coordinates (18). These were 2.9–3.4 mm caudal to the bregma, 1.1–1.3 mm lateral to the midline, and 8.6–8.7 mm ventral to the dorsal surface.

RVLM adrenal sympathetic premotor neurons are mingled with cardiovascular premotor neurons (5). Hence, the RVLM was identified by extracellular recording of cardiovascular sympathetic premotor neurons, which were inhibited by phenylephrine (10 μg/kg i.v.; Sigma-Aldrich; Supplementary Fig. 1) (5,19). These neurons were identified after antidromic field-potential mapping of the facial nucleus, elicited by electrical stimulation (0.5 Hz, 0.1 ms, 0.5–1.0 mA) of the facial nerve. Extracellular recordings were made using glass microelectrodes (2 mm outer diameter; 5–9 mol/LΩ) filled with 2% Pontamine Sky Blue in sodium acetate (0.5 mol/L). Extracellular potentials were recorded using a window discriminator and amplifier (×10,000; 400–4,000 Hz; Fintronics, Orange, CT). RVLM sympathetic premotor neurons were found at +0.1 rostral to −0.3 mm caudal, 0.1–0.3 mm medial, and 0.1–0.3 mm ventral to the caudal pole of the facial nucleus.

Glucoprivation and Microinjections

All experimental procedures were conducted after establishment of a euglycemic baseline (4.8–7.0 mmol/L; average: 6.1 ± 0.1 mmol/L; n = 60). Systemic glucoprivation was produced by 2DG (250 mg/kg i.v.; Sigma-Aldrich). Microinjections were performed using multibarrel micropipettes. All drugs were diluted in a solution of latex fluorescent beads 2% (Invitrogen) in artificial cerebrospinal fluid (aCSF; in mmol/L: NaCl, 128; KCl, 2.6; NaH_2PO_4, 1.3; $NaHCO_3$, 2; $CaCl_2$, 1.3; and $MgCl_2$, 0.9). All microinjections were 50 nL. Neuroglucoprivation was elicited by microinjections of 2DG (0.2–20 mmol/L) or 5-thio-D-glucose (5TG; 0.6–600 mmol/L; Sigma-Aldrich), using doses based on previous reports (2,20). Perifornical neurons were permanently inhibited by the γ-aminobutyric acid $(GABA)_A$ agonist muscimol (4 mmol/L; Sigma-Aldrich)

or disinhibited by the $GABA_A$ antagonist bicuculline (1 mmol/L; Sigma-Aldrich). Note that these agents were used primarily to inhibit or activate hypothalamic neurons and also to determine the role of their respective GABAergic inputs in glucose homeostasis. Orexin A (0.1–10 mmol/L; Sigma-Aldrich) was microinjected into the RVLM using doses based on a previous study (21). Orexin receptors in the RVLM were blocked using the nonselective antagonist TCS 1102 (5 mmol/L; Tocris Bioscience), diluted in 50% DMSO (Sigma-Aldrich), using a dose based on a previous report (22).

Histology

At the end of the experiments, animals were perfused with NaCl 0.9% (weight for volume), followed by 10% formalin. Brains were removed, fixed in formalin overnight, and cut with a Vibratome in 100-μm coronal sections. Sections were mounted onto gelatin-subbed slides for identification of the injection sites. Sections were examined under epifluorescence to locate the fluorescent bead deposits. The center of the injections were photographed (DXC-9100P; Sony, Tokyo, Japan) and plotted (Supplementary Fig. 1) with reference to a rat brain atlas (18).

In Vitro Experiments

Voltage-Clamp Recordings From Putative RVLM Sympathetic Premotor Neurons

Sprague-Dawley rat pups (P5–P20) were anesthetized with 2–5% isoflurane (Veterinary Companies of Australia) in oxygen and moved onto a heated pad. A dorsal laminectomy was performed and the T2 spinal cord exposed. Fluorescently conjugated cholera toxin β-subunit (CTB-Alexa 555, 0.5–1%; Invitrogen) was injected bilaterally at coordinates corresponding to the intermediolateral cell column (100 nL injections each side). After the microinjections were completed, the wound was closed with cyanoacrylate glue and anesthesia discontinued. Pups were allowed to recover on a warm pad until ambulatory and were then returned to the cage with their mother and littermates. Postoperative rats were carefully monitored and treated with additional analgesia (Carprofen, 2 mg/kg subcutaneous; Norbrook Pharmaceuticals, Australia) when indicated.

Whole-Cell Recordings From RVLM Medullospinal Neurons

Solutions (in mmol/L):

Cutting solution: 118 NaCl, 25 $NaHCO_3$, 3 KCl, 1.2 $NaH_2PO_4.H_2O$, 10 D-glucose, 1.5 $CaCl_2$, 1 $MgCl_2$; equilibrated with 95% O_2 and 5% CO_2 (23).

aCSF: 125 NaCl, 21 $NaHCO_3$, 2.5 KCl, 1.2 NaH_2PO_4. H_2O, 2 D-glucose, 2 $CaCl_2$, 2 $MgCl_2$; equilibrated with 95% O_2 and 5% CO_2 (pH = 7.35).

Potassium gluconate internal solution: 125 K-gluconate, 10 HEPES, 11 EGTA, 15 NaCl, 1 $MgCl_2$, 2 MgATP, 0.25 Na guanosine-5′-triphosphate, 0.05% biocytin (pH = 7.3; osmolarity 280–285 mOsm).

At 2–5 days after tracer microinjection, pups were anesthetized with isoflurane and quickly decapitated. The whole brain was quickly removed and dissected in ice-cold oxygenated cutting solution. The brainstem was mounted in a Vibratome, and 300-μm-thick coronal sections were cut under ice-cold carbogen-bubbled cutting solution. Three to four sections from the region immediately caudal to the facial nucleus were retained and transferred to carbogen-bubbled aCSF containing 2 mmol/L glucose at 34°C for at least 1 h. Recordings were performed at room temperature in the recording chamber of an Olympus microscope superfused at 1.5–2 mL/min with carbogen-bubbled aCSF.

Tracer-labeled neurons were identified under epifluorescence: CTB-filled neurons lying ventral to nucleus ambiguus and lateral to the inferior olive were identified as RVLM putative sympathetic premotor neurons. Whole-cell recordings were made in voltage- or current-clamp modes using borosilicate pipettes with 1.5- to 2-μm tip diameters (3–6 MΩ). After formation of a gigaseal, recordings were obtained using a Multiclamp 700B patch clamp amplifier (Molecular Devices LLC, Sunnyvale, CA). Baseline recordings were made for 300 s before 2DG administration. Series resistance compensation of 70–80% was used in voltage-clamp recordings. Recorded parameters were digitized using Spike2 with a Power 1401 mark II (Cambridge Electronic Design LTD). Data from three neurons recorded with the addition of 1 μmol/L tetrodotoxin (Jomar Bioscience) to the aCSF were included in the data set. At the conclusion of recordings, the pipette was withdrawn, and slices were fixed overnight in 4% paraformaldehyde and frozen in cryoprotectant before immunohistochemical processing for biocytin and tyrosine hydroxylase immunoreactivity.

Immunohistochemistry

Sections containing biocytin-labeled neurons were removed from the cryoprotectant, washed, and permeabilized in PBS with 0.5% Triton X-100 for 12 h at 4°C. The sections were incubated in blocking solution (5% BSA in PBS) for 4 h at room temperature, followed by incubation in mouse anti-tyrosine hydroxylase primary antibodies (1:2,000; Sigma-Aldrich) for 4 h at room temperature in 5% BSA. Sections were washed and incubated in secondary antibodies (Cy5 donkey anti-mouse and ExtrAvidin FITC, both 1:500; Jackson ImmunoResearch) with 5% BSA for 4 h at room temperature, and then washed, mounted, and coverslipped. Sections were visualized and photographed using a Zeiss Z1 microscope (Carl Zeiss, Thornwood, NY), under epifluorescence with appropriate filter sets.

Data Analysis

The effects of 2DG were assessed by comparing the holding current and the synaptic current frequency, averaged over 50 s before drug administration (baseline), to the mean over the last 50 s of drug perfusion (drug).

The dose of 2DG (5 mmol/L) was selected based on previous reports (4,13).

Statistics

The D'Agostino and Pearson omnibus test was performed to verify normal distribution of the data. Changes in ASNA are presented as mean ± SEM, determined from a 60-s window average, compared along time. Student *t* test, one-way ANOVA, and two-way ANOVA with the Bonferroni corrections were used for group comparisons. Correlations were determined by the Pearson or Spearman tests for parametric and nonparametric samples, respectively, with linear regression to determine CIs. Data that fit a normal distribution are presented as mean ± SEM, and nonparametric data are expressed as median (range). Statistical significance was determined when P was <0.05. All tests were performed using GraphPad Prism 5.0 software.

Experimental Protocols

1. ASNA was plotted against levels of circulating metanephrines to establish the relationship between nerve discharge and adrenaline release. Two samples were taken per experiment: during the resting condition when ASNA recordings had been stable for 10 min and ~6–10 min after intravenous injection of 2DG.
2. ASNA responses to intravenous 2DG were tested after microinjection of muscimol or bicuculline into the PeH to determine the role of GABAergic drive to perifornical neurons in adrenal sympathetic responses to glucoprivation. 2DG was also microinjected after bicuculline to determine its pharmacological effect in the absence of inhibitory tone to perifornical neurons. Lumbar sympathetic nerve activity (LSNA) and ASNA were recorded to determine whether sympathetic responses to glucoprivation are differentially regulated.
3. The effects of focal PeH neuroglucoprivation on ASNA were determined by bilateral microinjections of 2DG or 5TG, according to previous reports (2,20).
4. ASNA was compared before and after bilateral microinjections of 2DG into the RVLM to determine whether adrenal RVLM sympathetic premotor neurons were responsive to glucoprivation in vivo. Subsequent intravenous injection of 2DG confirmed that the ASNA responses were not dependent on a direct effect on RVLM neurons.
5. The intrinsic sensitivity of RVLM sympathetic premotor neurons to glucoprivation was also tested in vitro. After the establishment of stable recordings in aCSF containing 2 mmol/L glucose, slices were perfused for 300 s in aCSF containing 5 mmol/L 2DG (4,13). The effect of glucoprivation on membrane potential and spontaneous discharge frequency was assessed by comparing measurements made over the final 50 s of the control period to the final 50 s of 2DG application. Membrane resistance was monitored by measuring changes in membrane potential evoked by hyperpolarizing currents (−40 pA, 1 s) every 30 s and calculated using Ohm's Law (4). The average membrane resistance measured over the final three steps of the control period was compared with data measured at the corresponding periods of 2DG administration. Neuronal excitability was assessed by comparing the number of action potentials generated by depolarizing current pulses (20 pA, 3 s) every 60 s (13). As described above, data were averaged from the final three consecutive depolarizing steps in the control and 2DG periods. Voltage clamp ramps from 0 to −140 mV from a holding potential of −60 mV were performed to assess current-voltage relationships (4).
6. These experiments determined whether orexinergic activation of premotor neurons in the RVLM mediates the adrenal sympathoexcitation to glucoprivation. Orexin receptors were activated using microinjections of orexin A at different doses before and after microinjection of the antagonist TCS 1102. Adrenal sympathoexcitation in response to microinjection of 2DG into the PeH was also tested after microinjections of TCS 1102 or vehicle into the RVLM.

RESULTS

Correlation of ASNA and Plasma Metanephrines

At rest, the levels of blood glucose were 6.0 ± 0.1 mmol/L (n = 8); systemic glucoprivation (2DG, 250 mg/kg) increased the concentration of plasma metanephrine (3.4 ± 0.7 vs. 18.4 ± 4.4 pmol/L, n = 8; P = 0.008), a methylated metabolite of adrenaline, in direct proportion to the increase in ASNA (n = 15; r_s = 0.79, $P < 0.001$; Fig. 1). In contrast, 2DG failed to change the levels of normetanephrine (49.1 ± 9.9 vs. 44.3 ± 5.6 pmol/L, n = 8; P = 0.583), a methylated metabolite of noradrenaline. Hence, changes in the levels of normetanephrine were not correlated with ASNA (n = 15; r_s = −0.05, P = 0.849).

Role of Perifornical Neurons in Driving Sympathetic Responses to Glucoprivation

ASNA responses to systemic 2DG (250 mg/kg) in intact rats were compared with those measured after inhibition of perifornical neurons with microinjections of muscimol (4 mmol/L). Before 2DG administration, blood glucose was at 6.0 ± 0.2 mmol/L (n = 14). Systemic glucoprivation increased ASNA (165 ± 12%, n = 17; $P < 0.001$), which peaked at ~6 min (Fig. 2*A* and *B*). Bilateral microinjections of muscimol into the PeH abolished the ASNA increase to systemic 2DG (88 ± 9%, n = 6; $P < 0.001$; Fig. 2*C* and *D*). By contrast, after establishment of a stable glucose baseline (6.0 ± 0.2 mmol/L), unilateral microinjection of bicuculline (1 mmol/L) into the PeH increased ASNA (199 ± 14%, n = 8; $P < 0.001$), whereas subsequent microinjection of 2DG reduced ASNA (143 ± 12%, n = 8; $P < 0.001$; Fig. 2*E* and *F*). Systemic

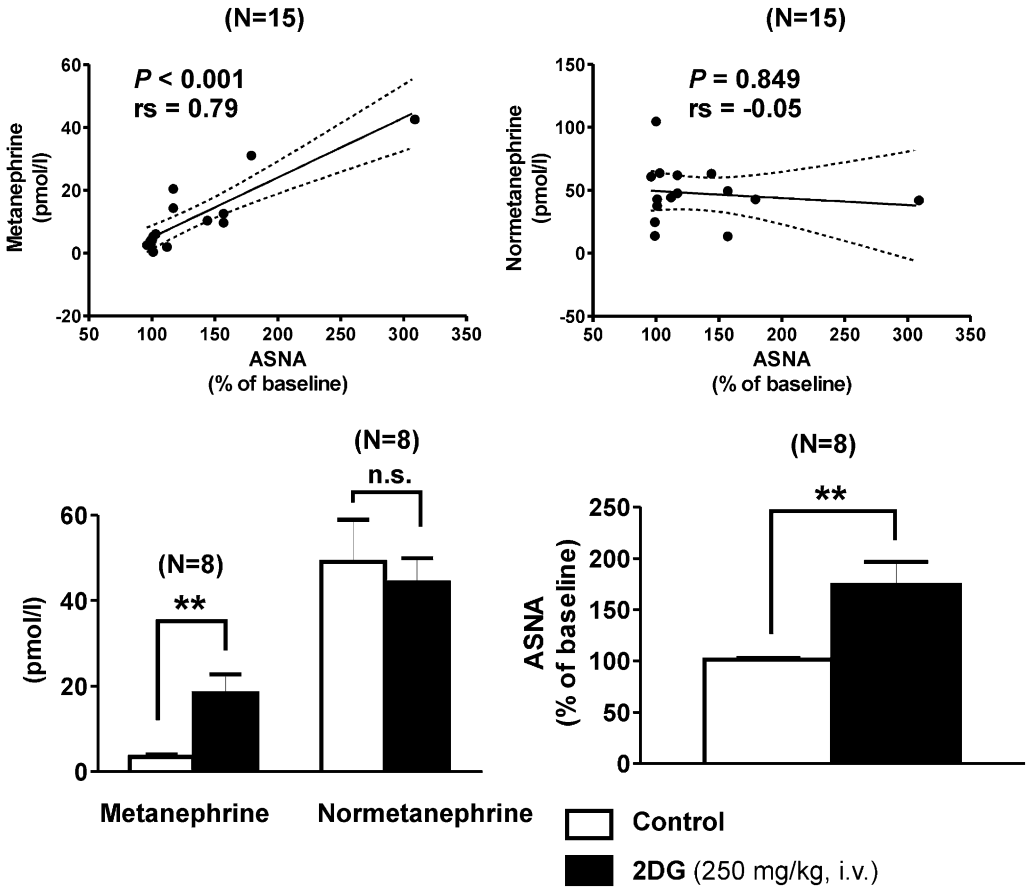

Figure 1—Glucoprivation elicits increases in ASNA correlated with the levels of metanephrines. Systemic injection of 2DG increased ASNA. The increase in ASNA correlated with plasma levels of metanephrine, a methylated metabolite of adrenaline. However, 2DG failed to alter the levels of normetanephrine, the corresponding methylated metabolite of noradrenaline. All data are presented as mean ± SEM. $^{**}P <$ 0.01; n.s., nonsignificant.

glucoprivation (2DG; 250 mg/kg) selectively increased ASNA (162 ± 9%, n = 6; $P < 0.001$) but did not affect LSNA (101 ± 6%, n = 6; $P = 0.22$). By contrast, elevation of blood pressure (phenylephrine, 10 μg/ kg) or blockade of sympathetic ganglionic transmission (hexamethonium, 40 mg/kg) reduced only LSNA (Fig. 2*G* and *H*).

Effects of Neuroglucoprivation in the PeH

Perifornical focal microinjection of 2DG or 5TG evoked adrenal sympathoexcitation (Fig. 3). Resting levels of blood glucose before 2DG and 5TG administration were 6.6 ± 0.3 mmol/L (n = 10) and 6.7 ± 0.1 mmol/L (n = 6), respectively. Bilateral microinjections of 2DG into the PeH (20) dose-dependently augmented ASNA (175 ± 10%, n = 10; $P < 0.001$). Bilateral 5TG also increased ASNA (145 ± 11%, n = 6; $P < 0.01$). The increases in ASNA in response to 2DG or 5TG were similar in magnitude (n = 6; $P > 0.05$) and correlated with the increases in arterial blood glucose (Fig. 3*D* and *F*).

Glucoprivation of RVLM Sympathetic Premotor Neurons In Vivo

At a blood glucose baseline of 6.4 ± 0.2 mmol/L (n = 6), bilateral microinjections of 2DG (2 mmol/L) into the RVLM evoked no effect on ASNA (90 ± 12%, n = 6; $P = 0.33$; Fig. 4). Subsequent systemic injection of 2DG (250 mg/kg i.v.) increased ASNA (162 ± 18%, n = 6; $P < 0.001$).

Glucoprivation of RVLM Sympathetic Premotor Neurons In Vitro

Sixteen sympathetic premotor neurons were recorded in 11 brainstem slices from five rats (Fig. 5). In all but three cases current- and voltage-clamp data were obtained from the same neurons. In no case did 2DG evoke any clear effect on any parameter recorded. In current clamp, the resting membrane potential was −52.7 ± 1.6 mV (n = 15 including three neurons recorded with tetrodotoxin), with spontaneous action potentials occurring at 3.7 ± 0.8 Hz (n = 12). At the end of the 2DG superfusion the membrane potential (−53.3 ± 1.6 mV, n = 15; $P = 0.55$), spontaneous discharge frequency (3.6 ± 0.8 Hz, n = 12; $P = 0.46$), and input resistance (335 ± 38 vs. 327 ± 41MΩ, n = 14; $P = 0.35$) were unchanged from baseline values. There was no significant change in the number of action potentials evoked by depolarizing current pulses by the addition of 2DG to the perfusate (11.8 ± 1.7 vs.

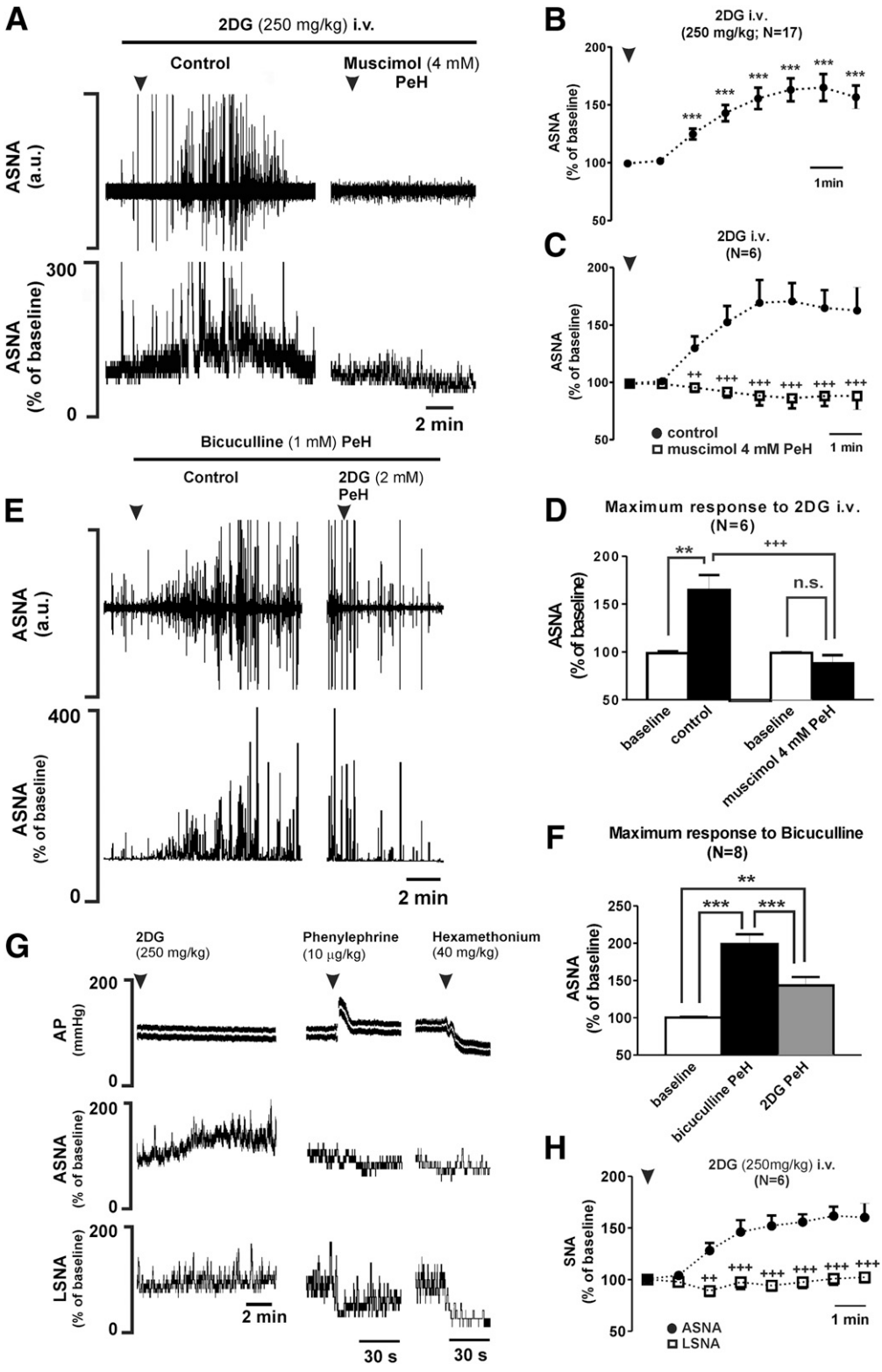

Figure 2—Selective effects of glucoprivation on ASNA depends on perifornical neurons. *A*: Neurograms of ASNA in arbitrary units (a.u.) (*top*) rectified, integrated, and normalized to the percentage of baseline (*bottom*). Systemic glucoprivation with 2DG increased ASNA, which was abolished by bilateral microinjections of muscimol into the PeH. *B*: Pooled increases in ASNA after 2DG. *C*: Group data of the response to 2DG after inhibition of the PeH. *D*: Muscimol in the PeH reduced the maximum increase in ASNA to systemic 2DG in the group. *E*: Microinjection of bicuculline into the PeH increased ASNA, and subsequent microinjection of 2DG reduced the evoked increase in ASNA. *F*: Group data of maximum ASNA increases to microinjection of bicuculline and 2DG into the PeH. *G*: Systemic 2DG increased only ASNA but did not affect LSNA. *H*: The differential sympathetic response to 2DG replicated within the group. All data are presented as mean ± SEM. $^{*}P < 0.05$, $^{**}P < 0.01$, $^{***}P < 0.001$ to baseline; $^{++}P < 0.01$, $^{+++}P < 0.001$ to control group. AP, arterial blood pressure; n.s., nonsignificant.

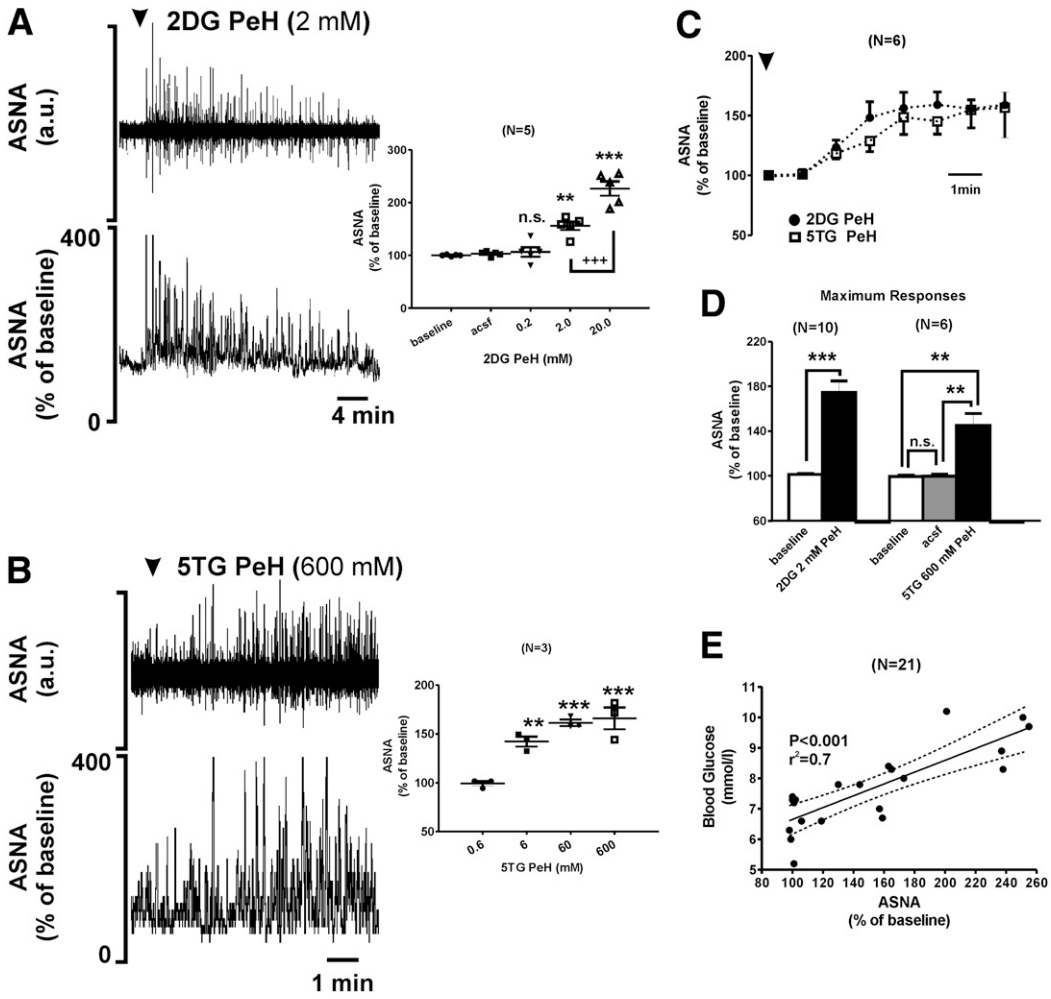

Figure 3—Glucoprivation in the PeH increases ASNA. *A*: Neurograms of raw and rectified, smoothed, and normalized ASNA (a.u., arbitrary units). Bilateral microinjections of 2DG into the PeH elicited dose-dependent increases in ASNA. *B*: Bilateral microinjections of 5TG into the PeH also augmented ASNA. *C*: Group data of sympathetic responses to microinjections of 2DG and 5TG. *D*: Pooled data of maximum increases in ASNA to 2DG or 5TG into the PeH. *E*: Increases in ASNA in response to microinjections of 2DG and 5TG into the PeH were directly correlated with levels of blood glucose. All data are presented as mean ± SEM. $^{**}P < 0.01$, $^{***}P < 0.001$ to baseline; $+++P < 0.001$ to 2DG (2 mmol/L); n.s. nonsignificant.

10.9 ± 1.6 spikes, $n = 12$; $P = 0.48$; Fig. 5*D*). In the voltage-clamp mode, no changes in holding current (−54.4 ± 7.5 vs. −55.9 ± 7.4 pA, $n = 13$; $P = 0.54$) or response to voltage ramps were noted after the addition of 2DG to the perfusion fluid.

Blockade of Orexin Receptors in the RVLM During Neuroglucoprivation of the PeH

Microinjection of orexin A into the RVLM produced an increase in ASNA (162 ± 16%, $n = 6$; $P < 0.001$) that was blocked by the nonselective antagonist TCS 1102 (99 ± 3%, $n = 6$; $P < 0.001$; Fig. 6*A–D*). Bilateral microinjections of 2DG (2 mmol/L) into the PeH increased ASNA (151 ± 16%, $n = 6$; $P < 0.01$) after microinjections of vehicle into the RVLM. By contrast, TCS 1102 in the RVLM abolished the increase in ASNA (95 ± 5%, $n = 6$; $P < 0.001$) produced by microinjection of 2DG into the PeH (Fig. 6*E–G*).

DISCUSSION

The principal finding in this study is that orexin modulates the activity of RVLM adrenal sympathetic premotor neurons, resulting in excitation of adrenal chromaffin cells. We showed that local glucoprivation or disinhibition of PeH neurons increased ASNA, whereas inhibition of PeH neurons abolished the ASNA response after systemic glucoprivation. Conversely, glucoprivation of perifornical neurons subsequent to activation by the $GABA_A$ antagonist bicuculline reduced the adrenal sympathoexcitatory response. In addition, local neuroglucoprivation in the RVLM failed to activate premotor neurons in vivo or in vitro, suggesting that RVLM neurons are not intrinsically glucose-sensitive. Finally, ASNA was directly correlated with plasma metanephrine levels but not normetanephrine levels, confirming that adrenal sympathoexcitation coincides with adrenaline release into the circulation. The

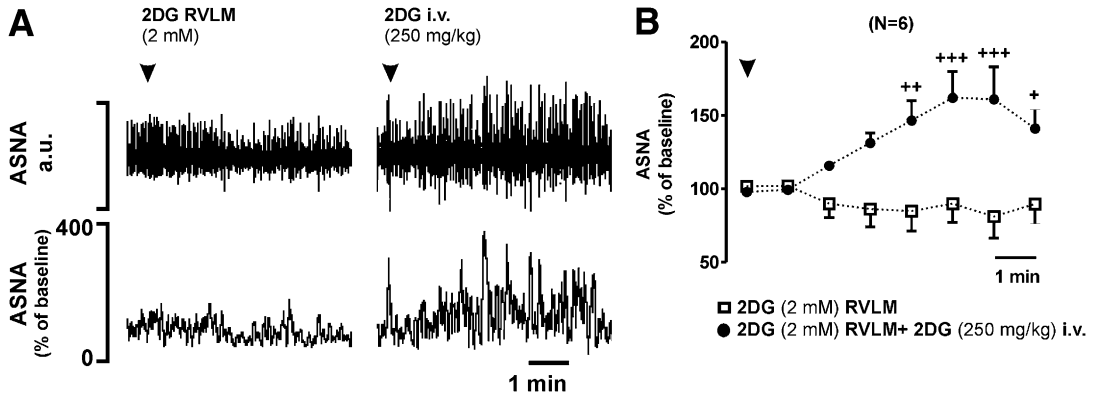

Figure 4—RVLM neurons are not glucose-sensitive in vivo. *A*: Neurograms of raw and rectified, smoothed, and normalized (% of baseline) ASNA (a.u., arbitrary units). Bilateral microinjections of 2DG into the RVLM, where premotor neurons are found, did not alter ASNA. However, a subsequent intravenous injection of 2DG in the same animal increased ASNA. *B*: Group data of ASNA responses to microinjections of 2DG into the RVLM, followed by systemic 2DG. All data are presented as mean ± SEM. +P < 0.05, ++P < 0.01, +++P < 0.001 to 2DG into the RVLM.

ASNA, noradrenaline, and adrenaline responses to glucoprivation noted in our study were consistent with previous reports of the effects of glucoprivation on sympathetic preganglionic neurons (24).

In this study, microinjection of 2DG/5TG or bicuculline into the PeH increased ASNA, whereas microinjection of the $GABA_A$ agonist muscimol into the PeH abolished the ASNA response to systemic injection of 2DG. Reports by

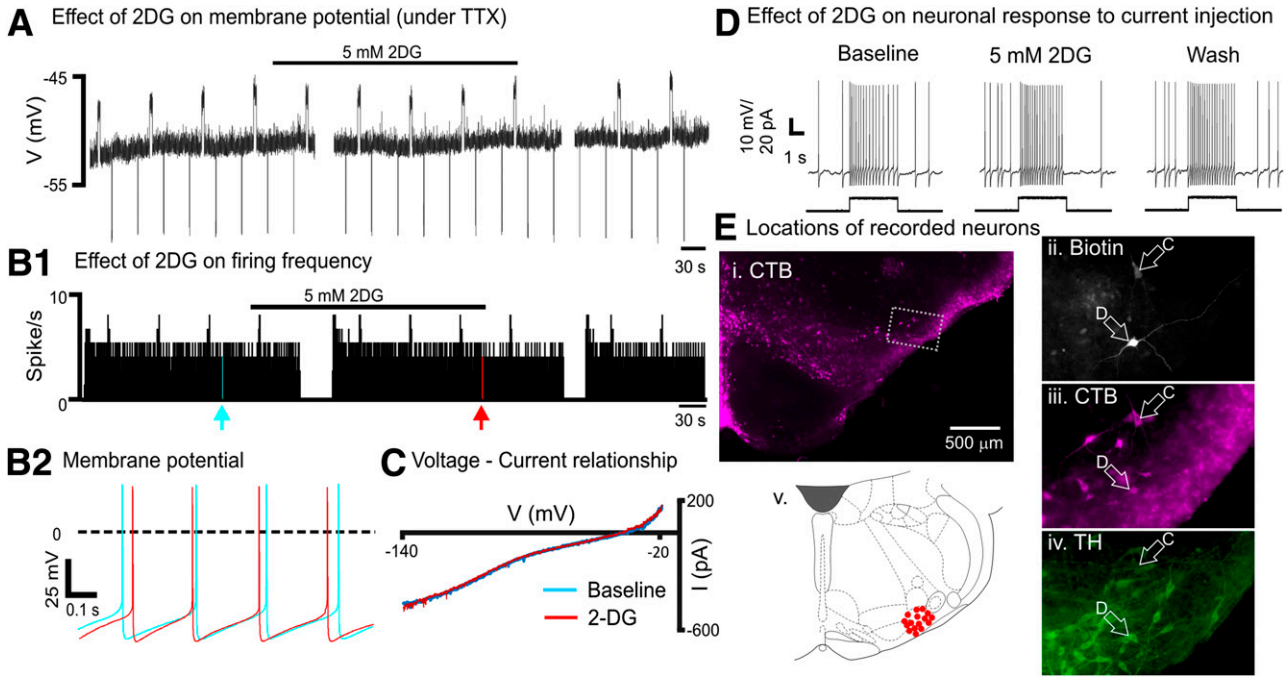

Figure 5—2DG exerts no direct effect on medullospinal RVLM neurons recorded in vitro. *A*: Whole-cell current-clamp recording performed in the presence of tetrodotoxin (TTX): bath application of 2DG exerts no effect on resting membrane potential or resistance. Deflections indicate responses to current injection. *B1*: Current clamp recording shows effect of 2DG on spontaneous discharge of medullospinal RVLM neuron. Regular increases in firing frequency indicate responses to depolarizing current injections. Breaks in recordings in panels *A* and *B1* indicate recording mode switch. *B2*: Raw data excerpts at points denoted (arrows) in panel *B1*. *C*: 2DG exerted no effect on current-voltage relationships recorded in voltage-clamp mode. *D*: 2DG exerted no effect on responsiveness to depolarizing currents (see also panel *B1*). *E*: In some cases, neurons were filled with biocytin during recording and subsequently examined histologically. *Ei*: Low-power photomicrograph shows distribution of CTB labeling. Field of view of high-powered images denoted by box. *Eii*: Two neurons were recorded and recovered in the experiment shown (indicated by arrows); raw data from each are shown in panels *C* and *D*. Both were CTB-labeled (*Eiii*), and under close examination, *C* was lightly tyrosine hydroxylase (TH)-positive whereas *D* was TH-negative (*Eiv*). *Ev*: Schematic diagram shows locations of recorded neurons.

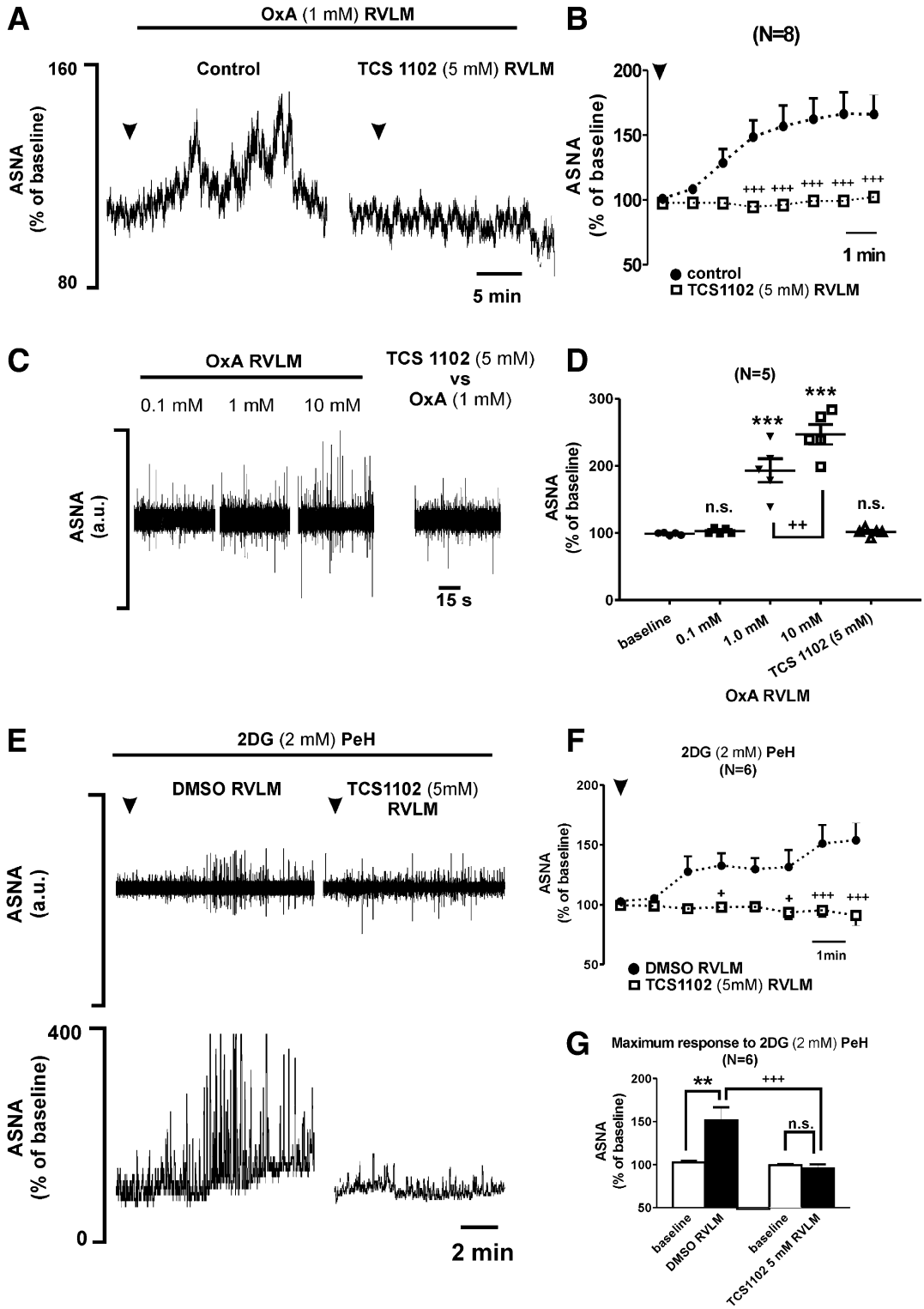

Figure 6—Orexin in the RVLM mediates the ASNA increase to glucoprivation. *A*: Neurograms of rectified, smoothed, and normalized (% of baseline) ASNA (a.u., arbitrary units). Microinjection of orexin A (OxA) into the RVLM produced sympathoexcitation, which was blocked by the nonselective antagonist TCS 1102. *B*: The blockade of the response replicated in a group of animals. *C*: Neurograms of raw ASNA. OxA into the RVLM evoked a dose-dependent increase in ASNA that was antagonized by TCS 1102. *D*: The dose-response effect replicated in a group of animals. *E*: Neurograms of raw (*top*) and rectified, smoothed, and normalized (*bottom*) ASNA. Bilateral microinjections of 2DG into the PeH after vehicle (50% DMSO) microinjection into the RVLM increased ASNA. However, bilateral injections of the antagonist TCS 1102 into the RVLM abolished the rise elicited by 2DG in the PeH. *F*: Blockade of the ASNA response replicated in a group of animals. *G*: Grouped data of maximum increases in ASNA to 2DG in the PeH, subsequent to DMSO or TCS 1102 in the RVLM. All data are presented as mean ± SEM. $^{**}P < 0.01$, $^{***}P < 0.001$ to baseline; $+P < 0.05$, $+++P < 0.001$ to control group; $++P < 0.01$ to OxA (1 mmol/L); n.s., nonsignificant.

others have shown that 2DG exerts a glucomimetic inhibition of orexinergic and GABAergic perifornical neurons (4,13,25). Thus, direct excitation of perifornical neurons by 2DG in our study is unlikely to be the mechanism underlying the increase in ASNA. Alternatively, adrenal sympathoexcitation could result from disinhibition of perifornical neurons that receive GABAergic drive (11). Orexinergic neurons express GABA receptors (26) and may receive inhibitory inputs from adjacent interneurons (25) or from the ventromedial hypothalamus (27,28). In our study, microinjection of 2DG into the PeH decreased the ASNA response evoked by prior administration of bicuculline into the same site, confirming the glucomimetic inhibitory effect of 2DG seen in vitro (4,13,25). One interpretation of this result is that 2DG acts at some location adjacent to the PeH. If so, this could explain the onset (~1 min) of the ASNA response to microinjection of 2DG into the PeH. Consistent with this notion are previous observations that injection of 2DG into the ventromedial hypothalamus (1) or into the ventrolateral portion of the lateral hypothalamus (29) elicits glucoprivic effects resulting in adrenaline release and adrenal sympathoexcitation, respectively. Although we have demonstrated that 2DG can exert inhibitory effects on PeH neurons, consistent with previous observations in vitro (4,13,25), the inevitable conclusion is that an excitatory response predominates in our in vivo study.

Blockade of orexin receptors in the RVLM by microinjection of TCS 1102 eliminated the adrenal sympathoexcitatory response to injections of 2DG into the PeH. The dose of the orexin antagonist used was sufficient to block the effects of the orexin microinjection into the RVLM on ASNA. On the basis of the density of the extracellular milieu (30) and histology, our injections extended for ~400 μm and so targeted most of the C1 neurons (6). The ASNA response to microinjection of orexin into the RVLM concurs with previous observations (21). Glucoprivation activates slow-conducting (<1 m/s) RVLM adrenal premotor neurons, which are intermingled with the cardiovascular premotor neurons (5). The slow-conducting axons suggest that they are C1 catecholaminergic cells (31). Glucoprivation also elicits Fos expression (6) and phosphorylation (32) in C1 neurons. Orexinergic neurons project to the C1 region of the RVLM (14,15), and their terminals make close appositions with C1 neurons (33). Moreover, neurotoxic ablation of C1 neurons eliminates the glucoregulatory response to 2DG (34). Together, the evidence suggests that orexinergic activation of adrenal sympathetic premotor neurons modulates the adrenal sympathoexcitatory response to glucoprivation. Although previous studies (35,36) have shown that selective glucoprivation of hindbrain neurons increases blood glucose, local application of 2DG failed to activate the RVLM adrenal premotor neurons. Thus, hindbrain glucose-sensitive neurons (6,37) are presumably located outside the RVLM but project to (38) and excite the adrenal C1 neurons.

The current study has explored the neural pathway(s) that relay the adrenal sympathoexcitatory response to neuroglucoprivation. We used 2DG as a glucoprivic agent because it allows the investigator to produce localized glucoprivation when injected into the brain parenchyma. Importantly, systemic 2DG produces secretion of adrenaline, glucagon, cortisol, and growth hormone (39,40). Because 2DG is also detected by most glucometers, we were unable to determine blood glucose changes after systemic 2DG. Nonetheless, glucoprivation elicits hyperglycemia via activation of glycogenolysis and gluconeogenesis in the liver (3,11,41). General anesthesia was essential for measurement of ASNA and eliminated the influence of stress, respiration, or body temperature (42–44). Anesthesia can alter neural metabolism and modulate glycemia, and intraperitoneal urethane is known to cause hyperglycemia (45). However, under the conditions of our experiment, we found that urethane produced normoglycemic animals (~6.1 mmol/L). Comparison of different methods for determining catecholamine levels indicated that plasma metanephrines determined by mass spectrometry is the most reliable method (16). Finally, the age of rat pups used the in vitro experiments correspond to previous electrophysiological studies (46), and the catecholaminergic neurons are likely to be mature and functional (47).

In conclusion, our findings suggest a key role for orexin in modulating the sympathetic drive to the adrenal chromaffin cells during glucoprivation. It is possible that during arousal, orexin changes the electrophysiological properties of adrenal premotor neurons facilitating adrenaline release in response to glucopenia, a mechanism that may be compromised when hypoglycemia unawareness develops in response to recurrent glucoprivation (3).

Acknowledgments. The authors thank Denise Massie, Clinical Pharmacology, Austin Health, for the analyses of metanephrines, and Andrew Ellis and Philip Zeglinski, Clinical Pharmacology, Austin Health, for important advice regarding measurements of catecholamines.

Funding. The authors' laboratories are supported by the National Health and Medical Research Council of Australia (1025031 and 604002), Australian Research Council (DP120100920), Austin Medical Research Foundation, the Rebecca L. Cooper Medical Research Foundation, and the Sir Edward Dunlop Medical Research Foundation.

Duality of Interest. No potential conflicts of interest relevant to this article were reported.

Author Contributions. W.S.K. conceived and designed the experiments, collected, analyzed, and interpreted the data, and drafted the manuscript. L.B.F. collected and analyzed the data from in vitro experiments. S.M. conceived and designed the in vitro experiments, interpreted the data, and critically reviewed the manuscript. A.J.M.V. conceived and designed the in vivo experiments, interpreted the data, and critically reviewed the manuscript. All authors approved the final version of the manuscript. W.S.K. is the guarantor of this work and, as such, had full access to all data in the study and takes responsibility for the integrity of the data and the accuracy of the data analysis.

Prior Presentation. This work was presented at the 34th Annual Meeting of the Australasian Neuroscience Society, Adelaide, South Australia, Australia, 28–31 January 2014, and at the Experimental Biology 2013 meeting, Boston, MA, 20–24 April 2013.

References

1. Borg WP, Sherwin RS, During MJ, Borg MA, Shulman GI. Local ventromedial hypothalamus glucopenia triggers counterregulatory hormone release. Diabetes 1995;44:180–184
2. Andrew SF, Dinh TT, Ritter S. Localized glucoprivation of hindbrain sites elicits corticosterone and glucagon secretion. Am J Physiol Regul Integr Comp Physiol 2007;292:R1792–R1798
3. Sanders NM, Ritter S. Acute 2DG-induced glucoprivation or dexamethasone abolishes 2DG-induced glucoregulatory responses to subsequent glucoprivation. Diabetes 2001;50:2831–2836
4. González JA, Jensen LT, Fugger L, Burdakov D. Metabolism-independent sugar sensing in central orexin neurons. Diabetes 2008;57:2569–2576
5. Verberne AJ, Sartor DM. Rostroventrolateral medullary neurons modulate glucose homeostasis in the rat. Am J Physiol Endocrinol Metab 2010;299:E802–E807
6. Ritter S, Llewellyn-Smith I, Dinh TT. Subgroups of hindbrain catecholamine neurons are selectively activated by 2-deoxy-D-glucose induced metabolic challenge. Brain Res 1998;805:41–54
7. Sakurai T, Amemiya A, Ishii M, et al. Orexins and orexin receptors: a family of hypothalamic neuropeptides and G protein-coupled receptors that regulate feeding behavior. Cell 1998;92:573–585
8. Briski KP, Sylvester PW. Hypothalamic orexin-A-immunpositive neurons express Fos in response to central glucopenia. Neuroreport 2001;12:531–534
9. Strack AM, Sawyer WB, Platt KB, Loewy AD. CNS cell groups regulating the sympathetic outflow to adrenal gland as revealed by transneuronal cell body labeling with pseudorabies virus. Brain Res 1989;491:274–296
10. Jansen ASP, Nguyen XV, Karpitskiy V, Mettenleiter TC, Loewy AD. Central command neurons of the sympathetic nervous system: basis of the fight-or-flight response. Science 1995;270:644–646
11. Yi CX, Serlie MJ, Ackermans MT, et al. A major role for perifornical orexin neurons in the control of glucose metabolism in rats. Diabetes 2009;58:1998–2005
12. Oomura Y, Ooyama H, Sugimori M, Nakamura T, Yamada Y. Glucose inhibition of the glucose-sensitive neurone in the rat lateral hypothalamus. Nature 1974;247:284–286
13. Burdakov D, Gerasimenko O, Verkhratsky A. Physiological changes in glucose differentially modulate the excitability of hypothalamic melanin-concentrating hormone and orexin neurons in situ. J Neurosci 2005;25:2429–2433
14. de Lecea L, Kilduff TS, Peyron C, et al. The hypocretins: hypothalamus-specific peptides with neuroexcitatory activity. Proc Natl Acad Sci U S A 1998;95:322–327
15. Peyron C, Tighe DK, van den Pol AN, et al. Neurons containing hypocretin (orexin) project to multiple neuronal systems. J Neurosci 1998;18:9996–10015
16. Lenders JW, Pacak K, Walther MM, et al. Biochemical diagnosis of pheochromocytoma: which test is best? JAMA 2002;287:1427–1434
17. Whiting MJ. Simultaneous measurement of urinary metanephrines and catecholamines by liquid chromatography with tandem mass spectrometric detection. Ann Clin Biochem 2009;46:129–136
18. Paxinos G, Watson C. The Rat Brain in Stereotaxic Coordinates. 4th ed. San Diego, Academic Press, Inc, 1998
19. Brown DL, Guyenet PG. Electrophysiological study of cardiovascular neurons in the rostral ventrolateral medulla in rats. Circ Res 1985;56:359–369
20. Shiraishi T, Simpson A. Central control of gastric acid secretion by extralateralhypothalamic nuclei. Brain Res Bull 1987;18:309–314
21. Shahid IZ, Rahman AA, Pilowsky PM. Orexin A in rat rostral ventrolateral medulla is pressor, sympatho-excitatory, increases barosensitivity and attenuates the somato-sympathetic reflex. Br J Pharmacol 2012;165:2292–2303
22. Hsiao YT, Jou SB, Yi PL, Chang FC. Activation of GABAergic pathway by hypocretin in the median raphe nucleus (MRN) mediates stress-induced theta rhythm in rats. Behav Brain Res 2012;233:224–231
23. Burdakov D, Ashcroft FM. Cholecystokinin tunes firing of an electrically distinct subset of arcuate nucleus neurons by activating A-Type potassium channels. J Neurosci 2002;22:6380–6387
24. Morrison SF, Cao WH. Different adrenal sympathetic preganglionic neurons regulate epinephrine and norepinephrine secretion. Am J Physiol Regul Integr Comp Physiol 2000;279:R1763–R1775
25. Karnani MM, Szabó G, Erdélyi F, Burdakov D. Lateral hypothalamic GAD65 neurons are spontaneously firing and distinct from orexin- and melanin-concentrating hormone neurons. J Physiol 2013;591:933–953
26. Alam MN, Kumar S, Bashir T, et al. GABA-mediated control of hypocretin- but not melanin-concentrating hormone-immunoreactive neurones during sleep in rats. J Physiol 2005;563:569–582
27. Chan O, Paranjape S, Czyzyk D, et al. Increased GABAergic output in the ventromedial hypothalamus contributes to impaired hypoglycemic counter-regulation in diabetic rats. Diabetes 2011;60:1582–1589
28. Chan O, Zhu W, Ding Y, McCrimmon RJ, Sherwin RS. Blockade of GABA(A) receptors in the ventromedial hypothalamus further stimulates glucagon and sympathoadrenal but not the hypothalamo-pituitary-adrenal response to hypoglycemia. Diabetes 2006;55:1080–1087
29. Yoshimatsu H, Egawa M, Bray GA. Adrenal sympathetic nerve activity in response to hypothalamic injections of 2-deoxy-D-glucose. Am J Physiol 1991;261:R875–R881
30. Nicholson C. Diffusion from an injected volume of a substance in brain tissue with arbitrary volume fraction and tortuosity. Brain Res 1985;333:325–329
31. Schreihofer AM, Guyenet PG. Identification of C1 presympathetic neurons in rat rostral ventrolateral medulla by juxtacellular labeling in vivo. J Comp Neurol 1997;387:524–536
32. Damanhuri HA, Burke PG, Ong LK, et al. Tyrosine hydroxylase phosphorylation in catecholaminergic brain regions: a marker of activation following acute hypotension and glucoprivation. PLoS ONE 2012;7:e50535
33. Puskás N, Papp RS, Gallatz K, Palkovits M. Interactions between orexin-immunoreactive fibers and adrenaline or noradrenaline-expressing neurons of the lower brainstem in rats and mice. Peptides 2010;31:1589–1597
34. Ritter S, Bugarith K, Dinh TT. Immunotoxic destruction of distinct catecholamine subgroups produces selective impairment of glucoregulatory responses and neuronal activation. J Comp Neurol 2001;432:197–216
35. DiRocco RJ, Grill HJ. The forebrain is not essential for sympathoadrenal hyperglycemic response to glucoprivation. Science 1979;204:1112–1114
36. Ritter RC, Slusser PG, Stone S. Glucoreceptors controlling feeding and blood glucose: location in the hindbrain. Science 1981;213:451–452
37. Dunn-Meynell AA, Routh VH, Kang L, Gaspers L, Levin BE. Glucokinase is the likely mediator of glucosensing in both glucose-excited and glucose-inhibited central neurons. Diabetes 2002;51:2056–2065
38. Aicher SA, Saravay RH, Cravo S, et al. Monosynaptic projections from the nucleus tractus solitarii to C1 adrenergic neurons in the rostral ventrolateral medulla: comparison with input from the caudal ventrolateral medulla. J Comp Neurol 1996;373:62–75
39. Goldsmith SJ, Yalow RS, Berson SA. Effects of 2-deoxy-D-glucose on insulin-secretory responses to intravenous glucose, glucagon, tolbutamide and arginine in man. Diabetes 1970;19:453–457
40. Ritter S, Scheurink A, Singer LK. 2-Deoxy-D-glucose but not 2-mercaptoacetate increases Fos-like immunoreactivity in adrenal medulla and sympathetic preganglionic neurons. Obes Res 1995;3(Suppl. 5):729S–734S
41. Watt MJ, Howlett KF, Febbraio MA, Spriet LL, Hargreaves M. Adrenaline increases skeletal muscle glycogenolysis, pyruvate dehydrogenase activation and carbohydrate oxidation during moderate exercise in humans. J Physiol 2001;534:269–278
42. Shah JH, Wongsurawat N, Aran PP, Motto GS, Bowser EN. A method for studying acute insulin secretion and glucose tolerance in unanesthetized and unrestrained rats. The effect of mild stress on carbohydrate metabolism. Diabetes 1977;26:1–6
43. Ehrentheil OF, Reyna LJ, Adams CJ, Giovanniello TJ, Chen ET. Studies in stress glycosuria. II. Glycosuria and blood sugar elevation in alloxanized subdiabetic white rats subjected to electric shock stress. Diabetes 1967;16:319–324

44. Guenther MA, Bruder ED, Raff H. Effects of body temperature maintenance on glucose, insulin, and corticosterone responses to acute hypoxia in the neonatal rat. Am J Physiol Regul Integr Comp Physiol 2012;302:R627–R633
45. Reinert H. Urethane Hyperglycaemia and Hypothalamic Activation. Nature 1964;204:889–891
46. Cotero VE, Routh VH. Insulin blunts the response of glucose-excited neurons in the ventrolateral-ventromedial hypothalamic nucleus to decreased glucose. Am J Physiol Endocrinol Metab 2009;296:E1101–E1109
47. Roux JC, Mamet J, Perrin D, et al. Neurochemical development of the brainstem catecholaminergic cell groups in rat. J Neural Transm 2003;110:51–65

Research Article

The Journal of Comparative Neurology
Research in Systems Neuroscience
DOI 10.1002/cne.23846

Somatostatin in the rat rostral ventrolateral medulla: origins and mechanism of action

L Bou-Farah*, BR Bowman*, P Bokiniec, S Karim, S Le, AK Goodchild#, S McMullan#

* Joint first author, # joint last author

Affiliation: The Australian School of Advanced Medicine, 2 Technology Place, Macquarie University, 2109, NSW Australia

Running title: Somatostatinergic projections to the RVLM

Corresponding Author: Simon McMullan

The Australian School of Advanced Medicine

2 Technology Place, Macquarie University, 2109, NSW Australia

Phone: +61 2 69850 2711

Fax: +61 2 9850 2701

Email: simon.mcmullan@mq.edu.au

Acknowledgements: This work was supported by the National Health and Medical Research Council of Australia (NHMRC 457068, APP1028183, APP1030301), the National Heart Foundation of Australia (NHF G09S4340), Australian Research Council (DP120100920), Macquarie University and Hillcrest Foundation (Perpetual).

Received: Feb 22, 2015; Revised: Jun 22, 2015; Accepted: Jun 23, 2015

ABSTRACT

Somatostatin (SST) or agonists of the SST-2 receptor (sst_2) in the rostral ventrolateral medulla (RVLM) lower sympathetic nerve activity, arterial pressure and heart rate, or when administered within the Bötzinger region, evoke apneusis. Our aims were to describe the mechanisms responsible for the sympathoinhibitory effects of SST on bulbospinal neurons and to identify likely sources of RVLM SST release. Patch clamp recordings were made from bulbospinal RVLM neurons (n = 31) in brainstem slices prepared from juvenile rat pups. 58% of neurons responded to SST, displaying an increase in conductance that reversed at -93 mV, indicative of an inwardly rectifying potassium channel (GIRK) mechanism. Blockade of sst_2 abolished this effect, but application of tetrodotoxin did not, indicating that the SST effect is independent of presynaptic activity. Fourteen bulbospinal RVLM neurons were recovered for immunohistochemistry; nine were SST insensitive and did not express sst_{2a}. Three out of five responsive neurons were sst_{2a} immunoreactive. Neurons that contained preprosomatostatin mRNA and cholera-toxin-B retrogradely transported from the RVLM were detected in: paratrigeminal nucleus, lateral parabrachial nucleus, Kölliker-Fuse nucleus, ventrolateral periaqueductal grey area, central nucleus of the amygdala, sublenticular extended amygdala, interstitial nucleus of the posterior limb of the anterior commissure nucleus and bed nucleus of the stria terminalis. Thus, those brain regions are putative sources of endogenous SST release that, when activated, may evoke sympathoinhibitory effects via interactions with subsets of sympathetic premotor neurons that express sst2.

INTRODUCTION

The inhibitory peptide somatostatin (SST) is expressed widely throughout the brain; its two isoforms, SST-14 and SST-28, act on six receptors, sst_{1-5}, with sst_2 receptors present in two subtypes, sst_{2a} and sst_{2b} (Bruno et al., 1992; O'Carroll et al., 1992; Vanetti et al., 1992; Vanetti et al., 1994; Yasuda et al., 1992).

The expression of SST and its receptors within the rostral ventrolateral medulla (RVLM), and the functional consequences of SST transmission in this region, has emerged as a topic of considerable interest in both the fields of central respiratory and central cardiovascular control. The medullary distribution of SST partially overlaps with putative markers of respiratory rhythm-generating neurons in the pre-Bötzinger Complex (Gray et al., 2010; Stornetta et al., 2003; Tupal et al., 2014), and pharmacogenetic silencing of SSTergic neurons in and around the pre-Bötzinger Complex causes apnea *in vivo* (Tan et al., 2008), leading to the proposal that SST may be a marker of pre-Bötzinger complex pacemaker neurons (Gray et al., 2010; Stornetta et al., 2003). Furthermore, microinjection of SST into the Bötzinger region, one target of pre-Bötzinger Complex SSTergic neurons (Tan et al., 2010), evokes apneusis, a gasping breathing pattern characterized by a lengthened inspiratory phase and a shortened expiratory period (Burke et al., 2010).

SST also causes dose-dependent sympathoinhibition, hypotension and bradycardia, as well as attenuation of chemo- and somatosympathetic reflexes, when microinjected into the pressor region of the RVLM (Burke et al., 2008). A direct effect of SST agonists on RVLM sympathetic premotor neurons is presumed to underlie this effect, as sst_{2a} receptors are the predominant receptor subtype expressed in the region and are widely expressed on RVLM C1 and non-C1 neurons (Burke et al., 2008; Spary et al., 2008), including those with bulbospinal projections (Burke et al., 2008). Involvement of other receptor subtypes is unlikely, as sst_5 mRNA is absent from the VLM, and isoforms 1, 2b and 4 are expressed at low levels (Ramírez-Jarquín et al., 2012; Spary et al., 2008). Similarly, we and others have reported pronounced VLM expression of sst_{2a} immunoreactivity, weak expression of sst_4, and no consistent neuronal expression of any other subtype (Burke et al., 2008; Spary et al., 2008). Finally, pre-treatment with the sst_2 selective antagonist BIM-23627 abolishes cardiovascular responses evoked by both SST and the sst_2 agonist lanreotide (Burke et al., 2008).

The cellular mechanisms that underlie the inhibitory effects of RVLM SST receptor activation, the sources of RVLM SST release, and the circumstances under which SST is released in the RVLM, are unknown. In general, the cellular responses evoked by SST receptor activation are wide ranging, modulating multiple second messenger systems. These include G-protein modulation of adenylate cyclase, Ca^{2+} and K^{+} channels, phospholipases, MAP kinase and phosphotyrosine protein phosphatases (Patel, 1999). When $sst_{2\text{-}5}$ receptors were co-expressed with a GIRK subunit in oocytes, sst_2 receptors were the most efficient in activating a GIRK mediated current (Kreienkamp et al., 1997). Similarly, whole cell patch clamp recordings of neurons in the periaqueductal grey (Connor et al., 2004) or the substantia gelatinosa of the spinal cord (Nakatsuka et al., 2008) show that SST application evokes a large outward current mediated by K^{+} channels consistent with GIRK characteristics, although calcium currents may also be activated (Connor et al., 2004).

Regions innervating the RVLM are well described and widely distributed (Bowman et al., 2013; Carrive et al., 1988; Dampney et al., 1987; Hopkins and Holstege, 1978; M'Hamed et al., 1993; Padley et al., 2007; Ross et al., 1985), as is the brain-wide distribution of neurons expressing SST-immunoreactivity or preprosomatostatin (PPS) mRNA (De León et al., 1992; Gray and Magnuson, 1992; Smith et al., 1994). However, whether or not RVLM-projecting neurons synthesize SST is largely unknown.

Therefore the aims of this study are, firstly, to determine the cellular mechanisms responsible for the inhibition of RVLM sympathetic premotor neurons by SST, using whole cell patch clamp in acute brainstem slices and, secondly, to define likely sources of SST by identifying RVLM-projecting neurons that contain PPS mRNA using a combination of retrograde tracing and *in situ* hybridization.

MATERIALS AND METHODS

All experiments were approved by the Macquarie University Animal Ethics Committee and performed in accordance with the Australian Code of Practice for the Care and Use of Animals for Scientific Purposes.

In vitro electrophysiology

Labelling of bulbospinal RVLM neurons

Sprague Dawley rat pups (P5 – P25) were anaesthetized with 2-5% isoflurane (Veterinary Companies of Australia, Pty) in oxygen and moved onto a heated pad. A dorsal laminectomy was performed and the T2 spinal cord exposed. Fluorescently conjugated cholera toxin β subunit (CTB-Alexa 555 or 488, 0.5 - 1%, Invitrogen) was injected bilaterally at co-ordinates corresponding to the interomediolateral cell column (1 to 3 100 nl injections each side). After completion of microinjections the wound was closed with cyanoacrylate glue and anesthesia discontinued. Pups were allowed to recover on a warm pad until ambulatory and were then placed back in the cage with their mother and littermates. Post-operative rats were carefully monitored for the duration of experiments and treated with additional analgesia when indicated (Carprofen, 2 mg/kg s.c. Norbrook pharmaceuticals, Australia).

Electrophysiology Solutions (all values in mM):

Cutting solution: 125 NaCl, 25 $NaHCO_3$, 3 KCl, 1.25 $NaH_2PO_4.H_2O$, 10 D-glucose, 1 $CaCl_2$, 6 $MgCl_2$; equilibrated with 95% O_2 – 5% CO_2.

Artificial cerebrospinal fluid (aCSF): 125 NaCl, 25 $NaHCO_3$, 3 KCl, 1.25 $NaH_2PO_4.H_2O$, 25 D-glucose, 2 $CaCl_2$, 1 $MgCl_2$; equilibrated with 95% O_2 – 5% CO_2 (pH = 7.35).

Potassium gluconate internal solution: 125 K-gluconate, 10 Hepes, 11 EGTA, 15 NaCl, 1 $MgCl_2$, 2 MgATP, 0.25 NaGTP, 0.05% biocytin (pH = 7.3, Osmolarity 280 - 285 mOsm).

Whole-cell recordings

Two to five days following tracer injection pups (P8 – P28) were anaesthetized with isoflurane and decapitated. The brain was rapidly removed and placed in ice-cold oxygenated cutting solution. The brainstem was isolated, mounted in a vibratome, and immersed in ice-cold aCSF solution. Coronal sections of 300 µm thickness were taken from the region immediately caudal to the caudal pole of the facial nucleus and transferred to continuously oxygenated aCSF at 36 °C and left for at least 1 hr. before

recordings in an oxygenated aCSF-filled chamber maintained at room temperature. Tracer-labelled neurons were viewed under epifluorescence: CTB-labelled neurons ventral to nucleus ambiguus and lateral to the inferior olive were identified as putative RVLM premotor neurons and targeted.

Whole-cell recordings were obtained from RVLM neurons in voltage clamp mode using borosilicate pipettes with 1.5 - 2 µm tip diameters (pipette resistance: 3 - 6 MΩ when filled with internal solution). After formation of a gigaseal, voltage clamp recordings were obtained using a Multiclamp 700B (Molecular Devices). Once the holding current and input resistance stabilized, baseline recordings were made for at least five minutes prior to commencement of the experimental protocol. Series resistance was compensated by 70-80%. All recorded parameters were digitized using Spike 2 version 6.11 (RRID: nlx_156886) with a Power 1401 mark II digitizer (Cambridge Electronic Design, UK). In some experiments two neurons were simultaneously recorded from the same slice.

Recorded neurons were labelled using 0.05% biocytin contained in the internal solution. At the conclusion of experiments slices were briefly fixed in 4% paraformaldehyde and cryoprotected until immunohistochemical processing.

Experimental protocol

The effect of SST on bulbospinal RVLM neurons was determined by superfusing slices with 50-300 nM SST (Auspep, Australia) in carbogen-equilibrated aCSF for up to 100 s, which was then washed out until recovery to baseline was achieved. 300 nM SST has been reported to evoke approximately 75% maximal inhibitory effect on spontaneously firing locus coeruleus neurons recorded in acute brain slices (Chessell et al., 1996) and 95% inhibition of calcium current in dissociated periaqueductal grey neurons (Connor et al., 2004). Membrane currents were evoked by voltage command steps from -60 to -130 mV in 10 mV increments and 250 ms duration before, at peak response to SST, and after return to baseline (see Figures 4 & 5). Voltage steps in SST-insensitive neurons were performed at equivalent times. In initial experiments the sensitivity of neurons to 10 µM Baclofen (Sigma Aldrich), an agonist of the metabotropic GABA B receptor that exerts its effects via activation of GIRK channels (Kerr and Ong, 1995; Lüscher et al., 1997), was used to ensure that the diminished responsiveness to repeated SST exposure was specific to SST receptor activation, rather than, for example, dialysis of intracellular GIRK effectors.

In order to assess whether the inhibition seen following SST application was mediated by SST_2 receptor activation, the effects of repeated SST application were compared before and after the addition of the sst_2 receptor antagonist cyanamid to the perfusate (CYN-154806, 300 nM, Tocris, UK). Baseline responses to 300 or 50 nM SST were assessed as described above; once a response to SST was detected sections were washed in aCSF for 1000 s then CYN-154806 was perfused for 500 s before the second application of SST.

To determine whether responses to SST were dependent on activity in putative presynaptic neurons we compared responses to 100 nM SST before and after addition of 10 μM tetrodotoxin (TTX, Jomar Bioscience) to the perfusion. This concentration blocked electrically-evoked synaptic currents in pilot experiments (data not shown) and exceeds that generally used elsewhere (Kawai et al., 1999; Kawashima et al., 2013). Baseline responses to SST were recorded and allowed to recover for 1000 s before incubation with TTX for 5 min and re-exposure to SST.

Data analysis

Responses to SST were quantified by measuring the peak change in holding current recorded immediately following SST application. The current-voltage relationship was calculated by plotting membrane current against holding potential (Connor et al., 2004). In some experiments hyperpolarization-activated currents were observed; these were quantified by subtracting initial from steady-state currents evoked by hyperpolarizing steps from a holding potential of -60 mV to -130 mV in -10 mV increments (Gao et al., 2012, see Figure 7).Repeated responses of bulbospinal neurons to SST following application of TTX or cyanamid to the perfusate were compared using Student's paired t-test for comparison of raw data within groups or unpaired t-test for comparison of normalized responses between groups. Grouped data are expressed as mean ± SEM for parametric series or median (range) for non-parametric series. Differences were judged significant at $p < 0.05$. Statistical analyses were performed using Graphpad Prism 6.0 (RRID: rid_000081) or Graphpad Quickcalcs (http://www.graphpad.com/quickcalcs/) for categorical data.

Immunohistochemical processing and analysis of recorded neurons

All slices were fixed overnight in 4% paraformaldehyde in phosphate buffer (0.1 M, pH 7.4) then frozen in cryoprotectant (30% sucrose plus glycerol). Slices were then

processed for sst_{2a} receptor immunoreactivity using a protocol based on that described by Gogolla et al. (2006).

Free-floating slices were washed in 20 ml pots for 10 min in 0.01 M PBS and incubated overnight at 4 °C in 0.5% Triton X-100 in 0.01 M PBS. Then slices underwent a blocking step in 5% bovine serum albumin (BSA) in 0.01 M PBS for 4 hr. at room temperature. Primary antibodies (see Table 1) were added to 5% BSA/0.01 M PBS for a 4 hr. incubation at room temperature then washed off with 30 min TPBS. Sections were then incubated at 4 °C overnight in 5% BSA/0.01 M PBS containing secondary antibody for detection of sst_{2a} receptor expression and ExtrAvidin-FITC for detection of biocytin-filled cells. Antibodies were washed off with TPBS for 30 min. Slices were wet-mounted on glass slides, coverslipped and viewed under epifluorescence to confirm labelling before mounting with DAKO fluorescent mounting medium. Fourteen slices contained intact recovered neurons and were imaged using an AxioImager Z2 microscope with ZEN software (2012 version, Carl Zeiss, RRID: SCR_013672). In some cases neurons were also imaged using a Leica SP5 TCS confocal microscope and processed using Leica LAS AF software (RRID: SCR_013673). All figures were prepared using Coreldraw and Corel Photopaint X4 (RRID: SCR_013674).

Antibody Characterization

The rabbit anti-sst_{2a} antibody used in the current study (Biotrend UMB-1) has previously been characterized by Western blot and immunoprecipitation experiments in wild-type and sst_2 knock-out mice, and is reported to specifically label HEK cells transfected with sst_{2a}, but not other SST receptor isoforms (Fischer et al., 2008). In initial experiments we directly compared the binding of the rabbit monoclonal sst_{2a} antiserum to that obtained using a guinea pig antiserum raised against the same antigen sequence. Binding of the guinea pig antiserum has previously been verified by dot blot and Western blot assay and screening in sst_2 knock-out animals (Allen et al., 2003; Korner et al., 2005; Schulz et al., 1998a; Schulz et al., 1998b; Spary et al., 2008), and its distribution in the RVLM has been used to define sst_{2a} expression in regions of the medulla associated with cardiovascular (Burke et al., 2008) and respiratory function (Gray et al., 2010), where it is colocalized with tyrosine hydroxylase (TH) and neurokinin-1 receptor (NK1R) respectively.

In pilot studies using 50 µm thick sections processed as described below, the binding distribution of the rabbit antiserum was consistent with that reported for the guinea-pig

antiserum: binding was colocalized with TH throughout the VLM and with NK1R between 600 and 1200 µm caudal to the facial nucleus, corresponding to the Pre-Bötzinger Complex (Figure 1).

No immunoreactivity was observed when either antibody was preincubated for 8 hours at 4 °C with the sst_{2a} antigen (Biotrend SS-801, 1:5 by weight, RRID: SCR_013675, Figure 2A & B). Binding of rabbit and guinea pig antisera overlapped completely in tissue incubated with both primary antibodies and visualised with different fluorescent secondary antibodies (Figure 2C).

Retrograde tracing of SSTergic neurons

Animal surgery

Experiments were performed on male Sprague Dawley rats (n = 10), 14-15 weeks old (400-550 g) from the Animal Resources Centre, Perth, Western Australia. The retrograde tracing and combined *in situ* hybridization and immunohistochemistry methods used here have been previously published (Kumar et al., 2009). In brief, rats were anaesthetized with ketamine (Parnell Laboratories, Australia) mixed with medetomidine hydrochloride (Pfizer Animal Health, 75 and 0.5 mg/kg respectively, i.p.) and treated with preoperative analgesia (carprofen, 5 mg/kg s.c.) and prophylactic antibiotics (cephazolin, 20 mg/kg i.m., Mayne Pharma, Australia). A flat skull approach was used to microinject the retrograde tracer cholera toxin subunit B (CTB, 1% in 200 nl saline; List Biological, Campbell, CA, USA) unilaterally into the RVLM. After conducting a small craniotomy through the occipital bone and incision through the dura, antidromic facial field potentials were evoked by stimulation of the facial nerve. CTB microinjections were made 0.3 mm caudal to the facial nucleus, 1.7-2.1 mm lateral to midline and 0.3 mm deep to the ventral margin of the facial field (that is, 8.8 - 9.2 mm from the dorsal surface of the brain). After withdrawal of the pipette, the wound was closed and 5 ml of physiological saline was administered i.p. Rats were then administered sedative reversal agent atipamezole hydrochloride (Pfizer Animal Health, Australia, 0.75 mg, 0.15 ml s.c.) and allowed to recover for 2-3 days under close monitoring.

Tissue preparation

Animals were deeply anaesthetized with sodium pentobarbitone (>100 mg/kg i.p.) and perfused transcardially with 250 ml heparinized 0.9% sodium chloride followed by 250 ml 4% paraformaldehyde in phosphate buffer (0.1 M, pH 7.4). The brain was removed,

the medulla dissected and fixed overnight at 4 °C. Brains were sectioned coronally at 40 µm into four series using a vibrating microtome (VT1200S; Leica, Germany). Sections in each series were thus separated by 160 µm. Fluorescent immunohistochemical detection of CTB was conducted using a rabbit anti-CTB primary antibody and a 488-conjugated donkey anti-rabbit alongside detection of mRNA using digoxigenin (DIG)-labelled riboprobes targeting PPS mRNA as described previously (Burke et al., 2008). Both anti-sense and sense probes were synthesized, with RNA polymerase T7 and SP6 promoters attached to the 5' end of the reverse and forward oligonucleotide primers respectively (primers listed below in lowercase with promoter attached in uppercase). PCR amplified cDNA template was then *in vitro* transcribed using T7 (AmpliScribe™ T7-Flash™ Transcription Kit, #ASF 3257, Epicentre Biotechnologies, Madison, WI) or SP6 (RiboMAX large scale RNA production system, #P1280, Promega, Madison, WI) *in vitro* transcription kits. Digoxigenin-11-UTP (Roche Applied Sciences, Mannheim, Germany) was incorporated into the riboprobes during *in vitro* transcription.

PPS Forward: GGATCCATTTAGGTGACACTATAGAAGctcaagctcggctgtctgag

PPS Reverse: GAATTCTAATACGACTCACTATAGGGAGAggaggagagggatcagaggt

Free floating brain sections were processed using the protocol described by Li et al. (2005). No labelling in any brain region was seen when the sense probe was substituted for the anti-sense probe.

Cell counts and analysis

Tissue sections were mounted on glass slides, coverslipped (Vectashield Hardset, Vector Laboratories, USA) and viewed and imaged using a Zeiss AxioImager Z1 microscope under epifluorescence. Images were acquired with Zeiss Axiovision software (Version 4.8, RRID: SciRes_000111). In each whole brain, sections separated by 160 µm were analyzed from Bregma level 5.16 mm to -15.24 mm. Six of the ten brains injected with CTB were selected for quantitative analysis, with every region quantified in at least three brains and confirmation assessed qualitatively in all other cases. Brains were selected due to their small CTB injection sites centered in the RVLM with little impingement on surrounding regions.

Each brain region containing CTB labelled neurons was assessed for expression of PPS mRNA. CTB immunoreactivity (-ir) was determined using the criteria described by Bowman et al. (2013), in which neurons were considered CTB-ir if distinct Dylight-488

labelling was apparent within the cytoplasm, organelles, and/or in the proximal dendrites. Where intense ISH signal obfuscated cytoplasmic CTB-ir, neurons were considered double labelled where CTB-ir proximal dendrites or organelles were clearly visible. When a region was found to contain double-labelled neurons, the section that contained the most CTB labelling was selected for counting, and, dependent upon the rostrocaudal extent of the region, a second and third section was also assessed for double labelling (> 300 µm apart). Regions of interest were imaged at multiple focal planes ("z-stack") so that CTB-positive proximal dendrites could be clearly discriminated in neurons in which intense ISH signal quenched the cytoplasmic CTB signal (Bowman et al., 2013).

Using these counts, the percentage of CTB-ir neurons that colocalized with PPS in that brain region, combining all sampled rostrocaudal levels, was determined for 3 - 4 animals and the mean ± SEM was calculated.

In addition, in order to describe those regions which provided the greatest number of retrogradely traced neurons containing PPS mRNA, the number of double-labelled neurons in each region (combining the selected rostrocaudal levels) was determined as a proportion of all double-labelled neurons and the results expressed as the mean percentage.

RESULTS

In vitro electrophysiology

Superfusion of 300 nM SST produced an outward current (I_{SST}) in 18/31 (58 %) bulbospinal neurons tested. The mean value of I_{SST} was 40.7 ± 4.8 pA (Figure 3). Subsequent application of $GABA_B$ agonist baclofen (10 μM) produced an outward current in SST-responsive (49.3 ± 5. 9 pA, *n* = 4, Figure 3A) and SST-insensitive neurons (42.6 ± 4.3 pA, *n* = 5, Figure 3B).

SST-sensitive neurons displayed desensitization to repeated application of 50 [*n* = 2], 100 [n = 2] or 300 nM [*n* = 1] SST. Responses to 50, 100 or 300 nM SST were reduced by 20.0 %, 32.4 %, or 43.8 % respectively: pooled responses were 36.6 ± 5.5 vs. 24.8 ± 2.4 pA, Paired t-test *t* = 3.4, *df* = 4, 2-tailed *p* = 0.027, Figure 4A. A similar reduction of response amplitude following repeated 100 nM SST application was observed following addition of TTX to the perfusate between SST trials (39.7 ± 4.9 vs. 25.9 ± 4.6 pA, Paired t-test *t* = 15.4, *df* = 4, 2-tailed *p* = 0.0001, *n* = 5, Figure 4B).

In order to assess whether sst_2-receptor activation underlies responses of bulbospinal neurons to SST, we reapplied SST to neurons previously shown to be SST-sensitive in the presence of the sst_2 antagonist cyanamid (300 nM). Baseline responses to 300 nM (*n* = 2) or 50 nM (*n* = 3) SST were of 40.15 ± 3.5 pA (300 nM) or 25.12 ± 2.9 pA (50 nM) respectively. Cyanamid reduced the amplitude of SST-evoked responses from 31.1 ± 4.1 pA to 2.8 ± 0.6 pA (Paired t-test *t* = 6.7, *df* = 4, 2-tailed *p* = 0.0025, *n* = 5, Figure 5). When normalized with respect to control responses, responses to second applications of SST were more attenuated in the presence of cyanamid (9.9 ± 2.7%) compared to repeated SST applications conducted in normal aCSF (70.3 ± 4.6%, unpaired t-test vs. cyanamid: *t* = 11.3, *df* = 8, *p*<0.0001, *n* = 5) or in the presence of TTX (63.4 ± 4.6%, unpaired t-test vs. cyanamid: *t* = 10, *df* = 8, *p*<0.0001, *n* = 5).

In 17 bulbospinal neurons in which SST induced an outward current at a holding potential of -60 mV, baseline slope conductances of 3 ± 0.4 nS and 3.7 ± 0.6 nS were measured between -60/-80 and -110/-130 mV respectively. Following 300 nM SST slope conductances increased to 3.6 ± 0.5 nS and 4.9 ± 0.6 nS over the same potentials, indicating inward rectification (2-way ANOVA: $F_{1, 32}$ = 10.57, *P* = 0.002, pooled data inset in Figure 6A(ii)). The SST-evoked current was greater at more

negative currents, had a reversal potential of -93 ± 6 mV, and was not detected in SST-insensitive neurons.

Hyperpolarizing steps beyond -70 mV were also associated with slowly activating inward currents in 10/26 neurons tested (Figure 7), which were consistent in timecourse and profile with activation of the hyperpolarization-activated cation channel, I_h. The amplitudes of hyperpolarization-activated currents were highly variable between neurons, with a median value of -55 pA at -130 mV (range: 10 – 291 pA). The proportion of SST-sensitive neurons was not significantly different in neurons that expressed I_h compared to those that did not (P = 1, Fisher's Exact Test).

sst_{2a} receptor expression on electrophysiologically characterized bulbospinal neurons

Fourteen biocytin-labelled bulbospinal neurons were recovered for histological processing. No sst_{2a} immunoreactivity was ever identified on SST-insensitive neurons (n = 9, Figure 8A). SST evoked responses of 42.3 ± 7.9 pA in the remaining 5 neurons: 3/5 were subsequently identified as sst_{2a}-positive (Figure 8B).

Retrograde tracing of SSTergic neurons

CTB injection sites were located in the RVLM and extended 0.7- 1.1 mm caudal to the facial nucleus (Bregma -11.64 mm) with the core of the injection sites centered between Bregma -11.8 and -12.3 mm (Figure 9).

The majority of brain regions that contained CTB-labelled neurons also contained neurons expressing PPS mRNA. Table 2 presents the distribution and relative density of cells containing CTB and/ or PPS mRNA in all brain regions that contained CTB labelled neurons.

Colocalization of PPS mRNA with CTB immunoreactivity was restricted to 8 brain regions: the paratrigeminal nucleus (Pa5), lateral parabrachial nucleus (LPB), Kölliker-Fuse nucleus (KF), ventrolateral periaqueductal grey area (VLPAG), central nucleus of the amygdala (CeA), sublenticular extended amygdala (SLEA), interstitial nucleus of the posterior limb of the anterior commissure nucleus (IPAC) and bed nucleus of the stria terminalis (BNST). Figure 10 shows examples of double labelling in the Pa5, VLPAG, CeA and BNST.

The proportion of CTB-labelled neurons that contain PPS mRNA within each region is shown in Figure 11. Of the eight brain regions, CTB-labelled cells in Pa5 contained the highest PPS-expression (40 ± 3%, 73/173 CTB-ir cells, n = 4), followed closely by the

SLEA (34 ± 6%, 65/180, *n* = 3). The lPAC possessed a small, variable population of double-labelled cells across animals (26 ± 10%, 20/68 CTB-ir cells, *n* = 3). The VLPAG contained PPS mRNA expression in approximately one fifth of its RVLM-projecting cell population (22 ± 3%), however this region also exhibited the highest number of double labelled cells of all regions analyzed (158/791, *n* = 4). Retrogradely traced populations of the LPB and BNST contained similar proportions of PPS (13 ± 1%, 47/369, *n* = 4 and 12 ± 2%, 48/406, *n* = 3 respectively), followed by the KF (10 ± 0.5%, *n* = 4) which furthermore contained the lowest number of double labelled cells of all RVLM-projecting populations. Despite the CeA possessing the lowest percentage of double labelled neurons (10 ± 1%), it contained a relatively large number of PPS-expressing CTB labelled cells (110/713 cells, *n* = 3), which was only overshadowed by the size of the VLPAG projection.

DISCUSSION

The main findings are: firstly, that SST evoked an outward current suggestive of activation of an inwardly rectifying potassium channel in approximately half of RVLM bulbospinal neurons. Second, this effect is most likely due to activation of sst_2 receptors, as SST-activated currents were blocked by cyanamid and sst_{2a} receptor expression was identified on SST-sensitive neurons. Thirdly, putative sources of SSTergic drive to the RVLM were identified in 8 distinct brain regions: the Pa5, KF, LPB, VLPAG, CeA, SLEA, IPAC and BNST.

SST hyperpolarizes spinally-projecting RVLM neurons via GIRK channels

SST hyperpolarized about 60% of bulbospinal neurons in acute brain slices from young rats. The response amplitudes obtained and dose range used were similar to those reported in SST-sensitive neurons in the periaqueductal grey (Connor et al., 2004). The SST-evoked responses were effectively blocked by cyanamid, a selective antagonist of sst_2 receptors (Nunn et al., 2003), suggesting specific involvement of sst_2 receptors in mediating the response in bulbospinal neurons. Addition of TTX to the perfusate did not alter outward currents evoked by SST, indicating that the evoked currents were mediated by postsynaptic rather than presynaptic mechanisms. The proportion of SST-sensitive neurons in the current study is consistent with the proportion of bulbospinal (35%) and C1 neurons (50%) that were previously identified as sst_{2a}-immunoreactive in adult animals (Burke et al., 2008), although higher than the overall proportion of biotin-labelled bulbospinal neurons identified as sst_{2a}-immunoreactive in the current study (21%). Of the five recovered neurons that responded to SST, only three clearly expressed sst_{2a} immunoreactivity, whereas all 9 non-responsive neurons were sst_{2a} negative. In neurons that expressed sst_{2a} it seems likely that the SST-evoked response was mediated via this receptor. In neurons that responded to SST in which sst_{2a} immunoreactivity was undetectable it is possible that other SST receptor isotypes mediated electrophysiological responses. This lower than expected expression of sst_{2a} on SST-sensitive neurons could also be an artefact that reflects the limited sensitivity of immunofluorescence for discriminating lightly immunoreactive neurons in thick slices, or could even be due to dialysis of SST receptors, which become internalized and migrate away from the cell membrane after agonist binding (Cescato et al., 2006).

The outward current evoked by SST resulted from an increase in inwardly rectifying potassium conductance, since at more negative potentials SST activated a greater

conductance and had a reversal potential approaching the Nernst potential calculated for potassium (-93 mV). This is in keeping with data indicating that sst_2 couples efficiently to GIRK1, examined by comparing dose-response curves and the maximum currents obtained by the five different rat SST receptor subtypes (sst_1 – sst_5) that were co-expressed with GIRK1 (Kreienkamp et al., 1997). Our results are consistent with the effects of SST on inwardly rectifying potassium conductance in neurons in other brainstem regions including the locus coeruleus (Inoue et al., 1988) and PAG (Connor et al., 2004). In addition, in different brain regions such as the superior cervical ganglion (Shapiro and Hille, 1993), amygdala (Viana and Hille, 1996) and PAG (Connor et al., 2004), SST directly activates potassium conductance and inhibits GABA release via a presynaptic calcium dependent mechanism and may contribute to the effects of SST on RVLM sympathetic premotor neurons.In the current study, repeated application of SST evoked hyperpolarizing responses that showed considerable desensitization. Following long exposure to agonists, G-protein coupled receptors mediate a signal that triggers receptor dephosphorylation (Bohm et al., 1997; Horie and Insel, 2000; Lefkowitz, 1998; Premont et al., 1995). Desensitization of SST receptors has been reported in rat hippocampal and neocortical neurons (Priestley, 1992; Wang et al., 1990; Yin et al., 2009; Young Shim et al., 2006), and, of particular relevance to the current study, Liu et al. (2008) found that SST_2 receptors internalize and desensitize following agonist stimulation within minutes.

An incidental finding of the current study is the presence of a hyperpolarization-activated channel in some bulbospinal RVLM neurons. Although not studied in detail, the time-course and activation threshold of the identified current is consistent with the distinctive profile of hyperpolarization and cyclic nucleotide channel-mediated current, I_h (reviewed by Robinson and Siegelbaum, 2003). This finding supports observations of I_h in bulbospinal RVLM neurons recorded in neonatal rats by previous investigators (Kangrga and Loewy, 1995; Li et al., 1995). Although I_h has been implicated in the generation of spontaneous pacemaker activity in other cell types (recently reviewed by He et al., 2014), it is not thought to play a critical role in driving autodepolarization in RVLM, as its blockade by ZD7288 evokes no significant effect on sympathetic nerve activity or blood pressure (Miyawaki et al., 2003).

Technical limitations

Electrophysiological recordings were confined to bulbospinal neurons encountered lateral to the pyramidal tract, ventral to nucleus ambiguous, and medial to the spinal trigeminal nucleus. Bulbospinal neurons in this region contain the highest density of TH expression and have been interpreted as putative sympathetic premotor neurons in similar studies (Kangrga and Loewy, 1995; Li et al., 1995; Li and Guyenet, 1996). Due to the technical difficulties associated with examining more than three fluorescent labels at a time we did not survey biocytin-labelled neurons for TH immunoreactivity in the current study. However, RVLM bulbospinal neurons selected using the same criteria were intermingled with and included TH-positive neurons in a recent study by our group (Korim et al., 2014).

Brain slices for recordings were made from 8 -28 days old rats. As global SST binding and brain-wide SST receptor expression undergo some lability in the neonatal period in rats (Gonzalez et al., 1989; Thoss et al., 1995), it is possible that changes in the relative expression of SST receptor isoforms in the brainstem could complicate interpretation of the current data. No developmental study has yet described the relative expression of SST receptor isoforms in the brainstem over the neonatal period. However, the expression of sst_{2a} in putative TH-positive neurons containing the Lmx1b and Phox2b transcription factors is already established by birth (Gray, 2013). Furthermore, the gross pattern of sst expression, including sst_{2a}, in P5 rats is similar to that observed in adults (Thoss et al., 1995). Although the quality of sst_{2a} labelling in thick brain slices reported here is inferior to that observed in conventional thin sections (Burke et al., 2008), sst_{2a}–like immunoreactivity was detected on all slices tested and the general pattern of expression was similar to that seen in adult rats, suggesting that sst_{2a} expression in juveniles is likely to be representative of older animals.

In common with many other studies using conventional retrograde tracers, interpretation of our anatomical study should be tempered with three caveats. First, CTB may be taken up by fibers that pass through the site of tracer deposition, an effect that is particularly prevalent following pressure-ejection (Chen and Aston-Jones, 1995; Luppi et al., 1990). We cannot therefore determine whether retrogradely labelled neurons form synaptic terminals within the RVLM or simply represent fibers of passage, and therefore urge conservative interpretation of our data. Second, assuming some CTB-labelled neurons do actually form terminals within the RVLM, we cannot determine the function or phenotype of their post-synaptic targets. Finally, significant numbers of neurons in the ventrolateral medulla express somatostatin and project to the ipsi- and

contralateral RVLM (Tan et al., 2010). However, discrimination of local SSTergic neurons was confounded by the tracer injection site; we therefore cannot exclude local interneurons as a potential source of SST release.

Finally, we and others (Giehl and Mestres, 1995; Kiyama and Emson, 1990; Stornetta et al., 2003) have interpreted the presence of PPS mRNA as indicative of SST synthesis and release. As discussed by Giehl and Mestres (1995), the correspondence between brain-wide SST mRNA and protein expression is generally robust, but PPS can be cleaved into a number of peptides other than SST-14 and SST-28 (Patel and O'Neil, 1988; Rabbani and Patel, 1990), including a recently discovered neuropeptide, neuronostatin (Samson et al., 2008). Therefore, although PPS mRNA expression is a sensitive assay of PPS production, PPS expression *per se* does not necessarily correspond with translation of SST peptide or its release. Interestingly, intracerebroventricular neuronostatin has been reported to drive a sympathetically mediated *rise* in arterial blood pressure (Samson et al., 2008; Yosten et al., 2011) via a proposed (Samson et al., 2008) but currently unproven action at the paraventricular nucleus of the hypothalamus. Preliminary experiments in our laboratory have revealed no effect of neuronostatin when microinjected into the RVLM pressor region in urethane-anaesthetized rats (Burke et al., unpublished data).

PPS mRNA is found in select groups of neurons projecting to the RVLM

The paratrigeminal nucleus

Distinct clusters of PPS mRNA-expressing neurons were found in the Pa5 in the current study, as previously noted (Kiyama and Emson, 1990). Both anterograde and retrograde studies have revealed projections from the Pa5 to the RVLM (Caous et al., 2001; de Sousa Buck et al., 2001), however this is the first study to describe a somatostatinergic phenotype in just under half the RVLM-projecting neurons in the region. Enkephalin, calbindin, and nNOS have been detected in Pa5 neurons that project to the dorsal motor nucleus of the vagus (Armstrong and Hopkins, 1998); these groups may also overlap with the PPS containing population described here. Pa5 microinjection of bradykinin evokes pressor effects (Lindsey et al., 1997) via direct activation of barosensitive RVLM neurons (Caous et al., 2004). Many (60-80%) Pa5 neurons are themselves barosensitive, increasing their firing rate in response to phenylephrine administration (Balan Jr et al., 2004; Sousa and Lindsey, 2009b), while

bilateral Pa5 ablation reduces cardiac barosensitivity (Sousa and Lindsey, 2009a). Whether SST participates in mediating such reflex modulation in the RVLM is unknown.

The Kölliker-Fuse and lateral parabrachial nuclei

Together, the KF and LPB form the pontine respiratory group, and while PPS expression has been explicitly demonstrated in the LPB (Kiyama and Emson, 1990), reporting of its localization in the KF has been overlooked prior to the current study (Giehl and Mestres, 1995; Kiyama and Emson, 1990). Projections from both KF and LPB to the RVLM region have been described (Smith et al., 1989). Although cardiovascular responses to chemical stimulation of parabrachial nuclei have been examined, they are inconsistent, brief and/ or small (Chamberlin and Saper, 1994; Lara et al., 1994; Ward, 1988), and the region's function in respiratory control is certainly better understood (Morschel and Dutschmann, 2009; Smith et al., 1989). At LPB/ KF sites corresponding to the location of PPS-expressing RVLM projecting neurons detected in the current study, glutamate microinjection has been reported to drive inspiratory facilitation (Chamberlin and Saper, 1994) or brief apnea (Chamberlin and Saper, 1994; Dutschmann and Herbert, 2006), whereas inhibition of the same sites drives apneustic prolongation of inspiratory phase duration (Dutschmann and Herbert, 2006), similar to that evoked by microinjection of SST into the Bötzinger Complex (Burke et al., 2010).

The ventrolateral periaqueductal grey (VLPAG)

PPS mRNA expression was observed in the VLPAG as previously described (Smith et al., 1994), and in neurons projecting to the raphe magnus (Beitz et al., 1983). Although projections from the VLPAG to the RVLM have been described (Carrive and Bandler, 1991), this is the first study to attribute a somatostatinergic phenotype to some elements of the pathway. Depressor responses associated with reductions in renal vascular resistance are evoked chiefly by stimulation of the caudal VLPAG (Carrive and Bandler, 1991), which overlaps anatomically with the PPS-expressing RVLM projecting neurons identified in the current study. On the other hand stimulation of the VLPAG also evokes vasodilation in the hindlimb (Lovick, 1992) and this has been attributed to a raphe-mediated pathway (Wang and Lovick, 1993). It is possible that raphe and RVLM projections arise from discrete regions of the VLPAG, as changes in iliac or renal blood flow are associated with different rostrocaudal levels of the VLPAG and corresponding RVLM termination sites (Carrive and Bandler, 1991). The caudal VLPAG has also been

implicated in hemorrhage as the activity of neurons in the region increase during the decompensatory or hypotensive phase (Cavun and Millington, 2001).

The central nucleus of the amygdala (CeA) and the extended amygdala

Somatostatinergic neurons have been described in the CeA (Vincent et al., 1985) and these project to the PAG (Gray and Magnuson, 1992) and/ or dorsal vagal complex, in particular the NTS (Gray and Magnuson, 1987; Saha et al., 2002; Veening et al., 1984). The present study however, is the first to demonstrate a dense PPS-expressing projection to the RVLM. Both coronal transection caudal to, or sagittal transection medial to the CeA reduce the amount of SST-ir fibers in the ventrolateral medulla (Kawai et al., 1982) supporting our findings. Furthermore the CeA also contains a glutamatergic population which projects to the RVLM (Takayama and Miura, 1991), and terminals arising from cells in the CeA appose barosensitive C1 neurons and non-C1 neurons (Cassell and Gray, 1989; Saha et al., 2005). Therefore it is possible that the PPS expressing neurons in the CeA described in the present study also contain glutamate.

The functional role of these neurons is more difficult to ascribe. Low frequency stimulation of CeA in the awake animal promotes inspiration, even respiratory entrainment (Harper et al., 1984). At higher frequencies (>10 Hz), phrenic nerve frequency is increased (Cox et al., 1987) and a prolonged period of inspiration occurs (Harper et al., 1984), while mostly pressor and some depressor effects have been reported (Frysinger et al., 1984; Gelsema et al., 1987; Harper et al., 1984; Iwata et al., 1987; Stock et al., 1978). It also appears that the responses evoked are state dependent, with sleep and anesthesia either dampening or reversing cardiorespiratory effects (Cox et al., 1987; Frysinger et al., 1984; Gelsema et al., 1987; Harper et al., 1984; Iwata et al., 1987; Stock et al., 1978). As the CeA forms a crucial link in the coordination of autonomic and behavioral responses to stress such as conditioned fear (LeDoux et al., 1988; Paré et al., 2004; Wilensky et al., 2006), it is possible that the somatostatinergic pathway identified in the current study may be involved in recovery responses such as the return of mean arterial pressure to baseline levels following freezing responses to conditioned fear (Carrive, 2000; Dielenberg et al., 2001) or the suppression of sympathetic responses during passive versus active coping (Roozendaal et al., 1991; Sherwood et al., 1990).

Extending dorsomedially from rostral parts of the CeA, the SLEA also contained a population of PPS-expressing RVLM-projecting neurons which has otherwise only been referred to briefly in studies of the developing and adult rodent brain (deCampo and Fudge, 2013; Real et al., 2009). Prior to this study knowledge of the SLEA's descending projections was restricted to the NTS/DMV and parabrachial complex (Grove, 1988; Sun et al., 1994; Waraczynski, 2006). Chemical stimulation of the SLEA elicits depressor responses (Gelsema et al., 1993). Although a respiratory relationship is associated with the SLEA, it is somewhat complex, as SLEA activity is normally synchronized with the onset of spontaneous breathing but suppressed during cognitive tasks which drive respiration (Evans et al., 2009). Activation of the SLEA is evident in subjects experiencing dyspnea, and is associated with the unpleasant emotional processing that occurs during a dyspneic episode (von Leupoldt et al., 2008). It is possible that the PPS-expressing pathway to the RVLM from the SLEA may be part of a complex circuit linking emotional state to cardiovascular and respiratory outflows.

The interstitial nucleus of the posterior limb of the anterior commissure (IPAC) expresses PPS mRNA in neurons projecting to the RVLM however very little is known about its function except for its role in reward and motivational processes (Waraczynski, 2003). Perhaps, as with other components of the extended amygdala, the IPAC is involved in the integration of emotional processing and autonomic outflows.

We have identified PPS-expressing neurons in the BNST that project to the RVLM despite the fact that such neurons have been found previously to project to the LPB, the PAG and dorsal vagal complex (Gray and Magnuson, 1987; Gray and Magnuson, 1992; Moga et al., 1989), and furthermore, neurochemically undefined neurons are known to project to the lateral tegmental field (Holstege et al., 1985). Although ablation of the region does not affect baseline arterial pressure or heart rate (Crestani et al., 2006), both chemical and electrical stimulation of the lateral subdivisions of BNST (where many PPS neurons in the present study were located) evoke a depressor response (Dunn and Williams, 1995). As PPS neurons projecting to the LPB and NTS are involved in feeding related responses (Li and Cho, 2006; Panguluri et al., 2009; Saggu and Lundy, 2008; Smith et al., 2005) it is possible that the projection identified here has a corresponding role. Alternatively, the BNST modulates MAP and HR during exercise (Alves et al., 2011), so whether the bradycardic and depressor responses evoked by SST microinjection in the RVLM (Burke et al., 2008) are simulating this function remains to be determined.

Conclusion

This study reveals that a discrete subset of brain regions provides somatostatinergic projections to the RVLM: the Pa5, KF, LPB, VLPAG, CeA, SLEA, IPAC and BNST, and we have provided evidence-based speculation as to the roles of these projections. The projection from the KF and LPB most likely has a respiratory function, however the role of the other pathways suggested remains to be tested. Nevertheless it is clear that SST released from these projection neurons activates G-protein coupled sst_2 (most likely sst_{2a}) receptors whereby GIRK channels are activated that serve to hyperpolarize neurons in the RVLM.

FIGURE LEGENDS

Figure 1 **Distribution of rabbit anti-sst_{2a} antibody binding in the ventrolateral medulla.** Confocal stack images demonstrate colocalization of rabbit anti-sst_{2a} immunoreactivity with tyrosine hydroxylase (TH) in the RVLM, 200 µm caudal to the facial nucleus (**A**) and with neurokinin-1 receptor (NK1R) in the Pre-Bötzinger Complex, 800 µm caudal to the facial nucleus (**B**). Individual channel images shown in panels 2 & 3. Arrowheads indicate double-labelled neurons.

Figure 2 Comparison of rabbit and guinea pig anti-sst_{2a} antibody binding. Epifluorescent images demonstrate binding of anti-sst_{2a} primary antibodies raised in guinea pig **(A1)** and rabbit **(B1)**, which was blocked by incubating alternate sections from the same animals with the antigen **(A2 & B2),** and resulted in overlapping patterns of expression when incubated together **(C1)**. **C2** and **C3** depict individual channels from merged image shown in **C1**. Box in **C4** shows region in which high powered images shown in **C** were taken. NA = nucleus ambiguus; NTS = nucleus of the solitary tract. IO = inferior olive; PY = pyramidal tract; SP5 = Spinal trigeminal nucleus.

Figure 3 Electrophysiological characterization of outward currents evoked by SST. (A). Voltage clamp recordings from CTB-labelled RVLM neurons: bulbospinal RVLM neurons in which SST and baclofen perfusion (black horizontal bars indicate time of application) evoked outward currents were categorized as SST-sensitive. **(B)** Bulbospinal RVLM neurons in which baclofen but not SST evoked outward currents were considered SST-insensitive.

Figure 4 Responses of bulbospinal RVLM neurons to repeated SST application exhibited desensitization. (A) Voltage-clamp recordings illustrate desensitization of responses to repeated application of 50 nM SST ('v' denotes timing of voltage steps; steps have been removed from traces to aid clarity). **(B)** Pooled data; responses to 50, 100 and 300 nM SST have been combined. **(C)** Experimental recording demonstrating that responses to repeated SST were unaffected by tetrodotoxin (TTX). **(D)** Pooled data of responses to 100 nM SST before and after addition of TTX to the perfusate. *: P<0.05, ***: P<0.001.

Figure 5 sst_2 blockade abolished SST-induced outward currents. **(A)** Voltage-clamp recordings of responses to SST application before and after superfusion with the sst_2 blocker CYN-154806 ('v' denotes timing of voltage steps). **B**: pooled data showing effects of SST_2 blockade on five SST-sensitive spinally projecting RVLM neurons. **: P<0.01.

Figure 6 Current-voltage relationship of SST-sensitive (A) and SST-insensitive (B) bulbospinal RVLM neurons. Examples of membrane currents evoked by voltage steps before, during and after 300 nM SST superfusion; experimental recordings are shown in i and iii, I-V plots are shown in ii and iv. 250 ms command voltages were stepped from -60 to -130 mV in 10 mV increments (v). Inset in A(ii) denotes pooled slope conductances from 17 SST-sensitive bulbospinal neurons. **: *P*<0.01, Bonferroni post-test.

Figure 7 Example of hyperpolarization-activated inward current recorded in a bulbospinal RVLM neuron. (A) Hyperpolarizing membrane steps from -70 to -130 mV evoked a slowly activating inward current. The amplitude of the hyperpolarization-activated current was estimated by measuring the difference between the instantaneous (open circle) and steady-state currents (closed circles) evoked by each step **(B)**.

Figure 8 Immunohistochemical recovery of electrophysiologically characterised RVLM bulbospinal neurons. (A1) Simultaneous voltage-clamp recordings from two bulbospinal RVLM neurons recorded with biocytin-filled pipettes; neither responded to 100 nM SST application. **(A2)** 22 µm thick confocal projection image of the same neurons; both biocytin-filled neurons were confirmed as CTB-positive and sst_{2a}-negative. **(B1)** Example of an SST-sensitive neuron recorded in a different experiment; the neuron was subsequently shown to be weakly sst_{2a}-

immunoreactive under epifluorescence **(B2)**. Breaks in recording B1 indicate switches in recording mode at which seal resistance was assessed.

Figure 9 CTB injection sites targeting the RVLM. The left coronal hemisection shows the CTB injection site from one animal. The right hemisection shows schematically the extents of six injection sites in animals used for quantitative analysis.

Figure 10 Combined PPS *in situ* hybridization and retrograde tracing reveals putative RVLM-projecting somatostatinergic neurons. (A) High power photomicrograph showing neurons labelled for PPS mRNA (brightfield) and CTB immunofluorescence (green channel). Double-labelled neurons are indicated by arrowheads; PPS mRNA is magenta in merged pseudocolored images. Merged epifluorescence images in **B – E** illustrate the distribution of double-labelled neurons in the paratrigeminal nucleus **(Pa5, B)**, ventrolateral periaqueductal grey **(VLPAG, C),** central nucleus of the amygdala **(CeA, D),** and bed nucleus of the stria terminalis **(BNST, E)**. A schematic diagram indicating the region shown (yellow box) and the rostrocaudal co-ordinate with respect to Bregma is superimposed onto each photomicrograph; schematic diagrams adapted from Paxinos and Watson (2006).

Figure 11 Brain regions containing RVLM projecting (CTB-ir) neurons that express PPS mRNA.

Table 1 Antibody details

Table 2 Relative abundance of neurons containing CTB-ir and/ or PPS mRNA in each brain region projecting to the RVLM. Scattered (+) labelling refers to sparsely distributed cells (<5 per region) Light (++) labelling indicates coverage of less than one third of the defined region. Moderate (+++) labelling indicates a range of labelling from approximately one to two thirds coverage of the cell group while dense (++++) labelling describes an area containing a high number of labelled cells which cover more than two thirds of the anatomically defined region.

CONFLICT OF INTEREST STATEMENT

The authors report no conflicts of interest

AUTHOR ROLES

SM & AKG conceived and designed study; LBF, PB & SK conducted in vitro electrophysiology; SM & BB conducted tracing studies. SL conducted antibody characterization. All authors analyzed data and prepared the manuscript.

REFERENCES

Allen JP, Hathway GJ, Clarke NJ, Jowett MI, Topps S, Kendrick KM, Humphrey PPA, Wilkinson LS, Emson PC. 2003. Somatostatin receptor 2 knockout/lacZ knockin mice show impaired motor coordination and reveal sites of somatostatin action within the striatum. European Journal of Neuroscience 17(9):1881-1895.

Alves F, Resstel L, Correa F, Crestani C. 2011. Bed nucleus of the stria terminalis α1 and 2-adrenoceptors differentially modulate the cardiovascular responses to exercise in rats. Neuroscience 177:74-83.

Armstrong CL, Hopkins DA. 1998. Neurochemical organization of paratrigeminal nucleus projections to the dorsal vagal complex in the rat. Brain Research 785(1):49-57.

Balan Jr A, Caous CA, Yu YG, Lindsey CJ. 2004. Barosensitive neurons in the rat tractus solitarius and paratrigeminal nucleus: A new model for medullary, cardiovascular reflex regulation. Canadian Journal of Physiology and Pharmacology 82(7):474-484.

Beitz AJ, Shepard RD, Wells WE. 1983. The periaqueductal gray-raphe magnus projection contains somatostatin, neurotensin and serotonin but not cholecystokinin. Brain Research 261(1):132-137.

Bohm SK, Grady EF, Bunnett NW. 1997. Regulatory mechanisms that modulate signalling by G-protein-coupled receptors. Biochem J 322 (Pt 1):1-18.

Bowman BR, Kumar NN, Hassan SF, McMullan S, Goodchild AK. 2013. Brain sources of inhibitory input to the rat rostral ventrolateral medulla. J Comp Neurol 521(1):213-232.

Bruno JF, Xu Y, Song J, Berelowitz M. 1992. Molecular cloning and functional expression of a brain-specific somatostatin receptor. Proceedings of the National Academy of Sciences 89(23):11151-11155.

Burke PG, Abbott SB, McMullan S, Goodchild AK, Pilowsky PM. 2010. Somatostatin selectively ablates post-inspiratory activity after injection into the Botzinger complex. Neuroscience 167(2):528-539.

Burke PG, Li Q, Costin ML, McMullan S, Pilowsky PM, Goodchild AK. 2008. Somatostatin 2A receptor-expressing presympathetic neurons in the rostral ventrolateral medulla maintain blood pressure. Hypertension 52(6):1127-1133.

Caous CA, Balan A, Lindsey CJ. 2004. Bradykinin microinjection in the paratrigeminal nucleus triggers neuronal discharge in the rat rostroventrolateral reticular nucleus. Can J Physiol Pharmacol 82(7):485-492.

Caous CA, de Sousa Buck H, Lindsey CJ. 2001. Neuronal connections of the paratrigeminal nucleus: a topographic analysis of neurons projecting to bulbar, pontine and thalamic nuclei related to cardiovascular, respiratory and sensory functions. Auton Neurosci 94(1-2):14-24.

Carrive P. 2000. Conditioned fear to environmental context: cardiovascular and behavioral components in the rat. Brain Research 858(2):440-445.

Carrive P, Bandler R. 1991. Viscerotopic organization of neurons subserving hypotensive reactions within the midbrain periaqueductal grey: a correlative functional and anatomical study. Brain Res 541(2):206-215.

Carrive P, Bandler R, Dampney RA. 1988. Anatomical evidence that hypertension associated with the defence reaction in the cat is mediated by a direct projection from a restricted portion of the midbrain periaqueductal grey to the subretrofacial nucleus of the medulla. Brain Res 460(2):339-345.

Cassell MD, Gray TS. 1989. The amygdala directly innervates adrenergic (C1) neurons in the ventrolateral medulla in the rat. Neurosci Lett 97(1-2):163-168.

Cavun S, Millington WR. 2001. Evidence that hemorrhagic hypotension is mediated by the ventrolateral periaqueductal gray region. Am J Physiol Regul Integr Comp Physiol 281(3):R747-R752.

Cescato R, Schulz S, Waser B, Eltschinger V, Rivier JE, Wester HJ, Culler M, Ginj M, Liu Q, Schonbrunn A, Reubi JC. 2006. Internalization of sst2, sst3, and sst5 receptors: effects of somatostatin agonists and antagonists. Journal of nuclear medicine : official publication, Society of Nuclear Medicine 47(3):502-511.

Chamberlin N, Saper C. 1994. Topographic organization of respiratory responses to glutamate microstimulation of the parabrachial nucleus in the rat. The Journal of Neuroscience 14(11):6500-6510.

Chen S, Aston-Jones G. 1995. Evidence that cholera toxin B subunit (CTb) can be avidly taken up and transported by fibers of passage. Brain Res 674(1):107-111.

Chessell IP, Black MD, Feniuk W, Humphrey PP. 1996. Operational characteristics of somatostatin receptors mediating inhibitory actions on rat locus coeruleus neurones. Br J Pharmacol 117(8):1673-1678.

Connor M, Bagley EE, Mitchell VA, Ingram SL, Christie MJ, Humphrey PP, Vaughan CW. 2004. Cellular actions of somatostatin on rat periaqueductal grey neurons in vitro. Br J Pharmacol 142(8):1273-1280.

Cox GE, Jordan D, Paton JF, Spyer KM, Wood LM. 1987. Cardiovascular and phrenic nerve responses to stimulation of the amygdala central nucleus in the anaesthetized rabbit. J Physiol 389:541-556.

Crestani CC, Alves FHF, Resstel LBM, CorrÃªa FMdA. 2006. The bed nucleus of the stria terminalis modulates baroreflex in rats. NeuroReport 17(14):1531-1535

Dampney RAL, Czachurski J, Dembowsky K, Goodchild AK, Seller H. 1987. Afferent connections and spinal projections of the pressor region in the rostral ventrolateral medulla of the cat. J Auton Nerv Syst 20(1):73-86.

De León M, Coveñas R, Narváez JA, Tramu G, Aguirre JA, González-Barón S. 1992. Distribution of somatostatin-28 (1–12) in the cat brainstem: an immunocytochemical study. Neuropeptides 21(1):1-11.

de Sousa Buck H, Caous CA, Lindsey CJ. 2001. Projections of the paratrigeminal nucleus to the ambiguus, rostroventrolateral and lateral reticular nuclei, and the solitary tract. Auton Neurosci 87(2-3):187-200.

deCampo DM, Fudge JL. 2013. Amygdala projections to the lateral bed nucleus of the stria terminalis in the macaque: Comparison with ventral striatal afferents. Journal of Comparative Neurology 521(14):3191-3216.

Dielenberg RA, Carrive P, McGregor IS. 2001. The cardiovascular and behavioral response to cat odor in rats: unconditioned and conditioned effects. Brain Res 897(1-2):228-237.

Dunn JD, Williams TJ. 1995. Cardiovascular responses to electrical stimulation of the bed nucleus of the stria terminalis. J Comp Neurol 352(2):227-234.

Dutschmann M, Herbert H. 2006. The Kolliker-Fuse nucleus gates the postinspiratory phase of the respiratory cycle to control inspiratory off-switch and upper airway resistance in rat. Eur J Neurosci 24(4):1071-1084.

Evans KC, Dougherty DD, Schmid AM, Scannell E, McCallister A, Benson H, Dusek JA, Lazar SW. 2009. Modulation of spontaneous breathing via limbic/paralimbic-bulbar circuitry: an event-related fMRI study. NeuroImage 47(3):961-971.

Fischer T, Doll C, Jacobs S, Kolodziej A, Stumm R, Schulz S. 2008. Reassessment of sst2 Somatostatin Receptor Expression in Human Normal and Neoplastic Tissues Using the Novel Rabbit Monoclonal Antibody UMB-1. The Journal of Clinical Endocrinology & Metabolism 93(11):4519-4524.

Frysinger RC, Marks JD, Trelease RB, Schechtman VL, Harper RM. 1984. Sleep states attenuate the pressor response to central amygdala stimulation. Experimental Neurology 83(3):604-617.

Gao LL, McMullan S, Djouhri L, Acosta C, Harper AA, Lawson SN. 2012. Expression and properties of hyperpolarization-activated current in rat dorsal root ganglion neurons with known sensory function. J Physiol 590(Pt 19):4691-4705.

Gelsema AJ, Copeland NE, Drolet G, Bachelard H. 1993. Cardiovascular effects of neuronal activation of the extended amygdala in rats. Brain Res 626(1-2):156-166.

Gelsema AJ, McKitrick DJ, Calaresu FR. 1987. Cardiovascular responses to chemical and electrical stimulation of amygdala in rats. Am J Physiol 253(5 Pt 2):R712-718.

Giehl K, Mestres P. 1995. Somatostatin-mRNA expression in brainstem projections into the medial preoptic nucleus. Exp Brain Res 103(3):344-354.

Gogolla N, Galimberti I, DePaola V, Caroni P. 2006. Staining protocol for organotypic hippocampal slice cultures. Nat Protoc 1(5):2452-2456.

Gonzalez BJ, Leroux P, Bodenant C, Laquerriere A, Coy DH, Vaudry H. 1989. Ontogeny of somatostatin receptors in the rat brain: biochemical and autoradiographic study. Neuroscience 29(3):629-644.

Gray PA. 2013. Transcription factors define the neuroanatomical organization of the medullary reticular formation. Front Neuroanat 7(APR):7.

Gray PA, Hayes JA, Ling GY, Llona I, Tupal S, Picardo MC, Ross SE, Hirata T, Corbin JG, Eugenin J, Del Negro CA. 2010. Developmental origin of preBotzinger complex respiratory neurons. J Neurosci 30(44):14883-14895.

Gray TS, Magnuson DJ. 1987. Neuropeptide neuronal efferents from the bed nucleus of the stria terminalis and central amygdaloid nucleus to the dorsal vagal complex in the rat. The Journal of Comparative Neurology 262(3):365-374.

Gray TS, Magnuson DJ. 1992. Peptide immunoreactive neurons in the amygdala and the bed nucleus of the stria terminalis project to the midbrain central gray in the rat. Peptides 13(3):451-460.

Harper RM, Frysinger RC, Trelease RB, Marks JD. 1984. State-dependent alteration of respiratory cycle timing by stimulation of the central nucleus of the amygdala. Brain Res 306(1-2):1-8.

He C, Chen F, Li B, Hu Z. 2014. Neurophysiology of HCN channels: from cellular functions to multiple regulations. Prog Neurobiol 112:1-23.

Holstege G, Meiners L, Tan K. 1985. Projections of the bed nucleus of the stria terminalis to the mesencephalon, pons, and medulla oblongata in the cat. Experimental brain research 58(2):379-391.

Hopkins DA, Holstege G. 1978. Amygdaloid projections to the mesencephalon, pons and medulla oblongata in the cat. Experimental Brain Research 32(4):529-547.

Horie K, Insel PA. 2000. Retrovirally mediated transfer of a G protein-coupled receptor kinase (GRK) dominant-negative mutant enhances endogenous calcitonin receptor signaling in Chinese hamster ovary cells. GRK inhibition enhances expression of receptors and receptor mRNA. J Biol Chem 275(38):29433-29440.

Inoue M, Nakajima S, Nakajima Y. 1988. Somatostatin induces an inward rectification in rat locus coeruleus neurones through a pertussis toxin-sensitive mechanism. Journal of Physiology 407:177-198.

Iwata J, Chida K, LeDoux JE. 1987. Cardiovascular responses elicited by stimulation of neurons in the central amygdaloid nucleus in awake but not anesthetized rats resemble conditioned emotional responses. Brain Res 418(1):183-188.

Kangrga IM, Loewy AD. 1995. Whole-cell recordings from visualized C1 adrenergic bulbospinal neurons: Ionic mechanisms underlying vasomotor tone. Brain Research 670(2):215-232.

Kawai Y, Inagaki S, Shiosaka S, Senba E, Hara Y, Sakanaka M, Takatsuki K, Tohyama M. 1982. Long descending projections from amygdaloid somatostatin-containing cells to the lower brain stem. Brain Research 239(2):603-607.

Kawai Y, Qi J, Comer AM, Gibbons H, Win J, Lipski J. 1999. Effects of cyanide and hypoxia on membrane currents in neurones acutely dissociated from the rostral ventrolateral medulla of the rat. Brain Research 830(2):246-257.

Kawashima T, Kitamura K, Suzuki K, Nonaka M, Kamijo S, Takemoto-Kimura S, Kano M, Okuno H, Ohki K, Bito H. 2013. Functional labeling of neurons and their projections using the synthetic activity-dependent promoter E-SARE. Nature Methods 10(9):889-895.

Kerr DIB, Ong J. 1995. GABAB receptors. Pharmacology & Therapeutics 67(2):187-246.

Kiyama H, Emson PC. 1990. Distribution of somatostatin mRNA in the rat nervous system as visualized by a novel non-radioactive in situ hybridization histochemistry procedure. Neuroscience 38(1):223-244.

Korim WS, Bou Farah L, McMullan S, Verberne AJ. 2014. Orexinergic activation of medullary premotor neurons modulates the adrenal sympathoexcitation to hypothalamic glucoprivation. Diabetes 63(6):1895-1906.

Korner M, Eltschinger V, Waser B, Schonbrunn A, Reubi JC. 2005. Value of immunohistochemistry for somatostatin receptor subtype sst2A in cancer tissues: lessons from the comparison of anti-sst2A antibodies with somatostatin receptor autoradiography. The American journal of surgical pathology 29(12):1642-1651.

Kreienkamp H-J, Hönck H-H, Richter D. 1997. Coupling of rat somatostatin receptor subtypes to a G-protein gated inwardly rectifying potassium channel (GIRK1). FEBS Letters 419(1):92-94.

Kumar NN, Ferguson J, Padley JR, Pilowsky PM, Goodchild AK. 2009. Differential muscarinic receptor gene expression levels in the ventral medulla of spontaneously hypertensive and Wistar-Kyoto rats: role in sympathetic baroreflex function. J Hypertens 27(5):1001-1008.

Lara JP, Parkes MJ, Silva-Carvhalo L, Izzo P, Dawid-Milner MS, Spyer KM. 1994. Cardiovascular and respiratory effects of stimulation of cell bodies of the parabrachial nuclei in the anaesthetized rat. The Journal of Physiology 477(Pt 2):321-329.

LeDoux J, Iwata J, Cicchetti P, Reis D. 1988. Different projections of the central amygdaloid nucleus mediate autonomic and behavioral correlates of conditioned fear. The Journal of Neuroscience 8(7):2517-2529.

Lefkowitz RJ. 1998. G protein-coupled receptors. III. New roles for receptor kinases and beta-arrestins in receptor signaling and desensitization. J Biol Chem 273(30):18677-18680.

Li C-S, Cho YK. 2006. Efferent projection from the bed nucleus of the stria terminalis suppresses activity of taste-responsive neurons in the hamster parabrachial nuclei. American Journal of Physiology - Regulatory, Integrative and Comparative Physiology 291(4):R914-R926.

Li Q, Goodchild AK, Seyedabadi M, Pilowsky PM. 2005. Preprotachykinin A mRNA is colocalized with tyrosine hydroxylase-immunoreactivity in bulbospinal neurons. Neuroscience 136(1):205-216.

Li YW, Bayliss DA, Guyenet PG. 1995. C1 neurons of neonatal rats: intrinsic beating properties and alpha 2-adrenergic receptors. Am J Physiol 269(6 Pt 2):R1356-1369.

Li YW, Guyenet PG. 1996. Activation of GABA(B) receptors increases a potassium conductance in rat bulbospinal neurons of the C1 area. American Journal of Physiology-Regulatory Integrative and Comparative Physiology 271(5):R1304-R1310.

Lindsey CJ, Buck HS, Fior-Chadi DR, Lapa RC. 1997. Pressor effect mediated by bradykinin in the paratrigeminal nucleus of the rat. J Physiol 502 (Pt 1):119-129.

Liu Q, Dewi DA, Liu W, Bee MS, Schonbrunn A. 2008. Distinct phosphorylation sites in the SST2A somatostatin receptor control internalization, desensitization, and arrestin binding. Molecular pharmacology 73(2):292-304.

Lovick TA. 1992. Inhibitory modulation of the cardiovascular defence response by the ventrolateral periaqueductal grey matter in rats. Exp Brain Res 89(1):133-139.

Luppi PH, Fort P, Jouvet M. 1990. Iontophoretic application of unconjugated cholera toxin B subunit (CTb) combined with immunohistochemistry of neurochemical substances: a method for transmitter identification of retrogradely labeled neurons. Brain Research 534(1-2):209-224.

Lüscher C, Jan LY, Stoffel M, Malenka RC, Nicoll RA. 1997. G protein-coupled inwardly rectifying K+ channels (GIRKs) mediate postsynaptic but not presynaptic transmitter actions in hippocampal neurons. Neuron 19(3):687-695.

M'Hamed S, B., Sequeira H, Poulain P, Bennis M, Roy JC. 1993. Sensorimotor cortex projections to the ventrolateral and the dorsomedial medulla oblongata in the rat. Neurosci Lett 164(1-2):195-198.

Miyawaki T, Goodchild AK, Pilowsky PM. 2003. Maintenance of sympathetic tone by a nickel chloride-sensitive mechanism in the rostral ventrolateral medulla of the adult rat. Neuroscience 116(2):455-464.

Moga MM, Saper CB, Gray TS. 1989. Bed nucleus of the stria terminalis: cytoarchitecture, immunohistochemistry, and projection to the parabrachial nucleus in the rat. J Comp Neurol 283(3):315-332.

Morschel M, Dutschmann M. 2009. Pontine respiratory activity involved in inspiratory/expiratory phase transition. Philos Trans R Soc Lond B Biol Sci 364(1529):2517-2526.

Nakatsuka T, Fujita T, Inoue K, Kumamoto E. 2008. Activation of GIRK channels in substantia gelatinosa neurones of the adult rat spinal cord: a possible involvement of somatostatin. The Journal of Physiology 586(10):2511-2522.

Nunn C, Schoeffter P, Langenegger D, Hoyer D. 2003. Functional characterisation of the putative somatostatin sst2 receptor antagonist CYN 154806. Naunyn-Schmiedeberg's archives of pharmacology 367(1):1-9.

O'Carroll AM, Lolait SJ, König M, Mahan LC. 1992. Molecular cloning and expression of a pituitary somatostatin receptor with preferential affinity for somatostatin-28. Molecular pharmacology 42(6):939-946.

Padley JR, Kumar NN, Li Q, Nguyen TB, Pilowsky PM, Goodchild AK. 2007. Central command regulation of circulatory function mediated by descending pontine cholinergic inputs to sympathoexcitatory rostral ventrolateral medulla neurons. Circ Res 100(2):284-291.

Panguluri S, Saggu S, Lundy R. 2009. Comparison of somatostatin and corticotrophin-releasing hormone immunoreactivity in forebrain neurons projecting to taste-responsive and non-responsive regions of the parabrachial nucleus in rat. Brain Res 1298:57-69.

Paré D, Quirk GJ, Ledoux JE. 2004. New Vistas on Amygdala Networks in Conditioned Fear. Journal of Neurophysiology 92(1):1-9.

Patel YC. 1999. Somatostatin and Its Receptor Family. Frontiers in Neuroendocrinology 20(3):157-198.

Patel YC, O'Neil W. 1988. Peptides derived from cleavage of prosomatostatin at carboxyl- and amino-terminal segments. Characterization of tissue and secreted forms in the rat. Journal of Biological Chemistry 263(2):745-751.

Paxinos G, Watson C. 2006. The Rat Brain in Stereotaxic Coordinates: Academic Press.

Premont RT, Inglese J, Lefkowitz RJ. 1995. Protein kinases that phosphorylate activated G protein-coupled receptors. FASEB J 9(2):175-182.

Priestley T. 1992. The effect of baclofen and somatostatin on neuronal activity in the rat ventromedial hypothalamic nucleus in vitro. Neuropharmacology 31(2):103-109.

Rabbani SN, Patel YC. 1990. Peptides derived by processing of rat prosomatostatin near the amino-terminus: Characterization, tissue distribution, and release. Endocrinology 126(4):2054-2061.

Ramírez-Jarquín JO, Lara-Hernández S, López-Guerrero JJ, Aguileta MA, Rivera-Angulo AJ, Sampieri A, Vaca L, Ordaz B, Peña-Ortega F. 2012. Somatostatin modulates generation of inspiratory rhythms and determines asphyxia survival. Peptides 34(2):360-372.

Real MA, Heredia R, del Carmen Labrador M, Dávila JC, Guirado S. 2009. Expression of somatostatin and neuropeptide Y in the embryonic, postnatal, and adult mouse amygdalar complex. The Journal of Comparative Neurology 513(4):335-348.

Robinson RB, Siegelbaum SA. 2003. Hyperpolarization-activated cation currents: from molecules to physiological function. AnnuRevPhysiol 65:453.

Roozendaal B, Koolhaas JM, Bohus B. 1991. Central amygdala lesions affect behavioral and autonomic balance during stress in rats. Physiology & Behavior 50(4):777-781.

Ross CA, Ruggiero DA, Reis DJ. 1985. Projections from the nucleus tractus solitarii to the rostral ventrolateral medulla. J Comp Neurol 242(4):511-534.

Saggu S, Lundy RF. 2008. Forebrain neurons that project to the gustatory parabrachial nucleus in rat lack glutamic acid decarboxylase. American Journal of Physiology - Regulatory, Integrative and Comparative Physiology 294(1):R52-R57.

Saha S, Drinkhill MJ, Moore JP, Batten TF. 2005. Central nucleus of amygdala projections to rostral ventrolateral medulla neurones activated by decreased blood pressure. Eur J Neurosci 21(7):1921-1930.

Saha S, Henderson Z, Batten TFC. 2002. Somatostatin immunoreactivity in axon terminals in rat nucleus tractus solitarii arising from central nucleus of amygdala: coexistence with GABA and postsynaptic expression of sst2A receptor. Journal of Chemical Neuroanatomy 24(1):1-13.

Samson WK, Zhang JV, Avsian-Kretchmer O, Cui K, Yosten GLC, Klein C, Lyu R-M, Wang YX, Chen XQ, Yang J, Price CJ, Hoyda TD, Ferguson AV, Yuan X-b, Chang JK, Hsueh AJW. 2008. Neuronostatin Encoded by the Somatostatin Gene Regulates Neuronal, Cardiovascular, and Metabolic Functions. Journal of Biological Chemistry 283(46):31949-31959.

Schulz S, Schreff M, Schmidt H, Händel M, Przewlocki R, Höllt V. 1998a. Immunocytochemical localization of somatostatin receptor sst2A in the rat spinal cord and dorsal root ganglia. European Journal of Neuroscience 10(12):3700-3708.

Schulz S, Schulz S, Schmitt J, Wiborny D, Schmidt H, Olbricht S, Weise W, Roessner A, Gramsch C, Höllt V. 1998b. Immunocytochemical detection of somatostatin receptors sst1 sst(2A), sst(2B), and sst3 in paraffin-embedded breast cancer tissue using subtype- specific antibodies. Clinical Cancer Research 4(9):2047-2052.

Shapiro MS, Hille B. 1993. Substance P and somatostatin inhibit calcium channels in rat sympathetic neurons via different G protein pathwavs. Neuron 10(1):11-20.

Sherwood A, Dolan CA, Light KC. 1990. Hemodynamics of Blood Pressure Responses During Active and Passive Coping. Psychophysiology 27(6):656-668.

Smith DV, Ye M-K, Li C-S. 2005. Medullary Taste Responses are Modulated by the Bed Nucleus of the Stria Terminalis. Chemical senses 30(5):421-434.

Smith GST, Savery D, Marden C, Costa JJL, Averill S, Priestley JV, Rattray M. 1994. Distribution of messenger RNAs encoding enkephalin, substance P, somatostatin, galanin, vasoactive intestinal polypeptide, neuropeptide Y, and calcitonin gene-related peptide in the midbrain periaqueductal grey in the rat. The Journal of Comparative Neurology 350(1):23-40.

Smith JC, Morrison DE, Ellenberger HH, Otto MR, Feldman JL. 1989. Brainstem projections to the major respiratory neuron populations in the medulla of the cat. J Comp Neurol 281:69-96.

Sousa LO, Lindsey CJ. 2009a. Cardiovascular and baroreceptor functions of the paratrigeminal nucleus for pressor effects in non-anaesthetized rats. Auton Neurosci 147(1-2):27-32.

Sousa LO, Lindsey CJ. 2009b. Discharge rate profiles of paratrigeminal nucleus neurons throughout a pressor event in non-anaesthetized rats. Auton Neurosci 147(1-2):20-26.

Spary EJ, Maqbool A, Batten TF. 2008. Expression and localisation of somatostatin receptor subtypes sst1-sst5 in areas of the rat medulla oblongata involved in autonomic regulation. J Chem Neuroanat 35(1):49-66.

Stock G, Schlör KH, Heidt H, Buss J. 1978. Psychomotor behaviour and cardiovascular patterns during stimulation of the amygdala. Pflügers Arch 376(2):177-184.

Stornetta RL, Rosin DL, Wang H, Sevigny CP, Weston MC, Guyenet PG. 2003. A group of glutamatergic interneurons expressing high levels of both neurokinin-1 receptors and somatostatin identifies the region of the pre-Botzinger complex. Journal of Comparative Neurology 455(4):499-512.

Takayama K, Miura M. 1991. Glutamate-immunoreactive neurons of the central amygdaloid nucleus projecting to the subretrofacial nucleus of SHR and WKY rats: A double-labeling study. Neuroscience Letters 134(1):62-66.

Tan W, Janczewski WA, Yang P, Shao XM, Callaway EM, Feldman JL. 2008. Silencing preBotzinger complex somatostatin-expressing neurons induces persistent apnea in awake rat. Nat Neurosci 11(5):538-540.

Tan W, Pagliardini S, Yang P, Janczewski WA, Feldman JL. 2010. Projections of preBotzinger complex neurons in adult rats. J Comp Neurol 518(10):1862-1878.

Thoss VS, Ferez J, Duc D, Hoyer D. 1995. Embryonic and postnatal mRNA distribution of five somatostatin receptor subtypes in the rat brain. Neuropharmacology 34(12):1673-1688.

Tupal S, Rieger MA, Ling GY, Park TJ, Dougherty JD, Goodchild AK, Gray PA. 2014. Testing the role of preBotzinger Complex somatostatin neurons in respiratory and vocal behaviors. Eur J Neurosci 40(7):3067-3077.

Vanetti M, Kouba M, Wang X, Vogt G, Höllt V. 1992. Cloning and expression of a novel mouse somatostatin receptor (SSTR2B). FEBS Letters 311(3):290-294.

Vanetti M, Ziolkowska B, Wang X, Horn G, Hollt V. 1994. mRNA distribution of two isoforms of somatostatin receptor 2 (mSSTR2A and mSSTR2B) in mouse brain. Brain Res Mol Brain Res 27(1):45-50.

Veening JG, Swanson LW, Sawchenko PE. 1984. The organization of projections from the central nucleus of the amygdala to brainstem sites involved in central autonomic regulation: A combined retrograde transport-immunohistochemical study. Brain Research 303(2):337-357.

Viana F, Hille B. 1996. Modulation of High Voltage-Activated Calcium Channels by Somatostatin in Acutely Isolated Rat Amygdaloid Neurons. The Journal of Neuroscience 16(19):6000-6011.

Vincent SR, McIntosh CHS, Buchan AMJ, Brown JC. 1985. Central somatostatin systems revealed with monoclonal antibodies. The Journal of Comparative Neurology 238(2):169-186.

von Leupoldt A, Sommer T, Kegat S, Baumann HJr, Klose H, Dahme B, BÃ¼chel C. 2008. The Unpleasantness of Perceived Dyspnea Is Processed in the Anterior Insula and Amygdala. American Journal of Respiratory and Critical Care Medicine 177(9):1026-1032.

Wang HL, Dichter M, Reisine T. 1990. Lack of cross-desensitization of somatostatin-14 and somatostatin-28 receptors coupled to potassium channels in rat neocortical neurons. Molecular pharmacology 38(3):357-361.

Wang WH, Lovick TA. 1993. The inhibitory effect of the ventrolateral periaqueductal grey matter on neurones in the rostral ventrolateral medulla involves a relay in the medullary raphe nuclei. Exp Brain Res 94(2):295-300.

Waraczynski M. 2003. Lidocaine inactivation demonstrates a stronger role for central versus medial extended amygdala in medial forebrain bundle self-stimulation. Brain Res 962(1-2):180-198.

Ward DG. 1988. Stimulation of the parabrachial nuclei with monosodium glutamate increases arterial pressure. Brain Research 462(2):383-390.

Wilensky AE, Schafe GE, Kristensen MP, LeDoux JE. 2006. Rethinking the Fear Circuit: The Central Nucleus of the Amygdala Is Required for the Acquisition, Consolidation, and Expression of Pavlovian Fear Conditioning. The Journal of Neuroscience 26(48):12387-12396.

Yasuda K, Rens-Domiano S, Breder CD, Law SF, Saper CB, Reisine T, Bell GI. 1992. Cloning of a novel somatostatin receptor, SSTR3, coupled to adenylylcyclase. Journal of Biological Chemistry 267(28):20422-20428.

Yin H, Lee KE, Park SA, Bhattarai JP, Suh BJ, Jeon JG, Kim BG, Park SJ, Han SK. 2009. Inhibitory effects of somatostatin on the substantia gelatinosa neurons of trigeminal subnucleus caudalis via somatostatin type 2 receptors in juvenile mice. Brain Res 1304:49-56.

Yosten GLC, Pate AT, Samson WK. 2011. Neuronostatin acts in brain to biphasically increase mean arterial pressure through sympatho-activation followed by vasopressin secretion: The role of melanocortin receptors. American Journal of Physiology - Regulatory Integrative and Comparative Physiology 300(5):R1194-R1199.

Young Shim E, Jung Kim H, Kim MJ, Rhie DJ, Jo YH, Kim MS, June Hahn S, Lee MY, Yoon SH. 2006. Desensitization of somatostatin-induced inhibition of low extracellular magnesium concentration-induced calcium spikes in cultured rat hippocampal neurons. Brain Res 1111(1):61-71.

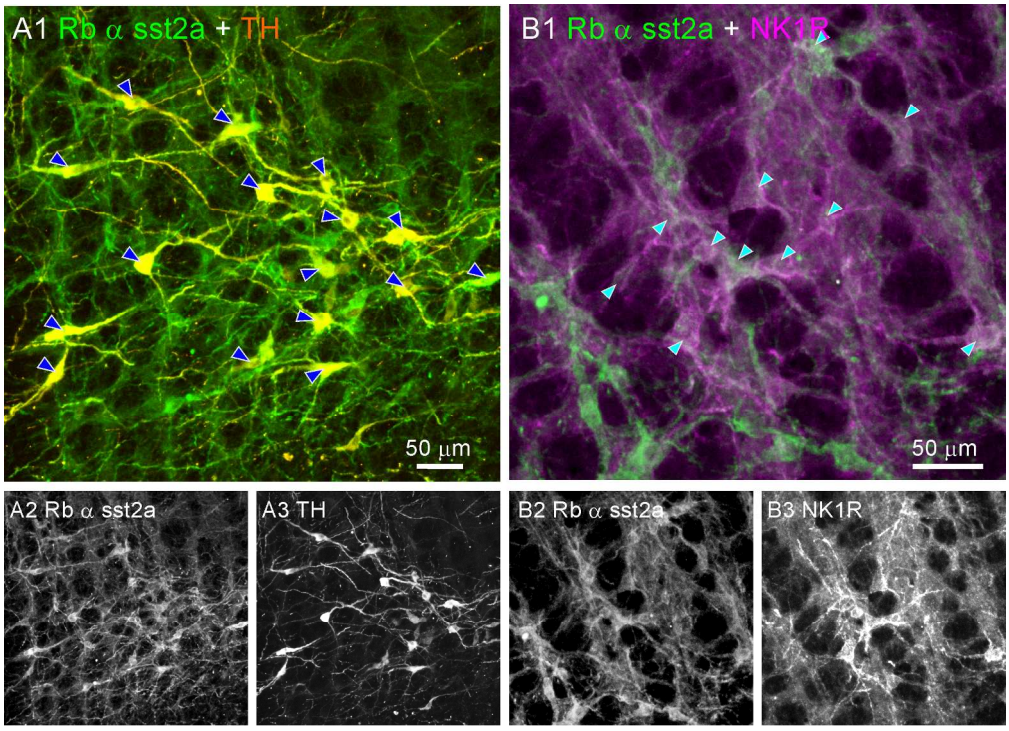

Figure 1 Distribution of rabbit anti-sst2a antibody binding in the ventrolateral medulla. Confocal stack images demonstrate colocalization of rabbit anti-sst2a immunoreactivity with tyrosine hydroxylase (TH) in the RVLM, 200 μm caudal to the facial nucleus (A) and with neurokinin-1 receptor (NK1R) in the Pre-Bötzinger Complex, 800 μm caudal to the facial nucleus (B). Individual channel images shown in panels 2 & 3. Arrowheads indicate double-labelled neurons.
211x152mm (300 x 300 DPI)

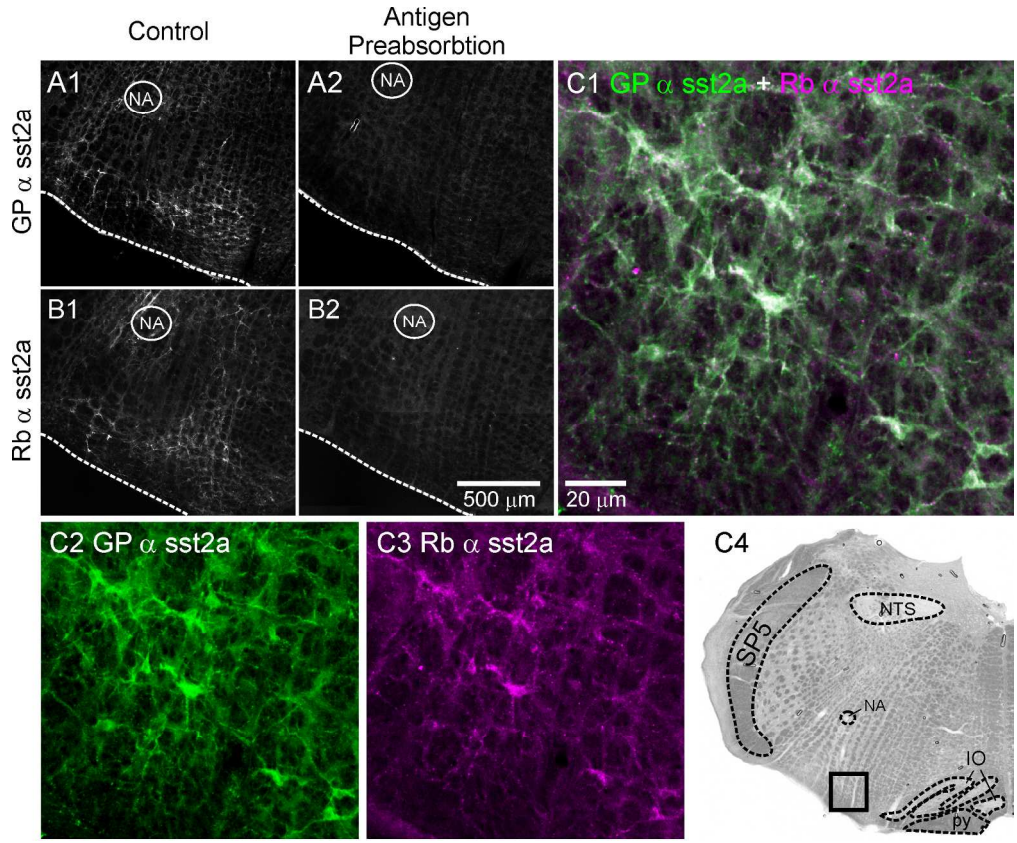

Figure 2 Comparison of rabbit and guinea pig anti-sst2a antibody binding. Epifluorescent images demonstrate binding of anti-sst2a primary antibodies raised in guinea pig (A1) and rabbit (B1), which was blocked by incubating alternate sections from the same animals with the antigen (A2 & B2), and resulted in overlapping patterns of expression when incubated together (C1). C2 and C3 depict individual channels from merged image shown in C1. Box in C4 shows region in which high powered images shown in C were taken. NA = nucleus ambiguus; NTS = nucleus of the solitary tract. IO = inferior olive; PY = pyramidal tract; SP5 = Spinal trigeminal nucleus.
204x169mm (300 x 300 DPI)

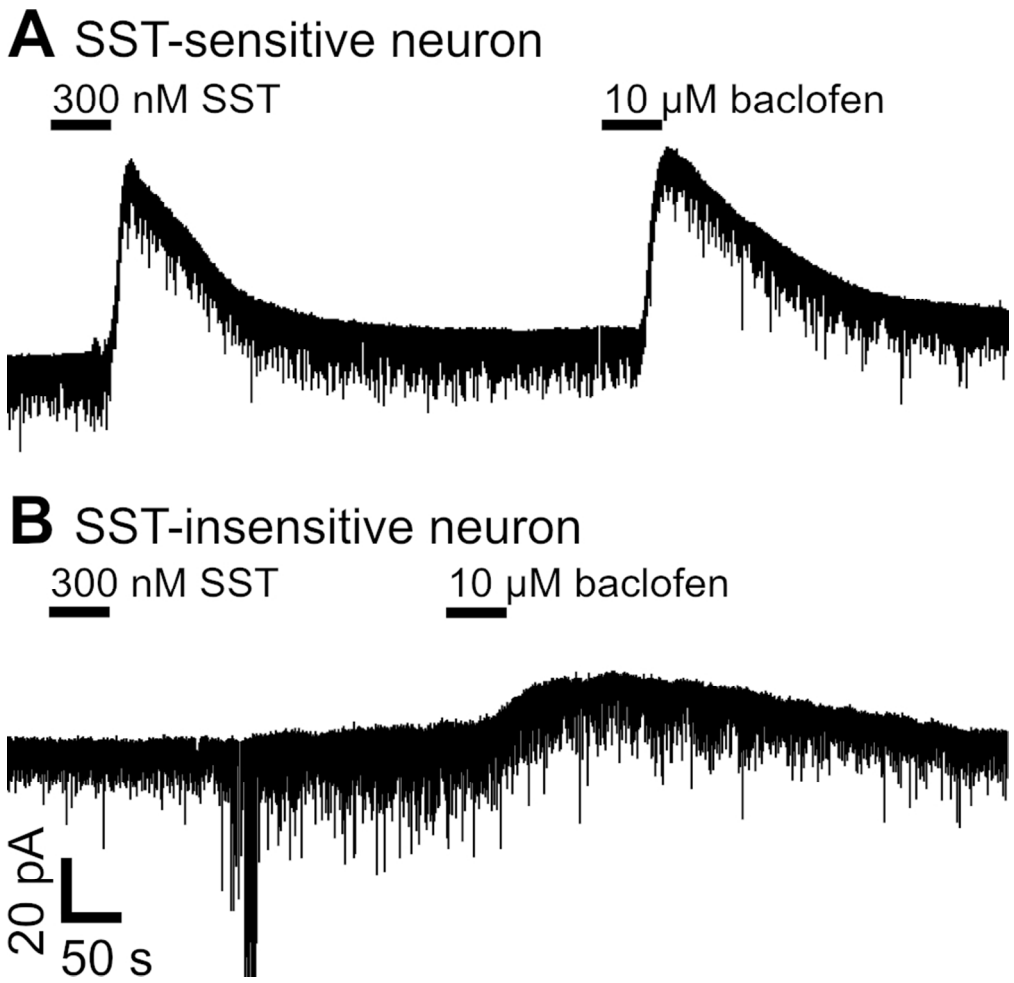

Figure 3 Electrophysiological characterization of outward currents evoked by SST. (A). Voltage clamp recordings from CTB-labelled RVLM neurons: bulbospinal RVLM neurons in which SST and baclofen perfusion (black horizontal bars indicate time of application) evoked outward currents were categorized as SST-sensitive. (B) Bulbospinal RVLM neurons in which baclofen but not SST evoked outward currents were considered SST-insensitive.
85x82mm (300 x 300 DPI)

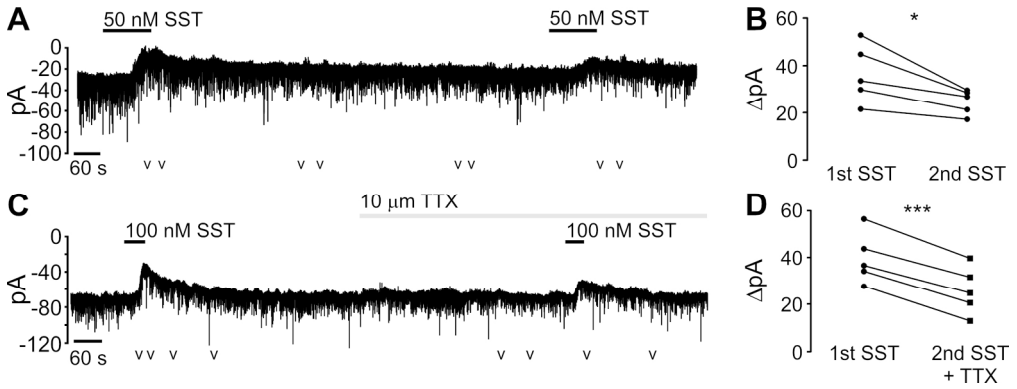

Figure 4 Responses of bulbospinal RVLM neurons to repeated SST application exhibited desensitization. (A) Voltage-clamp recordings illustrate desensitization of responses to repeated application of 50 nM SST ('v' denotes timing of voltage steps; steps have been removed from traces to aid clarity). (B) Pooled data; responses to 50, 100 and 300 nM SST have been combined. (C) Experimental recording demonstrating that responses to repeated SST were unaffected by tetrodotoxin (TTX). (D) Pooled data of responses to 100 nM SST before and after addition of TTX to the perfusate. *: P<0.05, ***: P<0.001.
177x66mm (300 x 300 DPI)

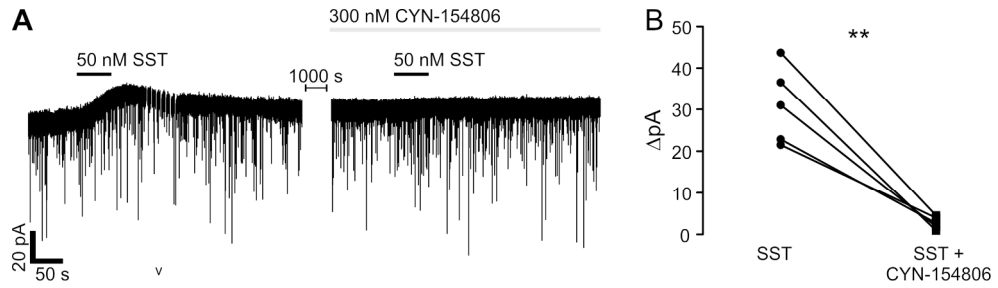

Figure 5 sst2 blockade abolished SST-induced outward currents. (A) Voltage-clamp recordings of responses to SST application before and after superfusion with the sst2 blocker CYN-154806 ('v' denotes timing of voltage steps). B: pooled data showing effects of SST2 blockade on five SST-sensitive spinally projecting RVLM neurons. **: P<0.01.
193x52mm (300 x 300 DPI)

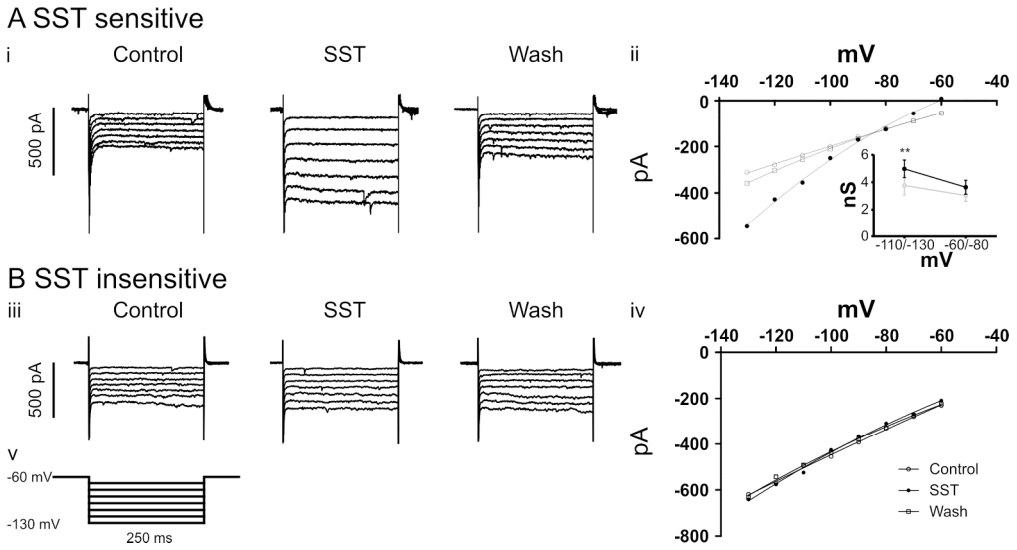

Figure 6 Current-voltage relationship of SST-sensitive (A) and SST-insensitive (B) bulbospinal RVLM neurons. Examples of membrane currents evoked by voltage steps before, during and after 300 nM SST superfusion; experimental recordings are shown in i and iii, I-V plots are shown in ii and iv. 250 ms command voltages were stepped from -60 to -130 mV in 10 mV increments (v). Inset in A(ii) denotes pooled slope conductances from 17 SST-sensitive bulbospinal neurons. **: P<0.01, Bonferroni post-test.
200x107mm (300 x 300 DPI)

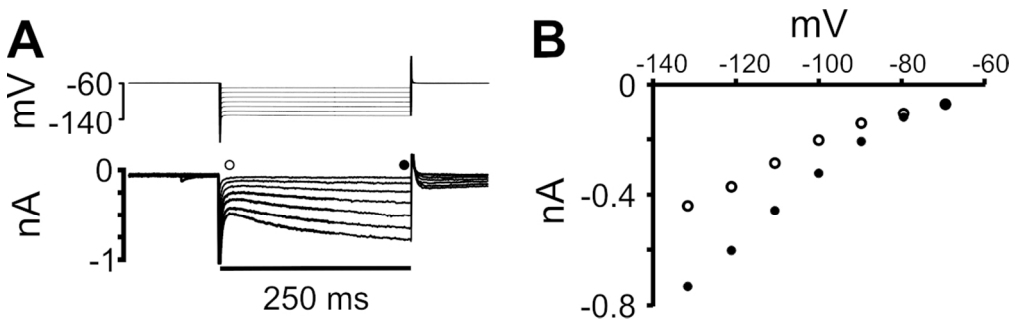

Figure 7 Example of hyperpolarization-activated inward current recorded in a bulbospinal RVLM neuron. (A) Hyperpolarizing membrane steps from -70 to -130 mV evoked a slowly activating inward current. The amplitude of the hyperpolarization-activated current was estimated by measuring the difference between the instantaneous (open circle) and steady-state currents (closed circles) evoked by each step (B).
108x33mm (300 x 300 DPI)

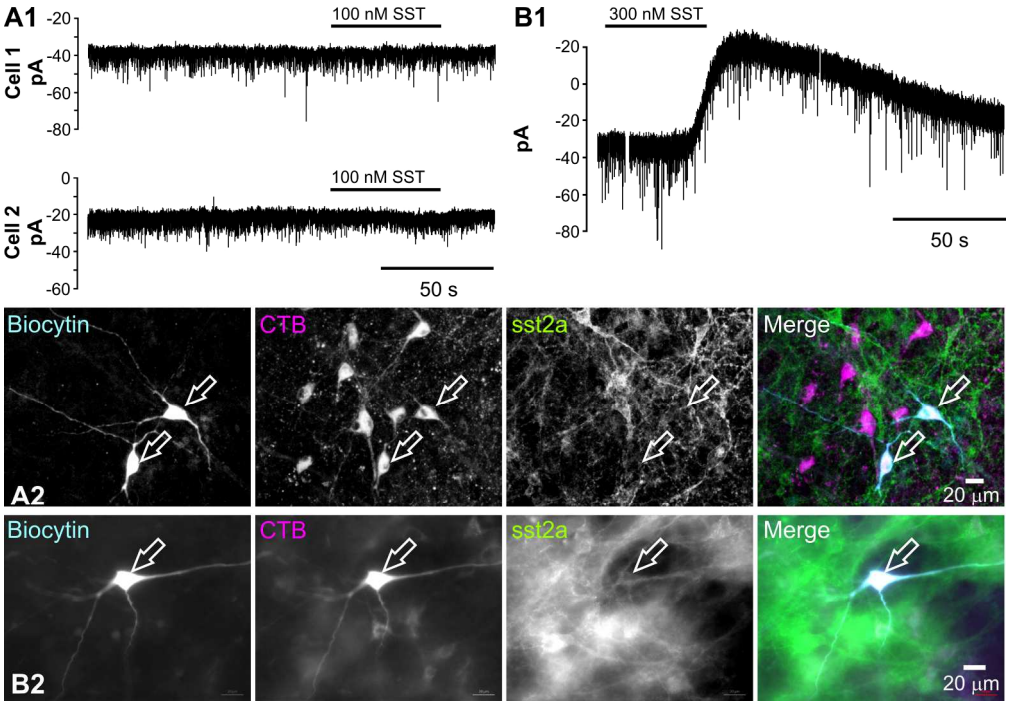

Figure 8 Immunohistochemical recovery of electrophysiologically characterised RVLM bulbospinal neurons. (A1) Simultaneous voltage-clamp recordings from two bulbospinal RVLM neurons recorded with biocytin-filled pipettes; neither responded to 100 nM SST application. (A2) 22 µm thick confocal projection image of the same neurons; both biocytin-filled neurons were confirmed as CTB-positive and sst2a-negative. (B1) Example of an SST-sensitive neuron recorded in a different experiment; the neuron was subsequently shown to be weakly sst2a-immunoreactive under epifluorescence (B2). Breaks in recording B1 indicate switches in recording mode at which seal resistance was assessed.
208x144mm (300 x 300 DPI)

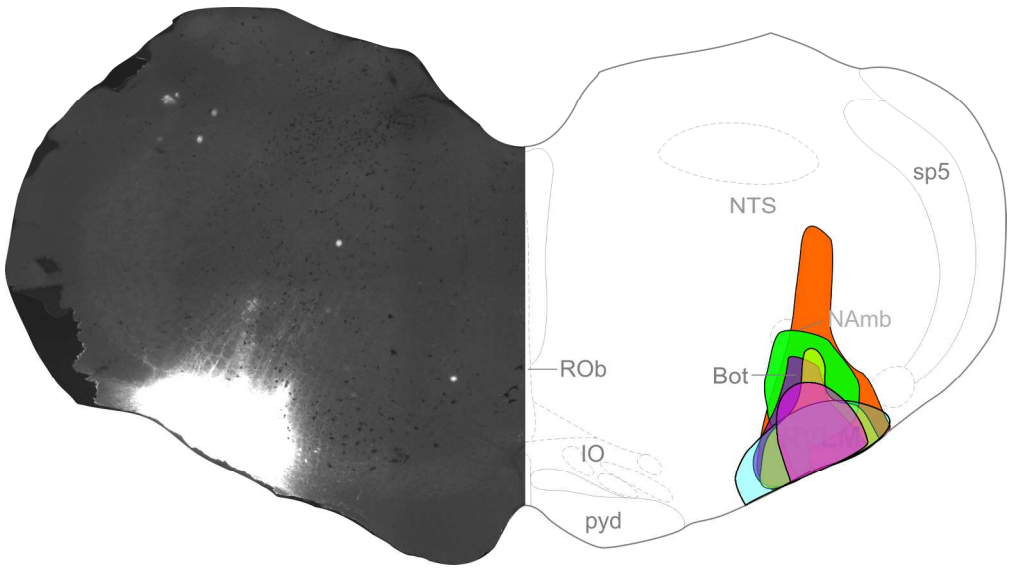

Figure 9 CTB injection sites targeting the RVLM. The left coronal hemisection shows the CTB injection site from one animal. The right hemisection shows schematically the extents of six injection sites in animals used for quantitative analysis.
197x109mm (300 x 300 DPI)

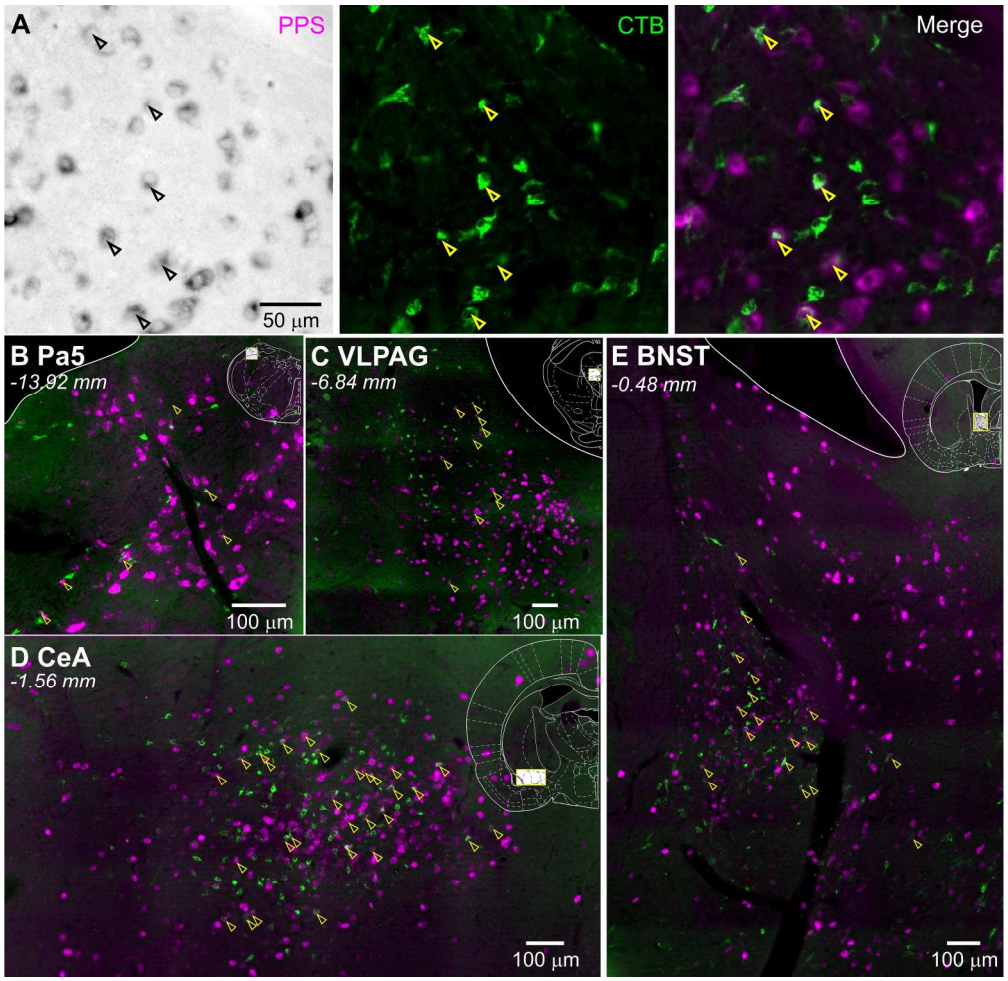

Figure 10 Combined PPS in situ hybridization and retrograde tracing reveals putative RVLM-projecting somatostatinergic neurons. (A) High power photomicrograph showing neurons labelled for PPS mRNA (brightfield) and CTB immunofluorescence (green channel). Double-labelled neurons are indicated by arrowheads; PPS mRNA is magenta in merged pseudocolored images. Merged epifluorescence images in B – E illustrate the distribution of double-labelled neurons in the paratrigeminal nucleus (Pa5, B), ventrolateral periaqueductal grey (VLPAG, C), central nucleus of the amygdala (CeA, D), and bed nucleus of the stria terminalis (BNST, E). A schematic diagram indicating the region shown (yellow box) and the rostrocaudal co-ordinate with respect to Bregma is superimposed onto each photomicrograph; schematic diagrams adapted from Paxinos and Watson (2006).
208x202mm (300 x 300 DPI)

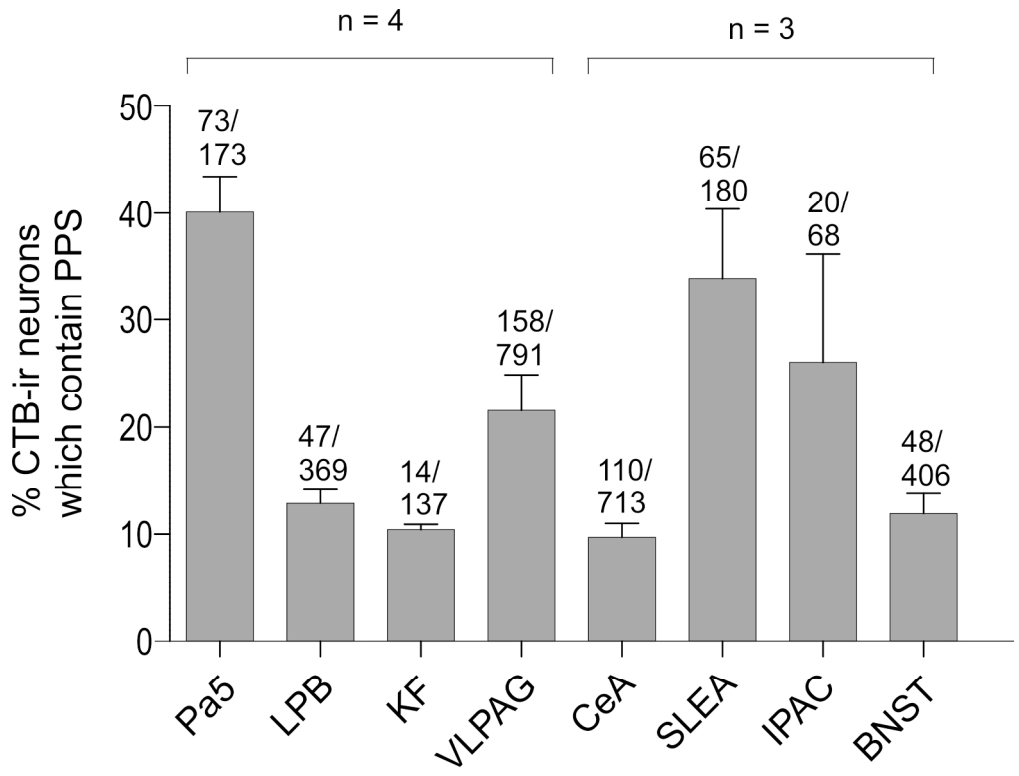

Figure 11 Brain regions containing RVLM projecting (CTB-ir) neurons that express PPS mRNA.
198x151mm (300 x 300 DPI)

Antibody Name	Immunogen	Manufacturer Details	Concentration
Primary Antibodies			
Guinea pig anti-SST_{2a}	C-terminus amino acid sequence 355-369 (ETQRTLLNGDLQTSI) of synthetic sst2a peptide	Gramsch Laboratories, Schwabhausen Germany Cat# SS-870 RRID: AB_2491104 Polyclonal	1:1000
Rabbit anti-SST_{2a}	C-terminus amino acid sequence 355-369 (ETQRTLLNGDLQTSI) of synthetic sst2a peptide	Bio-trend Cat# ss-8000-rmc Lot# a080826 RRID: AB_2491103 Monoclonal	1:100
Guinea pig anti-neurokinin 1 receptor (NK1R)	C-terminus synthetic rat NK1R	Millipore Cat# AB15810 Lot# LV1587443 RRID: AB_992894 Polyclonal	1:1000
Mouse anti-tyrosine hydroxylase (TH)	Rat tyrosine hydroxylase N-terminal region (approx. aa 9-16)	Sigma-Aldrich Cat# T1299 RRID: AB_477560 Monoclonal	1:8000
Rabbit anti-CTB	B subunit of cholera toxin	ViroStat, USA Cat# 7927 RRID: AB_2313635 Polyclonal	1:5000
Sheep anti-digoxigenin	Digoxigenin, whole	Roche Applied Science Cat# 11093274910 RRID: AB_514497 Polyclonal	1:1000
Secondary Antibodies			
ExtrAvidin®-FITC	n/a	Sigma-Aldrich Cat# E2761 RRID: AB_2492295	1:500
Alexa Fluor® 647-AffiniPure Donkey Anti-Rabbit IgG (H+L)	Whole molecule rabbit IgG	Jackson ImmunoResearch Laboratories, INC Cat# 711-605-152 Lot# 105115 RRID: AB_2492288 Polyclonal	1:250
Cy3®- AffiniPure Donkey anti-Goat IgG (H+L)	Whole molecule goat IgG	Jackson ImmunoResearch Laboratories, INC Cat# 705-165-147 Lot# 68839 RRID: AB_2307351 Polyclonal	1:250
Alexa Fluor® 488-AffiniPure Donkey Anti-Guinea Pig IgG	Whole molecule guinea pig IgG	Jackson ImmunoResearch Laboratories, INC	1:250

(H+L)		Cat# 706-545-148 Lot# 161406 RRID: AB_2340472 Polyclonal	
Dylight 488-conjugated Donkey anti-rabbit IgG (H+L)	Whole molecule rabbit IgG	Jackson Immunoresearch Laboratories, RRID: AB_2492289) Polyclonal	1:500
Alexa Fluor® 488 Donkey Anti-mouse IgG (H+L)	Mouse, IgG heavy & light chains	Life Technologies Cat# A21202 RRID: AB_10049285 Polyclonal	1:250

Location	Subregion	Laterality of CTB	CTB	PPS
Cortical	Motor Cortex (MC)	Bi	++	+++
	Sensory Cortex (SC)	Bi	++	++
	Infralimbic Cortex (IL)	Bi	+++	+++
	Prelimbic Cortex (PrL)	Bi	++	+++
	Insular Cortex (IC)	Bi	++	++
Subcortical	Vascular Organ, Lamina Terminalis	-	++	+
	Medial Preoptic Area (MPA)	bi	++	+
	Bed Nucleus, Stria Terminalis (BNST)	bi	+++	++++
	Interstitial Nucleus of Posterior Limb, Anterior Commissure (IPAC)	ipsi	++	+++
	Sublenticular Extended Amygdala (SLEA)	ipsi	+++	+++
		bi	++++	++
	Paraventricular Nucleus, Hypothalamus (PVN)			
	Ventromedial Hypothalamus (VMH)	Bi	+	+++
	Central Nucleus of the Amygdala (CeA)	ipsi	++++	+++
	Dorsomedial Hypothalamus (DMH)	bi	++	++
	Zona Incerta (ZI)	bi	++	
	Lateral Hypothalamic Area (LHA)	Bi	+++	++
Midbrain	Lateral PAG (LPAG)	bi	+	++
	Ventrolateral PAG (VLPAG)	bi	+++	+++

	Dorsomedial PAG (DMPAG)	bi	+++	++
	Oculomotor Nucleus, Parvicellular (3PC)	contra	+	++++
	Intermediate White Layer, Superior Colliculus (InWh)	contra	+	+
	Inferior Colliculus (InC)	bi	++	+++
	Dorsal Raphe, Caudal Part (DRC)	-	++	-
	Retrorubral Field (RRF)	Bi	++	+
Pons	Pedunculopontine Tegmental Area (PPTg)	Bi	++	+
	Lateral Parabrachial Nucleus (LPB)	Bi	+++	+++
	Medial Parabrachial Nucleus (MPB)	Bi	++	++
	Kölliker Fuse (KF)	Bi	+++	++++
	Locus Coeruleus (LC)	ipsi	++	+
	Subcoeruleus (SubC)	ipsi	++	-
	A5 region	Bi	++	+
Medulla	Midline Raphe	-	+++	++
	Vestibular Nucleus	bi	++	+++
	Gigantocellular Reticular Nucleus (Gi)	bi	+	+
	Caudal Ventrolateral Medulla (CVLM)	bi	+++	++
	Intermediate Reticular Nucleus	bi	+	+
	Nucleus of the Solitary Tract (NTS)	bi	++++	++
	Area Postrema (AP)	-	++++	-
	Paratrigeminal Nucleus (Pa5)	bi	+	+++
	A1 region/ Retro Ambiguus	bi	++	+

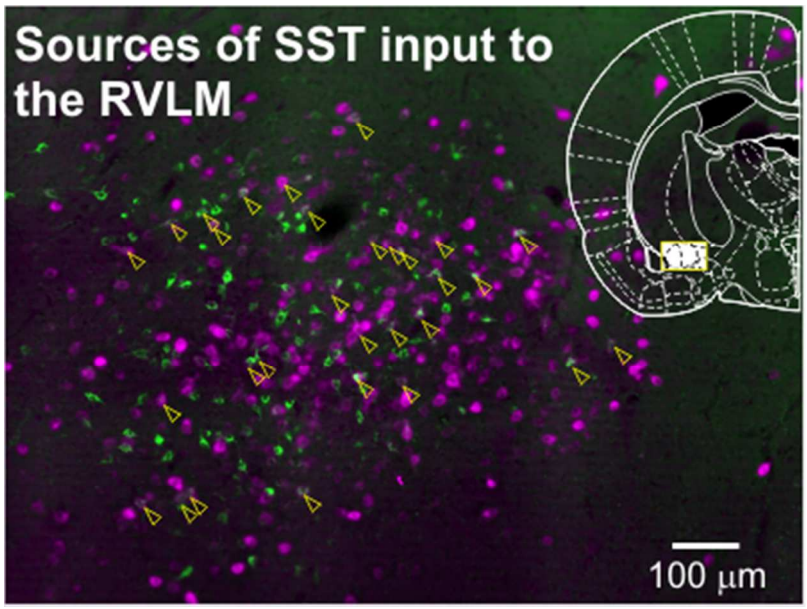

Somatostatin (SST) in the rostral ventrolateral medulla (RVLM) lowers sympathetic nerve activity, arterial pressure and heart rate and evokes apneusis when administered within the Bötzinger region. Here we describe the mechanisms responsible for the sympathoinhibitory effects of SST on bulbospinal neurons and identify brain-wide sources of RVLM SST release.
141x105mm (72 x 72 DPI)

Somatostatin (SST) in the rostral ventrolateral medulla (RVLM) lowers sympathetic nerve activity, arterial pressure and heart rate and evokes apneusis when administered within the Bötzinger region. Here we describe the mechanisms responsible for the sympathoinhibitory effects of SST on bulbospinal neurons and identify brain-wide sources of RVLM SST release.

APPENDIX II: ANIMAL RESEARCH AUTHORITIES

ANIMAL RESEARCH AUTHORITY (ARA)

AEC Reference No.: 2009/045 - 2 **Date of Expiry:** 31 March 2012

Full Approval Duration: *1 April 2010 to 31 March 2013 (36 months)*

This ARA remains in force until the Date of Expiry (unless suspended, cancelled or surrendered) **and will only be renewed upon receipt of a satisfactory Progress Report before expiry (see Approval email for submission details).**

Principal Investigator:
Dr Simon McMullan
Australian School of Advanced Medicine
Macquarie University NSW 2109
9850 4023
Simon.mcmullan@mq.edu.au

Associate Investigators:
Mr Stephen Abbott 0410 729 279
Dr Anita Turner 0411 283 223
Ms Lama Bou Farah 0406 164 456

In case of emergency, please contact:
Animal Welfare Officer Dr Miriam Meek: 9850 7758 / 0439 497 383
Central Animal House Manager Christine Sutter: 9850 7780 / 0428 861 163
or the Principal Investigator / Associate Investigator named above

The above-named are authorised by MACQUARIE UNIVERSITY ANIMAL ETHICS COMMITTEE to conduct the following research:

Title of the project: **NETWORK INTERACTIONS BETWEEN CARDIOVASCULAR CONTROL NEURONS IN THE BRAINSTEM UNDERLIE SYMPATHETIC TONE**

Type of animal research and aims of project:
Research (Pharmacology) – This project aims to clarify the network interactions between cardiovascular brainstem neurons.

Surgical Procedures category: 5 (Major Surgery with Recovery)

All procedures must be performed as per the AEC-approved protocol, unless stated otherwise by the AEC and/or AWO.

Maximum numbers approved:

Species	Strain	Age/Sex/Weight	*Year 1*	*Year 2*	*Year 3*	Total	Supplier/Source
Rat	Sprague-Dawley (SD)	Adult male(250-450g)	50	100	40	**190**	ARC Perth
Rat	Sprague-Dawley (SD)	Pups	50	100	50	**200**	ARC Perth
		TOTAL	**100**	**200**	**90**	**390**	

Location of research:

Location	*Full street address*
Australian School of Advanced Medicine	Level 1, Clinic Building, 2 Technology Place, Macquarie University NSW 2109
Central Animal House Facility	Building F9A, Research Park Drive, Macquarie University NSW 2109

Amendments approved by the AEC since initial approval:
1. Addition of Mr Stephen Abbott (approved June 2010)
2. Addition of Dr Anita Turner (approved Aug 2010
3. Addition of Ms Lama Bou Farah (approved Feb 2011)

Conditions of Approval: N/A

Being animal research carried out in accordance with the Code of Practice for a recognised research purpose and in connection with animals (other than exempt animals) that have been obtained from the holder of an animal suppliers licence.

Prof Michael Gillings (Chair, Animal Ethics Committee)

Progress Report Approval Date: ***17 March 2011***

ANIMAL RESEARCH AUTHORITY (ARA)

AEC Reference No.: 2011/055 **Date of Expiry:** 14 January 2013

Full Approval Duration: 15 January 2012 to 14 January 2015 (36 months)

This ARA remains in force until the Date of Expiry (unless suspended, cancelled or surrendered) **and will only be renewed upon receipt of a satisfactory Progress Report before expiry / is contingent upon receipt of a Final Report at the end of this period (see Approval email for submission details).**

Principal Investigator:
Dr Simon McMullan
ASAM
Macquarie University NSW 2109
0402 073 146
simon.mcmullan@mq.edu.au

Associate Investigators:
Anita Turner 0411 283 223
Anne Goodchild 0410 601 302

Other people participating:
Lama Bou Farah 0406 164 456
Bowen Dempsey 0403 831 090

In case of emergency, please contact:
Animal Welfare Officer: 9850 7758 / 0439 497 383
Manager, CAHF: 9850 7780 / 0428 861 163
or the Principal Investigator / Associate Investigator named above

The above-named are authorised by MACQUARIE UNIVERSITY ANIMAL ETHICS COMMITTEE to conduct the following research:

Title of the project: **Electrophysioloy and anatomy of cardiovascular control networks in the neonatal rat brainstem**

Purpose: 4 Research: animal or human biology
Aims: This project of electrophysiological and anatomical experiments aim to:

1. **Determine whether spinally projecting neurons in the brainstem receive monosynaptic inputs from neurons in the opposite side of the brain and to determine which neurotransmitters are responsible for these effects**

Examine whether pairs of spinally projecting neurons directly communicate with each other, i.e. to examine the hypothesis that cardiovascular control neurons are interconnected.

Surgical Procedures category: 2 (animal unconscious without recovery) & 5 (Major surgery with recovery)

All procedures must be performed as per the AEC-approved protocol, unless stated otherwise by the AEC and/or AWO.

Maximum numbers approved (for the Full Approval Duration):

Species	Strain	Age/Sex/Weight	Total	Supplier/Source
Rat	Sprague-Dawley (SD)	P7-25	**350**	ARC Perth
Rat	Sprague-Dawley (SD)	adult	**35**	ARC Perth
		TOTAL	**385**	

Location of research:

Location	*Full street address*
Australian School of Advanced Medicine	Level 1, Clinic Building, 2 Technology Place, Macquarie University NSW 2109
Central Animal House Facility	Building F9A, Research Park Drive, Macquarie University NSW 2109

Amendments approved by the AEC since initial approval: N/A

Conditions of Approval: N/A

Being animal research carried out in accordance with the Code of Practice for a recognised research purpose and in connection with animals (other than exempt animals) that have been obtained from the holder of an animal suppliers licence.
This authority remains in force from ***15 January 2012 to 14 January 2013***, unless suspended or surrendered, **and will only be renewed upon receipt of a PROGRESS REPORT annually.**

Prof Michael Gillings (Chair, Animal Ethics Committee) **Approval Date:** 8 December 2011